AD-773 195

INTEGRATED RADIOSOTOPE CATALYTIC MONOPROPELLANT HYDRAZINE ENGINE

Ronald A. Carlson

TRW Systems Group

Prepared for:

Air Force Rocket Propulsion Laboratory

December 1973

SECURITY CLASSIFICATION OF THIS PAGE (When Data Entered)

REPORT DOCUMENTATION PAGE

READ INSTRUCTIONS BEFORE COMPLETING FORM

1. REPORT NUMBER: AFRPL-TR-73-115
2. GOVT ACCESSION NO.:
3. RECIPIENT'S CATALOG NUMBER: AD 773 195

4. TITLE (and Subtitle): INTEGRATED RADIOISOTOPE CATALYTIC MONOPROPELLANT HYDRAZINE ENGINE

5. TYPE OF REPORT & PERIOD COVERED: FINAL REPORT March 72 thru Oct 73

6. PERFORMING ORG. REPORT NUMBER:

7. AUTHOR(s): Ronald A. Carlson

8. CONTRACT OR GRANT NUMBER(s): F04611-72-C-0064

9. PERFORMING ORGANIZATION NAME AND ADDRESS: TRW Systems Group, 1 Space Park, Redondo Beach, CA 90278

10. PROGRAM ELEMENT, PROJECT, TASK AREA & WORK UNIT NUMBERS:

11. CONTROLLING OFFICE NAME AND ADDRESS: Air Force Rocket Propulsion Laboratory/AFSC, Edwards, CA 93523

12. REPORT DATE: December 1973

13. NUMBER OF PAGES: ~~183~~ 188

14. MONITORING AGENCY NAME & ADDRESS (if different from Controlling Office):

15. SECURITY CLASS. (of this report): UNCLASSIFIED

15a. DECLASSIFICATION DOWNGRADING SCHEDULE: N/A

16. DISTRIBUTION STATEMENT (of this Report): APPROVED FOR PUBLIC RELEASE; DISTRIBUTION UNLIMITED

17. DISTRIBUTION STATEMENT (of the abstract entered in Block 20, if different from Report):

18. SUPPLEMENTARY NOTES

19. KEY WORDS (Continue on reverse side if necessary and identify by block number)

Hydrazine
Hydrazine Engine
Monopropellant Engine
Attitude Control Systems
Radioisotope Heaters

20. ABSTRACT (Continue on reverse side if necessary and identify by block number)

This report presents the results of AFRPL Contract No. F04611-72-C-0064 with TRW Systems Group. In this advanced technology program radioisotope heat sources were incorporated into an Integrated Radioisotope Catalytic Monopropellant Hydrazine Engine designed to maintain the catalyst bed above 200°F in an earth orbiting space environment. The impact of "ambient temperature starts" is thus reduced without requiring additional electrical power. (Continued on reverse side.)

DD FORM 1 JAN 73 1473 EDITION OF 1 NOV 65 IS OBSOLETE

SECURITY CLASSIFICATION OF THIS PAGE (When Data Entered)

20. ABSTRACT (Continued)

A limited development effort was conducted to upgrade a 5-pound thrust engine design originally developed during a TRW IR&D program. Iterations of the injector and headspace designs and variations to the catalyst bed were evaluated. Accelerated life testing of the selected design revealed a headscreen deformation problem and verified the design improvement incorporated to prevent recurrance.

Three Radioisotope Heater Units (RHU's), delivering 1 watt of thermal energy each, were designed and fabricated using previously flight qualified designs. A minimal nuclear safety effort was thus required. The three RHU's were incorporated with the 5-pound thrust engine and tested to a duty cycle involving over 200,000 cycles with 565 "ambient temperature starts" (defined as 200°F minimum). The results of this test program are presented herein.

AFRPL-TR-73-115

INTEGRATED RADIOISOTOPE CATALYTIC MONOPROPELLANT HYDRAZINE ENGINE

FINAL REPORT

TRW SYSTEMS GROUP
ONE SPACE PARK
REDONDO BEACH,
CALIFORNIA 90278

RONALD A. CARLSON

DECEMBER 1973

AIR FORCE ROCKET PROPULSION LABORATORY
DIRECTOR OF SCIENCE AND TECHNOLOGY
AIR FORCE SYSTEMS COMMAND
EDWARDS, CALIFORNIA 93523

AFRPL-TR-73-115

INTEGRATED RADIOISOTOPE CATALYTIC MONOPROPELLANT HYDRAZINE ENGINE

Contract F04611-72-C-0064

Final Report

December 1973

by

Ronald A. Carlson

TRW Systems Group
Redondo Beach, California, 90278

Air Force Rocket Propulsion Laboratory
Edwards Air Force Base
Edwards, California 93523

ic

"When U. S. Government drawings, specifications, or other data are used for any purpose other than a definitely related Government procurement operation, the Government thereby incurs no responsibility nor any obligation whatsoever, and the fact that the Government may have formulated, furnished, or in any way supplied the said drawings, specifications, or other data, is not to be regarded by implication or otherwise, or in any manner licensing the holder or any other person or corporation, or conveying any rights or permission to manufacture, use, or sell any patented invention that may in any way be related thereto."

ID

ABSTRACT

This report presents the results of AFRPL Contract No. F04611-72-C-0064 with TRW Systems Group. In this advanced technology program radioisotope heat sources were incorporated into an Integrated Radioisotope Catalytic Monopropellant Hydrazine Engine designed to maintain the catalyst bed above 200°F in an earth orbiting space environment. The impact of "ambient temperature starts" is thus reduced without requiring additional electrical power.

A limited development effort was conducted to upgrade a 5-pound thrust engine design originally developed during a TRW IR&D program. Iterations of the injector and headspace designs and variations to the catalyst bed were evaluated. Accelerated life testing of the selected design revealed a headscreen deformation problem and verified the design improvement incorporated to prevent recurrance.

Three Radioisotope Heater Units (RHU's), delivering 1 watt of thermal energy each, were designed and fabricated using previously flight qualified designs. A minimal nuclear safety effort was thus required. The three RHU's were incorporated with the 5-pound thrust engine and tested to a duty cycle involving over 200,000 cycles with 565 "ambient temperature starts" (defined as 200°F minimum). The results of this test program are presented herein.

TABLE OF CONTENTS

TABLE OF CONTENTS (Continued)

LIST OF ILLUSTRATIONS

LIST OF ILLUSTRATIONS (Continued)

LIST OF ILLUSTRATIONS (Continued)

LIST OF TABLES

1. INTRODUCTION AND SUMMARY

Anticipated requirements for monopropellant hydrazine reaction control thrusters to be used in future spacecraft missions include long operating life and numerous ambient starts. The rate of thruster performance degradation is influenced by the catalyst bed "ambient" temperature, leading to requirements for heating the catalyst bed. Electrical resistance heaters and radioisotope heaters are both capable of supplying the required heat energy. Resistance heaters require additional power from the spacecraft, however, and are comprised of components which are not conducive to high reliability for extensive spacecraft missions. Radioisotope heat sources do not have these limitations and are thus a promising approach to maintaining higher catalyst bed temperatures for extended times.

The objective of this program was to demonstrate the feasibility of an integrated radioisotope/catalytic 5-lbf class thruster with a capability of greater than 500,000 pulses independent of the number of ambient starts.

A limited development program was conducted to upgrade a 5-pound thrust engine design originally developed during a TRW IR&D program. The headspace injector design utilized in TRW thrusters has demonstrated excellent life capabilities, and the 5-lbf thruster was most directly applicable to the general requirements for this class. Pioneer 10 and 11 type Radioisotope Heater Units (RHU's) were then incorporated to supply 3 watts of nuclear heat energy. Three watts are sufficient to maintain a temperature of over 200°F for a thruster of this size in most earth orbiting spacecraft environments. The Pioneer 10 and 11 type RHU was selected for its flight-proven status, including nuclear safety approval for ground testing and launch. Minor modifications were required, however, to incorporate a pressure relief device in the isotope capsule. This was due both to higher temperature exposure (because of the close proximity to the catalyst bed), and to make it acceptable for earth orbiting applications.

A demonstration test was conducted which accumulated over 200,000 cycles on the radioisotope heated engine, including over 550 engine ambient starts. Engine ambient for this program was specified as 200°F minumum and for test purposes was defined as 210°F ± 10.

The overall program as conducted is summarized in the flow of diagram presented in Figure 1-1.

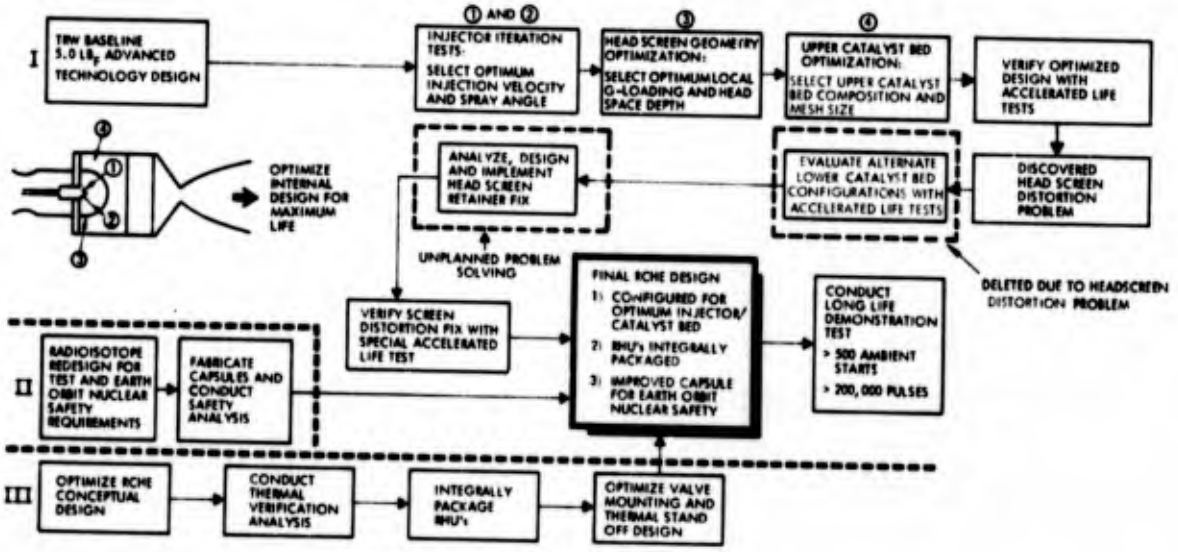

Figure 1-1. Program Flow Diagram

Engine performance shifted gradually throughout the test because of an increasing catalyst bed pressure drop. The resultant thrust shift was 15 per cent at the high propellant inlet pressure and 27 per cent at the low pressure. There was no step change in performance, however, and the engine appears capable of continuing to deliver acceptable performance for much greater durations.

The engine was X-rayed and disassembled for post test hardware evaluation. Catalyst weight loss was also determined to be 1.7 grams or 8 per cent of the catalyst loaded; the catalyst bed was found to be in relatively good condition. Some fines were present, but there was no indication of voiding, severe compaction, or sintering. The catalyst separator screen fractured and separated from the chamber wall, and a small hole appeared in the headscreen. These failures had some impact on the engine response characteristics, but would not prevent the engine from operating for a more extensive duty cycle.

An unheated engine, duplicating the pertinent design features of the heated engine, was fabricated and tested as part of the TRW IR&D program. The test exposure was the same as that for the heated engine except that each start was controlled to 70 $\pm$ 20°F. Performance of this engine throughout the duty cycle was comparable to the heated engine. Post test hardware condition was also comparable except for a greater catalyst loss (13 percent).

Highlights of the thruster development program are presented in the succeeding sections along with a description of the final engine design. The engine test program is presented and the results discussed.

2. THRUSTER DEVELOPMENT

TRW's headspace injection design has demonstrated long life capabilities at the 4 lb_f thrust level. This thruster operates with high inlet pressure and was originally designed for a nominal 3 lb_f thrust level, restricting its application within the 5 lb_f class. IR&D testing of a 5 lb_f thruster had demonstrated a good base point for a new thruster design which was more suitable to many current applications. A limited thruster development program was planned to select the final configuration.

This section summarizes the thruster development program. Starting with the baseline design, the test plans for the injector definition and for the lower catalyst bed definition tests are presented. Test results and resolution of specific problem areas are then discussed.

2.1 BASELINE DESIGN

A baseline design for a "new" thruster in the 5 lb_f thrust class is established from emperically derived criteria which include:

- Bed loading (G) $\leq$ 0.03 lb/sec-in^2 (based on engine cross-sectional area)
- Hemispherical headspace design to a nominal throughput of 0.05 lb/sec-in^2 (based on total area)
- Layered catalyst bed

  18-20 or 14-18 mesh upper bed
  20-30 mesh lower bed

- Injection velocity - 25-80 fps
- Injector spray pattern - 60-110° included angle

The final parameter required to establish the baseline design is length of the catalyst bed. Pressure Drop considerations are of importance, but offer considerable leeway. Experience has shown that approximately 0.5 inch of 20-30 mesh catalyst is required for the lower bed to insure that flooding (washout) will not occur during extensive duty cycles. The upper bed length must be 0.1 to 0.2 inch longer than the axial length of the headspace. Using these dimensions, a bolt-up thrust chamber is designed for an iteration test program.

The iteration test program establishes the final configuration of the injector, head space, and upper catalyst bed. Primary evaluation criteria are pulse repeatability (shape, impulse, and centroid) and chamber pressure roughness over the operating thrust range. Final adjustments to optimize the length of the lower catalyst bed are normally omitted due to the postulation that little benefit would be realized.

Figure 2-1 presents the bolt-up thruster design used for the test program, and Table 2-1 presents the baseline parameters. The bolt-on head end assembly provides rapid access to the catalyst bed and a removable injector element minimizes the cost of injector design iterations. The headscreen is held on the headplate by a pressed on retainer ring designed to an interference fit. Resistance welding or brazing are used at this attachment for extensive tests, while the interference fit has proven satisfactory for tests involving thousands of pulses. The catalyst separator screen is resistance welded to a ring which fits closely within the chamber and simulates a step in the chamber wall. For the bolt-up hardware, the location of this screen is set by the catalyst loading as the purpose of this this screen is usually to separate different mesh sizes of catalyst and is not a structural member.

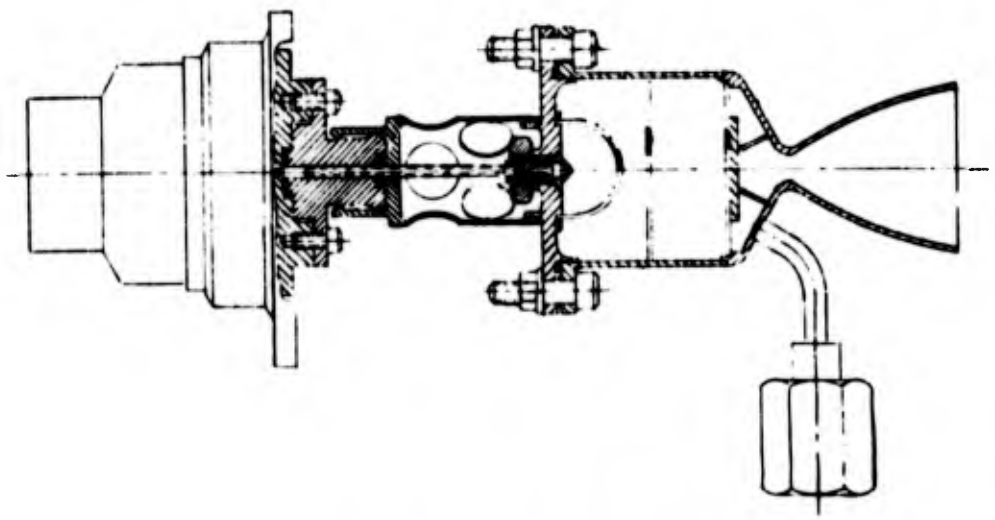

Figure 2-1. Bolt-Up Thruster

Table 2-1. Baseline Design Parameters

Parameter	Nominal	Range
Thrust (lbf)	5.0	2.1 - 5.6
Propellant Pressure (psia)	300	100 - 350
Chamber Pressure (psia)	180	70 - 200
Bed Loading (G = lbm/sec-in^2)	0.027	0.011 - 0.030
Total Bed Length (in.)	1.0	1.0

2.2 INJECTOR DEFINITION TEST PLAN

The design criteria presented above offer considerable leeway in establishing a specific design. This test sequence evaluated the influence of design variations within the above criteria to select the "best" design.

Each candidate design was subjected to the duty cycle presented in Table 2-2. Repeat and/or special tests dicated by test results were tested to abbreviated sequences, however, to obtain only the most pertinent data.

Table 2-2. Duty Cycle - Injector Definition Tests

Sequence	Duty Cycle	Propellant Feed Pressure(s) (psia)
1	500 Second Steady State	350
2	Duty Cycle A	350, 225, 100, 500, and 50
3	Pulse Sweep*	350, 225, 100, 500, and 50

Duty Cycle A

Sequence	On-Time (msec)	Off-Time (msec)	Number of Pulses
a	20	980	100
b	20	480	100
c	50	950	100
d	50	450	100
e	100	900	100
f	150	850	100
g	10 sec	Steady-State	/

*A pulse sweep consists of a 10-second steady-state firing to heat the thruster, followed by a single test varying the pulse width (on time) from 0.020 to 0.150 second at a constant pulse rate of one per second.

Chamber pressure, inlet pressure, and solenoid valve current were the primary data obtained. Chamber pressure and valve current were displayed on an oscilloscope and photographs taken which present several pulses superimposed. Data for selected portions of the tests were also recorded on an oscillograph as a backup for the oscilloscope photographs.

Evaluation criteria for the design selections are primarily chamber pressure oscillations, both during pulse mode and steady-state operation, and repeatability of pulse characteristics. Chamber pressure roughness is comparable on an absolute basis both in terms of nominal (average) magnitude and the magnitude of any pressure spikes or overshoots which may occur. Pulse repeatability is more subjective and is most easily evaluated using photographs of the oscilloscope trace. A semi-quantitative criteria for this evaluation is the number of distinct traces discernible from 10 superimposed pulses and/or the relative "line width" resulting.

Figure 2-2 presents the typical oscilloscope data obtained from a "pulse sweep." The 10 second steady state test is shown in the top photograph with an oscilloscope sweep rate of 1 sec/div. Immediately after the steady state test, pulsing is initiated at 0.150 sec ON - one pulse/sec and the oscilloscope set to sweep at 0.050 sec/div. The thruster is allowed to stabilize at this duty cycle and five (5) pulses are photographed. The pulse on time is then changed and the procedure repeated to show five (5) pulses each at pulse duration of 0.150, 0.100, 0.050, and 0.020 sec. on one photograph, After changing the oscilloscope sweep rate to 20 ms/div, the pulse duration is stepped up to again show five pulses each at the different pulse durations.

Fourteen (14) test sequences were planned to select the configuration of the injector and upper catalyst bed. Figure 2-3 summarizes the design iterations and test logic.

The first three tests were to determine the headscreen geometry and evaluate the low thrust operation of the baseline injector. TRW development experience has shown that thruster performance characteristics are more influenced by the addition of a small cylindrical extension of the headspace than by changes to the spherical radius, and that the headscreen design will not be significantly influenced by minor changes to the injector configuration.

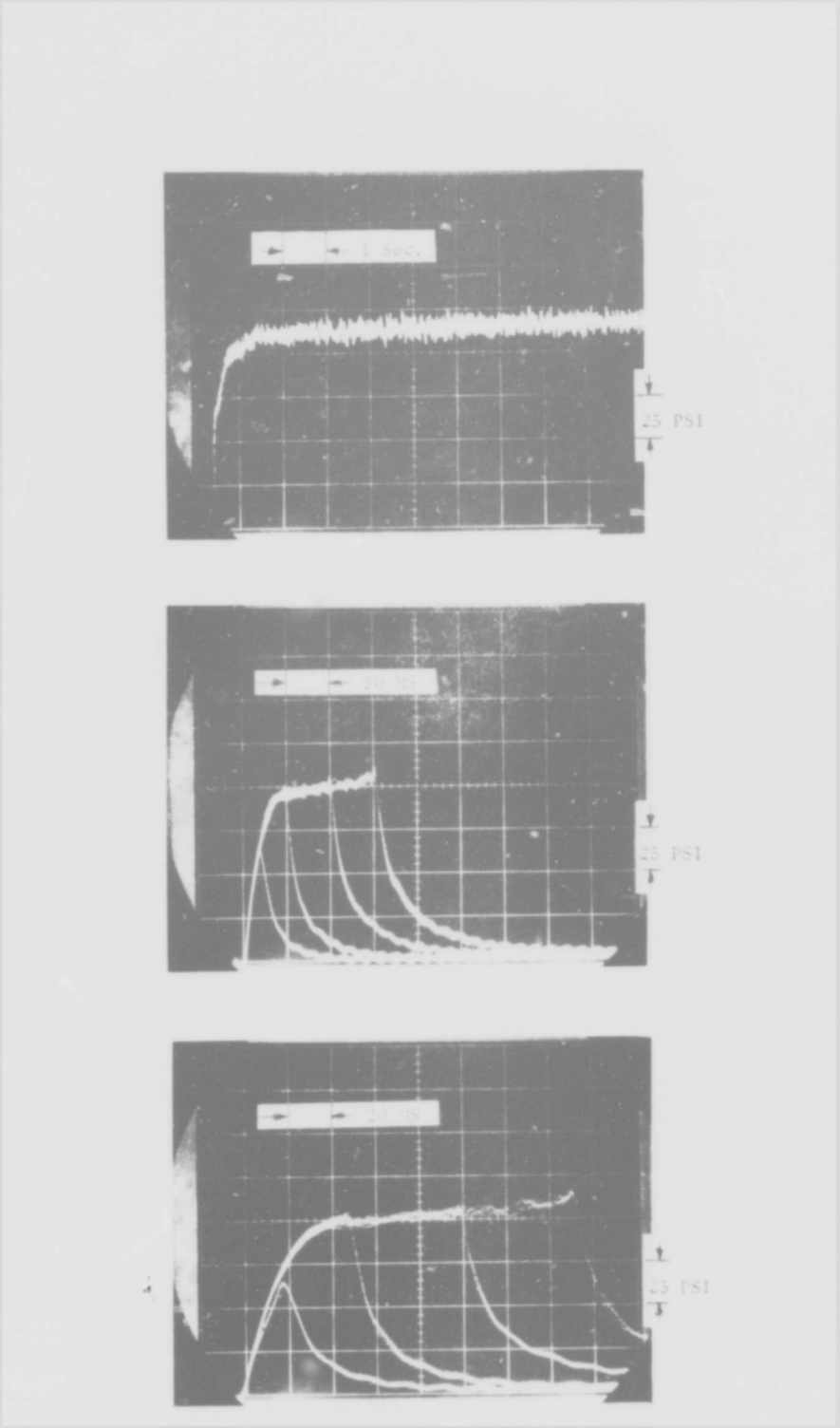

Tests shown consist of a 10 second steady-state firing (first picture) followed by a single test varying the pulse width (on time) from 0.150 to 0.020 second on (second picture) and then from 0.020 to 0.150 second on (third picture) at a constant pulse rate of one per second. Five pulses at each pulse width are shown in each picture.

Figure 2-2. Typical Pulse Sweep

HEADSCREEN ITERATIONS

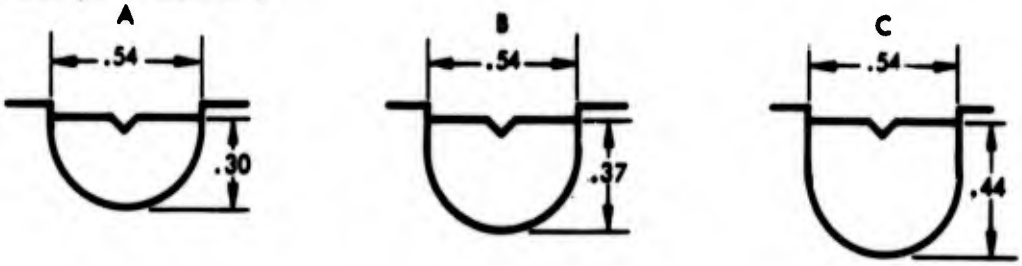

INJECTOR ITERATIONS

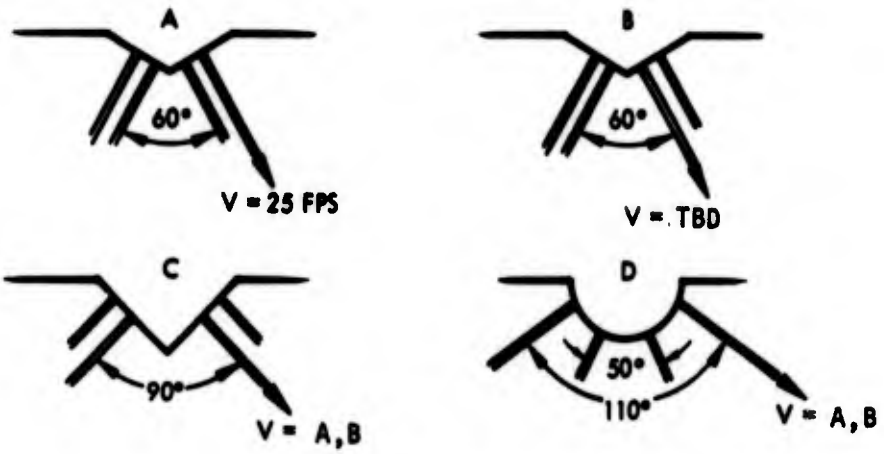

CATALYST COMPOSITION (UPPER BED)

A - 14 - 18 MESH SHELL 405 (75%)
14 - 18 MESH HA - 3 (25%)

B - 14 - 18 MESH SHELL 405 (75°)
18 - 20 MESH HA-3 (25°)

C - 18 - 20 MESH SHELL 405 (75°)
18 - 20 MESH HA-3 (25°)

	HEADSCREEN		
	A	B	C
INJECTOR A	●	●	●

SELECTED HEADSCREEN
SELECT INJECTOR B VELOCITY

	CATALYST COMPOSITION		
	A	B	C
INJECTOR A	●	●	●
INJECTOR B	●	●	●

SELECTED BED
SELECTED INJECTION VELOCITY

INJECTOR C	●
INJECTOR D	●

SELECTED INJECTOR
VERIFY HEADSCREEN

HEADSCREEN		
A	B	C
●	●	●

Figure 2-3. Injector/Upper Bed Test Logic

The three headscreen configurations selected (see Figure 2-3) are derived from prior test history at the 5 lb_f thrust level and scaling data from a series of tests which evaluated allowable tolerances for a 1.0 lb_f nominal thrust engine. Another primary goal for these tests was to aid in the establishment of minimum injection velocity. Previously tested thrusters of this design concept have utilized injection velocities of 50 to 80 fps at nominal thrust, yielding 25 fps when operated at the low end of their thrust range. Operation of the baseline injector at reduced thrust determined the adequacy of the injection velocity and contributed to selection of an alternate design (lower velocity desired, higher if required).

The second series of tests lead to final selection of the injection velocity and the upper catalyst bed composition. Two injectors, identical except for size of the orifices (velocity), were evaluated with three catalyst bed compositions.

Upper catalyst bed design involves a tradeoff between bed porosity (increased by larger mesh catalyst) required to enhance recirculation of hot gases within the headspace, and effective catalyst activity (resulting from smaller mesh catalyst) required to initiate decomposition. If the catalyst is too fine (i.e., 20-30 mesh), recirculation is restricted and propellant tends to collect within the headspace and cause pressure spikes through random decomposition. Too coarse a mesh (i,e., 14-18 in smaller reactors) will result in poor initial response and spikes occurring during the pulses. Previous testing at the 5 lb_f thrust level selected a bed composition consisting of 75 percent 14-18 mesh Shell 405 and 25 percent 18-20 mesh HA-3. This testing was very limited, however, and a more uniform mesh size is desirable to minimize catalyst migration.

Two additional injectors were then designed to evaluate alternate spray patterns, maintaining injection velocity constant. The baseline design was initially scaled up from smaller thrusters. The alternate designs selected (see Figure 2-3) represent a scaled down version of a larger thruster and an intermediate between the other two.

A final survey of the headspace design was planned to verify the selection of the headscreen for the specific injector selected.

2.3 LOWER CATALYST BED DEFINITION TEST PLAN

A significant factor in the life related degradation of thruster characteristics is the compaction of the catalyst bed and accumulation of catalyst fines, resulting in increased pressure drop. These tendencies can be reduced by increasing the porosity of the catalyst bed, decreasing the bed pressure drop, and/or decreasing bed length. These factors all interrelate, and all impact the performance characteristics. Increased bed porosity (larger mesh catalyst) impact the response characteristics and, generally, necessitates an increase in bed length to insure that flooding will not occur. Testing at the 1.0 lb_f thrust level indicated that a total bed length of 0.6 inch, comprised of 0.3 inch 18-20 mesh and 0.3 inch 20-30 mesh catalyst, was adequate. Real-time duty cycle tests (for the specific application) demonstrated an increasing tendency to flood (incomplete hydrazine decomposition), however, during long steady-state firings. At that time, cost and schedule dictated a conservative approach and the length of the lower catalyst bed was doubled. The fact that the initial design was marginal supports the theory that larger mesh catalyst could have been used to extend the lower bed with equal success in preventing flooding.

An approach used in the design of gas generators which utilize very long catalyst beds (to enhance ammonia dissociation) is to layer the bed. The screens used to define the layers support the catalyst, reducing the maximum compression load resulting from bed pressure drop. Additional porosity at each screen also enhances uniform flow distribution through the remainder of the bed.

Previous testing had demonstrated that 20-30 mesh catalyst was required for the lower bed in order to meet the response requirements imposed. A small compromise in response characteristics may, however, yield a better overall design for long life. Two additional tests (as used during the injector definition phase) were planned to evaluate the effects of using 18-20 and 14-18 mesh catalyst for the lower bed.

Four iterations of the lower bed design were planned to select a design least sensitive to clogging with catalyst fines and verify that the design would not be prone to flooding during steady-state firings. This was to be

accomplished by selecting two candidate designs and simultaneously subjecting them to the accelerated duty cycle presented in Table 2-3. The design demonstrating the least change in performance characteristics would then influence selection of two alternate configurations. Figure 2-4 presents the original logic and tentative design selections for the first test.

Table 2-3. Duty Cycle - Accelerated Life Test

Sequence	Duty Cycle	Propellant Feed Pressure(s) (psia)
1	500 Second Steady State	350
2	Duty Cycle A (Table 2-2)	350, 225, 100, 500 and 50
3	Duty Cycle A	350, 225, 100, 500 and 50
4	Pulse Sweep (Table 2-2)	350, 225, 100, 500 and 50
5	Duty Cycle B	350
6	Repeat 3, 4 and 5 - three times	
7	Repeat 3 and 4	
8	2,000 Second Steady State	350
9	Duty Cycle A	350, 225, 100, 500 and 50
10	1,000 Second Steady State	500

NOTE: Thrust data will be obtained for sequences 1, 2, and 9 only.

Duty Cycle B

Sequence	On-Time (m sec)	Off-Time (m sec)	Number of Pulses
a	20	230	1000
b	50	200	1000
c	100	150	1000
d	150	100	1000
e	100 sec	Steady State	1
f	Repeat a thru e, 6 times		24,006

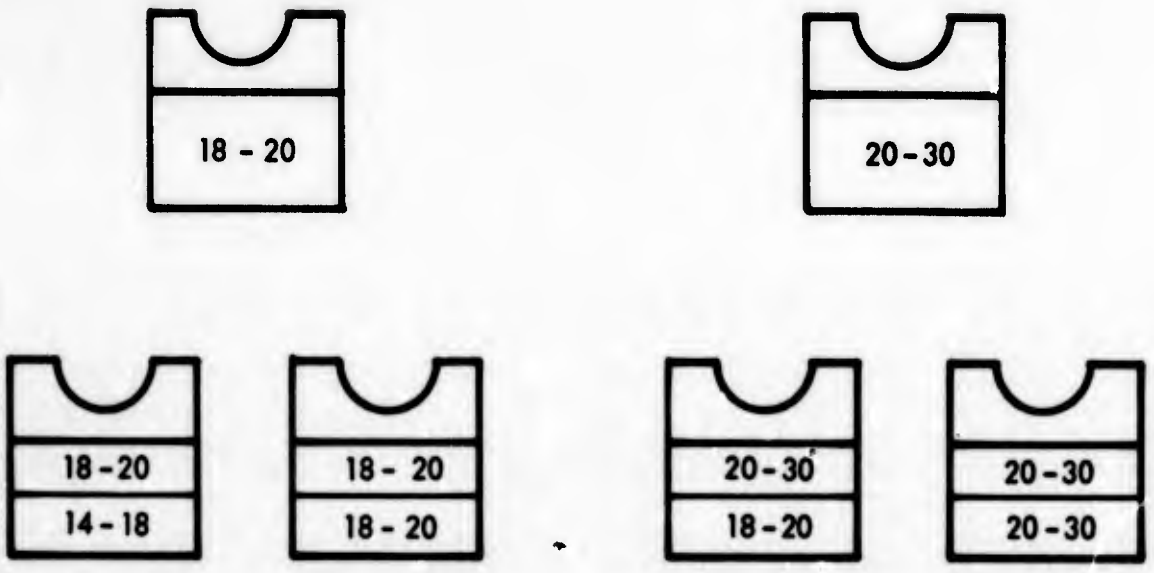

Figure 2-4. Lower Catalyst Bed Iteration Tests

2.4 INJECTOR DEFINITION TEST RESULTS

The headscreen iteration testing (see Figure 2-3) showed good steady state operation, particularly with Headscreens B and C. Pulse mode operation, however, showed pressure overshoots on startup followed by damped cyclic oscillations. Figure 2-5 presents a summary of the analog test data.

The pressure overshoot was attributed to insufficient liquid pressure drop, and the pressure distribution was re-evaluated. The IR&D thruster had been tested with a nominal chamber pressure of 100 psia (at 5 lb_f thrust). That design was dictated by the availability of a valve which had a high pressure drop. A higher chamber pressure was selected for this program to reduce the catalyst bed pressure drop and to reduce the nozzle exit diameter. The latter factor was primarily to reduce the heat loss by radiation. At this point, however, it was decided to revert back to the IR&D design having the lower chamber pressure (Reference Table 2-6).

Changing to the lower chamber pressure at this point necessitated a change to the nozzle expansion area ratio (ϵ). Preliminary design of the

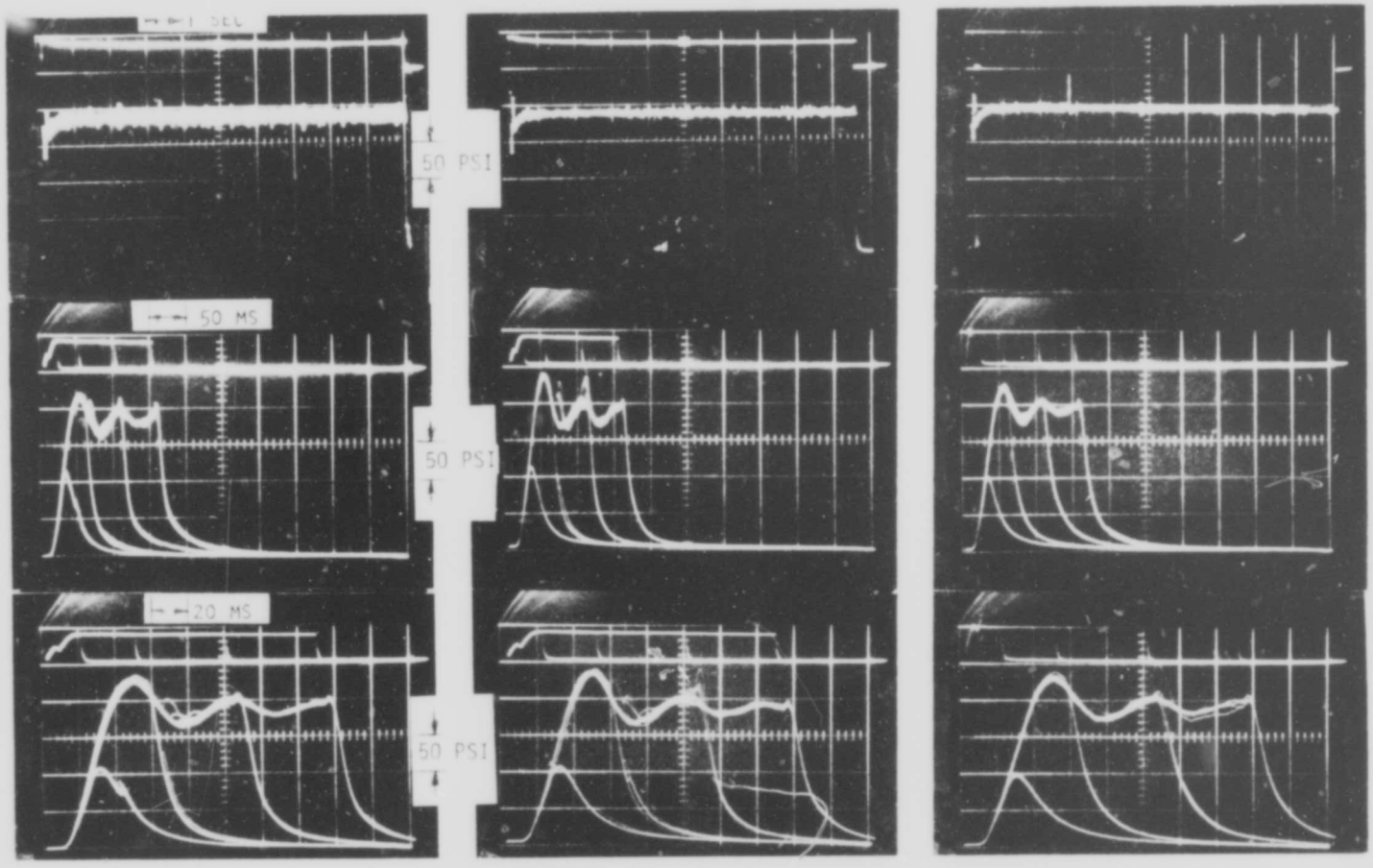

Figure 2-5. Injector Definition Test Results

final engine led to selection of a casting for the thrust chamber and ports for the radioisotope heater units (RHU's). Accounting for the lead time to receive castings, a casting was designed which provided adequate flexibility for any anticipated design iterations. Only minor changes to this design were necessary to increase the nozzle throat diameter (thus lower chamber pressure) provided the nozzle exit diameter remained essentially unchanged. The nozzle expansion area ratio was thus changed from 40 to 24.

Limited testing was continued with the baseline design, pending fabrication of new nozzles, Headscreen C (0.44 inch length) was selected as shown in Table 2-4. The design for Injector B was also selected from this test series. An increase to the injector velocity appeared desirable for operation at lower thrust levels. Slightly less than twice the injection velocity was chosen for the second injector (Injector B). An orifice diameter of .009 inch, yielding a nominal velocity of 44 fps, was selected.

Table 2-4. Headscreen Performance Comparison

P_{inlet} (psia)	Headscreen A			Headscreen B			Headscreen C		
	Steady-State	Pulse Mode		Steady-State	Pulse Mode		Steady-State	Pulse Mode	
	Pc Roughness	Overshoot	Repro.*	Pc Roughness	Overshoot	Repro.*	Pc Roughness	Overshoot	Repro.*
350	+10%	52%	2	±5%	30%	2	±4%	22%	1
225	±90%	23%	1	±7%	0	1	±7%	0	1
100	±22%	0	2	+31%	0	1	±22%	0	1

*Reproducibility Ratings:

1) Good Reproducibility
2) Minor Variations
3) Erratic pulse-to-pulse variations

Catalyst for the above tests was 100 percent Shell 405, 14-18 mesh for the upper and 20-30 mesh for the lower catalyst beds. Tests were then conducted to evaluate the alternate upper catalyst beds as well as the alternate injection velocities. These tests were first conducted with the high Pc chamber. Injector A (25 fps) performed best with catalyst C (18-20 mesh) and Injector B (44 fps) performed best with catalyst A (14-18 mesh). The results were verified using the low Pc (100 psia) chamber as shown in Figure 2-6. The lower injection velocity was selected for further testing, in conjunction with catalyst C (18-20 mesh). Table 2-5 presents the comparison of the three injector spray patterns and Figure 2-7 presents a summary of the analog data. For overall performance Injectors A and D (60° and 50-110° injector spray pattern angles respectively) were rated essentially equal. Injector D was thus tested with an alternate headscreen (B) to verify that the prior headscreen selection was also applicable to this injector. No improvement was noted with the alternate headscreen. Injector A was selected at this point primarily because of similarity to the other TRW thruster designs.

Table 2-6 summarizes the results of the Injector/Upper Catalyst Bed Testing, presenting the baseline design parameters and the selected design.

Table 2-5. Injector Performance Comparison

P_{inlet} (psia)	Injector A			Injector B		
	Steady-State Pc Roughness	Pulse Mode		Steady-State Pc Roughness	Pulse Mode	
		Overshoot	Reproducibility*		Overshoot	Reproducibility*
350	±3%	0	1	±9%	0	1
225	±4%	0	1	±9%	0	2
100	±7%	0	1	±7%	0	1

P_{inlet} (psia)	Injector C			Injector D		
	Steady-State Pc Roughness	Pulse Mode		Steady-State Pc Roughness	Pulse Mode	
		Overshoot	Reproducibility*		Overshoot	Reproducibility*
350	±3%	0	1	±4%	0	1
225	±6%	0	1	±4%	12%	1
100	±15%	0	1	±7%	0	1

*Reproducibility Ratings:

1) Good Reproducibility
2) Minor Variations
3) Erratic pulse-to-pulse variations

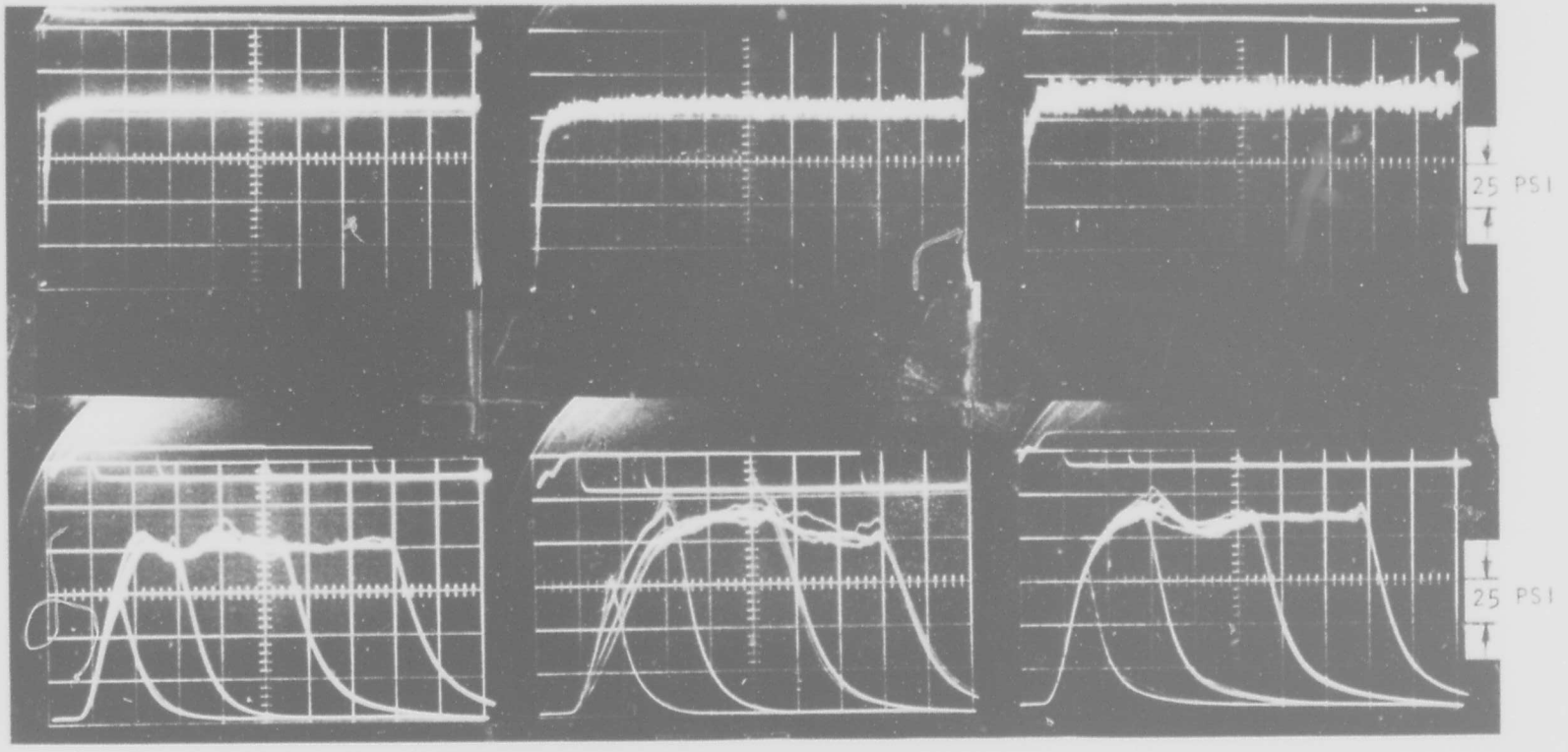

Injector A
Headscreen C
Catalyst C
Pc = 100

Injector B
Headscreen C
Catalyst A
Pc = 100

Injector B
Headscreen C
Catalyst C
Pc = 100

Figure 2-6. Injection Velocity/Catalyst Composition Test Results

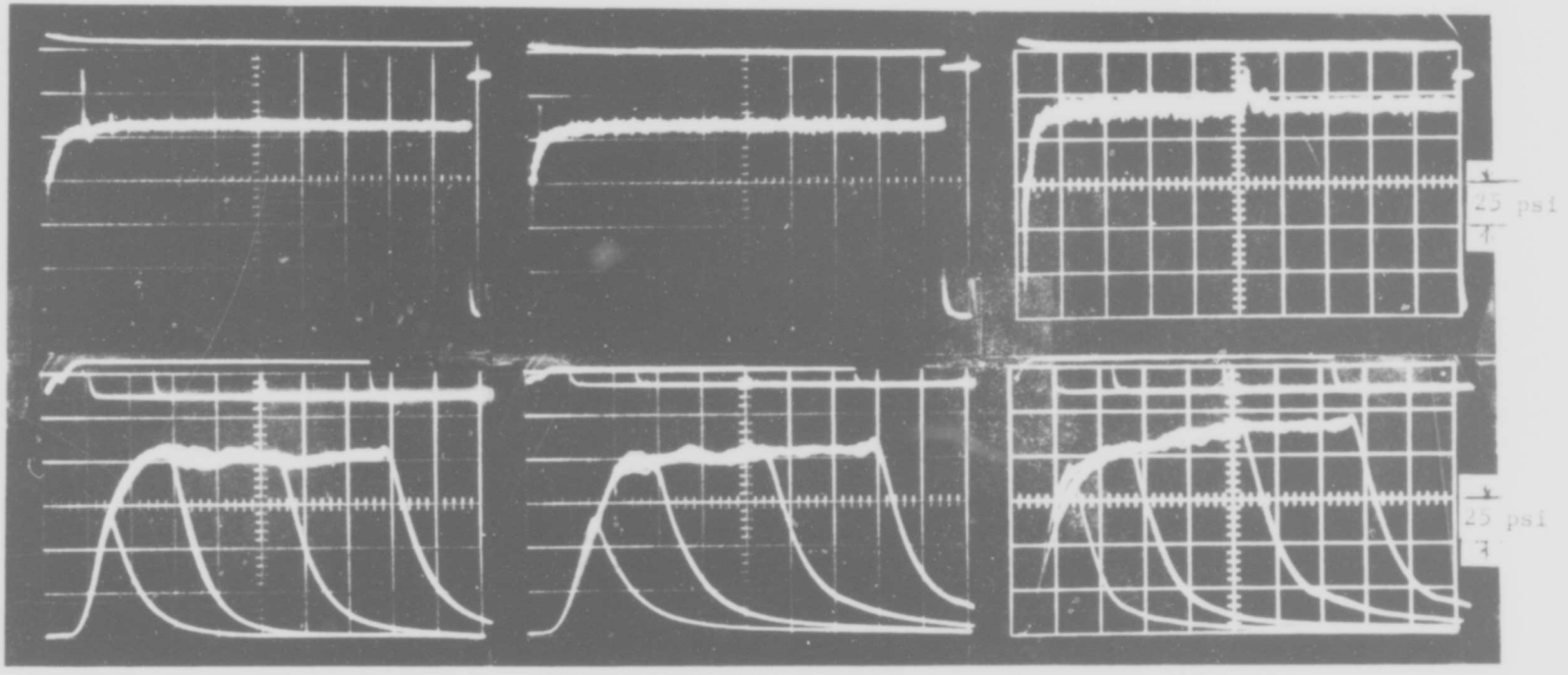

Injector A
Screen C
Catalyst C

Injector C
Screen C
Catalyst C

Injector D
Screen C
Catalyst C

Figure 2-7. Alternate Injector Evaluation

Table 2-6.

Thruster Design Comparison

Parameter	Baseline Design	Selected Design
Propellant Pressure	300	300
Thrust (lb_f)	5	5
Chamber Pressure (psia)	180	100
Llquid Pressure Drop (psid)	105	173
Catalyst Bed Loading (G - lb/in^2 sec)	0.03	0.03
Catalyst Bed Pressure Drop (psid)	15	27
Nozzle Expansion Area Ratio (ε)	40	24
Injector Spray Angle	TBD	60° (Injector A)
Headscreen Length (inch)	TBD	0.47
Upper Catalyst Bed	TBD	18 - 20 mesh (Catalyst C - 25% HA-3)

2.5 LOWER CATALYST BED TEST RESULTS

Two "new" injectors were fabricated to the same drawings as the "selected" Injector A, and two thrusters assembled. One of the thrusters utilized 20-30 mesh and the other 18-20 mesh catalyst for the lower bed, with all other parameters identical. The "acceptance" test of these thrusters did not demonstrate the same performance characteristics as previously measured, however. Both thrusters demonstrated higher chamber pressure oscillations than anticipated. Figure 2-8 shows the steady state characteristics of these thrusters.

The difference between the thrusters was traced to fabrication differences of the injector element. The first injector was out of tolerance on wall thickness, yielding a low L/D for the orifices. Comparing this injector to the "new" injector A's showed the first to produce greater atomization and distribution of the propellant. All of the injectors were then

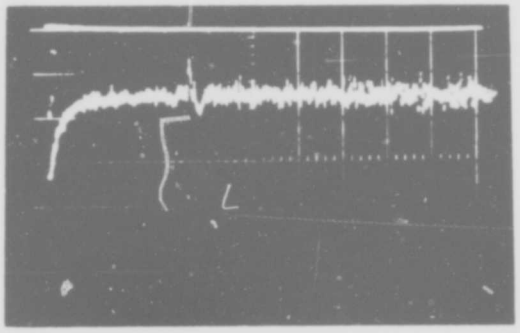

Engine #1
18-20 mesh lower bed

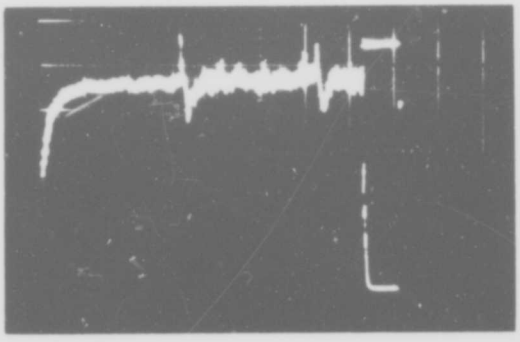

Engine #2
20-30 mesh lower bed

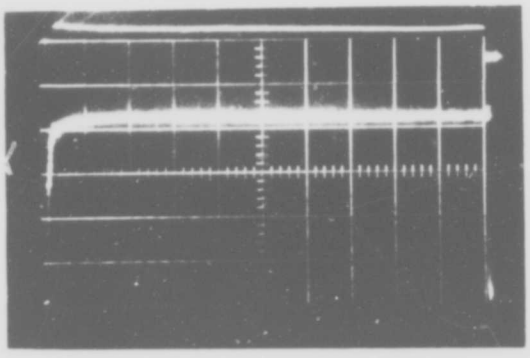

Prior Test
Original Injector A
(Reference)

Figure 2-8. Accelerated Life Test First Attempt

re-evaluated in water flow and visual inspection, and the original A was the only one found discrepant.

Reviewing the selection of Injector A (Section 2.4), it and Injector D (50° and 110°) were rated essentially equal. A second injector of this configuration (Injector D) was then fabricated and tested to verify that it repeated the earlier test results. Program scope limitation dictated continuation of the planned testing with Injector D rather than pursuing a further investigation of injector design parameters and/or attempting to reproduce the first injector.

Each engine was successfully "acceptance" tested, including measurement of thrust and propellant flow. Both engines were then installed to fire simultaneously and measure chamber pressure only. The intent was to rapidly accumulate 130,000 pulses on both thrusters, per the duty cycle of Table 2-3, then mount each thruster separately for thrust measurement for comparison of the lower catalyst bed compaction (as indicated by thrust shift). The 1,000 second steady state test at the high (500 psia) inlet pressure was to test for washout. Testing of the thruster having the 20-30 mesh lower catalyst bed was terminated after 83,600 pulses, however, due to a failure of the chamber pressure tap. Attempts to reweld this tube were unsuccessful. The remainder of the test was thus completed using only one thruster design. Data from these tests are presented in Figures 2-9 through 2-16, and Figure 2-17 summarizes the analog characteristics via pulse sweeps at various stages. Engine No. 1 has 18-20 mesh and engine No. 2 has 20-30 mesh catalyst for the lower bed.

Two variances from the plan evolved from the results of this test. The digital data revealed lower impulse and specific impulse at duty cycles of two (2) pulses/sec that at one (1) pulse/sec, leading to a re-evaluation of the catalyst blend. Post test evaluation of the hardware then revealed severe deformation of the headscreens. These factors are discussed separately in the following sections.

2.5.1 Catalyst Blend Evaluations

Catalyst blends consisting of 25% HA-3 and 75% Shell 405 have been utilized to improve steady state chamber pressure roughness in certain thrusters. The blend has also been used in the upper catalyst bed of a

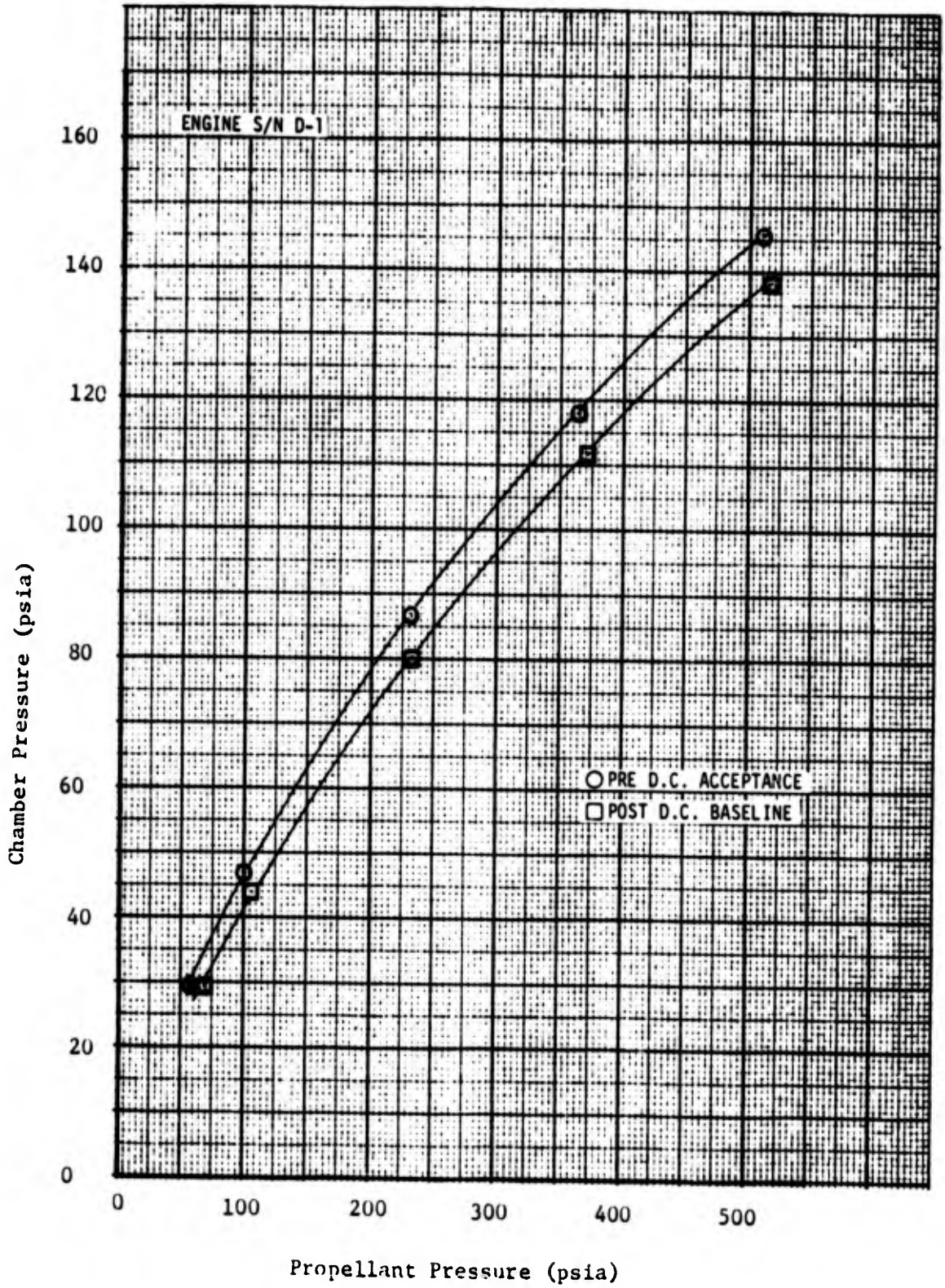

Figure 2-9.

Engine No. 1 - Chamber Pressure vs Inlet Pressure

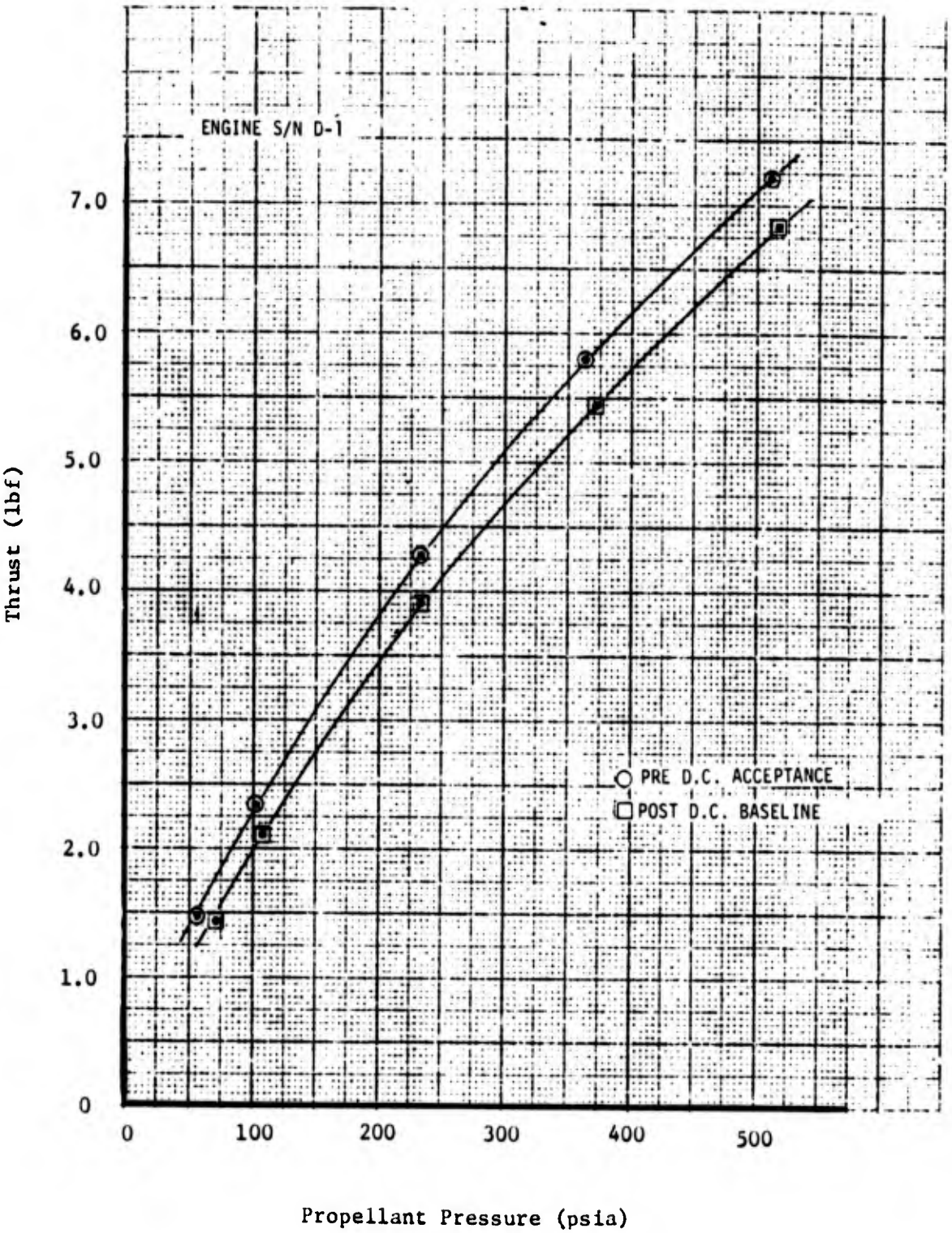

Figure 2-10.

Engine No. 1 - Thrust vs Inlet Pressure

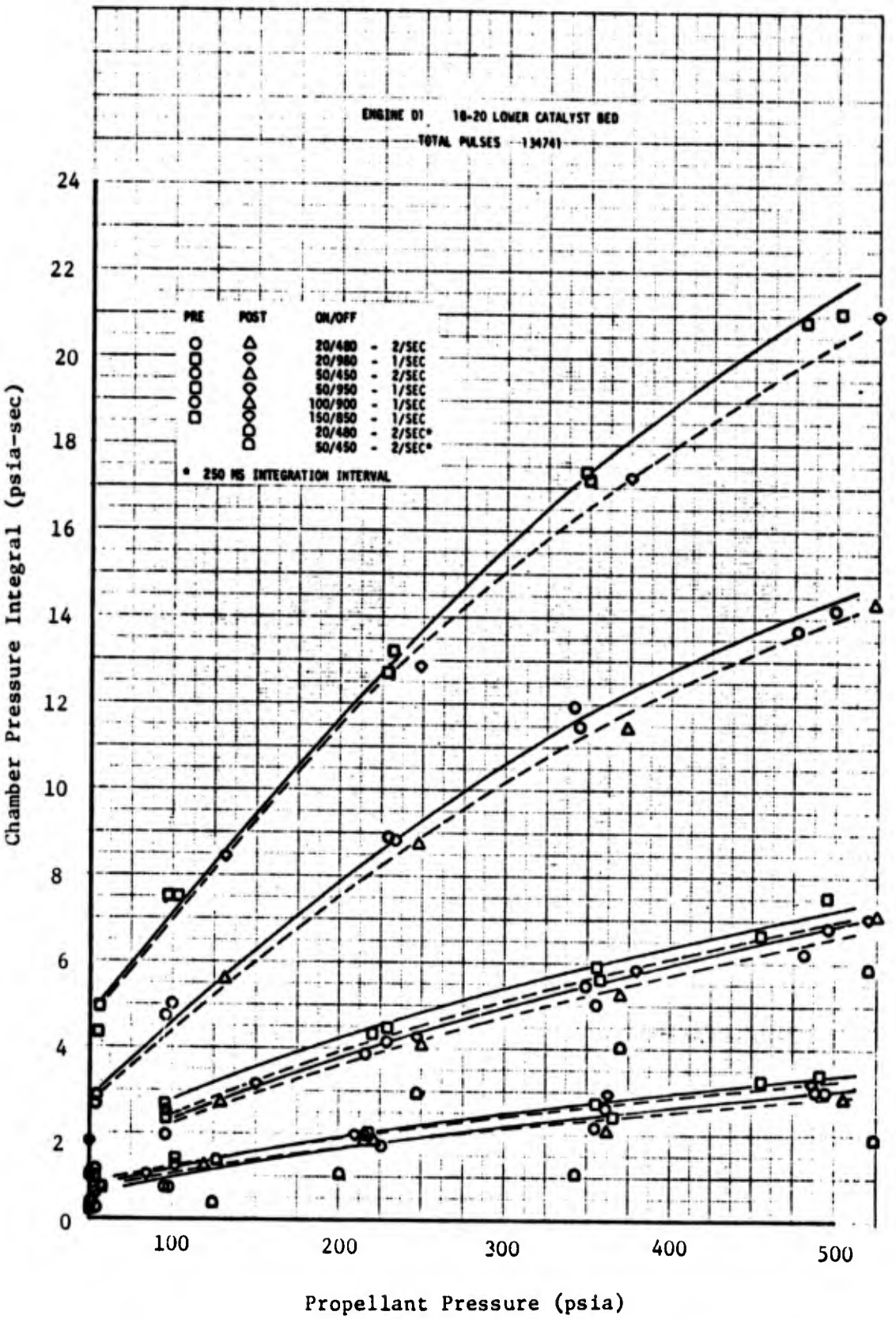

Figure 2-11. Engine No. 1 - Pc Integral vs Inlet Pressure

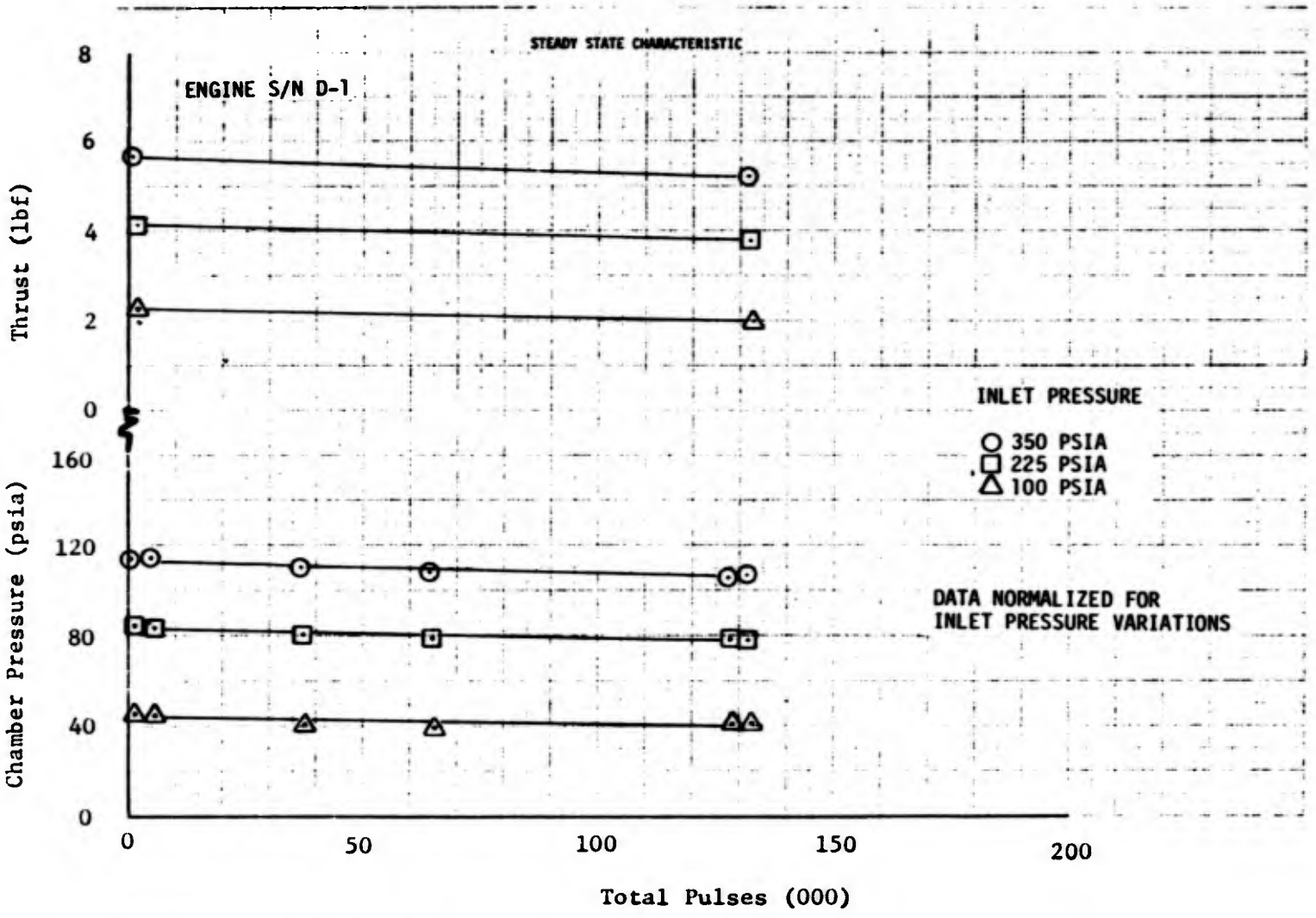

Figure 2-12. Engine No. 1 - Steady State Characteristics vs Life

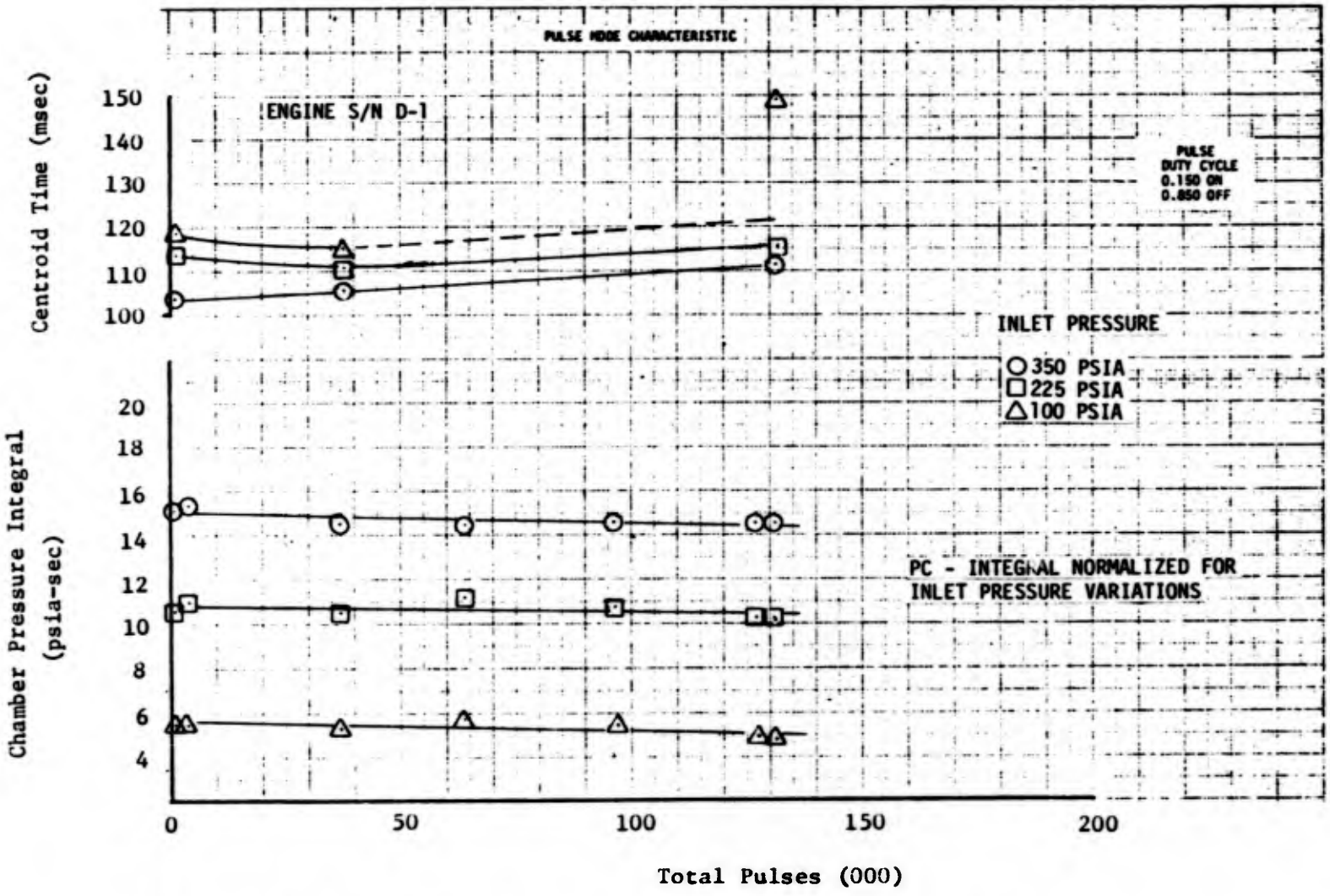

Figure 2-13. Engine No. 1 - Pulse Mode Characteristics vs Life

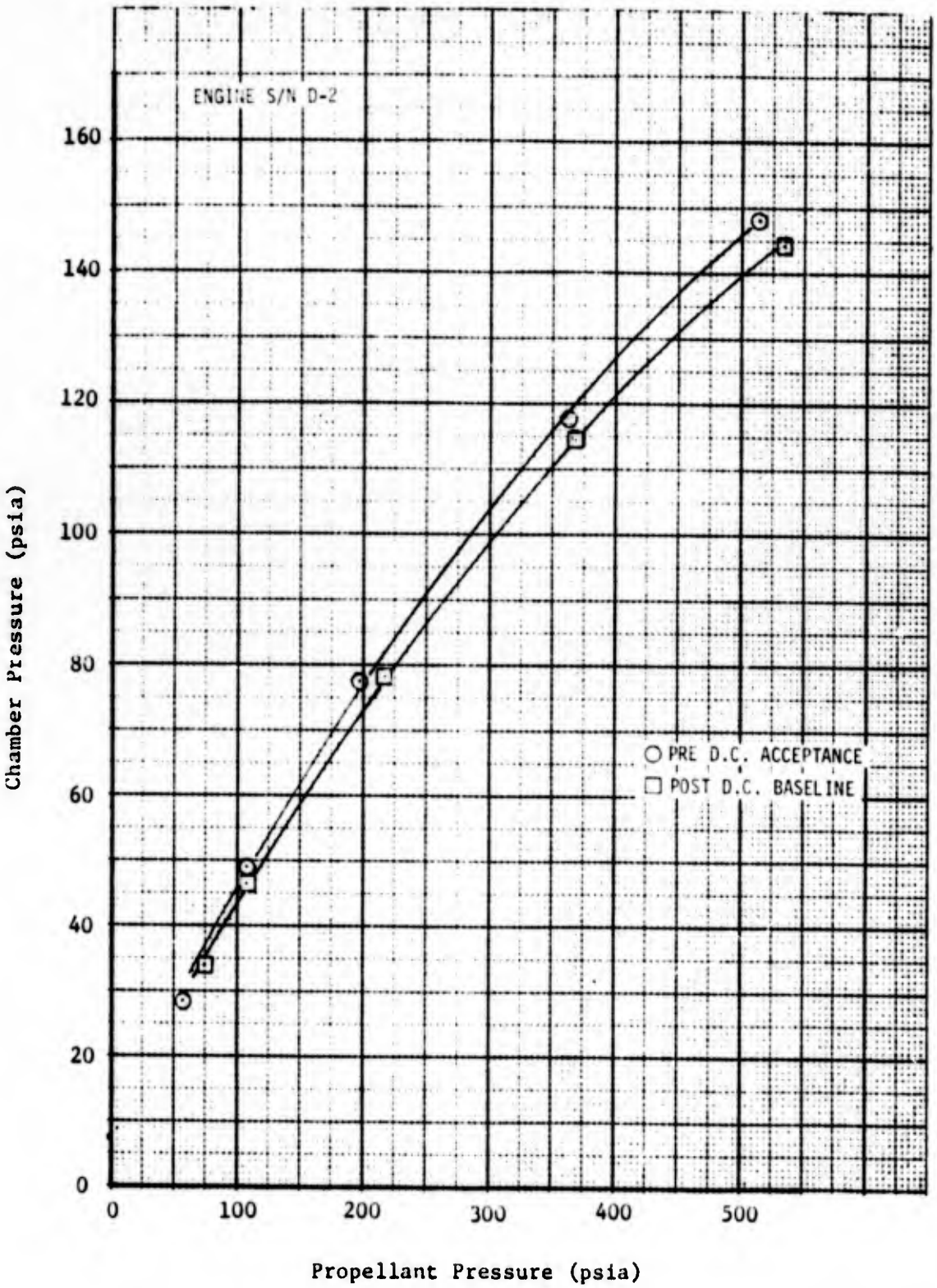

Figure 2-14.

Engine No. 2 - Chamber Pressure vs Inlet Pressure

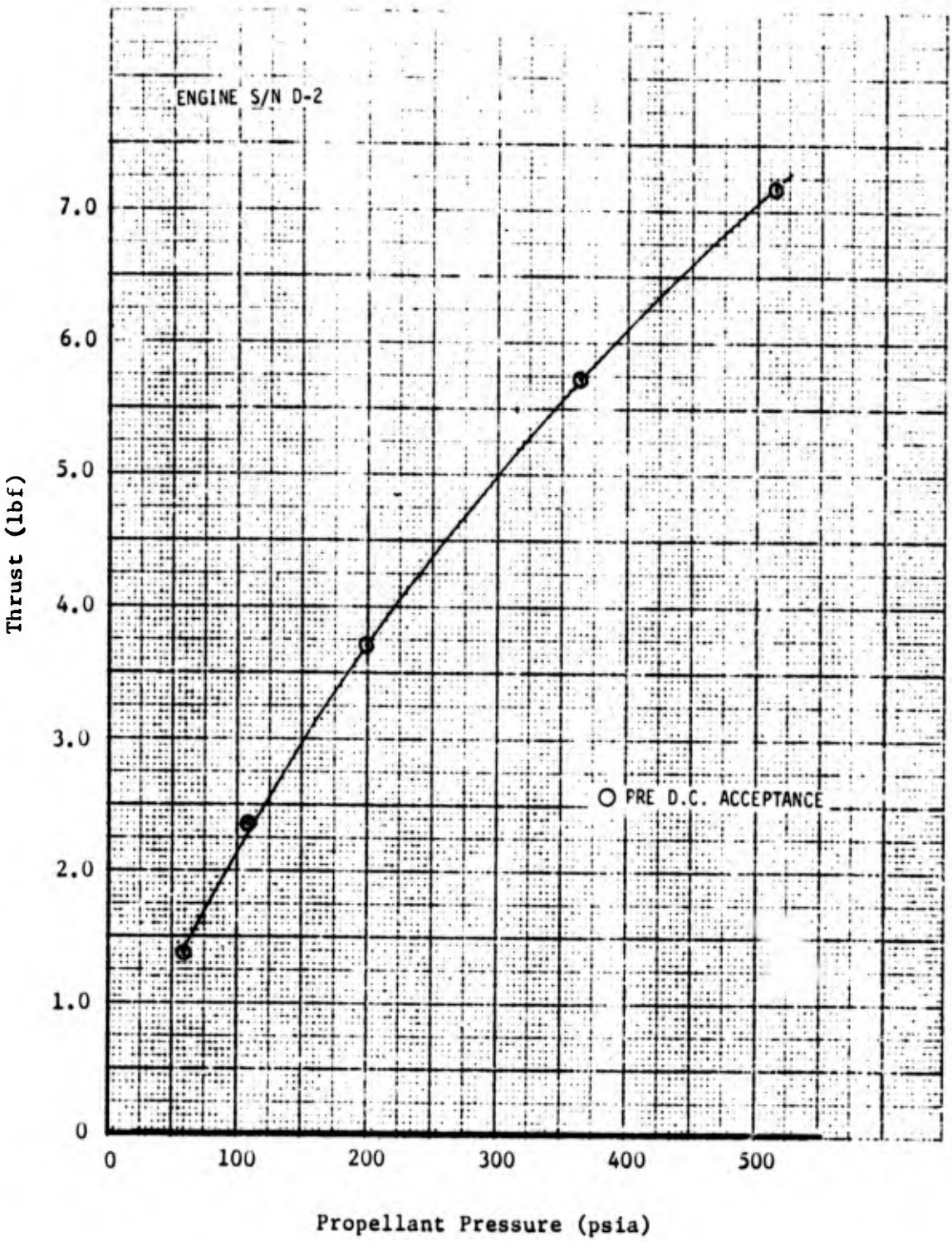

Figure 2-15

Engine No. 2 - Thrust vs Inlet Pressure

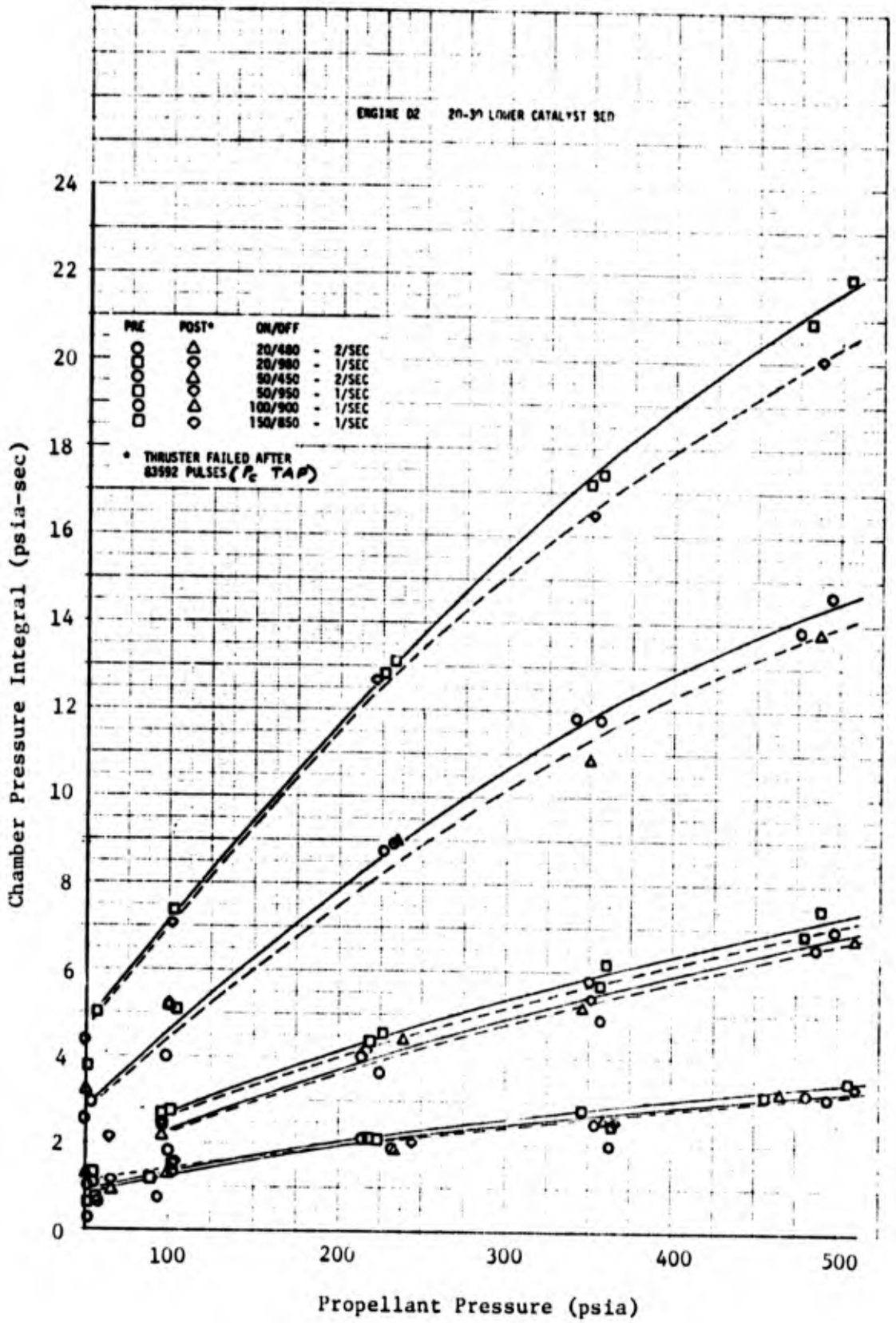

Figure 2-16
Engine No. 2 - Pc Integral vs Inlet Pressure

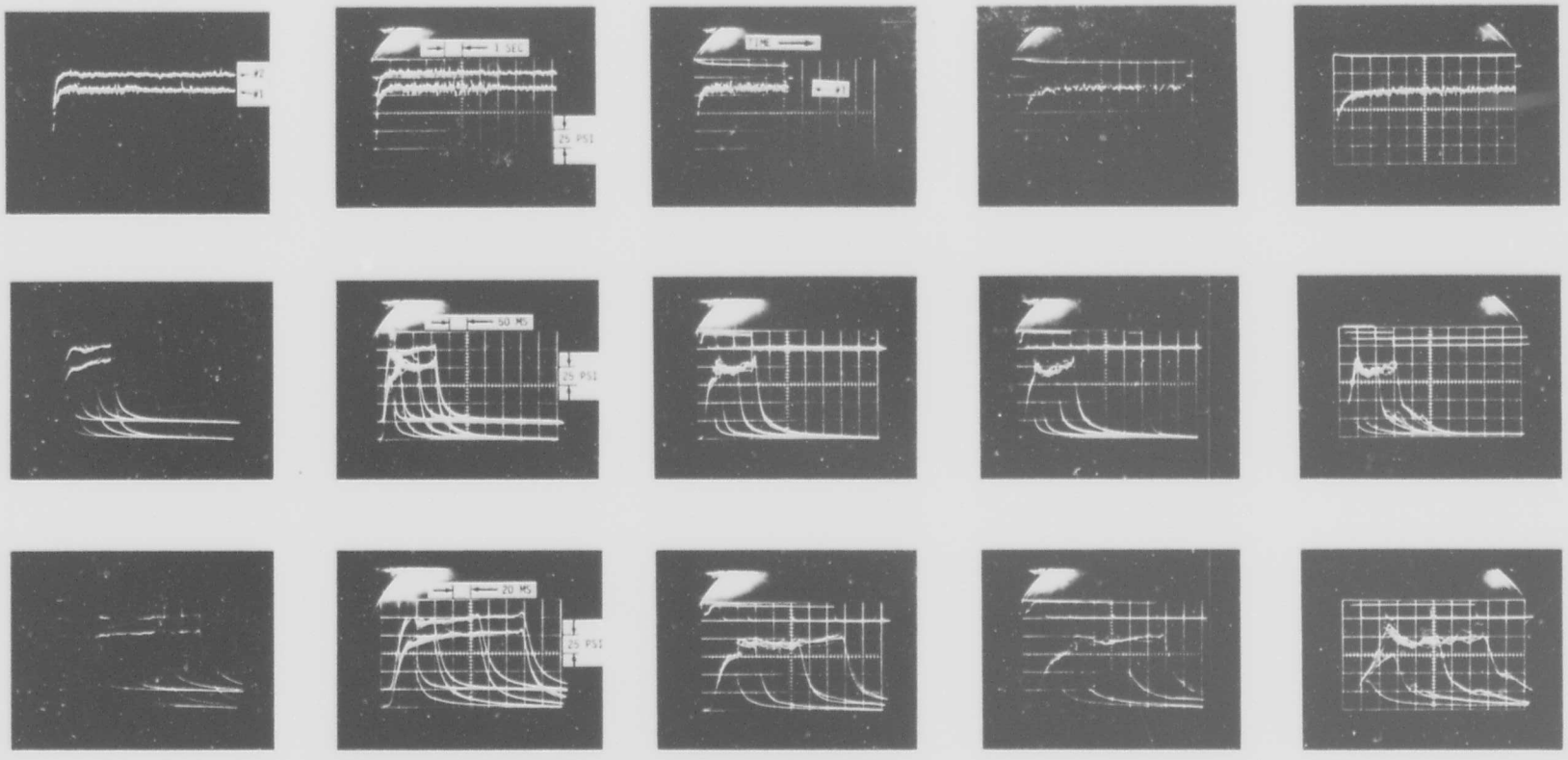

Data shown at 350 psia inlet pressure

Thruster #2 terminated after 83,600 pulses due to failed Pc port.

Tests shown consist of a 10 second steady-state firing (first picture) followed by a single test varying the pulse width (on time) from 0.150 to 0.020 second on (second picture) and then from 0.020 to 0.150 second on (third picture) at a constant pulse rate of one per second. Five pulses at each pulse width are shown in each picture.

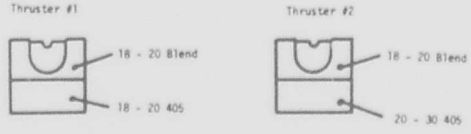

Figure 2-17. Summary of Operating Characteristics - Accelerated Life Test No. 1

0.5 lb_f thruster for high pulse rate (10 cps) operation. Review of the digital data from the acceptance tests of the accelerated life test engines, noting lower impulse from two pulse/second than from one pulse/second operation, led to a re-evaluation of the use of a catalyst blend.

A comparison of the performance of the blended catalyst and all Shell 405 is presented in Figure 2-18 and Table 2-7. Steady state roughness is clearly reduced by the addition of HA-3 (±3% vs ±12%). The impact on pulse performance is less clear, however. As shown in Figure 2-18, the chamber pressure response improves at the higher pulse rate for the all Shell 405 catalyst bed whereas the opposite is true for the catalyst blend. Further investigation into the use of catalyst blends was deemed beyond the scope of this program, and the use of 100% shell 405 catalyst was considered most appropriate. A compromise in steady state roughness was thus accepted and HA-3 catalyst deleted from further testing.

Table 2-7. Catalyst Performance Comparison

P_{inlet} (psia)	Catalyst C 75% Shell 405/25% HA-3			All Shell 405		
	Steady-State	Pulse Mode		Steady-State	Pulse Mode	
	Pc Roughness	Overshoot	Reproducibility*	Pc Roughness	Overshoot	Reproducibility*
350	±2%	13%	2	±6%	13%	1
225	±2%	0	1	±7%	6%	1
100	±4%	0	1	±11%	0	1

*Reproducibility Ratings:

1) Good Reproducibility
2) Minor Variations
3) Erratic pulse-to-pulse variations

2.5.2 Headscreen Deformation Evaluation

Disassembly of the two thrusters used for the first accelerated life test revealed gross deformation of both headscreens as shown in Figure 2-19. Potential causes of this deformation include differential expansion of the catalyst and chamber, and thermal stresses in the headscreen due to localized cooling.

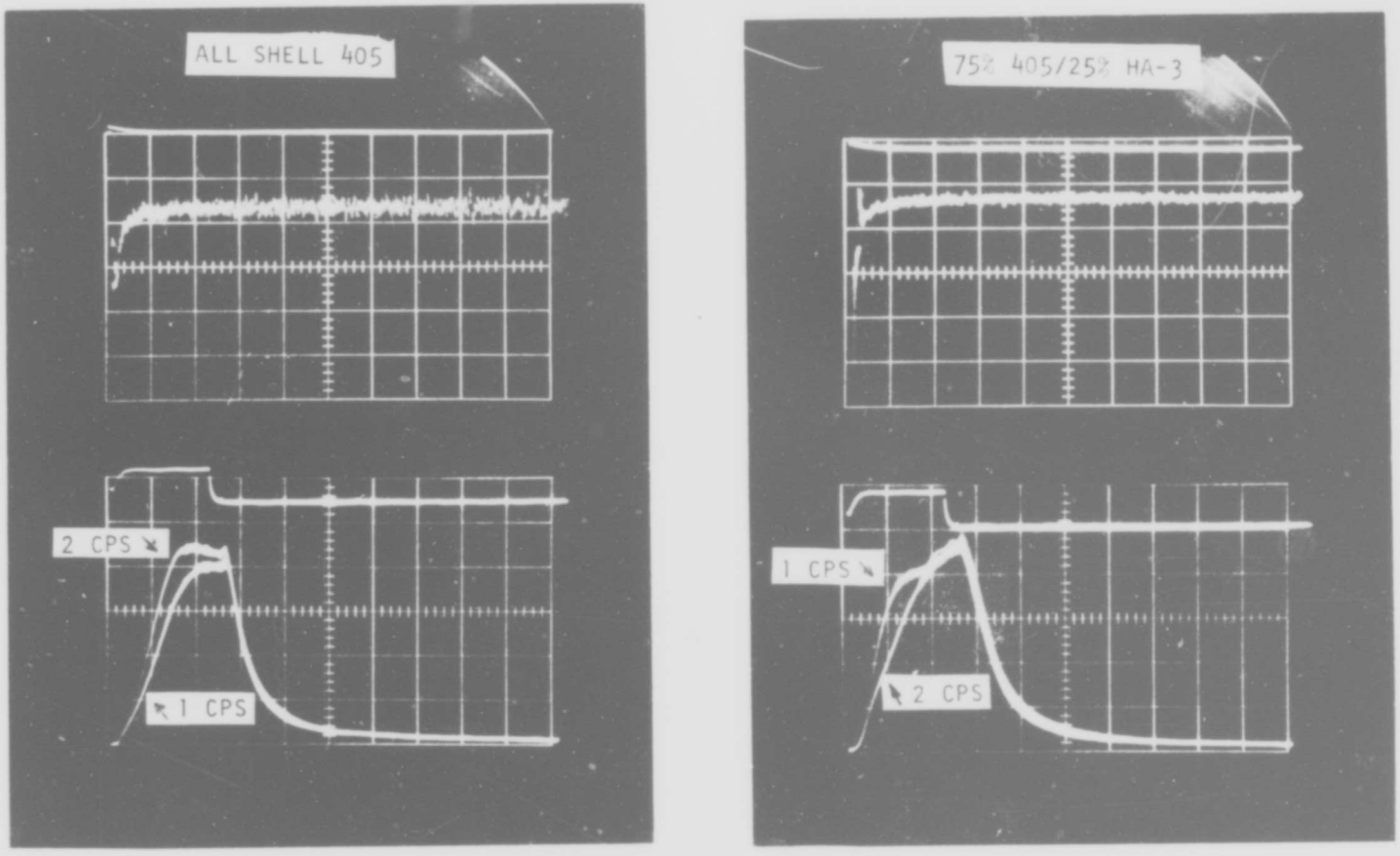

Figure 2-18. Catalyst Composition, Shell 405 vs HA-3 Blend

Both headscreens grossly deformed.

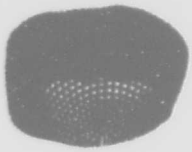

THRUSTER #1
134,740 PULSES

THRUSTER #2
83,600 PULSES

Figure 2-19. Headscreen Condition, Post Life Test No.1

The startup transient, particularly from an ambient start, involves heating of the catalyst and the chamber wall. Heating of the catalyst occurs faster than the chamber wall, as represented in Figure 2-20. The resultant temperature differential causes thermal stresses in the form of a compressive load on the catalyst. The compression load is in part supported (or applied) by the headscreen, which is also likely to heat rapidly due to its small mass. The resultant compression load on the headscreen may cause a slight deformation. As thermal equilibrium is attained, the greater coefficient of thermal expansion of the Haynes 25 chamber compared to the catalyst relieves this compressive load and loosens the catalyst bed. Migration of catalyst is then possible, due to the forces of gravity and/or flow forces, to fill the void generated by the screen deformation. After shutdown, compressive forces again occur via the chamber wall cooling faster and having a greater expansion coefficient than the catalyst. This cycle repeats with every restart from below equilibrium temperature for the given duty cycle. Hot restarts may, in fact, be more severe than cold starts due to reduced strength of the headscreen.

The above discussion readily explains some headscreen deformation. It is difficult to accept that as the total explanation, however, for the gross deformation experienced. Thermal stresses within the screen wire resulting from localized cooling by incoming propellant could, however, add to the above forces and result in the gross deformation experienced.

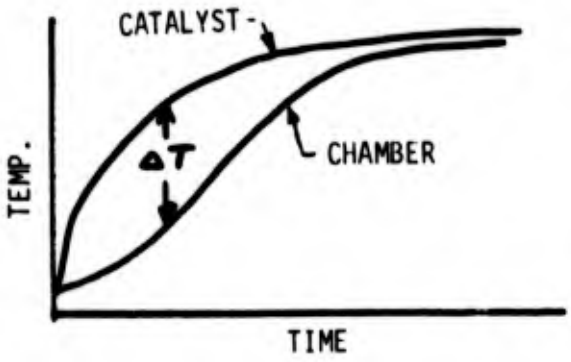

Figure 2-20. Startup Temperature Transient

Tests were conducted to aid in the understanding of the problem and investigate alternate solutions. One proposed solution was a compartmentalized catalyst bed which would limit catalyst migration. A cylindrical screen was added to the headscreen, slightly smaller in diameter than the headscreen and extending to the catalyst separator screen. This would prevent catalyst migration from the periphery of the headscreen to the area of the deformation. This and a control engine (identical to one of the accelerated life test engine) were tested simultaneously to 20 thermal cycles from ambient temperature to over 1500°F (chamber wall temperature). This was accomplished by firing for 5 seconds steady state, then force cooling back to ambient temperature. Neither headscreen exhibited noticeable deformation.

Two more engines were then built up and subjected to 30,000 pulses. This test was very similar to the first accelerated life test, mostly at 4 pulses/second and stepping through the four pulse durations (0.020, 0.050, 0.100, and 0.150) every 1000 pulses. In addition, the engines were force cooled to below 150°F every 1000 pulses. After this test, the control engine showed moderate deformation of the headscreen. The headscreen with the added cylindrical screen also showed deformation but much less than the control engine. Relating the deformation in the control engine to the orientation to gravity during firing (the engines were fired horizontally) showed greater deformation on the bottom side, indicating some effect of catalyst migration. Deformation of the other screen, however, was more indicative of thermal stresses. The conclusion drawn from these results

was that the catalyst expansion, related to heating faster than the chamber shell, contributes to headscreen deformation but is not the sole cause. Thermal stresses resulting from portions of the headscreen being cooled by the propellant on hot restarts may be the most important contributor.

Two approaches were then pursued to support the headscreen and/or reduce the thermal stresses. A headscreen retainer was designed and fabricated, as were alternate injectors. Figure 2-21 summarizes these configurations.

The headscreen retainer consists of six (6) equally spaced webs to support the screen. It appeared that the impact of this addition on thruster performance would be minimized by rotating the inner set of injector orifices, allowing maximum clearance for the webs between orifices (Injector E of Figure 2-21 as compared to the baseline of Injector D). Another injector (Injector F) was fabricated with an added orifice, in line with the thruster axis, to improve distribution of the propellant over the headscreen. Additional headscreens were fabricated using 30X30 mesh, 0.010 wire diameter screen as compared to 40X40 mesh, 0.009 wire diameter. This offers some increase in wire strength and an increase in porosity.

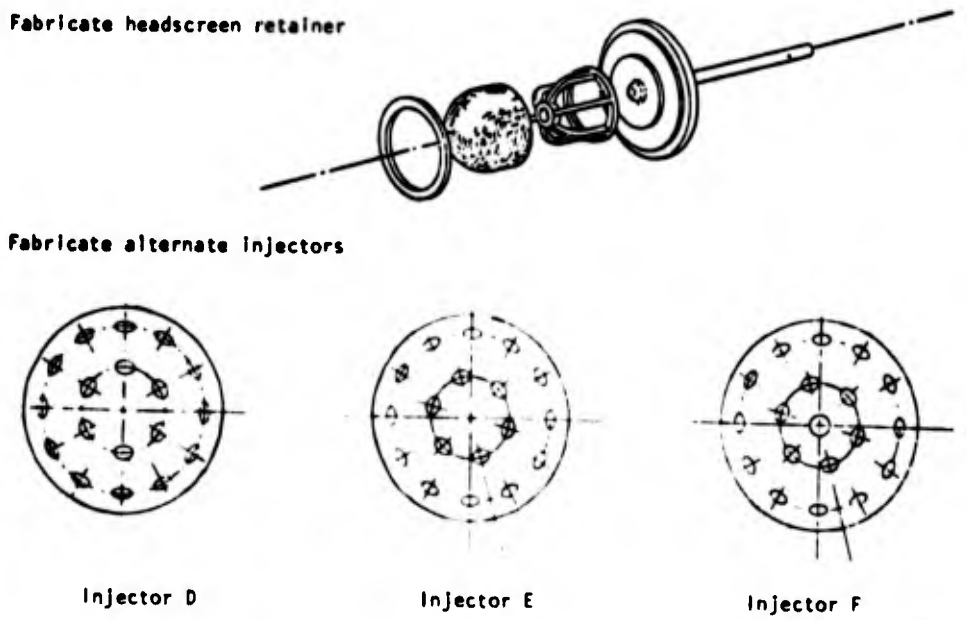

Figure 2-21. Headscreen Evaluation Tests

An accelerated life test as presented in Table 2-8 was conducted using Injector D with a 40 mesh headscreen and without the retainer (control engine) and Injector F with a 40 mesh headscreen and without the retainer. Following 80,000 pulses, both headscreens showed moderate deformation. Injector F caused greater deformation, however, and was eliminated from further testing.

A series of iteration tests was then conducted to evaluate performance effects of 30 versus 40 mesh headscreens and of the headscreen retainer. These tests are summarized in Table 2-9.

Table 2-8. Duty Cycle - Accelerated Life Test

Sequence	Duty Cycle	Propellant Feed Pressure(s) (psia)
1	Pulse Sweep	350, 225, 100, 500, and 50
2	100 sec SS	350, 225, 100, 500, and 50
3	Duty Cycle C, 8 times	350
4	100 sec SS	350, 225, 100, 500, and 50
5	Pulse Sweep	350, 225, 100, 500, and 50

Duty Cycle C

Sequence	On-Time (m sec)	Off-Time (m sec)	Number of Pulses*
a	20	230	2400
b	50	200	2400
c	100	150	2400
d	150	100	2400

* Approximate Number, change On-Time every 10 minutes.

Table 2-9. Iteration Tests

Injector D1,*	40 mesh headscreen with retainer
Injector E	40 mesh headscreen without retainer
Injector E	40 mesh headscreen with retainer
Injector D1	30 mesh headscreen without retainer
Injector D1	30 mesh headscreen with retainer
Injector E	30 mesh headscreen without retainer
Injector D2	30 mesh headscreen without retainer
Injector E	30 mesh headscreen with retainer
Injector D2	30 mesh headscreen with retainer
Injector D1	30 mesh headscreen without retainer

*Injector designations D1 and D2 represent the first and second of two identical injectors fabricated for the accelerated life test. The complete designation is included only as a record of the exact hardware tested.

Injector D and a 30 mesh headscreen were selected for use with the headscreen retainer. The close proximity of the propellant streams to the headscreen support webs evidently helps to prevent propellant accumulation. Another accelerated life test was then conducted with this configuration and an identical engine except for the headscreen retainer (D1 30 mesh without and D2 30 mesh with). Both engines looked very good after 80,000 pulses. The screen supported by the retainer deformed slightly over the retainer, assuming somewhat a hexagonal shape following the support webs. The unsupported screen deformed less than 40 mesh screens but in the same fashion, indicating that changing to 30 mesh screen is an improvement but gross deformation would ultimately occur.

A final accelerated life test was then conducted in which Duty Cycle C (Table 2-8) was repeated 29 times accumulating 280,000 pulses. The configurations tested were the same as the previous test (Injector D, 30 mesh screen, and with and without the headscreen retainer) to obtain another data point for a longer exposure. Results of this test were similar to the previous test, with even less deformation of the supported screen. Figure 2-22 shows the port test condition of the (6) headscreen subjected to accelerated life testing, and Figure 2-33 summarizes the engine characteristics over the final life test.

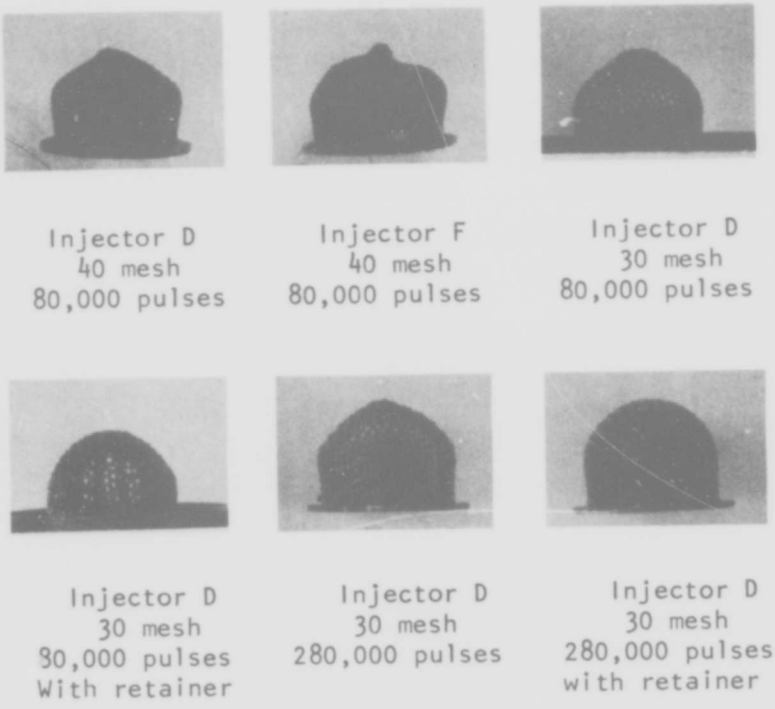

Figure 2-22. Headscreen Evaluation Test Results

None of the accelerated tests reproduced the gross deformation experienced from the first life test. The gross deformation is evidently the synergistic effect of several factors which are not clearly understood. Changing to the 30 mesh screen and adding the headscreen retainer grossly in increase the strength of the assembly, however, and no visual signs of damage to the retainer appeared. A single retainer was used for two tests, accumulating 360,000 pulses, adding to the confidence that it would survive the life goal.

HEADSCREEN DEFORMATION TEST DATA

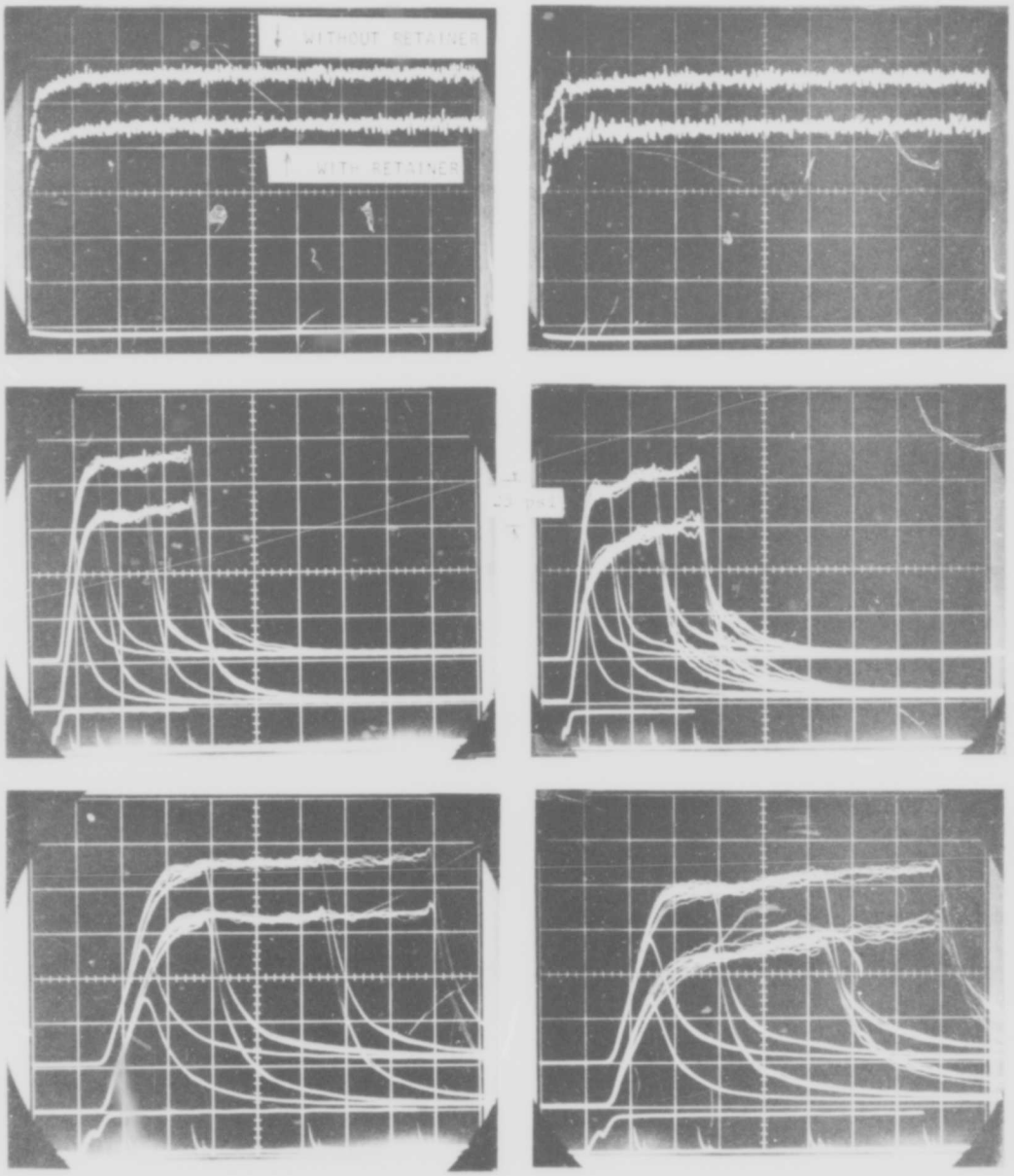

Figure 2-23. Headscreen Deformation Test Data

3. ENGINE DESIGN AND FABRICATION

An iterative process was involved in arriving at the RCHE* design. Several concepts were reviewed in arriving at a base point from which to establish the final design. Some of these concepts, together with appropriate comments, are shown in Figure 3-1.

Based on the specified requirement of a 200°F catalyst bed and assuming a typical spacecraft environment in earth orbital missions, a heat source of about three (3) watts was assumed. Later thermal analyses proved this to be a reasonable assumption. The baseline design and the evolution into test hardware are discussed in the following sections.

3.1 BASELINE DESIGN

Selection of the baseline design was largely influenced by program scope implications of a "new" heat source design. The design presented in Figure 3-2 utilizes Radioisotope Heater Units (RHU's) of the type flown on the Pioneer 10 and 11 Spacecraft, requiring a minimum nuclear safety effort to test and later to launch such an engine.

A casting was considered to provide the housing for three RHU's in close proximity to the catalyst bed. The chamber assembly bolts to the mount with thermal standoffs. Ceramic washers are shown as the standoffs, but thin walled titanium soon replaced the more brittle ceramic as the baseline. A Parker propellant valve, developed and qualified for use on the P-95 program, also bolts to the mount.

Analyses of this design, as discussed in the following section, demonstrated the feasibility of attaining the 200°F goal using Pioneer type RHU's.

3.2 THERMAL ANALYSES

A preliminary thermal model of the engine was constructed to determine the severity of the temperature requirements and examine the effect of varying model parameters such as standoff and feed tube geometry, insulation thickness, and component emissivities (Figure 3-3). The model has 24 nodes and is coded to be run on a timeshared version of the TRW Thermal Analyzer Program (TAP). The relation of model nodes and resistances to the physical

*Radioisotope Catalytic Heated Engine.

	CONFIGURATION	WEIGHT, LB_M	ADVANTAGES	DISADVANTAGES
1	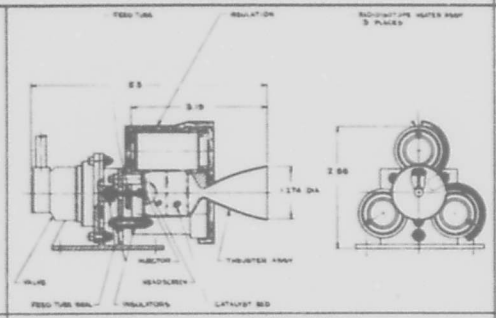	THRUSTER SHELL .61 INSULATION .20 BRACKET .36 HEATER .33 VALVE .40 MISC. .20 2.10	◦ CONVENTIONAL THRUST CHAMBER DESIGN ◦ EXISTING RHU DESIGN ◦ REMOVABLE RHU'S WITH MAXIMUM FLEXIBILITY ◦ LEAST EXPENSIVE TO DEVELOP	◦ HEAVIEST
2	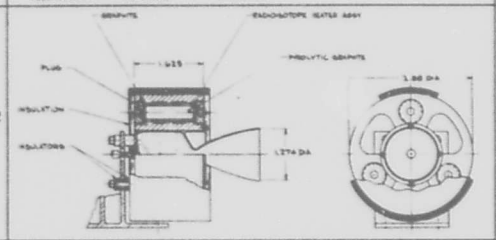	THRUSTER SHELL .33 INSULATION .20 BRACKET .24 HEATER .51 VALVE .40 MISC. .20 1.88	◦ WEIGHT IMPROVEMENT ◦ REMOVABLE HEAT SOURCE ◦ CONVENTIONAL THRUST CHAMBER DESIGN	◦ SPECIALIZED RHU RE-ENTRY BODY
3	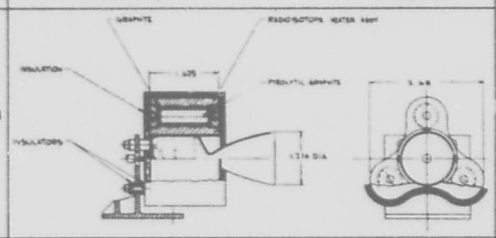	THRUSTER SHELL .33 INSULATION .20 BRACKET .24 HEATER .38 VALVE .40 MISC. .20 1.75	◦ WEIGHT IMPROVEMENT ◦ REMOVABLE HEAT SOURCE ◦ CONVENTIONAL THRUST CHAMBER DESIGN	◦ SPECIALIZED RHU RE-ENTRY BODY
4	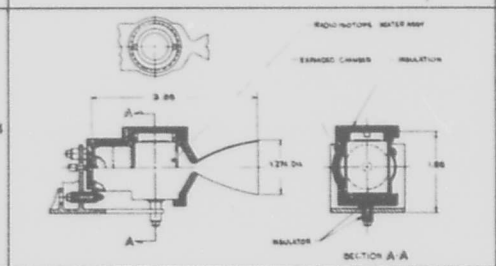	THRUSTER SHELL .46 INSULATION .09 BRACKET .20 HEATER .17 VALVE .40 MISC. .20 1.52	◦ MINIMUM WEIGHT ◦ EXISTING RHU DESIGN CONCEPT ◦ SMALLER DIAMETER	◦ IMPACTS THRUST CHAMBER DESIGN ◦ MORE COMPLICATED MOUNTING ◦ LONGER
5	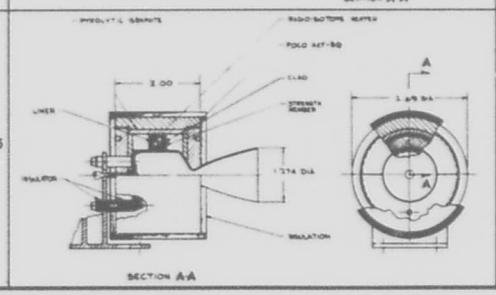	THRUSTER SHELL .32 INSULATION .12 BRACKET .24 HEATER .85 VALVE .40 MISC. .20 2.13	◦ BETTER POSITIONING OF HEAT SOURCE ◦ CONVENTIONAL THRUST CHAMBER DESIGN	◦ SPECIALIZED CAPSULE AND RE-ENTRY BODY ◦ MOST DIFFICULT RHU DEVELOPMENT

Figure 3-1. Comparison of Design Approaches

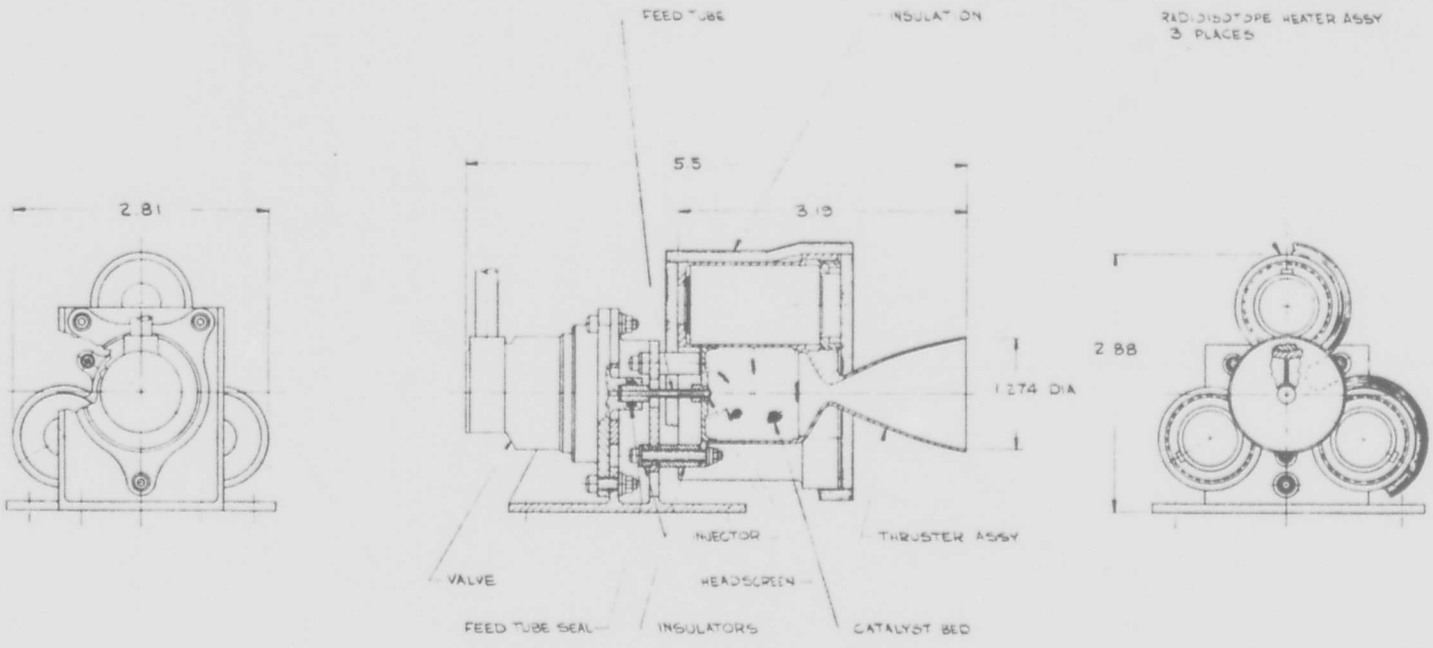

Figure 3-2. RCHE Baseline Design

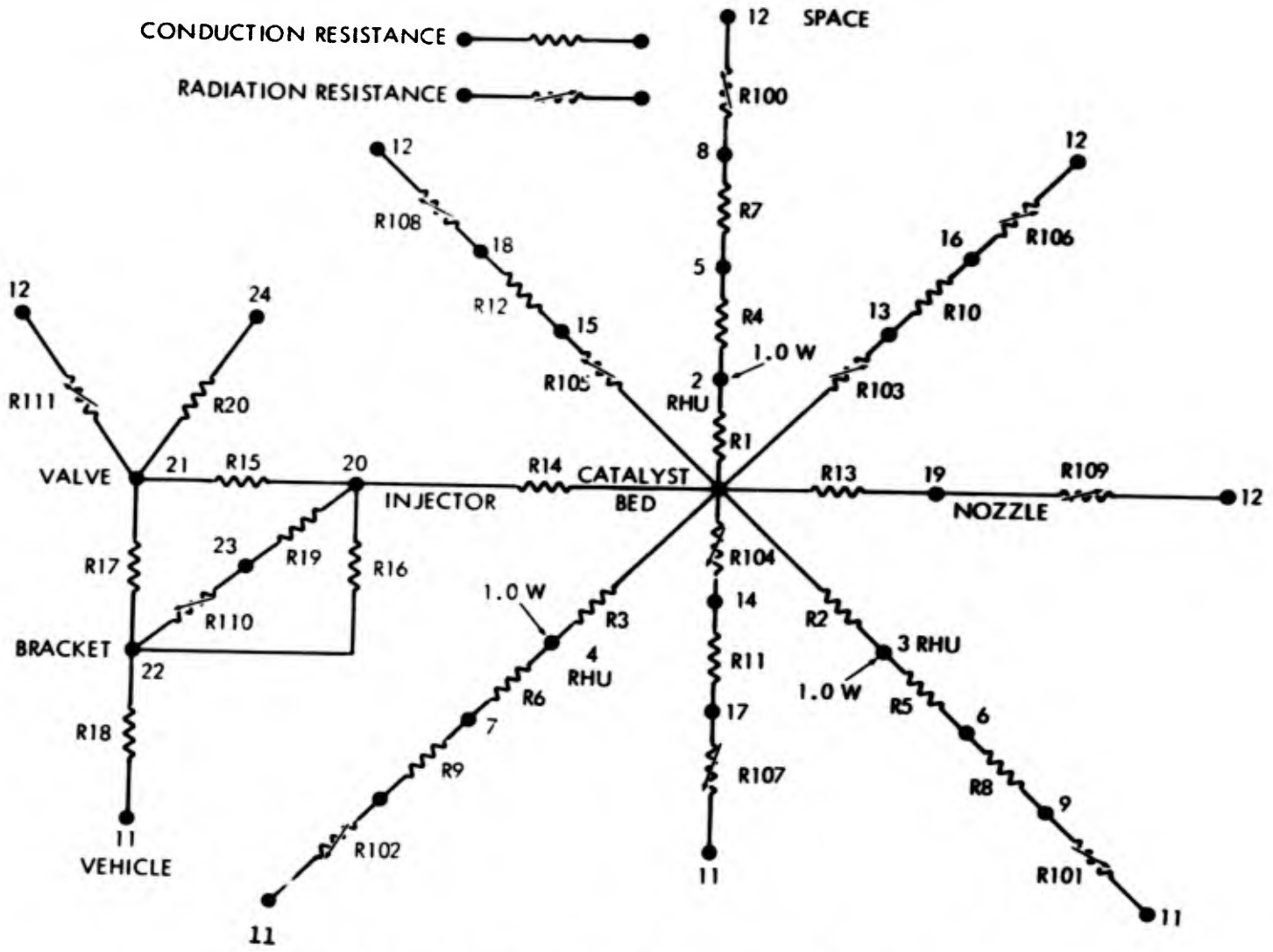

Figure 3-3. Preliminary RCHE Thermal Model

engine is indicated in Figure 3-4. The assumptions of the model are:

- Thruster housing and feed tube are L-605. Propellant valve case is 300 series stainless steel. Mount bracket and threaded fasteners are 6Al-4V titanium alloy.

- Thruster is attached to bracket with three 6Al-4V titanium alloy cylindrical standoffs, each 0.250 OD by 0.005 wall by 0.707 long or equivalent.

- Propellant valve is connected to thruster with 0.090 OD by 0.010 wall by 0.47 long L-605 tube or equivalent.

- Perfect thermal contact exists between all attached parts, except valve to bracket and bracket to vehicle resistances, which are arbitrarily set at one-tenth the net standoff resistance.

- The exterior surface of the uninsulated nozzle radiates to space with an emissivity of 0.18. The interior of the nozzle radiates to space with an emissivity of 0.43.

- In advance of detailed shape factor calculations, the upper three radial direction branches are assumed to radiate entirely to space at absolute zero, while the lower three radial branches radiate entirely to vehicle sink temperature.

- The multi-layer insulation covers a total radiant housing area of 25.3 square inches. The insulation is a 0.13-inch thick blanket of separated nickel 200 foils with an equivalent thermal conductivity of 0.17 Btu/hr-ft°F. The emissivity of nickel foil is 0.10.

Briefly, the six principal radial directions from the catalyst bed (node 1) are represented by six branches in the model ending in radiation to space (node 12) or to the vehicle (node 11). A seventh branch transmits heat loss from the nozzle (node 19) to space, while the final branch represents the forward conduction path from thruster to valve and bracket. The cooling effect of propellant flow on the valve is modeled by attaching it to a node maintained at an assumed propellant temperature of 40°F (node 24) through a resistance representing the convective hydrazine cooling inside the valve. In pulse mode simulation, this convective resistance (R_{20}) has a low value during on-time and a very high value during off-time. A 0.13-inch thick blanket of multi-layer nickel foil insulation with an equivalent thermal conductivity of 0.17 Btu/hr-ft-°F was assumed to cover the catalyst bed-RHU housing. This conductivity can be obtained by either interweaving the nickel foil layers with layers of quartz fabric or by dimping the foil

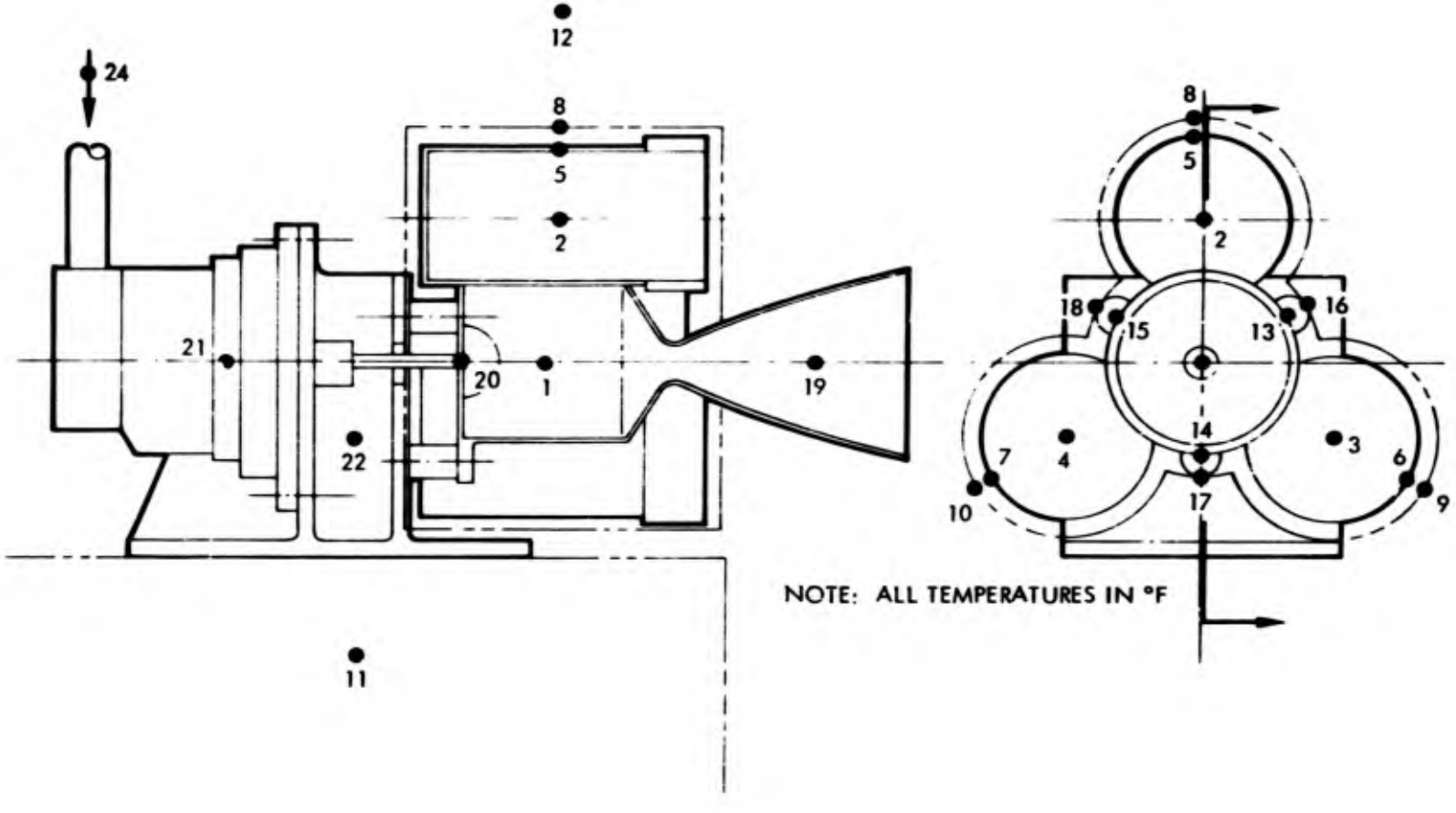

Figure 3-4. Location of Thermal Model Nodes

layers so as to maintain their separation. Either separation method is adequate from a thermal standpoint, and the final selection of insulation type would be made on the basis of fabrication cost, weight, and envelope.

Several runs of the preliminary thermal model were made using resistances consistent with current flight designs to determine temperatures of baseline configuration engine components in worst case cold soaks and worst case thruster firing modes. Figure 3-5 illustrates steady-state temperatures during space vacuum cold soak.

The model node representing the vehicle is maintained at 40°F during cold soak. As the catalyst bed temperature of 382°F exceeds the 200°F minimum temperature by over 100 degrees, some tradeoffs can be made to ease thermal standoff, feedtube length, or RHU power requirements while still maintaining a margin over the 200°F minimum catalyst bed temperature.

A preliminary search for the worst case thruster firing duty cycle was conducted by first running the model for the steady-state temperature distribution with the catalyst bed held at an assumed hydrazine decomposition temperature of 1800°F and a nozzle temperature of 1200°F. Figure 3-6 illustrates the resultant temperature distribution. The 40°F flowing propellant maintains the valve node at 48°F during steady state firing. Next, a transient soakback run was made using the temperature of Figure 3-6 as an initial condition, but with the propellant flow shut off. Heat soakback from the thruster to the propellant valve is shown in Figure 3-7. A peak valve temperature of 184°F was reached 3400 seconds after shutdown from steady-state operation (this is consistent with the analysis and test results for the Pioneer F/G TCA in which the peak valve temperature occurs 3600 to 3800 seconds after shutdown). Temperature distribution at this time slice are presented in Figure 3-8.

A 5 percent pulsing duty cycle (0.05 second ON/0.95 second OFF) initiated at the time of peak valve temperature was also evaluated and the results are shown in Figure 3-9. The valve temperature decreases in this case as the cooling from the propellant flow exceeds the increased heat input from the reactor.

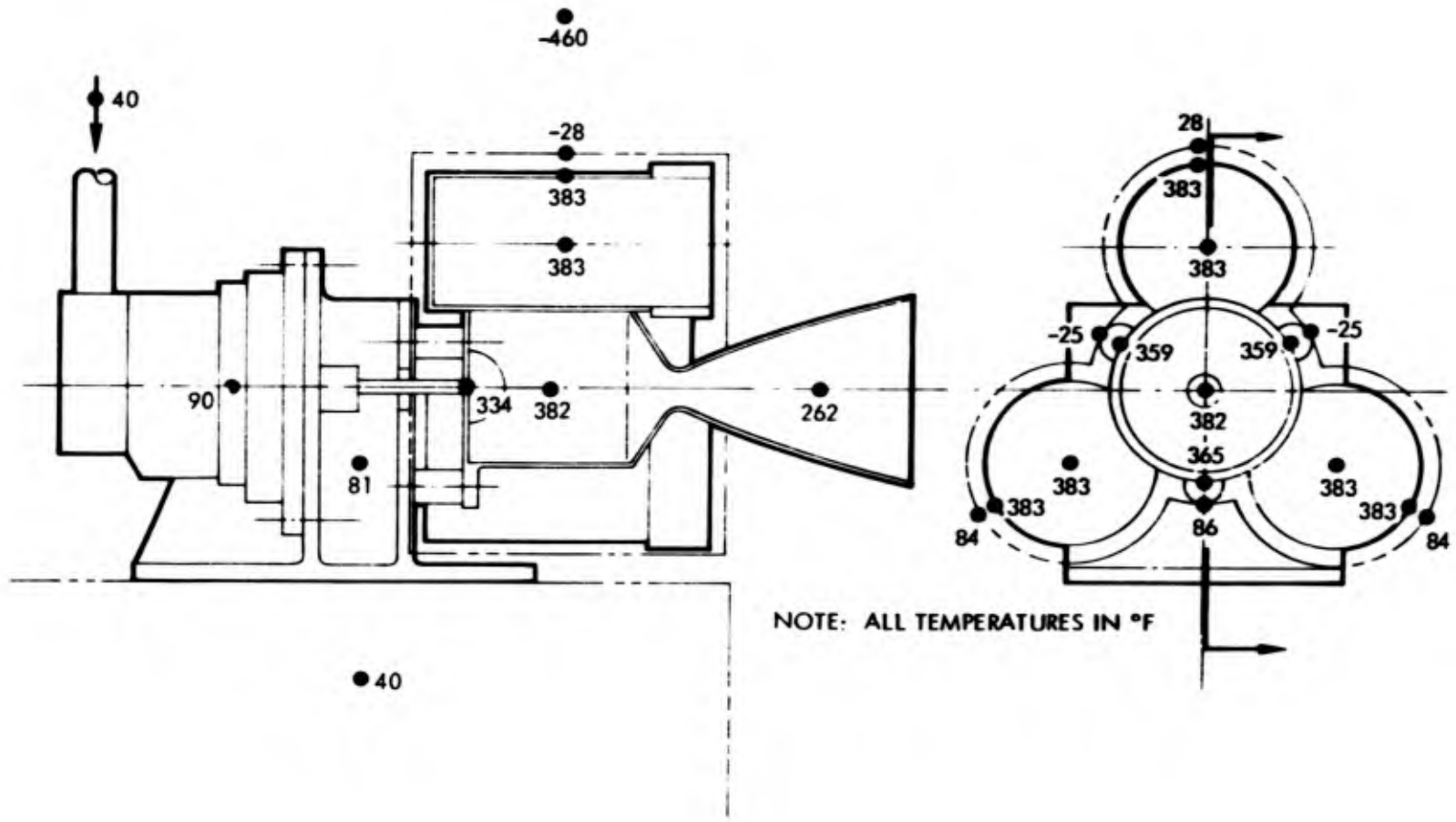

Figure 3-5. Space Vacuum Cold Soak Temperature

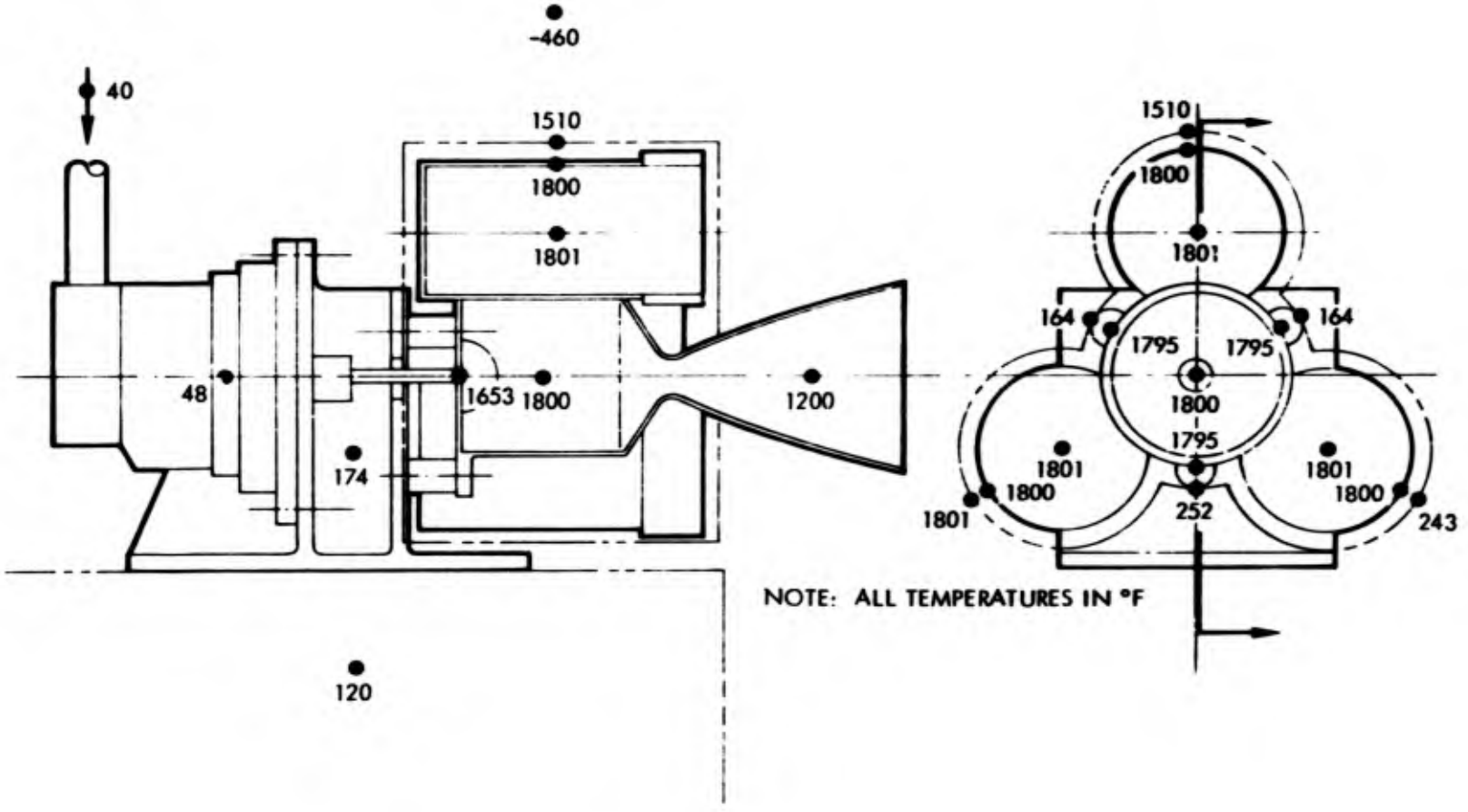

Figure 3-6. Steady-State Temperatures During Thruster Firing

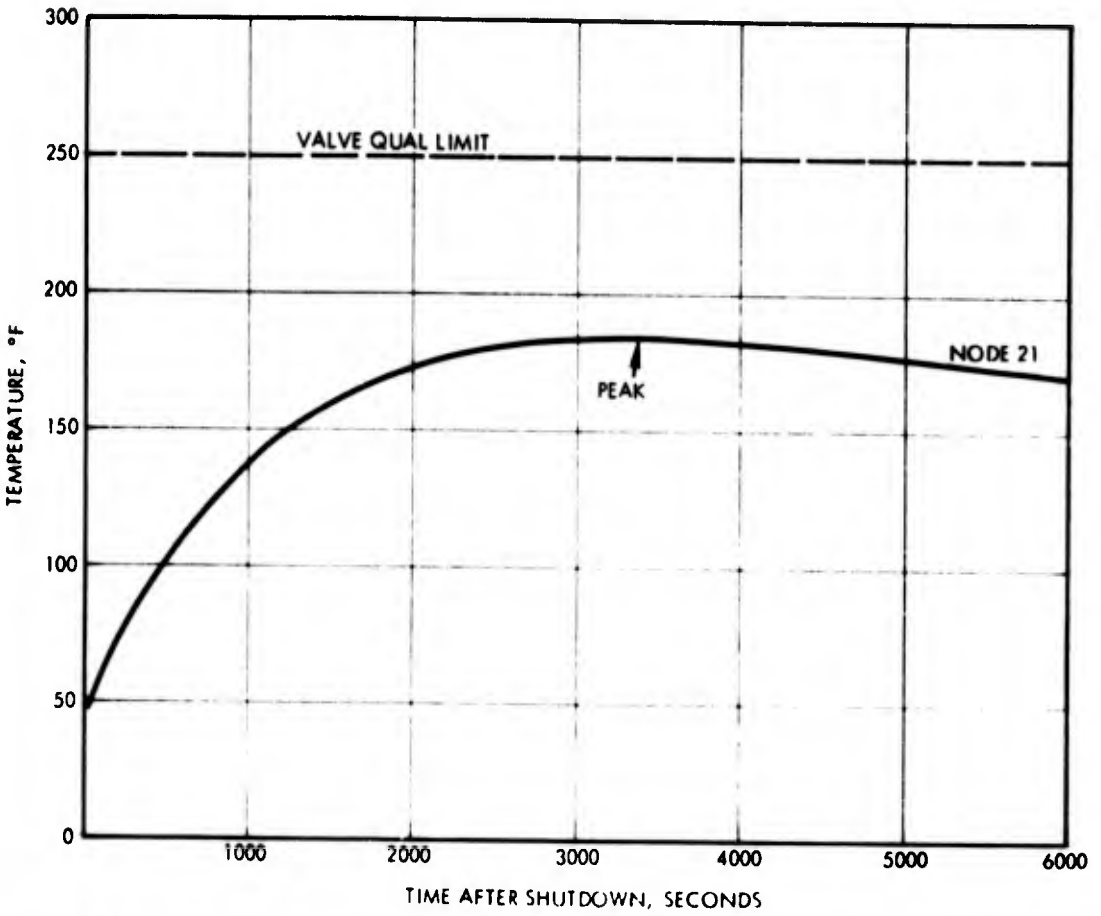

Figure 3-7. Propellant Valve Temperature After Shutdown from Steady-State Thruster Firing

3.3 SELECTED DESIGN

The final design of the RCHE, less thermal insulation, is presented in Figure 3-10, and a photograph of the engine is shown in Figure 3-11. A machined casting is utilized to provide three RHU ports intimately attached to the catalyst bed. The catalyst retainer plate and screens are inserted through the head end and resistance-welded in place as part of the catalyst loading operation. The furnace-brazed injector assembly, including the injector, headscreen, and headscreen support, is then EB welded as the final closure.

Thin-walled titanium standoffs attach the chamber assembly to the mount, providing high thermal isolation. The valve bolts to the mount using spacers to provide clearance from the standoffs. An O-ring seal is provided at the valve/injector feed tube interface, allowing for the thermal expansion of the feed tube. Location of the end of the feed tube within

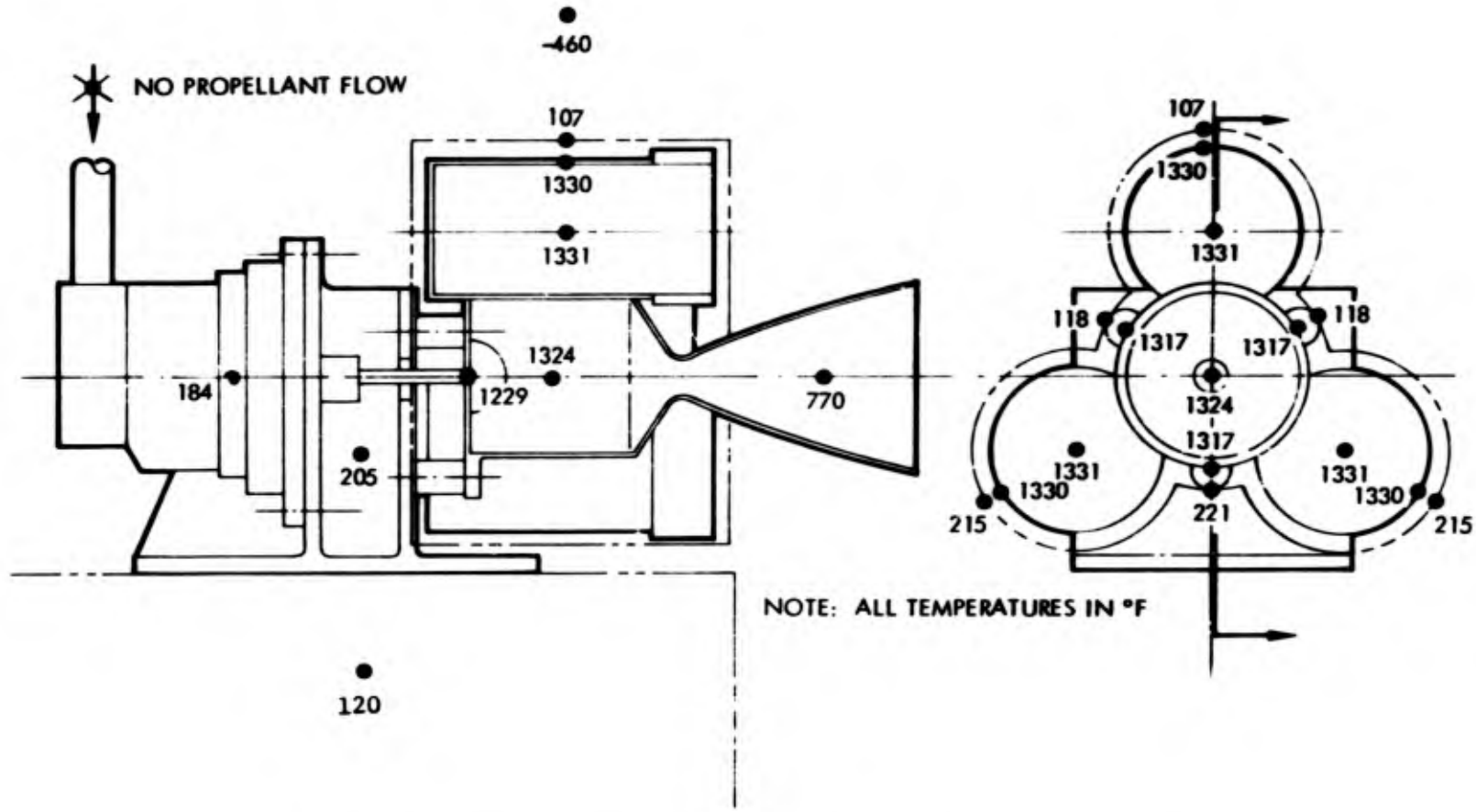

Figure 3-8. Engine Temperature at 3400 Seconds after Shutdown from Steady-State Thruster Firing

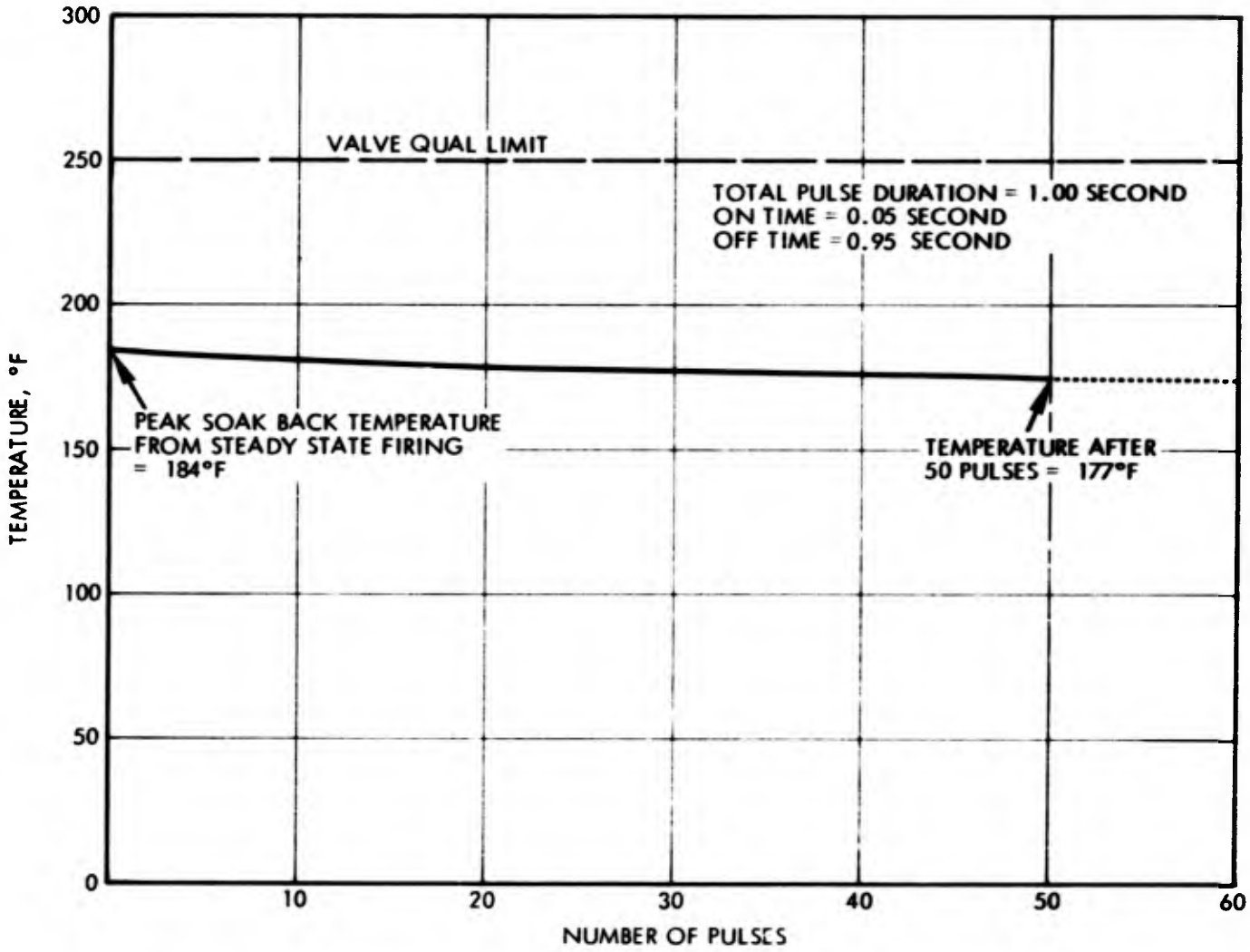

Figure 3-9. Propellant Valve Temperature with Typical Engine Pulsing at Peak Soakback Temperature

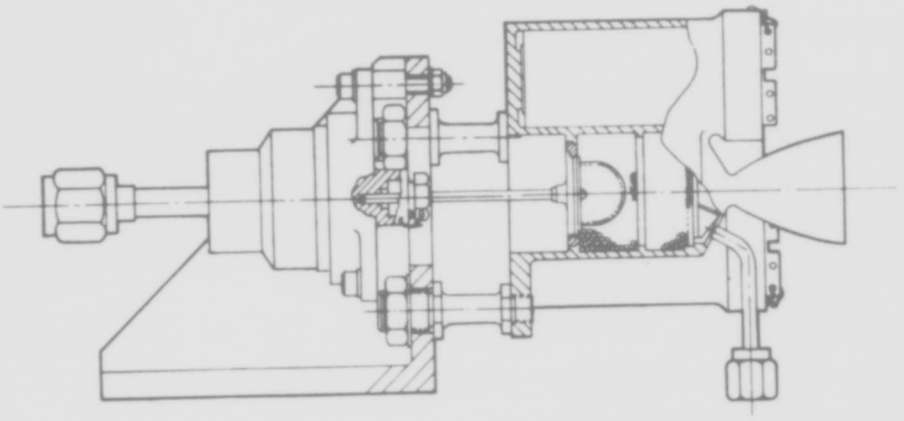

Figure 3-10. RCHE Design

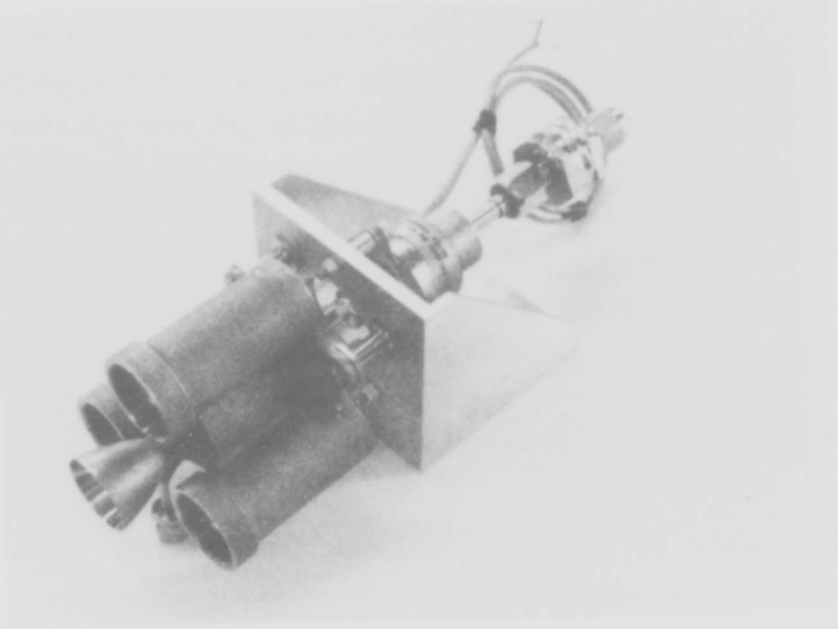

105440-73

Figure 3-11. RCHE

the valve outlet is established by measurements during engine assembly and cutting the valve spacers to the appropriate length. This minimizes the dribble volume while preventing an interference fit.

Adjustment of the liquid pressure drop (thus the thrust versus propellant inlet pressure) is accomplished with an orifice at the valve inlet. The orifice consists of a drilled hole in a blank VOI-SHAN soft seal. For test purposes, a filter was attached to the valve inlet with the orifice and this joint not broken unless mandatory.

Thermal insulation was delted from the design for test purposes. A multi-layer insulation was assumed for the analysis. In order for this or alternate types of insulation to be effective, a vacuum on the order of 10^{-5} torr must be maintained. This being impractical for hot fire testing, it was decided to delete insulation entirely and supplement the RHU's with a radiant heater in order to maintain 210 $\pm$ 10°F.

3.4 FABRICATION

Based upon the baseline design, the longest lead time components were the propellant valve and the thrust chamber casting. The valve interface was thus established early in the program and the procurement inititated. Definition of the chamber casing was required, however, before the thruster design iterations were tested. The design was thus established to provide for any anticipated iteration. As discussed in Section 2.4, the iteration testing led to a change in the thruster nozzle diameter to reduce chamber pressure. This change occurred after the casting procurement had been initiated, but before the tooling had been completed. Only a minor tooling change was required to change the outside nozzle contour for the larger throat diameter, provided the nozzle exit diameter was not changed. This factor influenced the design which yielded a nozzle expansion area ratio (ϵ) of 24.

Following completion of the iteration test program, machining of the casting and fabrication of the remaining piece parts were completed. The assembly sequence started with the injector. Orientation of the headscreen and headscreen retainer with the injector were established during water flow. The headscreen and the retainer are lightly held in place by the retainer ring, and this assembly rotated relative to the injector to

determine the orientation which yields the least indication of water collecting within the headspace. Once the optimum orientation is selected, the retainer ring is pressed into place. The flow characteristics are then verified as satisfactory (unchanged) and the assembly prepared for brazing.

A one shot braze was planned to attached the headscreen, headscreen support, propellant feed tube, and an insert (adapter for feed tube to headplate) to the headplate. The first braze attempt was not satisfactory, however. A slight movement of the headscreen and support resulted in a gap of approximately 0.015 inch between the headscreen support and the headplate. Prior to attempting any repair, the assembly was water flowed and the injector spray pattern through the headscreen assembly deemed acceptable. A second braze cycle, using a slightly lower melting point alloy, then successfully filled the gap.

The injector assembly was again water flowed to verify spray pattern and to set the pressure drop. An orifice was added at the valve inlet yielding a total pressure drop of 159 psia at a flow of 0.0225 lbm/sec. The orifice consists of a blank VOI-SHAN soft seal drilled and reamed to 0.029 inch diameter. After water flow, the valve and injector were flushed with alcohol and dried.

Loading of the catalyst was the next operation, and it was desired to determine the mass of catalyst loaded. All components of the thrust chamber together weighed 324.5 grams, and adding the weld fixture yielded 1192.7 grams. The catalyst to be loaded was also weighed at 26.5 grams with the "tin" used to contain it. After loading the catalyst, the weight of catalyst (with tin) remaining was 5.9 grams and the weight of the (unwelded) assembly with fixture was 1213.4 grams. These numbers yield 20.6 and 20.7 grams of catalyst loaded, implying an accuracy of approximately 0.1 gram.

The first attempt at the final EB closure weld of the injector assembly to the chamber yielded cracks in the weld. A review of the weld joint design revealed a design error allowing too great a gap at the joint, leading to the weld cracks. An EB weld repair was then attempted by first machining a groove, approximately 0.020 inch deep, and adding 0.020 diameter Hasteloy W weld rod. Cracks again appeared at the point where the

weld started and stopped. TIG welding, using Hasteloy W filler, was then successfully utilized to repair the weld. This welding was done in small increments, with an Argon purge through the catalyst bed and with wet asbestos packed around the chamber to minimize the impact on the catalyst bed. Subsequent dye penetrant inspection and proof pressure and leak tests proved the weld sound.

3.5 ENGINE WEIGHT AND COST COMPARISON

The actual weights of the RCHE and the unheated IR&D engine (XMRE-5) are presented in Table 3-1, showing 0.97 lb_m difference. This weight difference could be reduced somewhat as weight was not a primary concern of this program.

Table 3-1. Engine Weight Comparison

	RCHE	XMRE-5
Thruster Shell	.72 lb_m	.19 lb_m
Catalyst	.05	.05
Caps for RHU Ports (3)	.14	-
Bracket	.47	.47
Valve	.40	.40
Miscellaneous	.23	.23
RHU's (3)	.30	-
	2.31 lb_m	1.34 lb_m

A cost comparison for the two designs is less straightforward, as unit costs are greatly influenced by quantities and specific program constraints. The chamber casting for the RCHE had a non-recurring cost of $1600 and a unit price of $65. Subsequent costs for machining, welding, and fabrication of other piece parts are comparable to an unheated engine. The Radioisotope Heater Units will have a non-recurring cost of approximately $20,000 and a unit cost of $6,500, assuming that the prior qualification status is acceptable for the specific application.

4. HEAT SOURCE

4.1 DESCRIPTION

The heat source design selected was chosen because it is essentially an off-the-shelf heat source. Except for the PRD*, it is identical to the Pioneer RHU which has been flight qualified and is being used in Pioneer 10 and 11. The PRD, however, is also a component which has been flight qualified for the Transit and Pioneer RTG heat sources. These Pioneer heat sources are aboard the same spacecraft as the RHU's. By using all flight qualified heat source materials, components, and fabrication and inspection techniques, the risk and development effort required were practically non-existent. The specifications to which the Pioneer RHU's were qualified represent the most stringent set of spacecraft and aerospace nuclear safety requirements imposed on any radioisotope heat source to date. All required material, process, and inspection specifications are available. Hence, the selection of this design offered the greatest possibility of program success at minimum cost.

The RCHE and Pioneer RHU's are illustrated in Figure 4-1. Note that the only difference between the two heat sources is that the foam spacers at the ends of the radioisotope fuel have been removed and replaced by a PRD at one end. In the PRHU, a void volume was provided inside the liner so that helium from the radioisotope decay process could be accumulated without increasing internal pressure to unacceptable levels. To prevent the fuel from rattling in this void, foam spacers were used. The foam spacers were less than 10 percent of maximum theoretical density and hence over 90 percent of the void was available for helium storage. By using a PRD to relieve helium pressure, the void, and hence the spacers, were not required.

The RCHE heat source is a cylinder 0.875 inch in diameter and 1.860 inches long. Three RHU's are used in an RCHE; each RHU weighs 0.11 pound. The components are described in Table 4-1.

* Pressure Relief Device

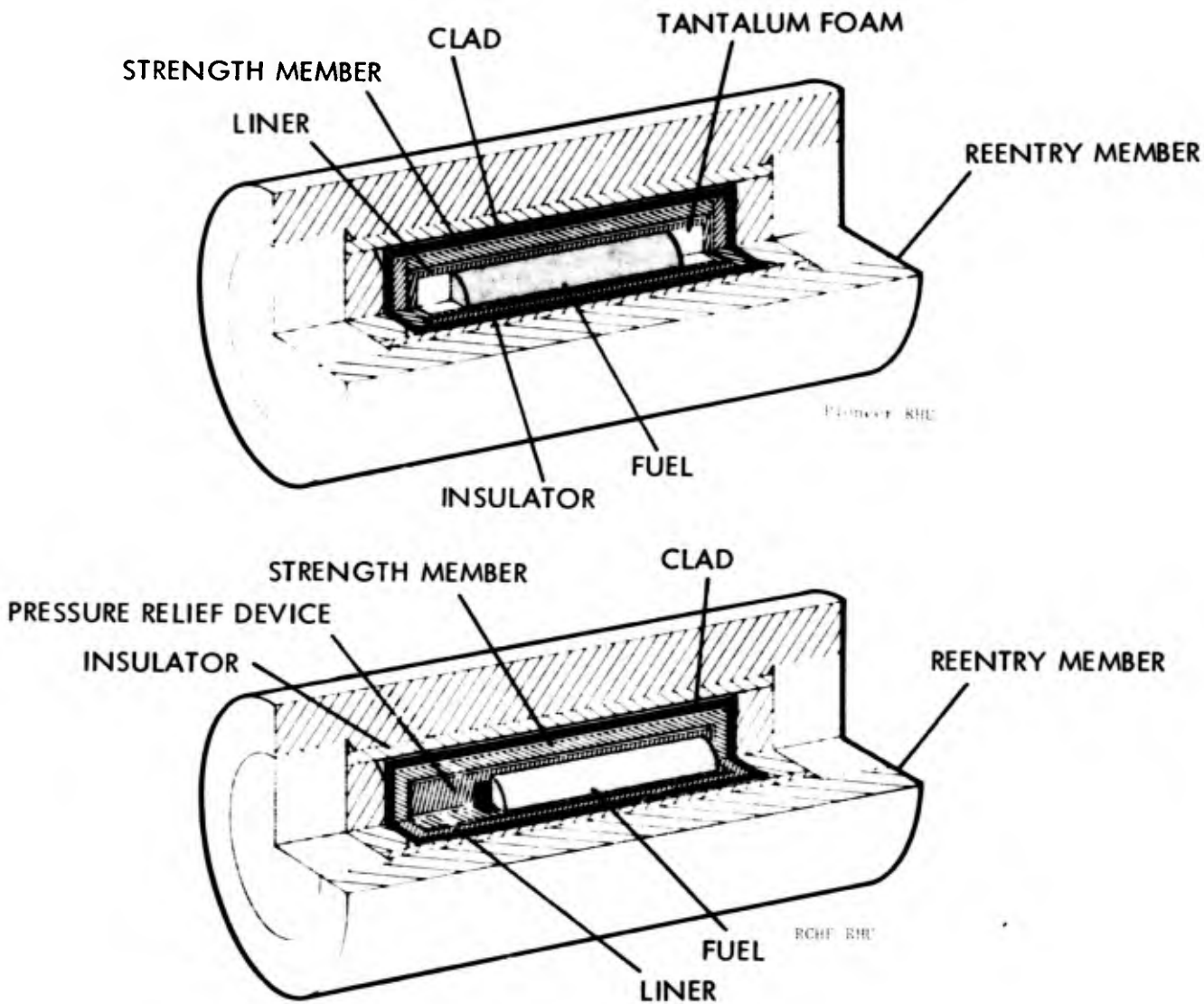

Figure 4-1. One-Watt Radioisotope Heater Unit

Table 4-1. Heat Source Components

Component	Principal Function	Material	Outside Diameter (in)	Thickness (in)	Outside Length (in)	Weight (lb)
Radioisotope	One watt source	PuO_2 solid	0.191	---	0.675	0.0072
Pressure relief device	Release helium, retain fuel	---	0.210	---	0.270	0.0055
Liner	Provide fuel compatibility and containment	Ta-10W	0.250	0.020	0.986	0.0097
Strength member	Provide impact resistance	T-111	0.346	0.040	1.085	0.0287
Clad	Provide oxidation protection for strength member	Pt-20Rh	0.380	0.010	1.127	0.0103
Insulator	Thermal protection of capsule during reentry	Pyrolytic graphite	0.516	0.063	1.400	0.0111
Reentry	Reentry protection and aerodynamic profile to limit impact velocity	Poco AXF-5Q	0.875	0.177	1.860	0.0415
				Total Weight		0.1140

4.2 HEAT SOURCE FABRICATION AND ASSEMBLY

The materials of construction and the configurations of the heat source have, as mentioned above, been successfully fabricated and utilized in the Pioneer RHU program. Raw material and process specifications, including material heat treatment and cleaning procedures, for the materials were available from the Pioneer RHU and Transit RTG programs. Figure 4-2 is a typical manufacturing plan showing inspection, acceptance, and qualification test steps planned to assure conformance with an equipment specification. Methods for producing the piece parts and the assembly procedures for the heat source are discussed below.

4.2.1 Piece Part Fabrication

All RHU components, including the fuel, were fabricated or purchased by TRW. Tube stock to the finished OD and ID was purchased and then machined to the proper length for the pressure relief device (PRD), liner, strength member and clad. Ta-10W rod is used to produce the filter component and seal plugs for the PRD. The filter component consists of a solid core having a thin layer of Al_2O_3 applied by plasma arc spraying. The liner and clad end discs are stamped from sheet stock of the finished thickness and then coined to the final diameter. The strength member end discs are fabricated from sheet stock and ground to the required thickness. These parts are all inspected at TRW, then shipped to the fueling agency for fueling and welding. Meanwhile, at TRW, the pyrolytic graphite insulator bodies were finished machined on the OD and ID from tube stock and the end plugs were made from sheet stock. All heat shield reentry components were machined from blocks of Poco AXF-5Q graphite.

4.2.2 Capsule Fueling and Heat Source Assembly

The fueling of the RCHE was unique in that it was accomplished at a commercial facility. TRW issued a commercial contract to Donald W. Douglas Labs of Richland, Washington, to purchase the fuel in powder form, press and sinter it then assemble it into the structural components by welding. Typically, this operation would have been conducted at a government facility which typically requires AEC involvement and interagency agreements. A recent AEC policy statement, however, encourages the use of commercial fueling facilities by properly licensed contractors. The fuel

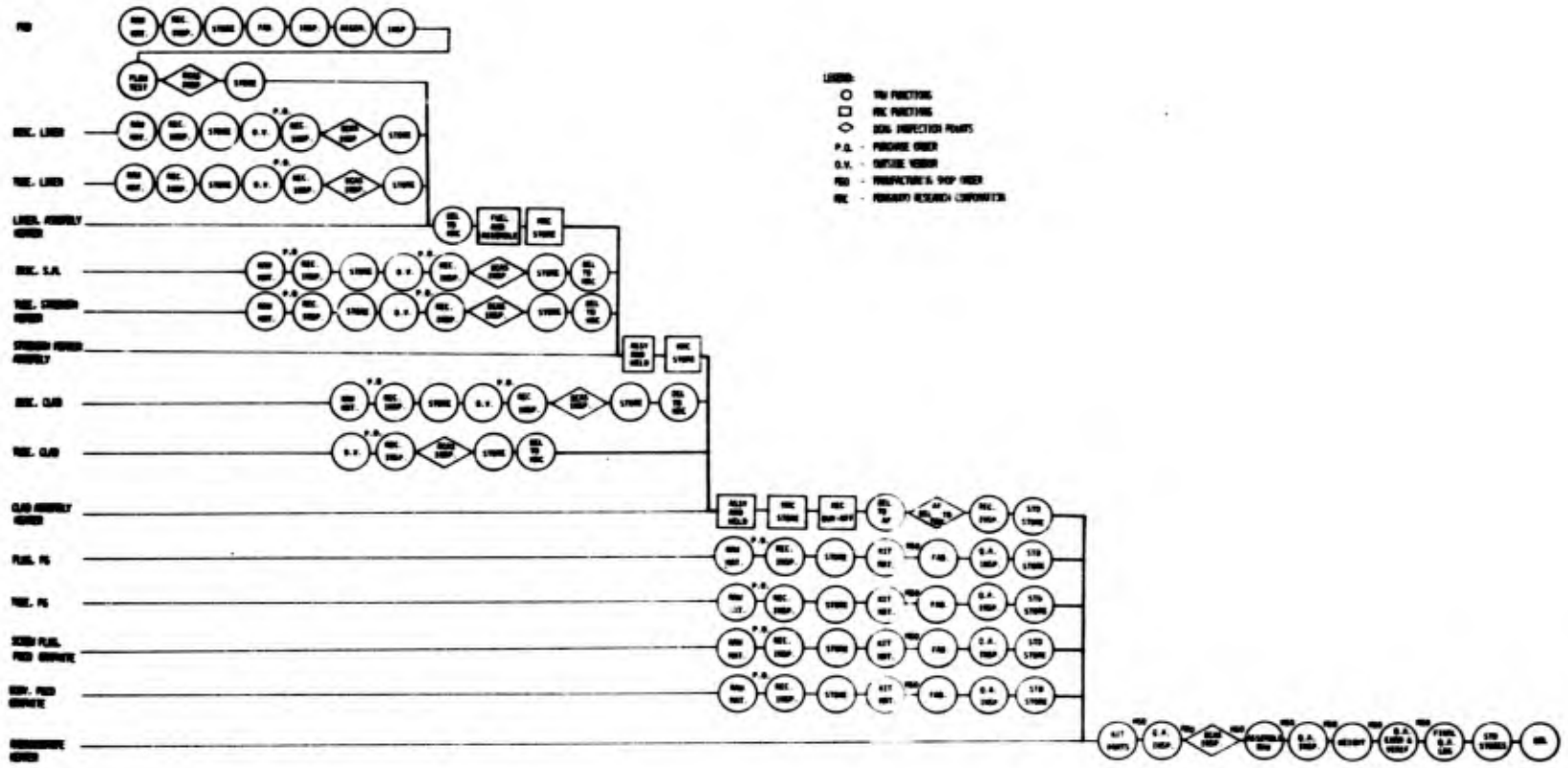

Figure 4-2. Radioisotope Catalytic Hydrazine Engine RHU Manufacturing Flow Chart

capsules are then returned to TRW where they are assembled into the graphite components.

Fueling of the radioisotope capsule is an eight-step process as follows:

1) The PRD is welded into one end of the liner tube
2) One end closure disc is welded to the clad tube
3) The fuel is inserted into the liner body subassembly
4) The end closure disc is welded to the open end of the liner body
5) The liner subassembly is decontaminated
6) The PRD seal plug is punctured
7) The fuel/liner subassembly is inserted into the strength member and the end closure disc is welded to the end of the strength member body, decontaminated, and its seal is punctured.
8) The fuel/liner/strength member subassembly is inserted into the clad and the end closure disc is welded to the end of the clad body to produce the capsule, and decontaminated.

Assembly of the capsule into the graphite heat shield is a two-step process as follows:

1) The clad is punctured and the capsule is slid into the pyrolytic graphite tube body and the pyrolytic graphite end cap discs are fitted into each end of the tube
2) The capsule/pyrolytic graphite subassembly is slid into the Poco graphite heat shield body and the Poco graphite end plugs are screwed in place to produce the RHU.

For live-fueled units, visual examination only was utilized to assure surface integrity. The internal quality of all weldments was assured by microstructural analyses of simulated assemblies welded prior to and after completing the fabrication of the lot of capsules, as well as X-ray radiography. A lot is defined as all subassemblies welded at the same time by the same operator. Criteria for acceptance was based on the experience gained during the Pioneer RHU and Transit RTG programs.

4.3 OPERATIONAL CHARACTERISTICS

The radioactive decay process of Pu-238 produces alpha particles (helium), gamma rays, and neutrons, and as a result, heat. The rates at

which these products are created establish thermal power output versus time, helium release rates, and nuclear radiation fields. During the development of the Pioneer heaters, analyses and tests were conducted to determine the resultant operational characteristics of the heat source. Additionally, analyses and tests were conducted to determine the effects of the launch vibration, shock, and spin environments on the heater components. All of these data are directly applicable to the RCHE.

4.3.1 Thermal Power Output

The equation for thermal power output versus time for the radioactive decay of Pu-238 is

$$P = P_o e^{-\lambda\theta}$$

where P_o = initial power
λ = decay constant = 7.93×10^{-3} (years^{-1})
θ = time (years)

Using this equation and an initial thermal output of 1 watt, the plot in Figure 4-3 was generated. Note that the power decays at a rate of approximately 3/4 of 1 percent a year and is nearly linear for the relatively short period of 10 years (short in comparison to the Pu-238 half life of 87.5 years). One watt of Pu-238 will thus decay to 0.93 watt in 10 years. If the mission duration is 10 years, this power is referred to as the end-of-life power. It is this end-of-life power output that must establish the minimum thruster operating temperature of 200°F (using three heat sources).

4.3.2 Radiation Characteristics

Calculations were made to determine the gamma ray and neutron dose rates expected in the vicinity of each RHU. The gamma ray dose rates were computed with the QAD point kernel code using thirteen gamma ray groups, energy-dependent build-up factors, flux-to-dose conversion factors, and attenuation coefficients. The analyses were based on the characteristics of the cermet fuel form. The source spectrum used in the calculations was that for 2-year old plutonium dioxide having 1.2 parts per million Pu-236 and 80 percent Pu-238. The neutron calculations assumed a source of 3.0×10^4 neutrons/sec-gram of plutonium and attenuation inversely proportional

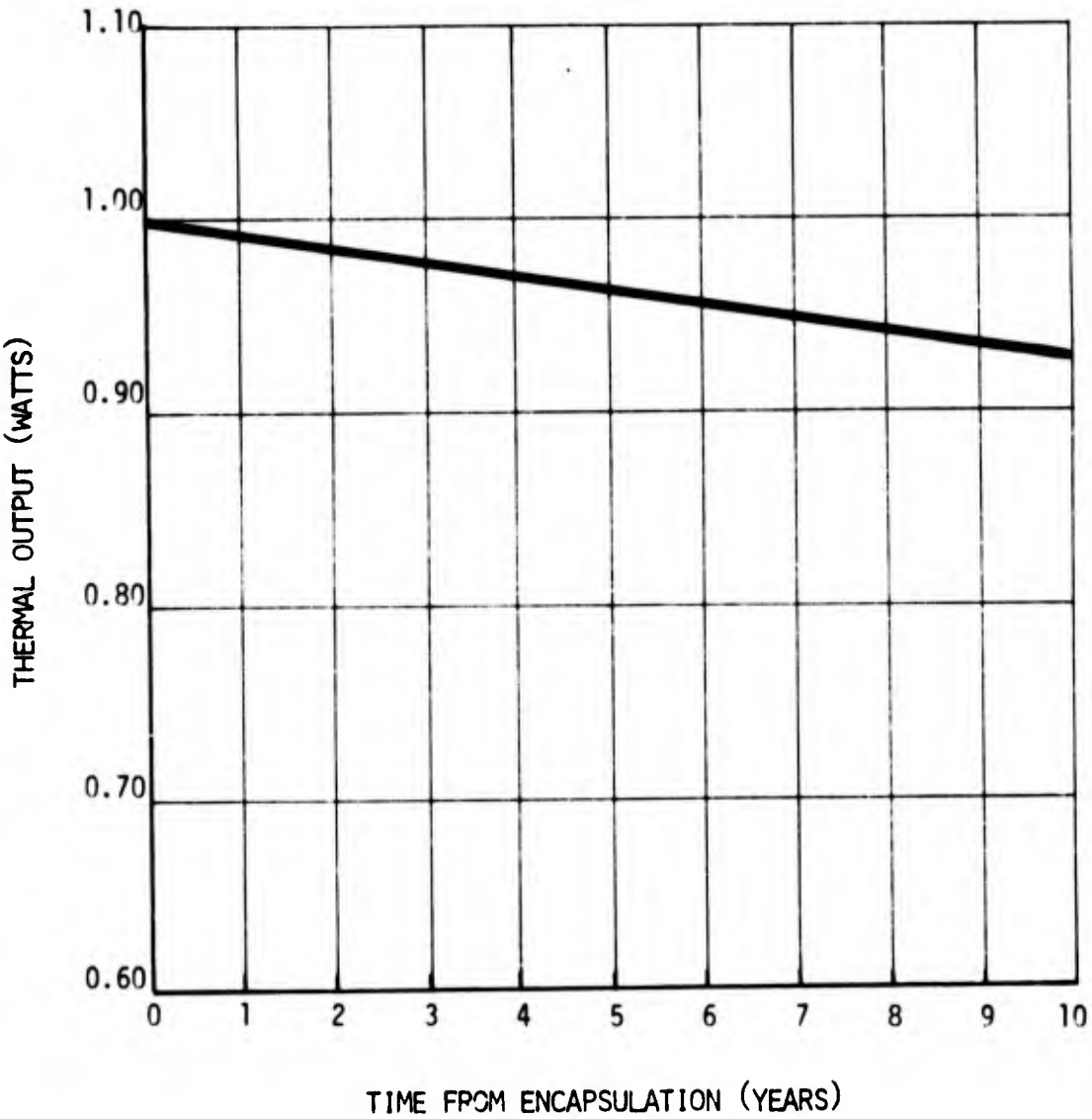

Figure 4-3. Thermal Power Output Vs Time Per Watt of Initial Pu-238 Fuel

to the square of the distance. The self-attenuation for neutrons in the RHU was estimated to be only 5 percent. The flux-to-dose conversion factor was taken to be 0.13 mrem/hr per N/cm^2-sec. The neutron production rate was assumed to be independent of time.

The results of the radiation calculations are shown in Figure 4-4 for 1 watt of radioisotope. The dose from 3 watts is three times as large if the 3 watts are in close proximity. The neutron dose rate is seen to be approximately a factor of ten higher at all locations than the gamma ray dose rate.

4.3.3 Helium Management

The operating characteristics of the PRD have been analytically and experimentally verified in the Transit development effort.* The characteristics may be summarized as follows:

- The helium permeation rates of all PRD assemblies tested remained stable not only through short-term testing, but also during long-term, high temperature operation. (Test temperatures ranged from 70° to 2700°F and pressure differentials varied from 0.0015 to 300 psi.) Figure 4-5 shows the stable helium permeation history of a Transit PRD undergoing long-term testing.

- There is good correlation between predicted and experimental flow rates at various pressure differentials from room temperature to 2700°F, as shown for the Transit PRD's in Figures 4-6 and 4-7.

- At high pressure differentials, relative to normal operating conditions, the permeation mechanism of these vents changes from slip flow to viscous laminar flow, as shown in Figure 4-7. During this change, the effect of the pressure gradient on the permeation rate changes from a first order dependency (proportional to Δp) to a second order dependency [proportional to $(\Delta p)^2$]. Thus, the PRD's have, in effect, a built-in safety valve. If the helium pressure in the capsule should suddenly rise to a very high value in an accident mode due to sudden (nonsteady state) release of excess helium from the fuel, the flow increases rapidly to relieve the pressure.

* 1. Transit RTG Updated Safety Analysis Report, Volume III. Nuclear Safety Analysis Document, September 15, 1970 TRW (A)-11464-291

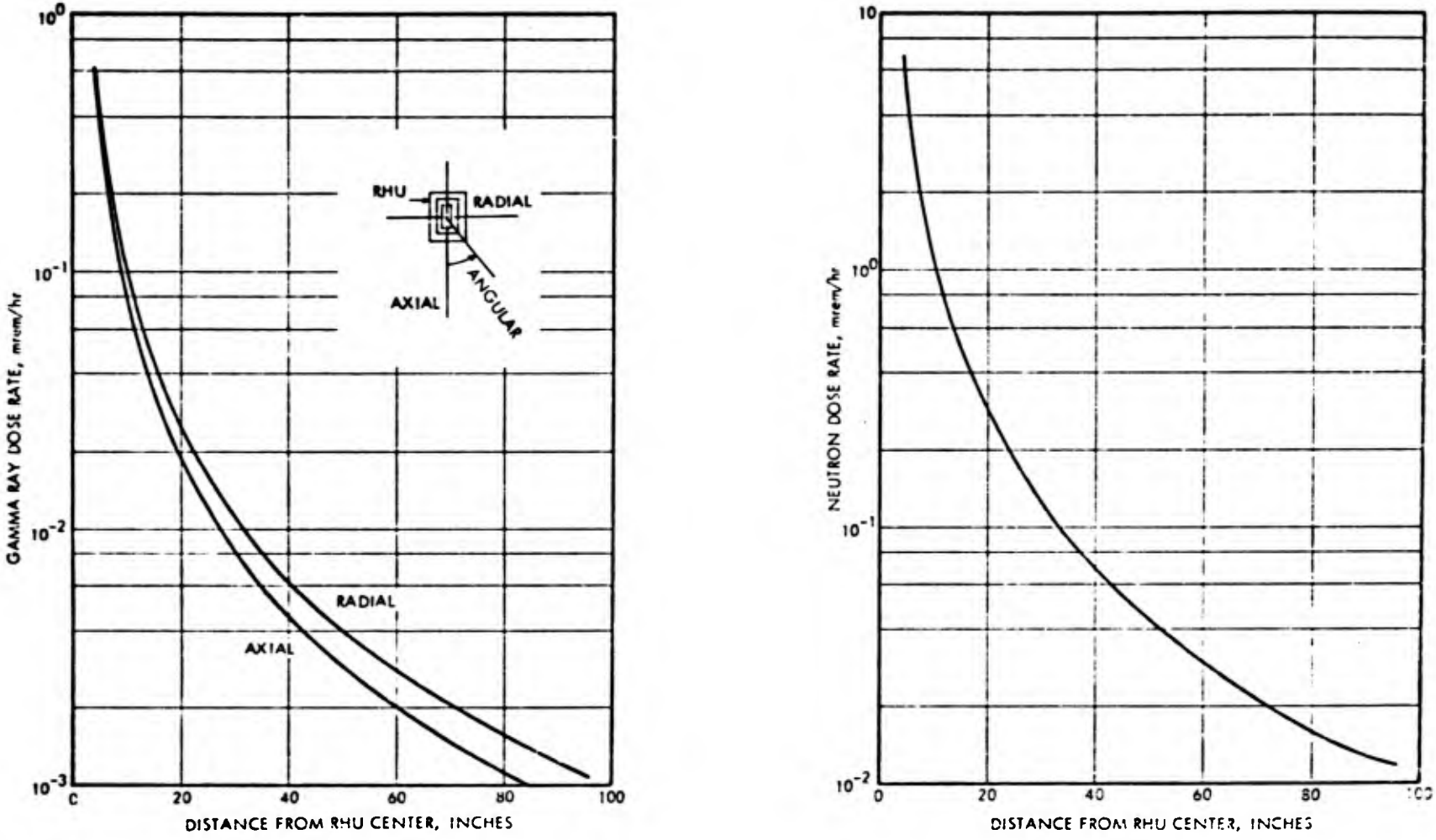

Figure 4-4. Radiation Dose/Watt of Radioisotope Vs Distance

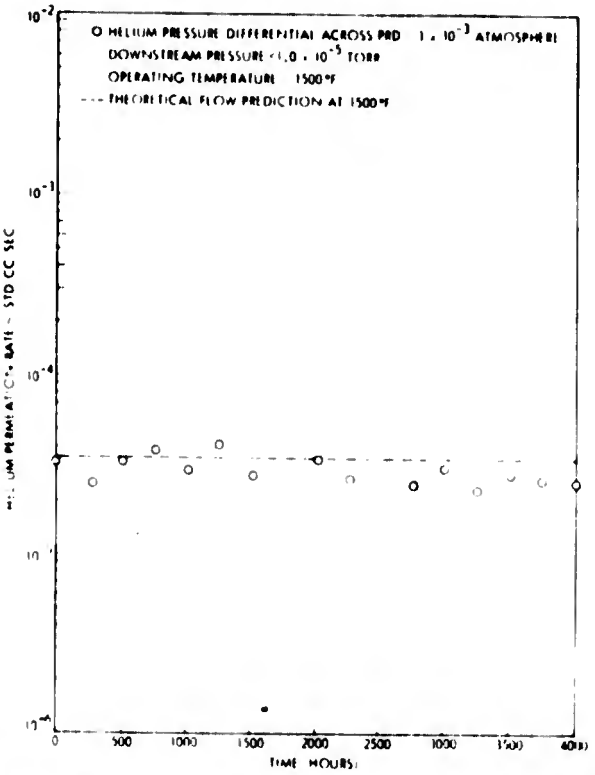

Figure 4-5. Long-Term Helium Permeation History for PRD S/N 128

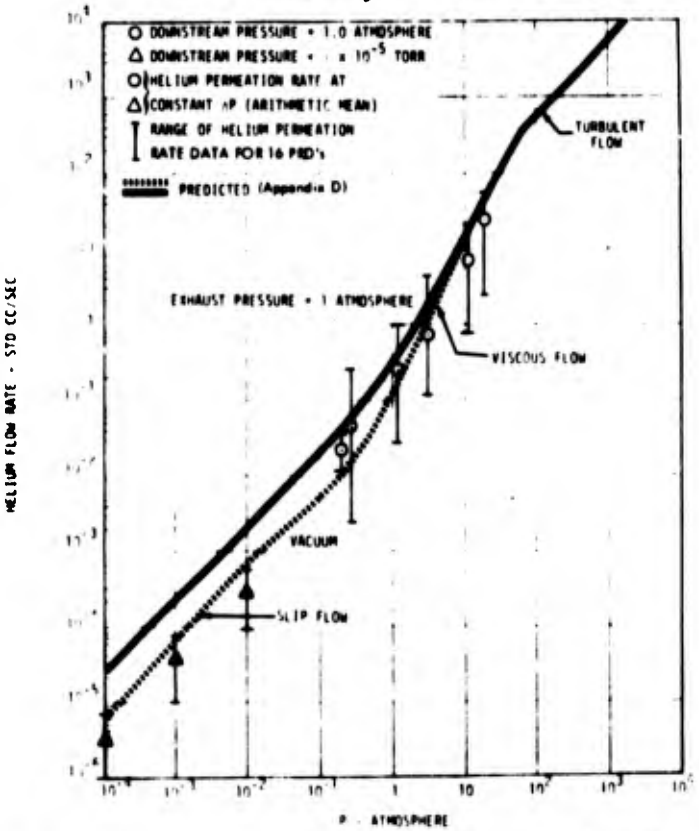

Figure 4-6. Correlation Between Predicted and Experimental Flow Rate of Transit PRD's at Room Temperature

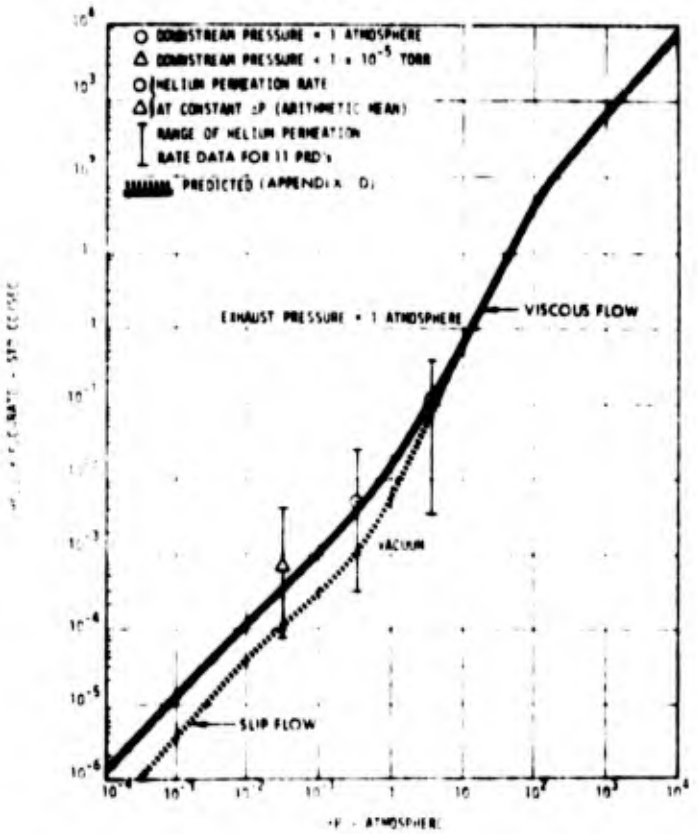

Figure 4-7. Correlation Between Predicted and Experimental Flow Rate of Transit PRD's at 2700°F

- Experimental testing has demonstrated the ability of the PRD to retain submicron thoria fuel simulant while maintaining a stable helium flow at all flow rates measured. The conclusions obtained from the fine-retention test were verified by a test series conducted independently by Monsanto Research Corporation, Mound Laboratory, utilizing plutonium-238 dioxide (PuO_2) powder consisting of particles of less than 1 micron.*

4.3.4 Launch Vibration and Shock

The one watt heat sources have been vibration tested and qualified for the Pioneer mission. These units were contained in a thruster assembly similar to the RCHE design. The vibration input requirements are shown in Table 4-2. In early tests the heat sources survived an input approximately 100 percent higher than these requirements (56g peak).

The pyrotechnic shock environment to which the heat sources have been qualified is shown in Figure 4-8.

* 1. Transit RTG Updated Safety Analysis Report, Volume III. Nuclear Safety Analysis Document, September 15, 1970 TRW (A)-11464-291

Table 4-2. Qualification Level Vibration Spectrum

Random

9 Minutes each Axis

Frequency (cps)	PSD Level g^2/cps
20 - 100	Increasing from 0.0023 to 0.056 at a rate of 6 db/octave
100 - 1000	0.056
1000 - 2000	Roll off from 0.056 at 1000 cps to 2000 cps at rate of 12 db/octave

Sinusoidal

Hz	g's (zero to peak)
5 - 38	*
38 - 55	29.2
55 - 90	15.0
90 - 200	3.0

*0.4 inch double amplitude

Sweep rate one octave per minute

4.4 NUCLEAR SAFETY

As discussed in Section 4.0, the baseline RCHE heat source design is essentially identical to the Radioisotope Heater Unit (RHU) which was developed for the Pioneer 10 and 11 spacecraft. The only difference is that the RCHE RHU incorporates a vent to relieve the helium that is generated, which eliminates the need for tantalum foam spacers. Therefore, the extensive safety analyses and tests which were conducted for the Pioneer RHU* are directly applicable to the RCHE RHU. This section summarizes the safety analyses and tests which were conducted for the Pioneer RHU.

*"Safety Analysis Summary Report for the Pioneer Radioisotope Heater Unit," PFG-273-324, TRW Systems, February 19, 1971.

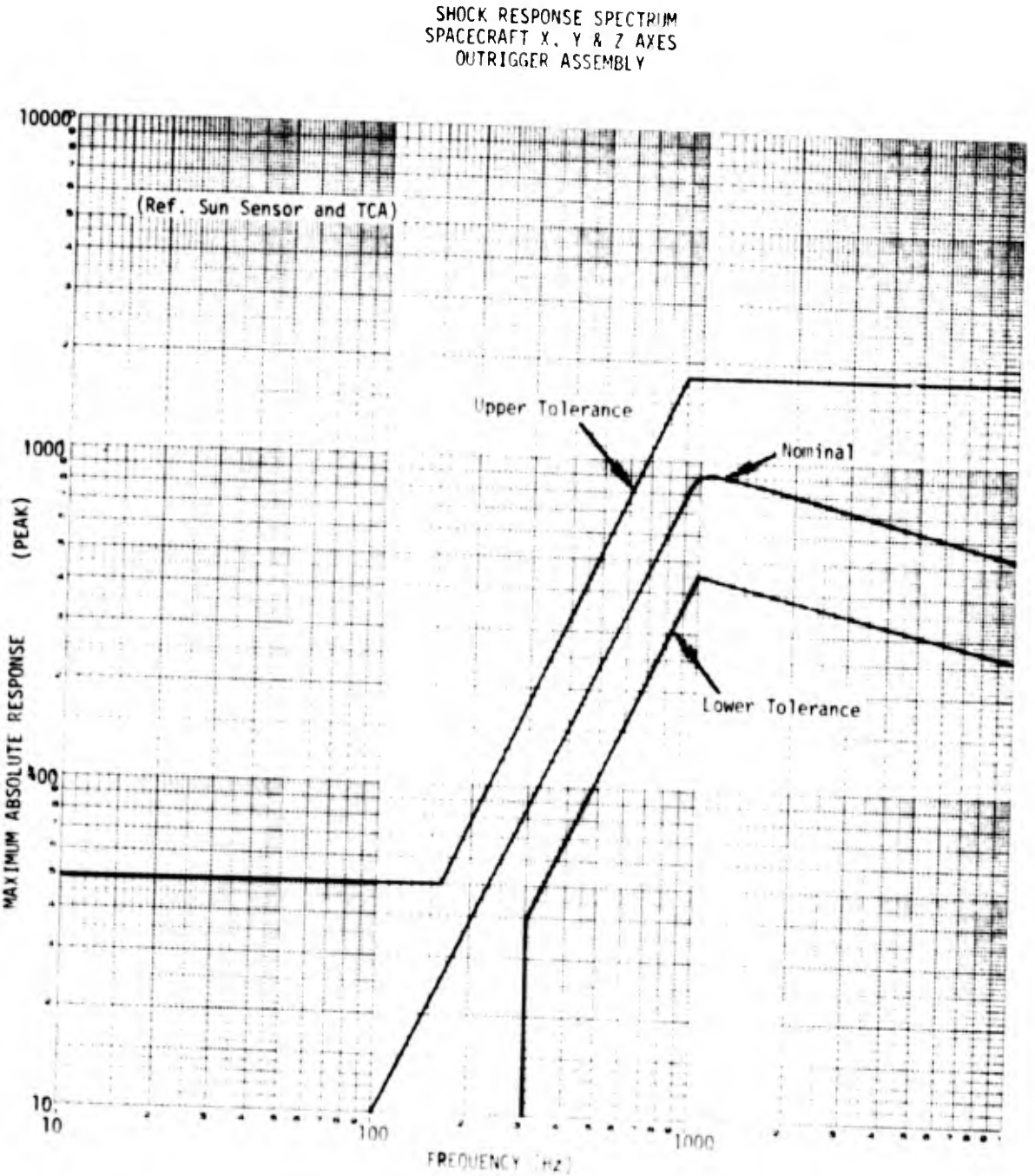

Figure 4-8. Pyrotechnic Shock

For the RHU, extensive analyses and tests were conducted to verify fuel containment during and after launch pad aborts and ascent aborts. The launch vehicle for the RHU-equipped Pioneer Jupiter spacecraft is the Atlas/Centaur/TE 364-4 configuration. Abort of this launch vehicle on or near the launch pad could expose the RHU's to a combination of overpressure, shrapnel, prompt liquid propellant fireball, impact onto the pad, and the residual fire associated with burning of liquid or solid propellants. Analysis was utilized to determine the extent of these environments and to predict their effects on the RHU, and tests were utilized to verify the predicted effects. Launch pad abort tests to which the RHU's were exposed consisted of: (1) 915 psia shock overpressure, simulating a 12.8 percent TNT yield ground burst of the TE 364-4 motor, (2) simulated shrapnel from the TE 364-4 motor casing at a velocity of 1900 ft/sec, (3) a simulated liquid propellant, prompt fireball with a heat flux history similar to that resulting from conflagration of all the liquid propellants, (4) impact of the RHU's onto a smooth, unyielding medium at 160 ft/sec, and (5) a solid propellant fire of maximum possible duration (based on the maximum web thickness from a burning chunk of the TE 364-4 solid propellant). These test conditions represented the most severe launch pad abort environments expected. In no case was radioisotope fuel released from the fuel capsules during or after exposure to these test environments. It was predicted, however, that fuel could be released during a solid propellant fire, depending on the fire temperature, if the capsule contained only one or two months of accumulated helium. Fuel release could be caused by capsule rupture because of internal pressure.

Ascent aborts of the Pioneer launch vehicle may result in spacecraft reentry and breakup, RHU terminal reentry, impact of the RHU's onto land, and long-term exposure of the RHU's to air and soil after impact. These environments and their effects on the RHU's were extensively analyzed, and the results were verified through tests. The initial reentry conditions at 400,000 feet altitude which could be achieved through attitude misorientations

of the launch vehicle's final stage were calculated using a digital computer program which presented the spectrum of potential initial reentry velocities and flight path angles. An analysis was conducted to determine the altitudes at which the RHU's would be released from the spacecraft for a range of initial reentry conditions. The aerothermodynamic environments experienced by the RHU's were then computed and their effects, in terms of reentry member ablation, reentry member thermal stress, and capsule structural integrity, were predicted. Several tests were conducted in which the most severe predicted aerodynamic heating rates were imposed on the RHU's. These reentry tests indicated that, for the Pioneer Jupiter mission, fuel could be released from the RHU's during reentry in only two cases, (1) if the attitude misorientation of the final stage were such as to cause the RHU's to undergo a grazing reentry 25 months after fuel encapsulation, and (2) if the launch vehicle failure resulted in random orbital decay and reentry of the RHU's in excess of 20 years after fuel encapsulation. Both of these types of failures were due to the sealed configuration of the fuel capsule. That is, for the elapsed times discussed above, which resulted in an accumulation of helium, and for the corresponding reentry temperatures, the internal pressures at these reentry temperatures would cause rupture of the fuel capsules.

Drop tests from high altitude were conducted in order to measure the terminal velocity of the RHU's. Impact tests were then conducted in which the RHU's were impacted against smooth granite, at various angles of attack, at a velocity of 125% of the predicted sea-level impact velocity. In no test was fuel released, and in no case was even one of the capsule components breached. In the post-impact environment, in which the RHU could be exposed to air and soil, the near-ambient temperature of the RHU, as predicted and later measured, indicated that complete fuel containment would be provided.

Further verification of the reentry, impact, and post-impact capabilities of the RHU was provided in a test in which two RHU's were released from a U.S. Air Force booster during reentry. Although the conditions at which the RHU's were released from the booster did not simulate a severe reentry such as might be obtained by ascent aborts of the Pioneer launch vehicle, the RHU's were recovered and were found to be completely intact. The reentry members underwent an immeasurably small amount of ablation, and were not cracked by impact.

Figure 4-9 presents a summary of the post-test conditions of the RHU. The RHU capsule was only slightly deformed as the result of the overpressure test, as shown in Figure 4-9a and the clad was intact. The capsule which was exposed to simulated shrapnel is shown at the top of Figure 4-9b, and the simulated piece of shrapnel is shown in the lower portion of the photograph. Extensive clad removal is evident, but fuel was completely contained. Figure 4-9c shows the results of the liquid fireball test, in which partial clad melting occurred. In Figure 4-9d, for the solid propellant fire, interaction between the clad and strength member is evident, but fuel was not released. Figure 4-9e shows the RHU reentry members which were exposed to simulated random orbital decay, grazing, and steep angle reentries. In all tests, the reentry member remained integral. Finally, Figure 4-9f shows the impacted capsules, where it can be seen that only slight deformation occurred because of impact.

Addition of the pressure relief device (PRD) to the RHU eliminates the two potential failure modes defined for the Pioneer RHU. Both failure modes required a pressure buildup within the capsule prior to specific reentry conditions. The vent eliminates the pressure buildup and thus the failure modes.

In response to an AFRPL request, AFWL/SECQ conducted a preliminary Nuclear Safety Analysis of the RCHE. They conclude that the RHU's used in this engine design are improved versions of those already flown on the Pioneer 10 and 11 missions and that no further effort is required until an actual flight application is identified. It is expected that the Nuclear Safety Analyses conducted by AFWL and TRW will facilitate a quick approval.

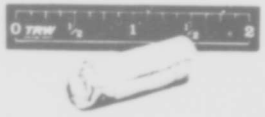

a. OVERPRESSURE

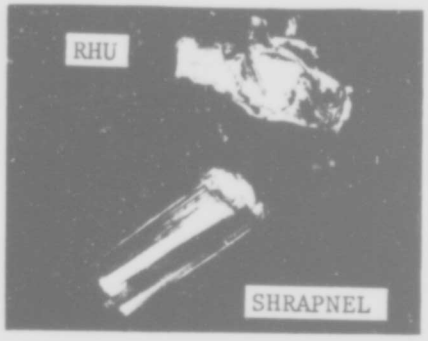

b. SHRAPNEL

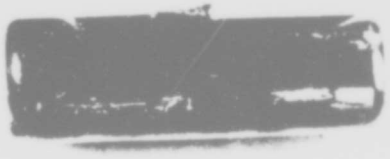

c. LIQUID PROPELLANT FIRE

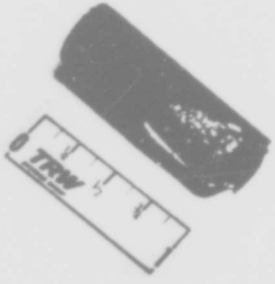

d. SOLID PROPELLANT FIRE

e. REENTRY

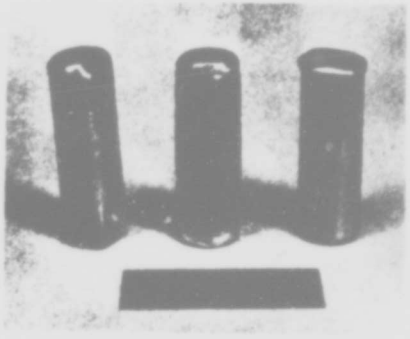

f. IMPACTED CAPSULES

Figure 4-9. RHU Post-Test Conditions

5. RCHE TESTING

Testing of the RCHE followed the sequence typical of a qualification test program. The engine was acceptance tested, including hot fire tests, then subjected to a qualification level vibration environment prior to the duty cycle demonstration test. These tests are discussed in the following sections.

5.1 ACCEPTANCE TESTS

Following a visual inspection of the assembly, a proof pressure test was conducted. A nozzle throat plug was installed, and connections made to the valve inlet (filter) and chamber pressure tap. The valve was then opened and the assembly pressurized to 600 psig with GN_2 for 5 minutes. The pressure was then reduced to 200 psig and all potential leak paths checked with a snoop solution. No leaks were detected. With the valve closed, the inlet pressure was raised to 300 psig, the thrust chamber vented through the chamber pressure tap, and internal leakage of the propellant valve checked. This was a bubble type test measuring through the chamber pressure tap. No leakage was detected over a 10 minute period.

The engine was then installed on the thrust stand for hot fire acceptance test. The tests outlined in Table 5-1 were conducted at propellant inlet pressures of 350,225, and 100 psia. A simulated altitude of greater than 100,000 feet was maintained throughout all testing. Measurements included thrust (F), chamber pressure (Pc), propellant inlet pressure (Pinj), steady-state propellant flow rate ($\dot{m}$), and pulse mode propellant consumption ($\int \dot{m} dt$).

Table 5-1. Acceptance Test Duty Cycle

Sequence	On Time (msec)	Off Time (msec)	No. of Pulses
a	20	980	100
b	20	480	100
c	50	950	100
d	50	450	100
e	100	900	100
f	150	850	100
g	10 sec	Steady-State	1

Prior to initiation of testing, the RHU's were installed and the engine held at vacuum (120,000 feet) overnight. The chamber temperature, with no insulation, stabilized at 115°F. A wrap of microquartz insulation was then installed around the chamber casting, leaving both ends uninsulated, and again left at vacuum overnight. The equilibrium temperature was 155°F, in an environment of approximately 60°F. Adding free convection (air at 120,000 feet altitude) to the thermal model, and using appropriate insulation properties, yielded predictions of 120°F and 180°F for the above conditions. Additional refinement of the model is required to accurately predict the catalyst bed temperature in space, but the above data yield confidence that the 200°F goal would be exceeded in high vacuum (10^{-5} torr). An electric radiant heater was then added as shown in Figure 5-1 to supplement the RHU's and maintain 210±10°F at the initiation of every test.

No specific accept/reject criteria were established for this test. It was intended, however, to verify that the engine would repeat the operating characteristics of trh development thrusters. It was also intended to simulate a flight type application where the launch environment would follow an acceptance hot fire test. Data from this test sequence are presented in Section 5.3.

105529-73

Figure 5-1. Photo of RCHE on Test Stand

Following the hot fire test, the propellant valve was removed from the engine assembly, flushed with Isopropyl Alcohol (IPA), and vacuum dried. The engine was then re-assembled in preparation for a vibration test.

5.2 VIBRATION TEST

A vibration test was planned to simulate the effects of a launch environment on the catalyst bed. The exposure, as presented in Table 5-2, is representative of a flight qualification vibration exposure. Figures 5-2 and 5-3 show the RCHE mounted on the test fixture in preparation for the first (X-X) axis test. The engine was subjected to the random and sine vibration exposures in this axis, after which the fixture was rotated 90° (to the Y-Y axis) and the exposure repeated. During the random vibration exposure, however, the valve inlet tube separated from the valve. Tape was placed over the opening, to minimize particulate contamination, and testing in this axis completed. The fixture was then mounted for vibration in the vertical (Z-Z) axis to complete the vibration exposure. Accelerometer data from these tests are presented in Figures 5-4 to 5-9.

Table 5-2. Vibration Spectrum

Random Vibration
About three orthogonal axes:
Flat from 300 to 1200 cps at 0.25 g^2/cps
Roll up to 300 cps at 3 db/octave
Roll off above 1200 cps at 6 db/octave
Integrated load - 19.5 g rms
Test time - 180 seconds/axes
Sinusoidal Vibration
About three orthogonal axes:
Sweep at spectrum of 5 to 2000 cps at a rate of 2.0 minutes per octave at a level of 1.0 g (zero to peak)

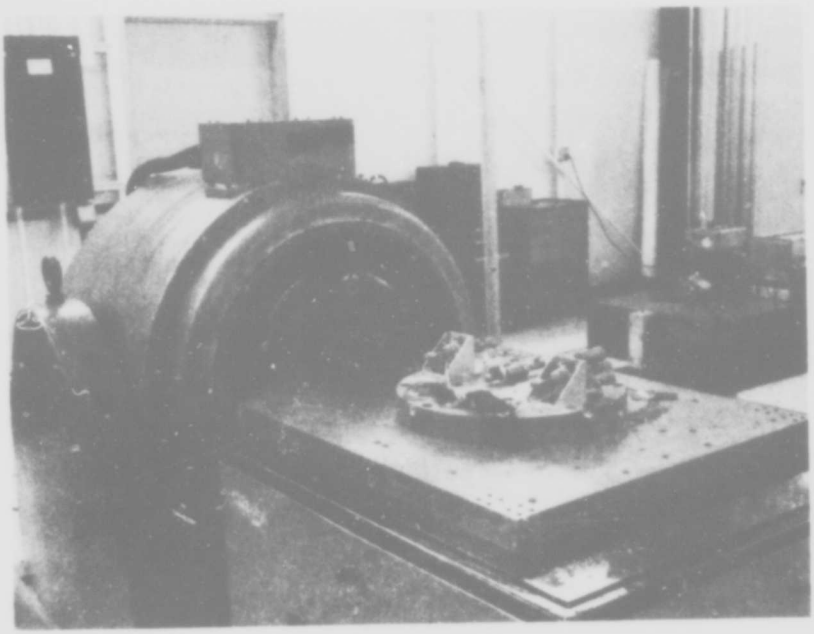

101896-73

Figure 5-2. Vibration Test Setup

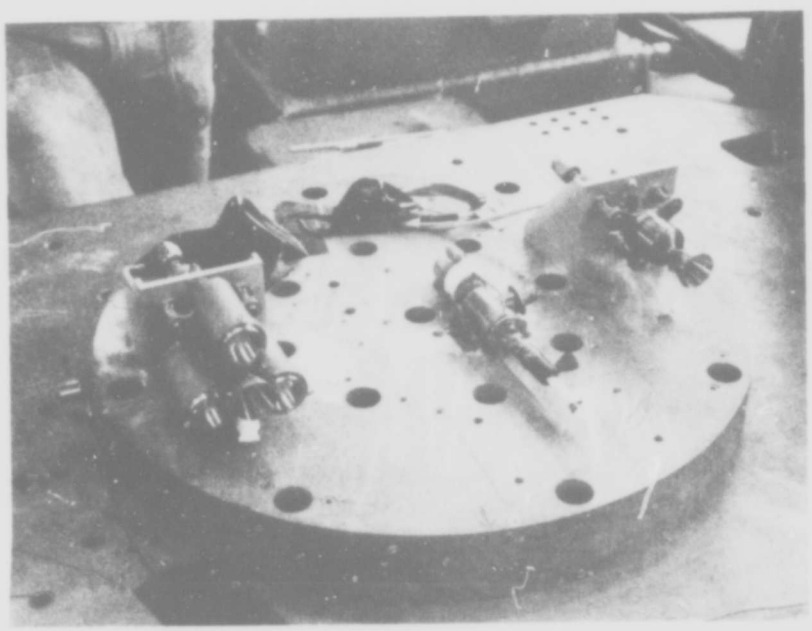

101897-73

Figure 5-3. RCHE on Vibration Fixture

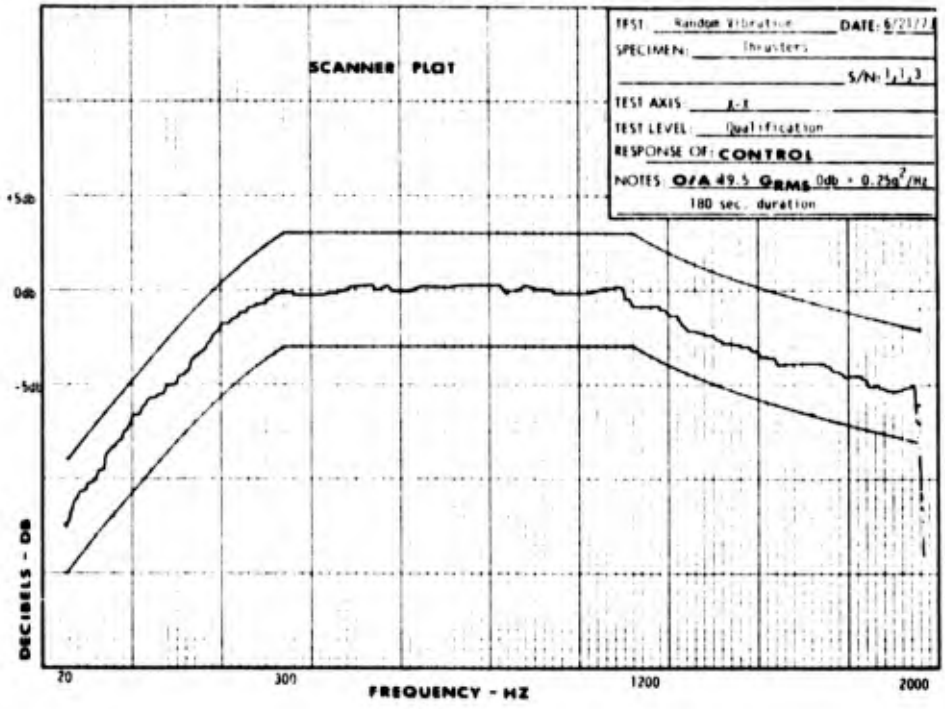

Figure 5-4. Accelerometer Data - X-X Random

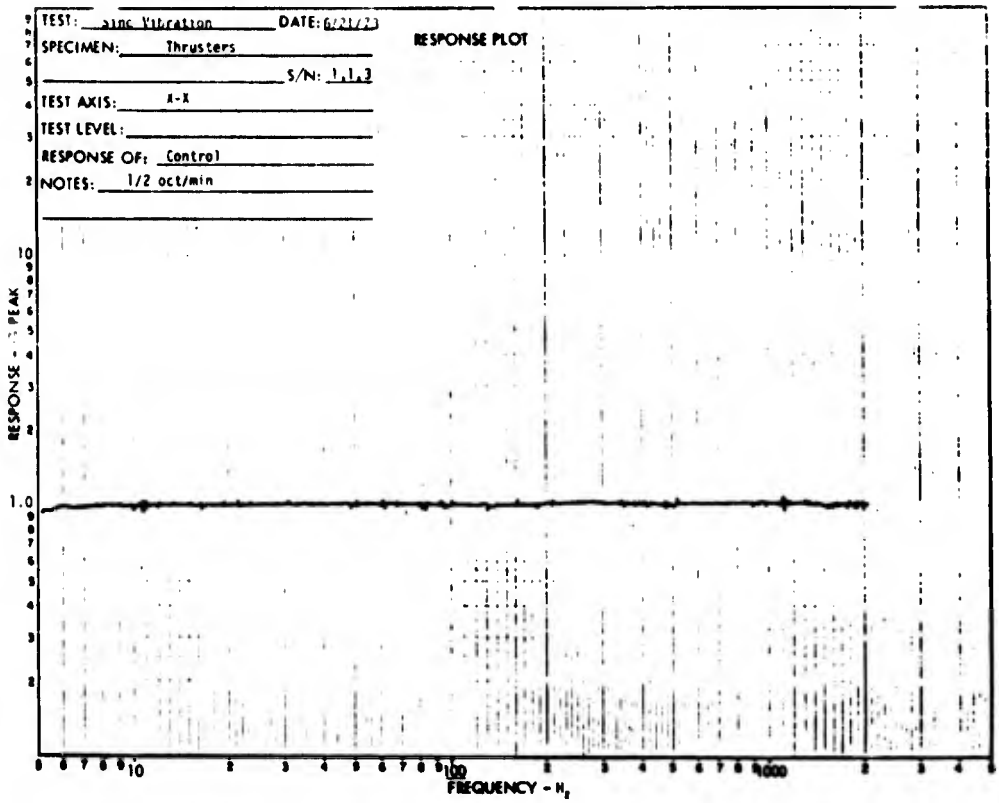

Figure 5-5. Accelerometer Data - X-X Sine

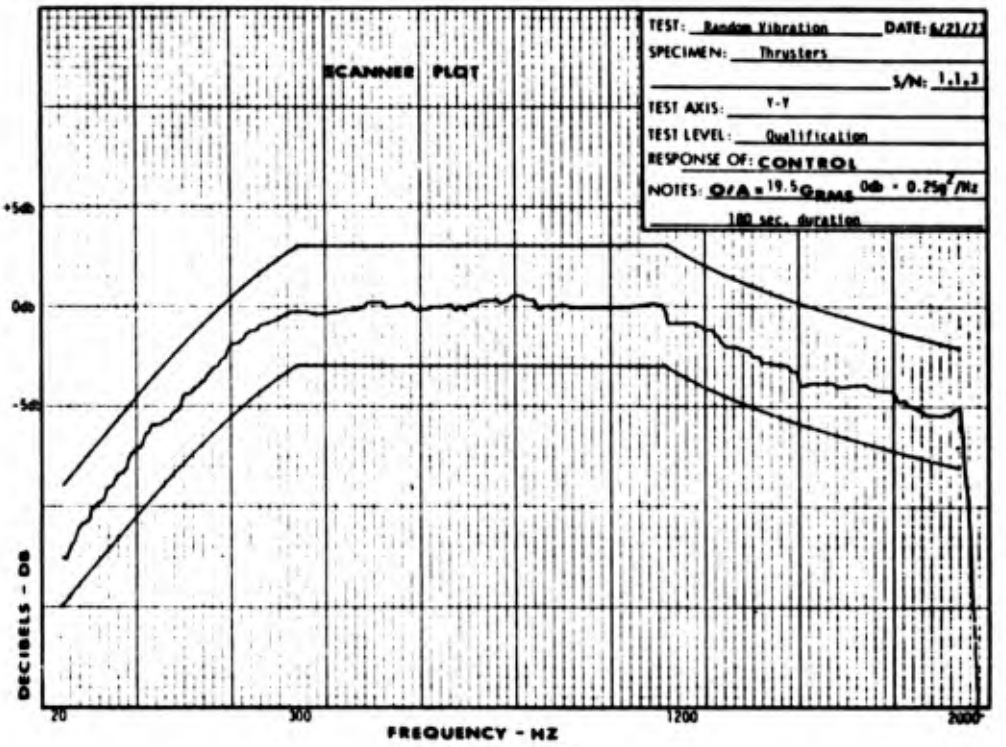

Figure 5-6. Accelerometer Data - Y-Y Random

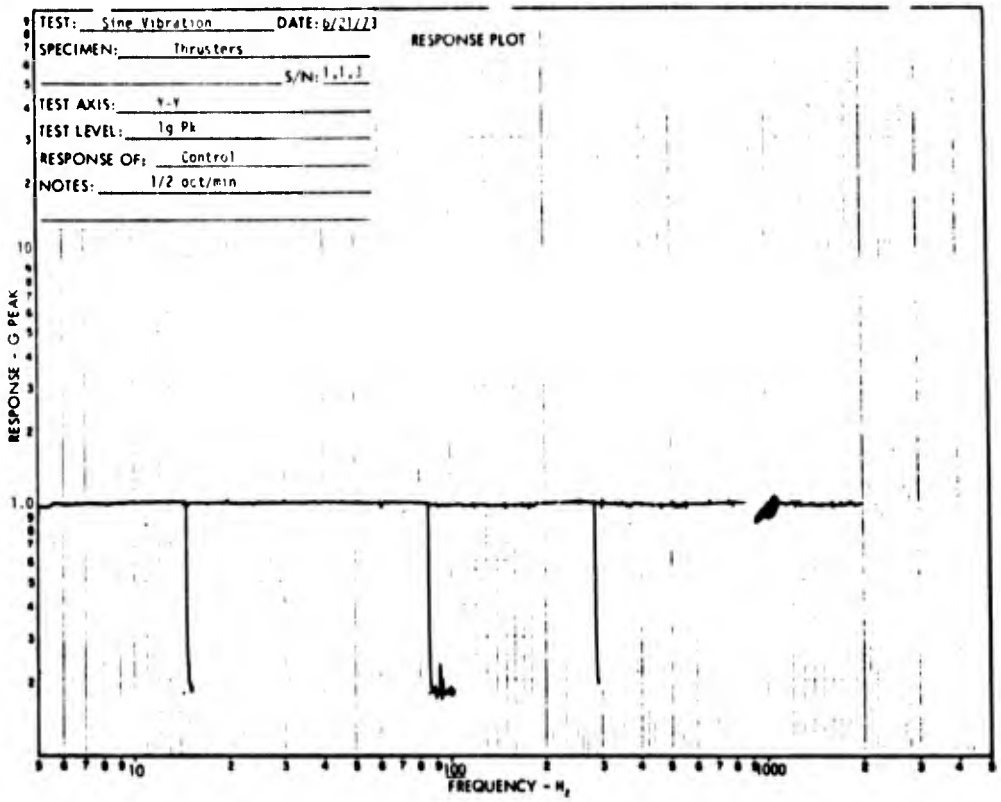

Figure 5-7. Accelerometer Data - Y-Y Sine

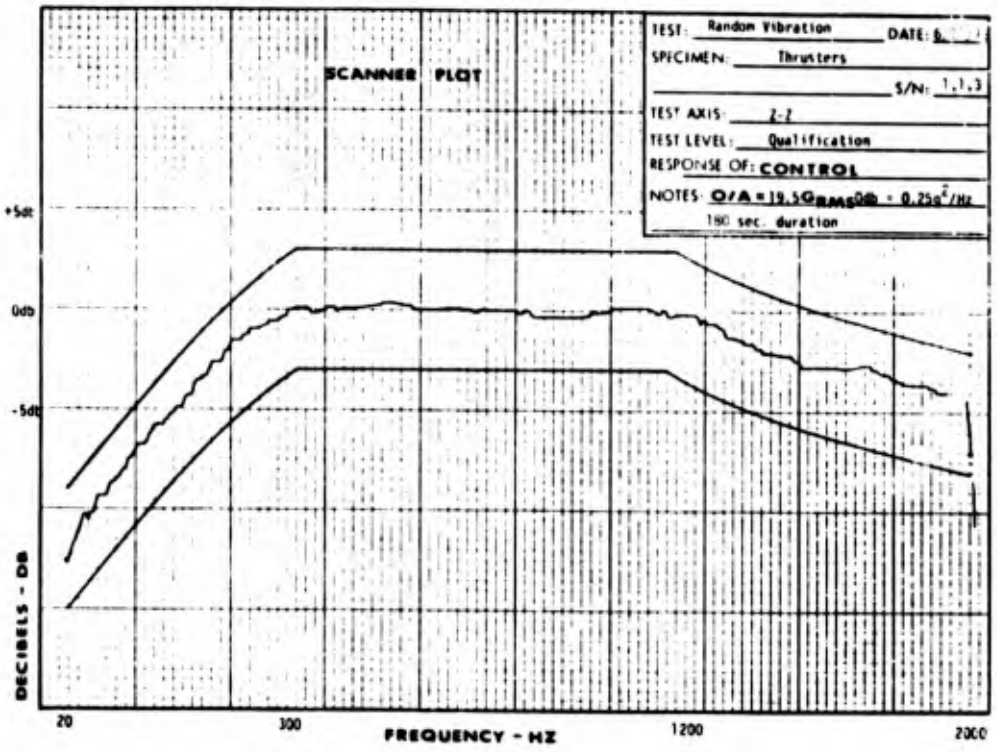

Figure 5-8. Accelerometer Data - Z-Z Random

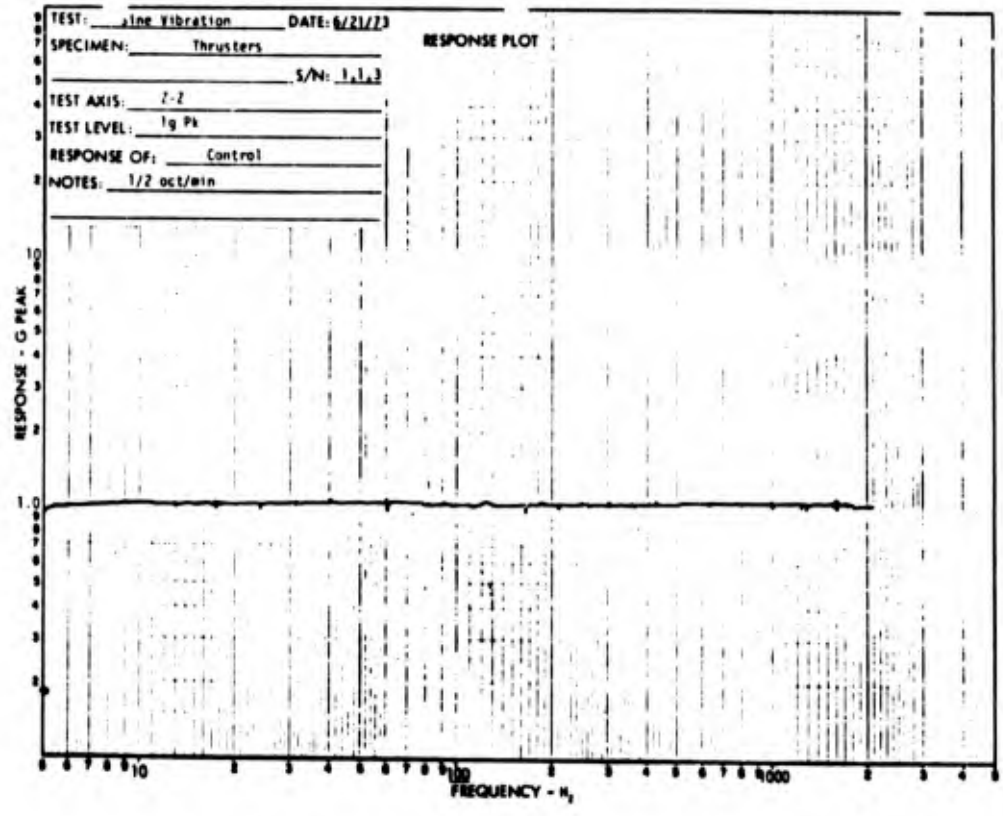

Figure 5-9. Accelerometer Data - Z-Z Sine

Examination of the valve inlet and separated inlet tube revealed that the tube had fractured. The tube had been EB welded to the end plate of the valve from the back side, and the fracture appeared to occur at the bottom of the weld penetration. This is deemed a minor problem with the valve which would readily be correct for any future application. TIG welding was then utilized to re-attach the valve inlet, maintaining an argon purge and minimizing heat input to the valve.

Proof pressure and internal and external leakage tests were then successfully completed, verifying that the unit was ready to continue the test program.

5.3 DUTY CYCLE DEMONSTRATION

The engine was installed on the thrust stand as for the acceptance test, including the radiant heater and GN_2 coolant purge. Vacuum was attained and then maintained continuously for 9 weeks, 2 weeks beyond the end of the duty cycle. The planned duty cycle was as presented in Tables 5-3 and 5-4, with every test sequence to start at 210 $\pm$10°F. As indicated in Table 5-4, digital data was scheduled to be acquired at approximately 25,000 pulse increments and/or every 50 ambient starts.

The test was conducted essentially as planned, except that 37 extra ambient starts were accumulated. Minor problems with the data acquisition system and/or other test problems resulted in repeating certain tests. Tests were added at the start, middle, and end of the duty cycle to obtain oscilloscope photographs of pulse sweeps. The total accumulated life on the engine is summarized in Table 5-5.

Table 5-3. Duty Cycle Definitions

DUTY CYCLE A

Sequence*	On Time (msec)	Off Time (msec)	No. of Pulses
a	20	980	100
b	20	480	100
c	50	950	100
d	50	450	100
e	100	900	100
f	150	850	100
g	10 sec	Steady-State	1

*Propellant feed temperature is 40°F ±5°F

DUTY CYCLE B

Sequence*	On Time (msec)	Off Time (msec)	No. of Pulses
a	20	980	500
b	20	480	500
c	50	950	500
d	50	450	500
e	100	900	500
f	150	850	500
g	1 min	Steady-State	1

DUTY CYCLE C

Sequence*	On Time (msec)	Off Time (msec)	No. of Pulses
a	100	900	1000
b	10 sec	Steady-State	1

*Propellant feed temperature is 40°F ±5°F

TEST NO.	DUTY CYCLE (Table 4-8)	STATIC FEED PRESSURE (PSIA) 100	225	350	CUMULATIVE Ambient Starts	Cycles	DIGITAL DATA
1	10 sec steady-state			X	1	1	X
	10 sec steady-state		X		2	2	X
	10 sec steady-state	X			3	3	X
2	A			X	10	604	X
	A		X		17	1205	X
	A	X			24	1806	X
3	B			X	31	4807	X
	B		X		38	7808	X
	B	X			45	10,809	X
4	C			X	47	11,810	
	C		X		49	12,811	
	C	X			51	13,812	
5	Repeat Test No. 4, 8 times				99	37,836	
6	Repeat Test No. 4				105	40,839	X
7	Repeat Test No. 4, 4 times				129	52,851	
8	Repeat Test No. 2				150	54,654	X
9	Repeat Test No. 4, 9 times				204	81,681	
10	Repeat Test No. 4,				210	84,684	X
11	Repeat Test No. 4, 5 times				240	99,699	
12	Repeat Test No. 2				261	101,502	X
13	Repeat Test No. 4, 6 times				297	119,520	
14	Repeat Test No. 4				303	122,523	X
15	Repeat Test No. 4, 8 times				351	146,547	
16	Repeat Test No. 4				357	149,550	X
17	Repeat Test No. 2				378	151,353	X
18	Repeat Test No. 4, 7 times				420	172,374	
19	Repeat Test No. 4				426	175,377	X
20	Repeat Test No. 4, 9 times				480	202,404	
21	Repeat Test No. 2, 2 times				522	206,010	X
22	Repeat Test No. 1				525	206,013	X
23	60 Sec. steady-state	X	X	X	528	206,016	X

Table 5-4. Rocket Engine Assembly Demonstration Test Duty Cycle

Table 5-5. Engine Test Summary

Total Ambient (200°F) Starts	566
Total Pulses	210,098
Total Steady-State	2,646 seconds
Total ON Time	23,941 seconds
Total Propellant Thruput	431 pounds

Engine performance at the beginning and end of the duty cycle is summarized in Figures 5-10 through 5-13. The thrust shift which resulted from the duty cycle test is nominally 15% and 27% at high and low propellant inlet pressures respectively. Thrust level and ISP versus life are presented in Figures 5-14 and 5-15 for three inlet pressures, and Figures 5-16 and 5-17 summarize pulse mode life trends. A second order, least squares fit, was used to curve fit the data. Additional data are presented in Appendices A and B. The specific test sequence and the data obtained are tabulated and plots presented where applicable.

Typical characteristics of the engine at the start, middle, and end of the duty cycle are shown via oscilloscope photos in Figure 5-18. The pressure overshoots, which appear at the end of the duty cycle, started occurring on a few pulses during the warmup transient after approximately 100 ambient starts. After nearly 500 ambient starts, random pressure overshoots occurred after thermal equilibrium had been attained. The frequency of the overshoots increased until they occur on nearly every pulse. It is noteworthy that even though the pressure overshoots are occurring, the slope of the life plots at the end of the duty cycle indicate much greater life capability still remaining.

In parallel with the RCHE effort, TRW fabricated and tested an unheated IR and D thruster of the RCHE design (less RHU ports). All starts on this engine were controlled to 70°F $\pm$20, and only chamber pressure data were obtained. The overall shift in performance characteristics at the end of the duty cycle is essentially the same as the RCHE. The analog data, as summarized in Figure 5-19, revealed fewer pressure overshoots, of lower magnitude, of the duty cycle, however.

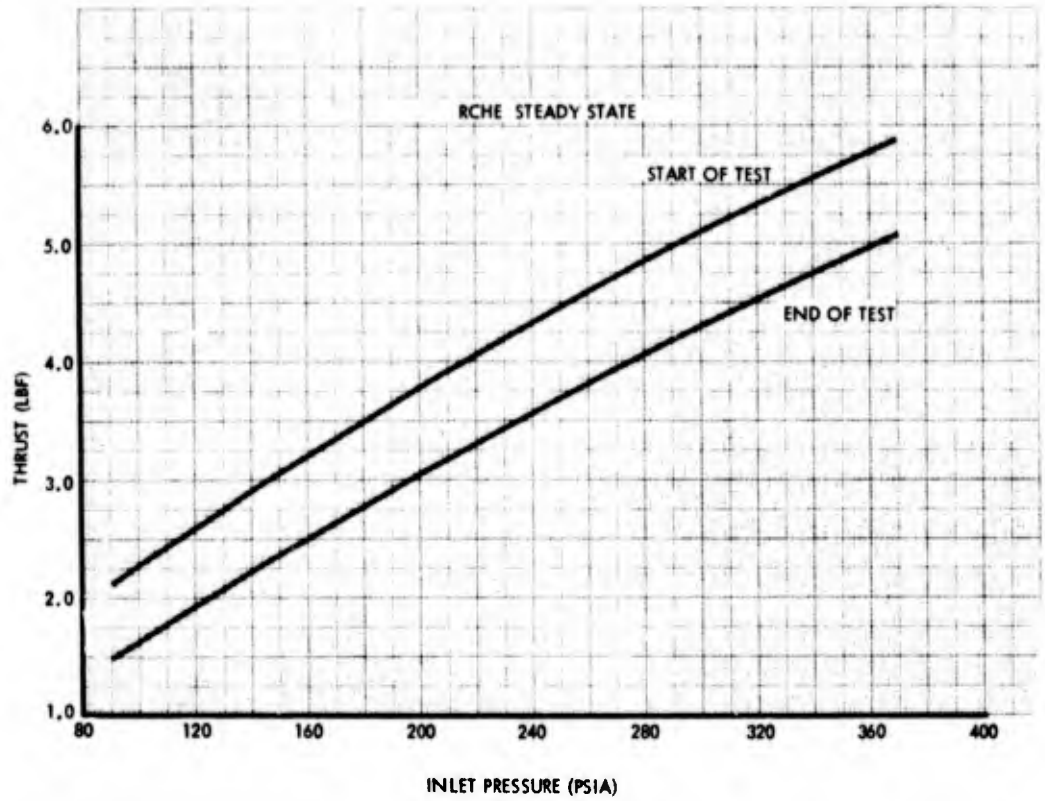

Figure 5-10. Steady-State Thrust vs Inlet Pressure

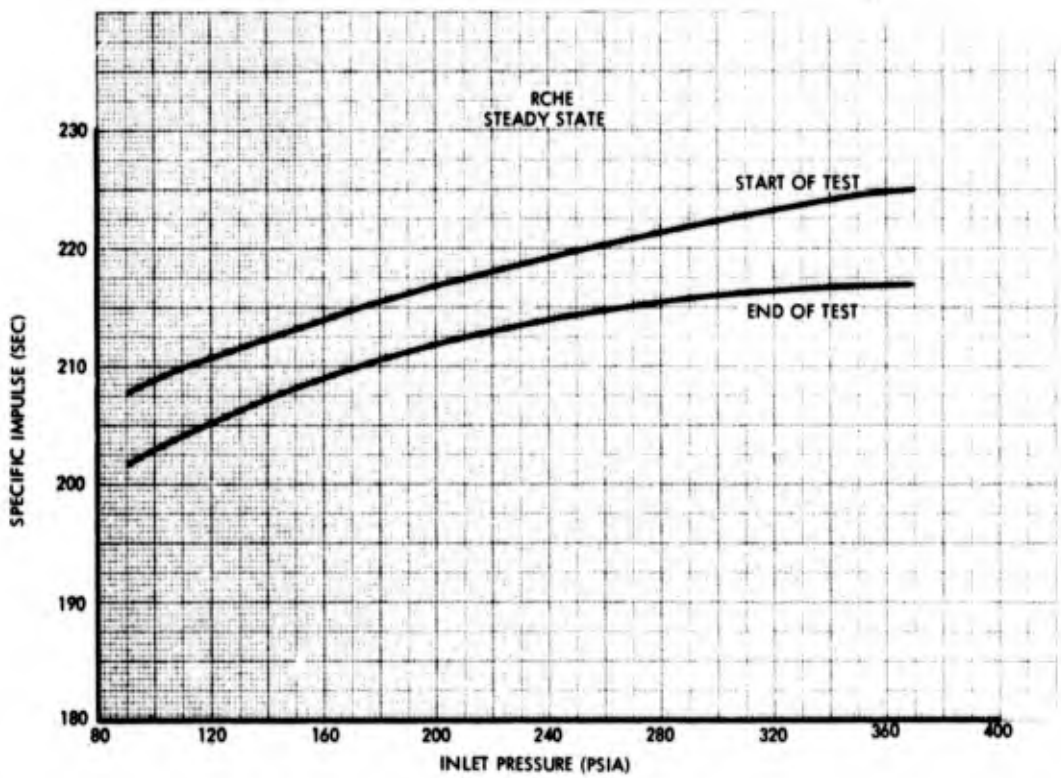

Figure 5-11. Steady-State Specific Impulse vs Inlet Pressure

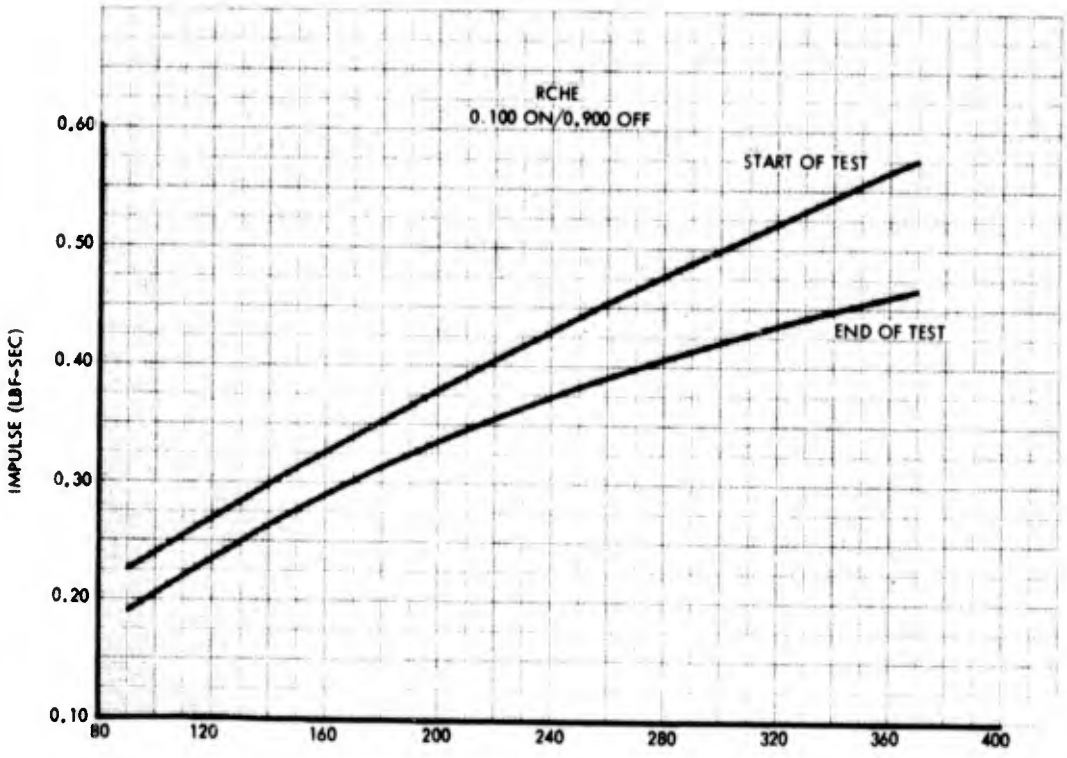

Figure 5-12. Impulse vs Inlet Pressure

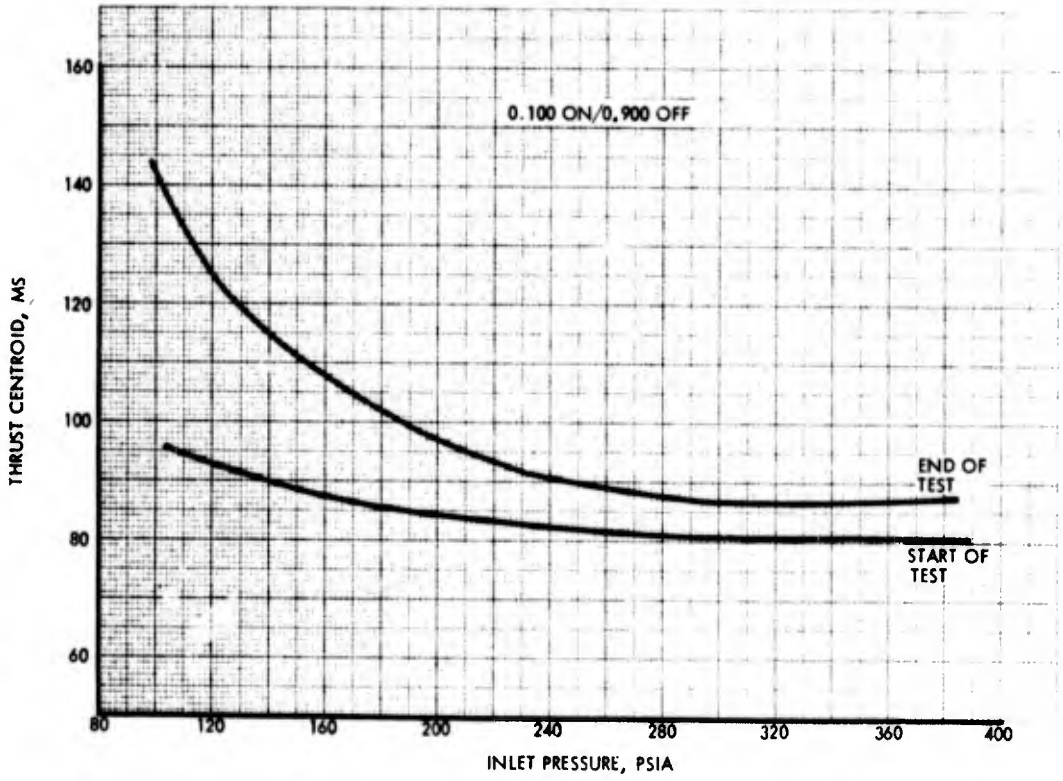

Figure 5-13. Pulse Centroid vs Inlet Pressure

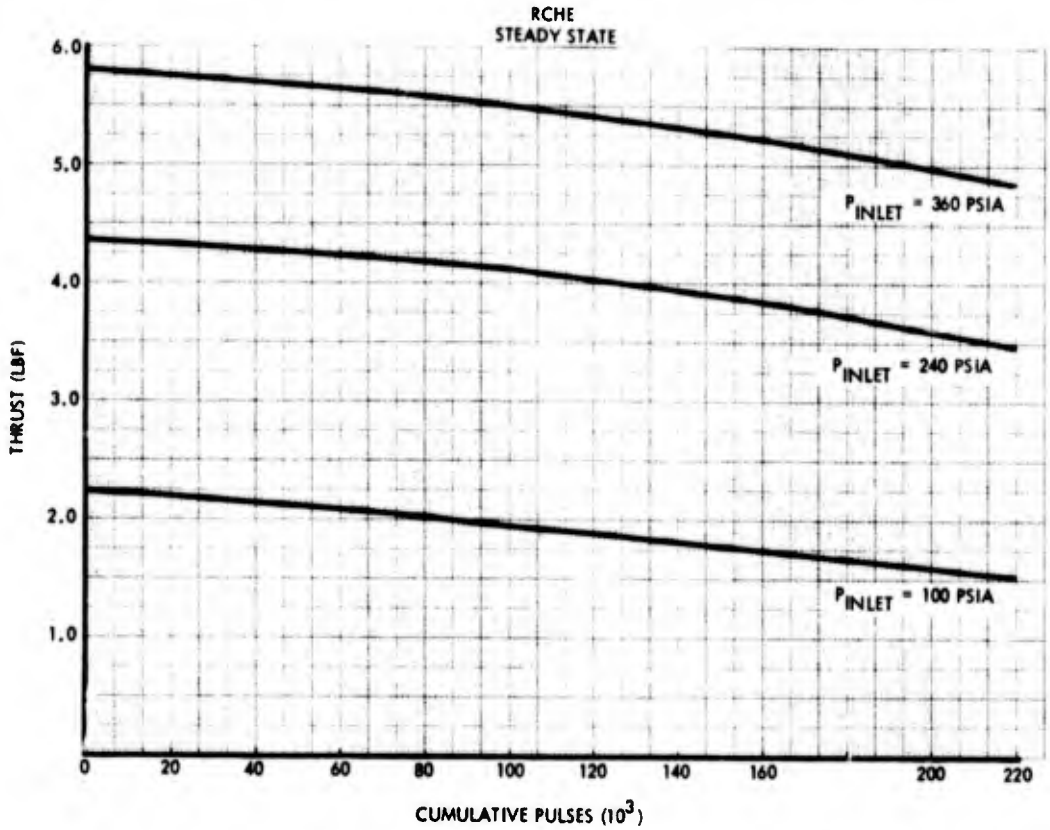

Figure 5-14. Thrust vs Life

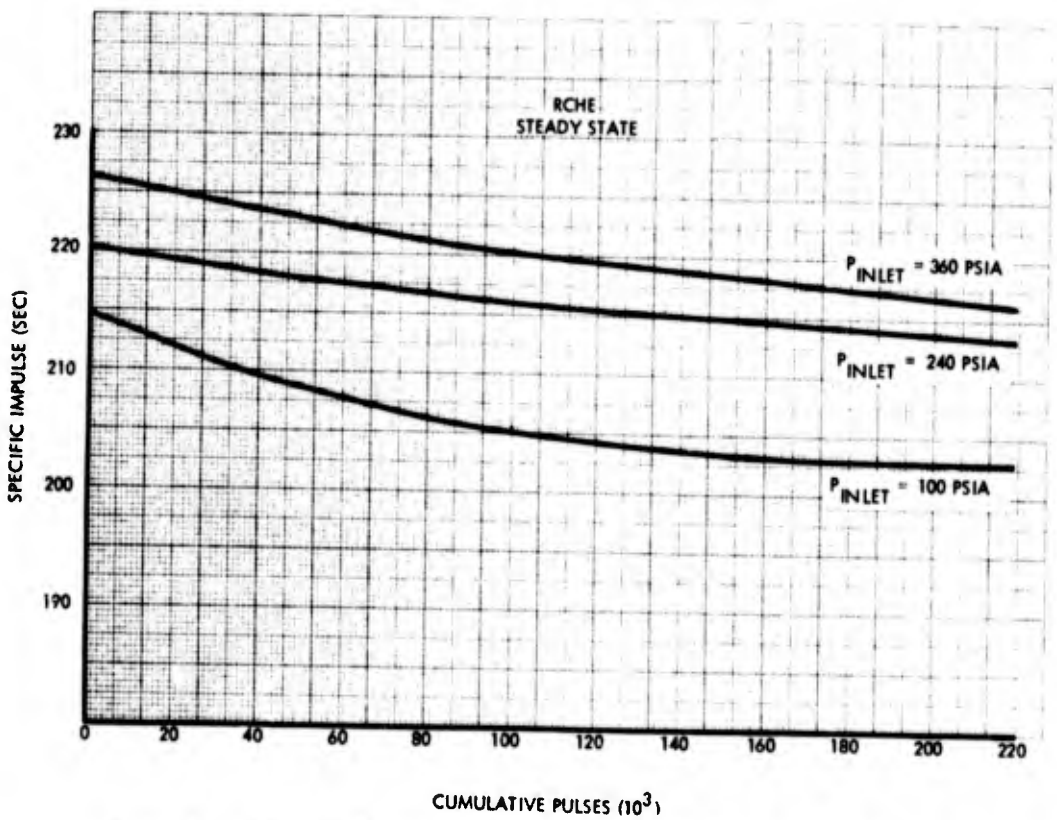

Figure 5-15. Steady-State Specific Impulse vs Life

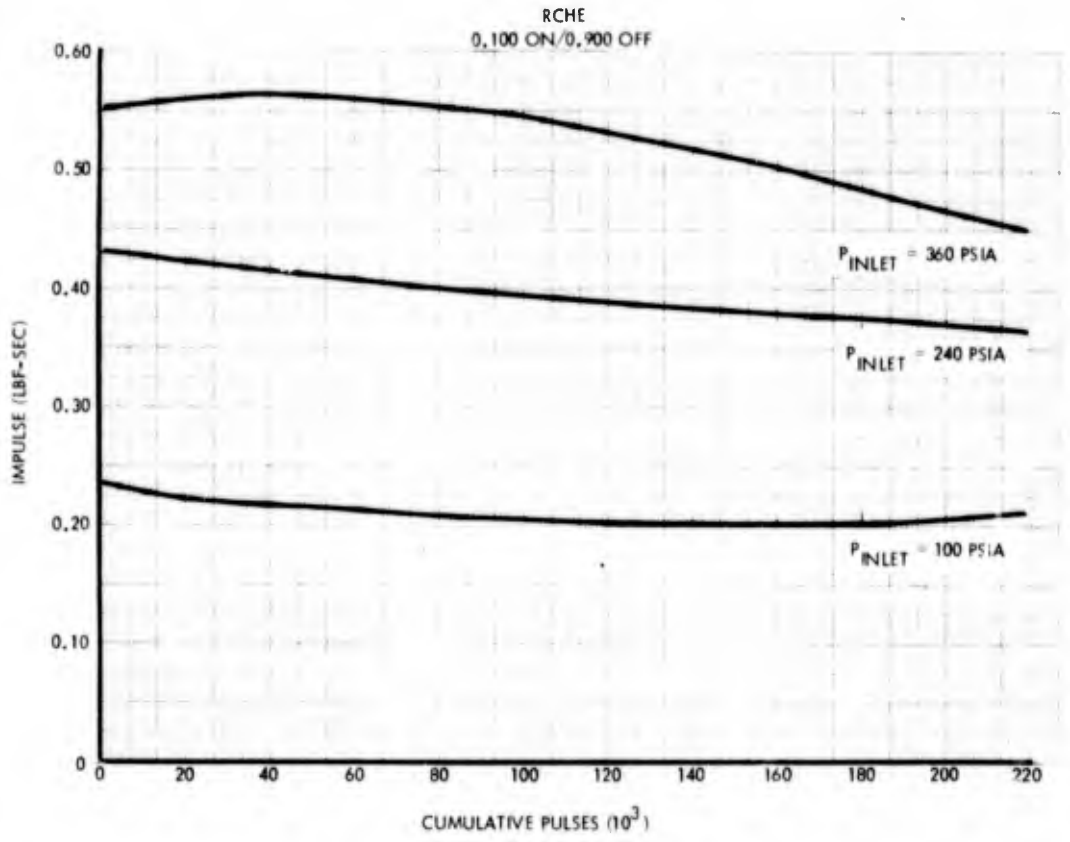

Figure 5-16. Impulse vs Life

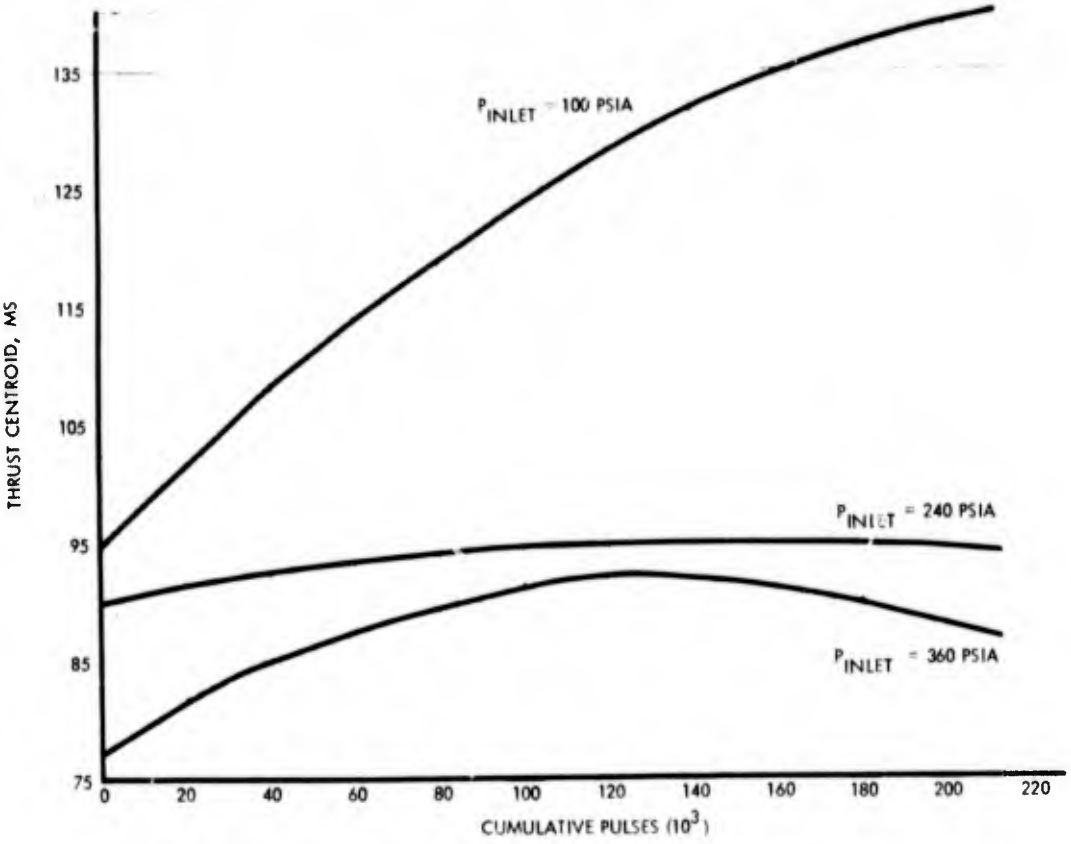

Figure 5-17. Pulse Centroid vs Life

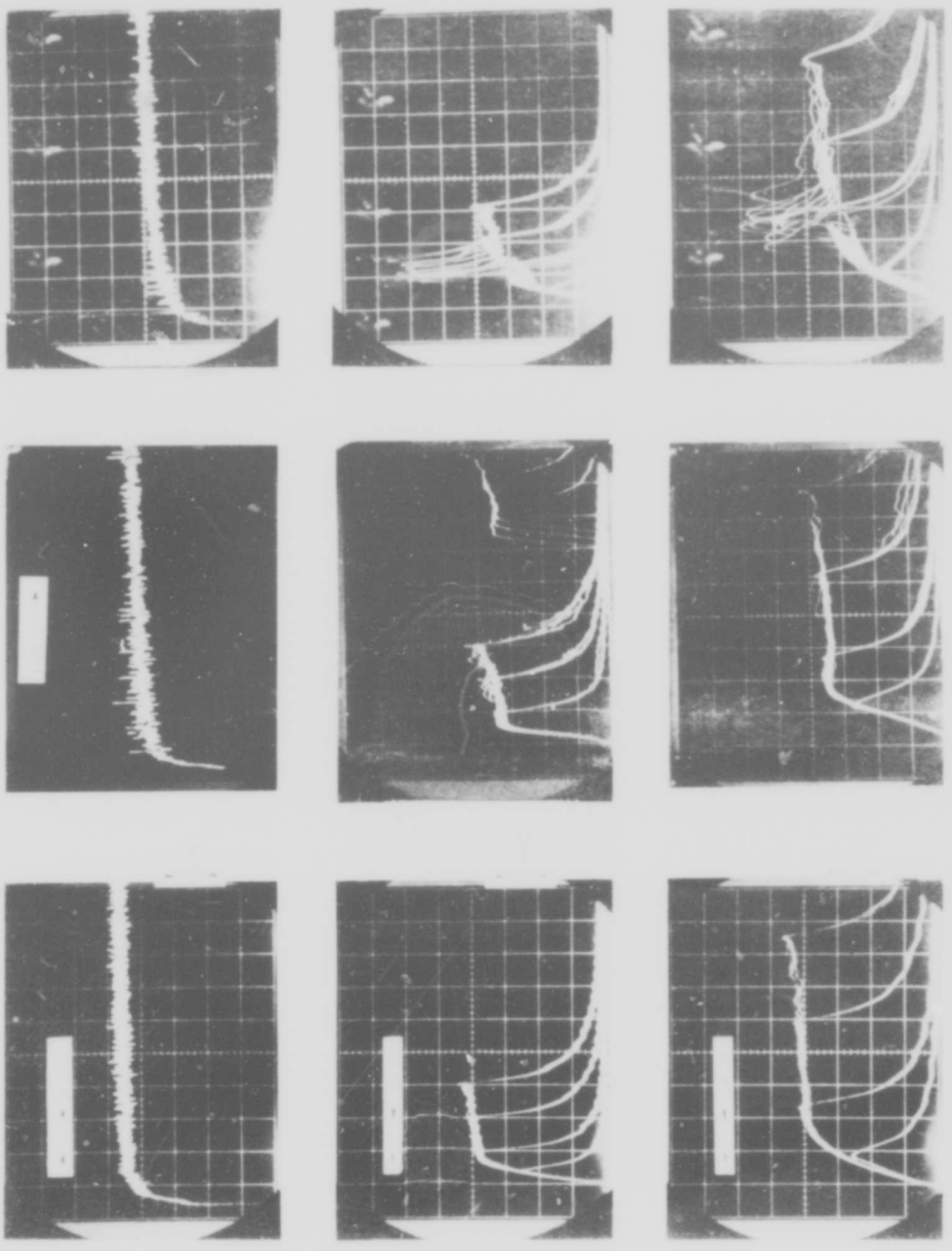

Figure 5-18. RCHE Analog Characteristics

Data shown at 350 psia inlet pressure

Tests shown consist of a 10 second steady-state firing (first picture) followed by a single test varying the pulse width (on time) from 0.150 to 0.020 second on (second picture) and then from 0.020 to 0.150 second on (third picture) at a constant pulse rate of one per second. Five pulses at each pulse width are shown in each picture.

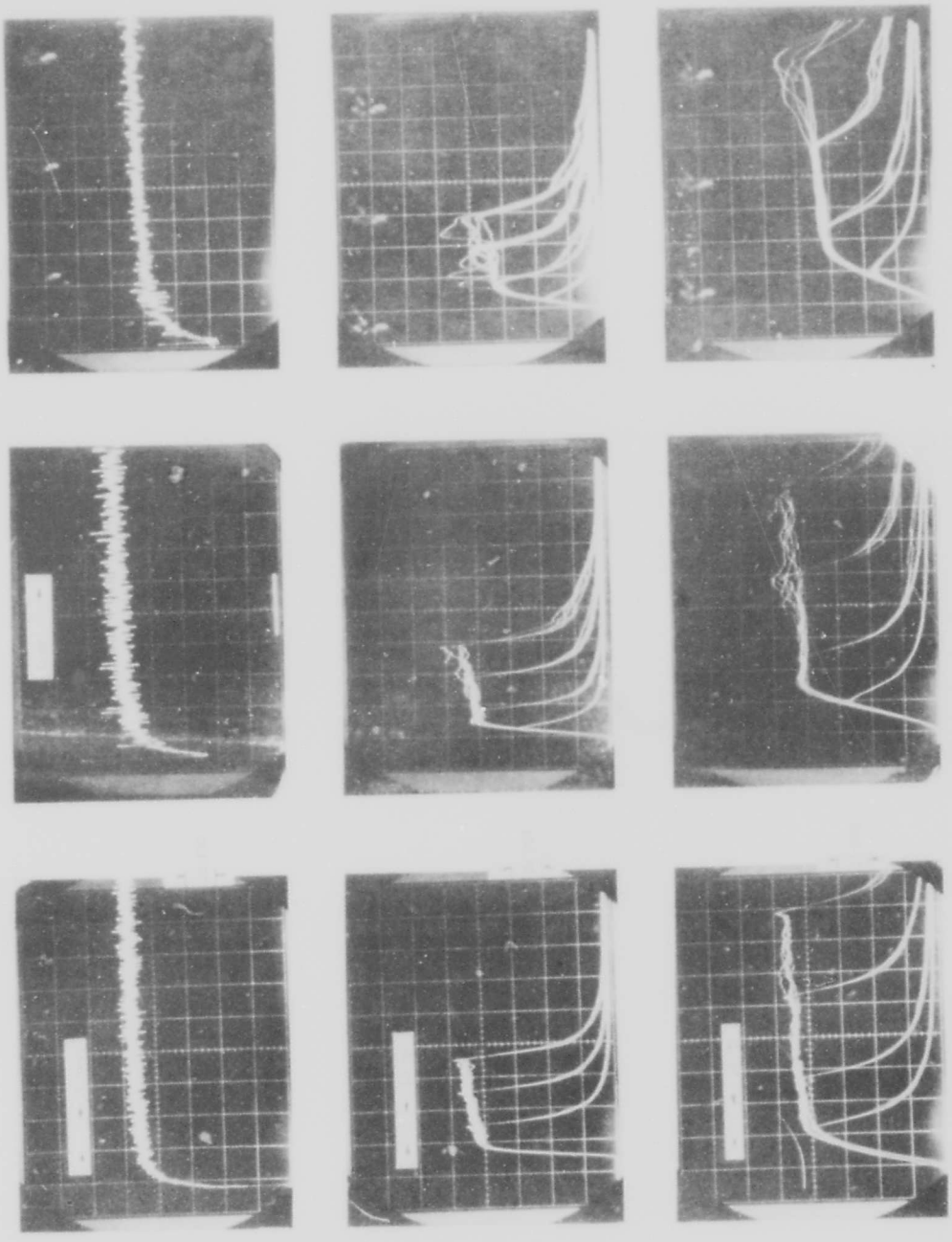

Figure 5-19. XMRE-5 Analog Characteristics

Data shown at 350 psia inlet pressure

Tests shown consist of a 10 second steady-state firing (first picture) followed by a single test varying the pulse width (on time) from 0.150 to 0.020 second on (second picture) and then from 0.020 to 0.150 second on (third picture) at a constant pulse rate of one per second. Five pulses at each pulse width are shown in each picture.

6. POST TEST EXAMINATIONS

Post test condition of the RCHE was evaluated via weight, X-ray, and disassembly of the thrust chamber. The IR and D thruster condition was similarly evaluated.

The quantity of catalyst loaded in the engines was 20.6 grams in the RCHE and 20.2 grams in the IR and D engine. The measured weight change of the assemblies, post versus pre-test, was 1.7 and 2.6 grams, respectively. This translates to 8 percent catalyst loss for the RCHE and 13 percent for the unheated IR and D engine.

Examination of the X-rays of the two engines yields results consistent with the weight data. X-rays of the RCHE were somewhat limited due to the mass of the RHU ports, but did show that the catalyst bed was relatively intact. No voids were evident, nor was any deformation of screens. The IR and D thruster X-rays, however, indicate some catalyst loss from the upper catalyst bed.

Electric-discharge machining (EDM) was chosen for disassembly of the RCHE to minimize vibration of the catalyst bed. Isopropyl Alcohol was used as the dielectric fluid for this operation so that any fluid contacting the catalyst could be readily removed. A circular cut was made through the headplate, between the outer periphery of the headscreen and the weld joint to the chamber wall. After the cut was made, the injector and upper catalyst bed were removed. The lower catalyst bed was vacuum dried before removal, however, to eliminate residual alcohol.

The catalyst bed was found in relatively good condition. Some fines were present, but there was no indication of voiding, severe compaction or sintering. All of the catalyst was removed by inverting the chamber and lightly tapping it with a pair of tweezers. Some catalyst was found in the headspace. A hole had formed in the headscreen, apparently allowing penetration of the catalyst. The quantity was very small, however, filling only 10 to 15 percent of the volume and may have entered the headspace after the test. A fracture of the midscreen also occurred, along with a separation of the weld over about one-third of the circumference. The screen had curled toward the injector after fracturing and was thus close enough to the headscreen that it may have been in contact.

A view of the injector, through the hole in the headscreen, is shown (as first removed from the RCHE) in Figure 6-1. This unusual appearance was first interpreted as severe nitriding of the injector, with flakes from inside the flow passage partially blocking the injector orifices. Water flow, however, showed no change in flow characteristics, and the water dissolved and/or removed the deposit responsible for the flakey appearance, leaving the injector as shown in Figure 6-2. A similar appearing deposit results from evaporating the alcohol used as the dielectric for EDM, leaving the metallic particles resulting from the cut. The appearance in Figure 6-1 is thus attributed to this type of deposit from the disassembly operation.

Figure 6-1. RCHE Injector Upon Disassembly (20X Size)

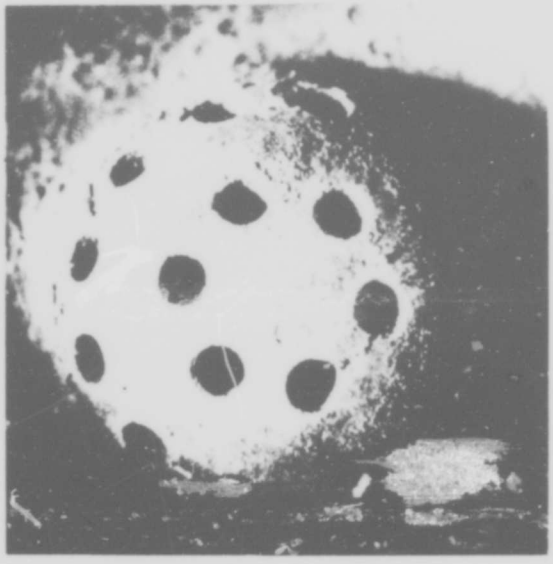

Figure 6-2. RCHE Injector Post Water Flow (20X Size)

The test data were further analyzed to assess the possibility that the above deposit was not from the EDM process, was in-soluble in hydrazine (though soluble in water) and had affected the engine performance. This evaluation showed that the increase to the total pressure drop (thus the thrust shift) was essentially a linear function of flow rate, yielding the conclusion that the thrust shift is the result of increasing catalyst bed pressure drop. Had the shift been due to the injector, it would relate to flowrate squared.

The IR and D thruster was disassembled by making a circumferential cut in the chamber shell slightly below the headplate. During removal of the headplate it was noted that the catalyst bed had settled approximately 0.1 inch below the headplate, indicating about 7% loss of catalyst volume. The condition of the catalyst bed was very similar to that of the RCHE except for the greater loss and, accordingly, a somewhat greater quantity of catalyst fines in the lower bed.

This headscreen also had numerous broken wires with some pieces missing. Figure 6-3 shows the IR and D headscreen and Figure 6-4 shows the RCHE headscreen. A section through one of the headscreen wires is shown in Figure 6-5, showing the nitride penetration along the grain boundaries. The large grain size, relative to the wire diameter, and the nitride penetration result in an extremely brittle and weakened condition. Both the injector and the headscreen retainer exhibited a nitride layer of nominally .001 inch, with much deeper penetration along the grain boundaries. A section through a web of the headscreen retainer is shown in Figure 6-6, midway through the thinner (.020 inch) demension. Nitride penetration along grain boundaries had also occurred here, but the relative size of the grains to the part is such that structural adequacy retained.

Figure 6-3. IR&D Headscreen

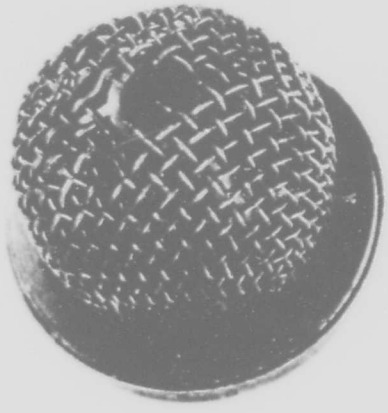

Figure 6-4. RCHE Headscreen

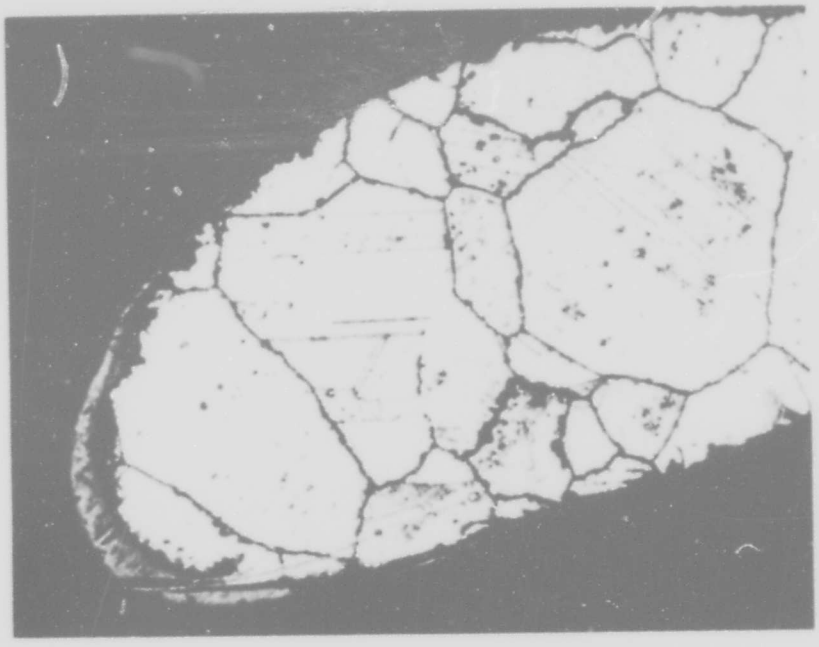

Figure 6-5. Section through Headscreen Wire (315 X)

Figure 6-6. Section through Headscreen Retainer (50 X)

The RHU's were also inspected after the test. They were first removed from their graphite reentry members and visually inspected. There was no apparent damage to the outer surface of the Pt-Rh clad. A test was then conducted to verify that the pressure relief device was releasing the helium generated by the radioisotope decay of the fuel. Each assembly was placed separately into a vacuum chamber which was then connected to a Veeco helium leak detector. The chamber was then evacuated and the helium flow measured. Data recorded during this series of tests are noted in Table 6-1.

Table 6-1.

Unit	Helium Permeation Rate (Std cc/sec)
S/N 234	3.4×10^{-7}
S/N 235	1.1×10^{-7}
S/N 236	2.0×10^{-7}

The helium flow rates recorded indicate that the pressure relief devices are functioning properly.

Post-test sealed source radiography studies were performed to verify the integrity of the capsule components including the radioisotope fuel pucks. Each heat source was exposed to a 2 curie, Cesium-137, sealed source for a period of thirty minutes. The radiographs showed no indication of damage or failure of any of the capsule components. However, one fuel puck, loaded in RHU S/N 235 appeared to be cracked circumferentially resulting in a complete break. A portion of this puck also appears to be fractured at one end.

In conclusion, the RHU's appear to be integral and are functioning normally. The fractured puck in unit S/N 235 does not affect the integrity or function of these heat sources. A smear survey and direct reading alpha radiation monitor detected no evidence of fuel contamination.

7. RELIABILITY AND MAINTAINABILITY

The formal demonstration of specific reliability levels and maintainability characteristics was not a goal of the Integrated Radioisotope Catalytic Monopropellant Hydrazine (RCHE) advanced technology program. However, attainment of the required program goals did require a large number of engine ambient starts and pulses on slightly varying engine configurations even through a large amount of firing time was not generated. The successful completion of a large number of engine ambient starts and pulses on very similar configurations does indicate what reliability levels could be expected from a production program where field utilization missions require a large number of ambient starts and pulses.

Figure 7-1 shows the program test history. All configurations considered similar enough to be representative of the selected configurations for the purposes of reliability evaluation are indicated. Two (2) malfunctions occurred during the applicable engine runs. Both of the malfunctions can be discounted as not chargeable to the engine. One Malfunction (failure at the chamber pressure tap) was a side effect of the goals and practical methods used to make the many hardware changes required during that early phase of the program. This element is an in-process test appendage only that would have no impact on flight hardware. The second failure (valve inlet tube separated from the valve) occurred during vibration testing and is chargeable to the valve and not to the engine. In all the testing only the failure at the chamber pressure tap which occurred early in the development program caused premature shutdown of the engine. The data applicable to reliability evaluation shown on Table 7-1 can be summarized as follows:

TOTAL PROGRAM APPLICABLE DATA FOR RELIABILITY EVALUATION:

1. Total pulses accumulated on all hardware representative of the final design — 1,230,241

2. Total ambient starts accumulated on all hardware representative of the final design. — 626

3. Total pulses accumulated on the final design hardware unit without repair/refurbishment. — 210,000

4. Total ambient starts accumulated on the final design hardware unit without repair/refurbishment. — 566

5.	Total failures experienced on all hardware representative of the final design.	1
6.	Total chargeable failures experienced on all hardware representative of the final design.	0

No chargeable failures in 626 ambient engine starts demonstrates an ambient engine start probability of 0.9950 at a 95% confidence level based on binomial sampling techniques. Likewise, no chargeable failures in 1,230,241 engine pulses demonstrates an engine pulse probability of 0.99999 at a 95% confidence level. Data is not sufficient to make a numerical life expectancy calculation on a single hardware item (i.e., A RCHE is good for 500,000 pulses at a reliability level of X_1 at a confidence level of Y_1 or, a RCHE is capable of 1,000 ambient starts at a reliability level of X_2 at a confidence level of Y_2.) However, condition of the RCHE at teardown after extensive duty cycle testing indicated useable life remaining.

The RCHE is essentially one-piece construction with only the valve being easily removed for maintenance. The following welds are made:

Resistance-welds

Catalyst retainer plate and screens as part of the catalyst loading operations.

EB Welds

Injector assembly (injector, headscreen, and headscreen support) to chamber.

However, the only time dependent (degradating) components on the RCHE other than the valve which can be removed for maintenance are the O-ring seal used for the valve/injector feed tube interface and a Voi-Shan soft seal used at the valve inlet. Therefore, any maintenance required (other than the Valve) is likely to be as a result of usage rather than periodic maintenance required because certain parts have passed their storage capability.

PROGRAM PHASE/HARDWARE CONFIGURATION	TYPE OF TEST	NUMBER OF PULSES AND AMBIENT STARTS	ALLOWABLE DATA FOR RELIABILITY EVALUATION	FAILURES/CHARGEABLE FAILURES	COMMENTS
Thruster Development					
A. Baseline 5-lb_f thrust Engine.	Hot-Firing Tests	*A large number of pulses were accumulated but not formally recorded.	No	*0/0	Selected 18 to 20 mesh catalyst for the upper bed.
A-1 Bolt-up thruster configuration allowing parametrical evaluation of variations of injector, headscreen, and catalyst mesh size for the upper catalyst bed.					
A-2 Final injector/upper catalyst bed configurations per A-1. Evaluations of variations to lower catalyst bed.	Accelerated Life Tests	83,600 pulses (0.020, 0.050, 0.100, and 0.150 second on times) at *4 pulses per second.	Yes	*1/0	Used 20 to 30 mesh catalyst for lower bed. Disassembly revealed deformation of the headscreen.
		134,740 pulses (0.020, 0.050, 0.100, and 0.150 second on times) at *4 pulses per second.	Yes	0/0	Used 18 to 20 mesh catalyst for lower bed. Disassembly revealed deformation of the headscreen.
A-3 Headscreen Evaluation Tests. Added headscreen retainer and designed two alternate injectors.	Special Accelerated Life Tests				Headscreens were changed from 40X40 mesh, .009 wire diameter to 30X30 mesh, .010 wire diameter.
	Injector F	80,000 pulses	No	0/0	40 mesh headscreen.
	Injector E		No	0/0	
	Injector D	80,000 pulses	Yes	0/0	40 mesh headscreen
		80,000 pulses	Yes	0/0	30 mesh headscreen
		280,000 pulses	Yes	0/0	30 mesh headscreen
		80,000 pulses	Yes	0/0	30 mesh headscreen with retainer
		280,000 pulses	Yes	0/0	30 mesh headscreen with retainer
RCRE Design					
Final design features: (1) Configured for optimum injector/catalyst bed, (2) RHU's integrally packaged, (3) Improved capsule for earth orbit nuclear safety.	Acceptance Tests				
	Proof Pressure Test. Leak Test (external/internal (valve)	0	Yes	0/0	
	Hot Fire Test	1803 (including 21 ambient starts)	Yes	0/0	
	Vibration	0	Yes	1/0	Valve inlet tube separated from the valve.
	Proof Pressure Test. Leak (external/internal (Valve) Test.	0	Yes	0/0	These tests (Proof Pressure and Leakage) required to verify fix of valve inlet tube failure
	Duty Cycle Demonstration.	210,098 pulses (including 565 ambient starts)	Yes	0/0	Life plots of test data indicate much greater life capability remaining. Post test examination showed: A 8% catalyst loss, the catalyst bed was relatively intact, no voids evident, no deformation of screens, catalyst bed in good condition, few fines present, no indication of voiding, severe compaction or sintering, a hole was found in the headscreen, midscreen fractured, and separation of the weld over about 1/3 of the circumference.

TOTAL PROGRAM APPLICABLE ALLOWABLE DATA FOR RELIABILITY EVALUATION:

1.	Total pulses accumulated on all hardware representative of the final design	1,230,261
2.	Total ambient starts accumulated on all hardware representative of the final design	626
3.	Total pulses accumulated on the final design hardware unit without repair/refurbishment.	210,000
4.	Total ambient starts accumulated on the final design hardware unit without repair/refurbishment.	566
5.	Total failures experienced on all hardware representative of the final design.	1
6.	Total chargeable failures experienced on all hardware representative of the final design	0

*The goals of the thruster development program in this phase were not conducive to the tracking of thruster pulse accumulation. The thrusters were tested, changed slightly and tested again through many variations to obtain the optimum injector, headscreen, and catalyst mesh size. Normal production phase aerospace hardware handling procedures would have been inefficient and a hinderance to the goals of this phase of the program. The hardware therefore was subjected to handling abuse far in excess of what would be experienced in a qualification or production program. It is highly probable that the failure of the chamber pressure tap during the Accelerated Life Tests was at least contributed to by the excessive rough handling it had experienced. Therefore, this failure is considered non-chargeable to the basic design.

Figure 7-1. Test/Failure Program History

8. CONCLUSIONS

This program successfully demonstrated the integration of radioisotope heat sources into a catalytic hydrazine engine. Over 210,000 pulses were accumulated, with 565 "ambient" temperature starts and with indications of much greater life capability. Comparison of the test results of 200°F versus 70°F "ambient" starts indicates that to the extent of the test conducted, the headspace type thruster performance is not sensitive to the difference. Post test hardware condition, however, reveals greater catalyst attrition in the 70°F engine. Had the test been more extensive, therefore, the heated engine would most likely demonstrate a greater ultimate life capability.

Nitriding of the Haynes Alloy 25 (L605) headscreens and midscreens yielded several broken wires in both engines. Nitriding of other elements of the engine was less severe and no material problems are anticipated for much more extensive duty cycles. A material change is recommended for the screens, however, to increase the life capability.

Both 5-pound engines demonstrated less sensitivity to ambient temperature starts than other existing TRW flight qualified designs. The mode of degradation with life is also consistent, showing a gradual increase in catalyst bed pressure drop yielding a reduced thrust level.

APPENDIX A
ADDITIONAL TEST DATA

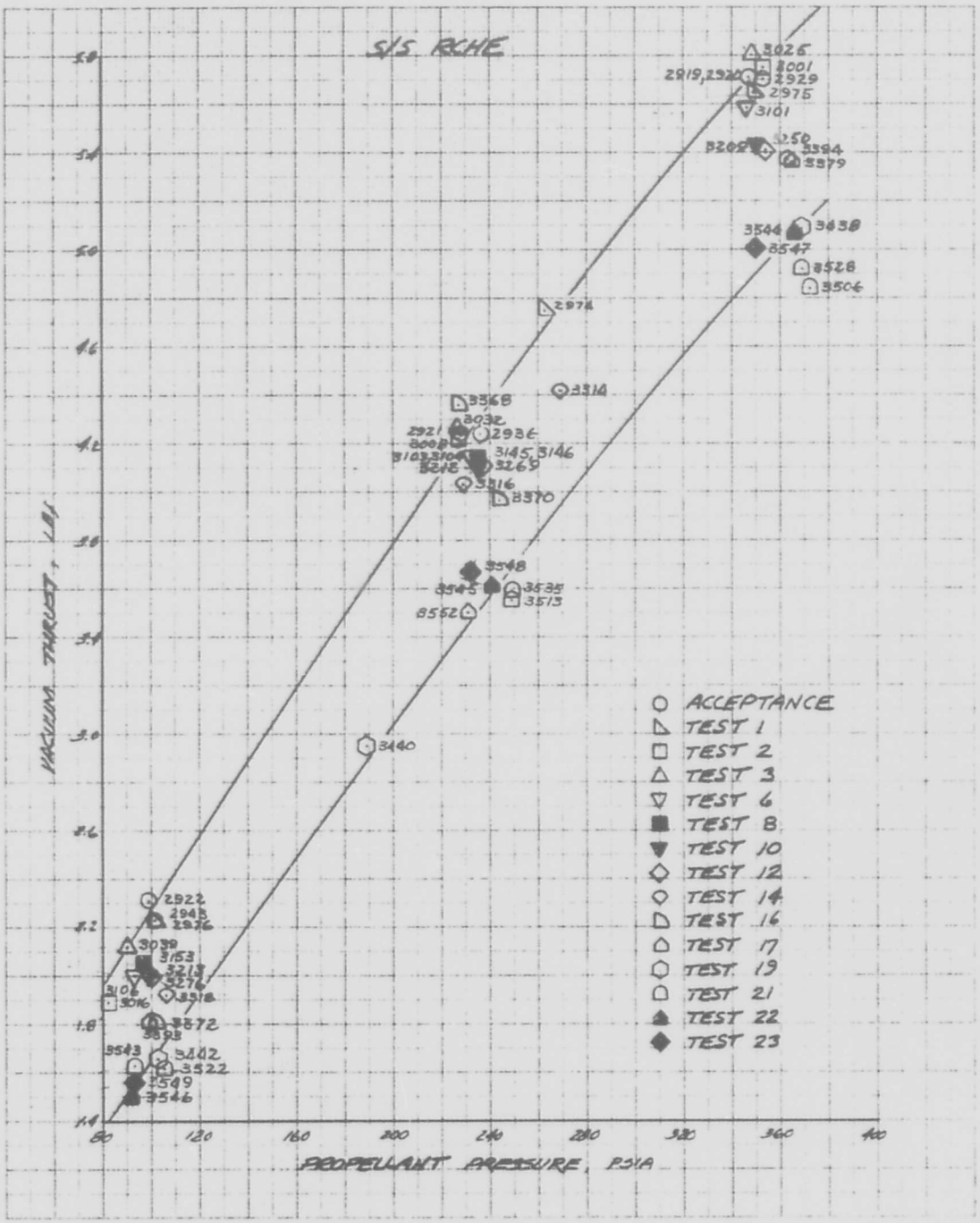
S/S RCHE
VACUUM THRUST, LBF
PROPELLANT PRESSURE, PSIA
ACCEPTANCE
TEST 1
TEST 2
TEST 3
TEST 6
TEST 8
TEST 10
TEST 12
TEST 14
TEST 16
TEST 17
TEST 19
TEST 21
TEST 22
TEST 23

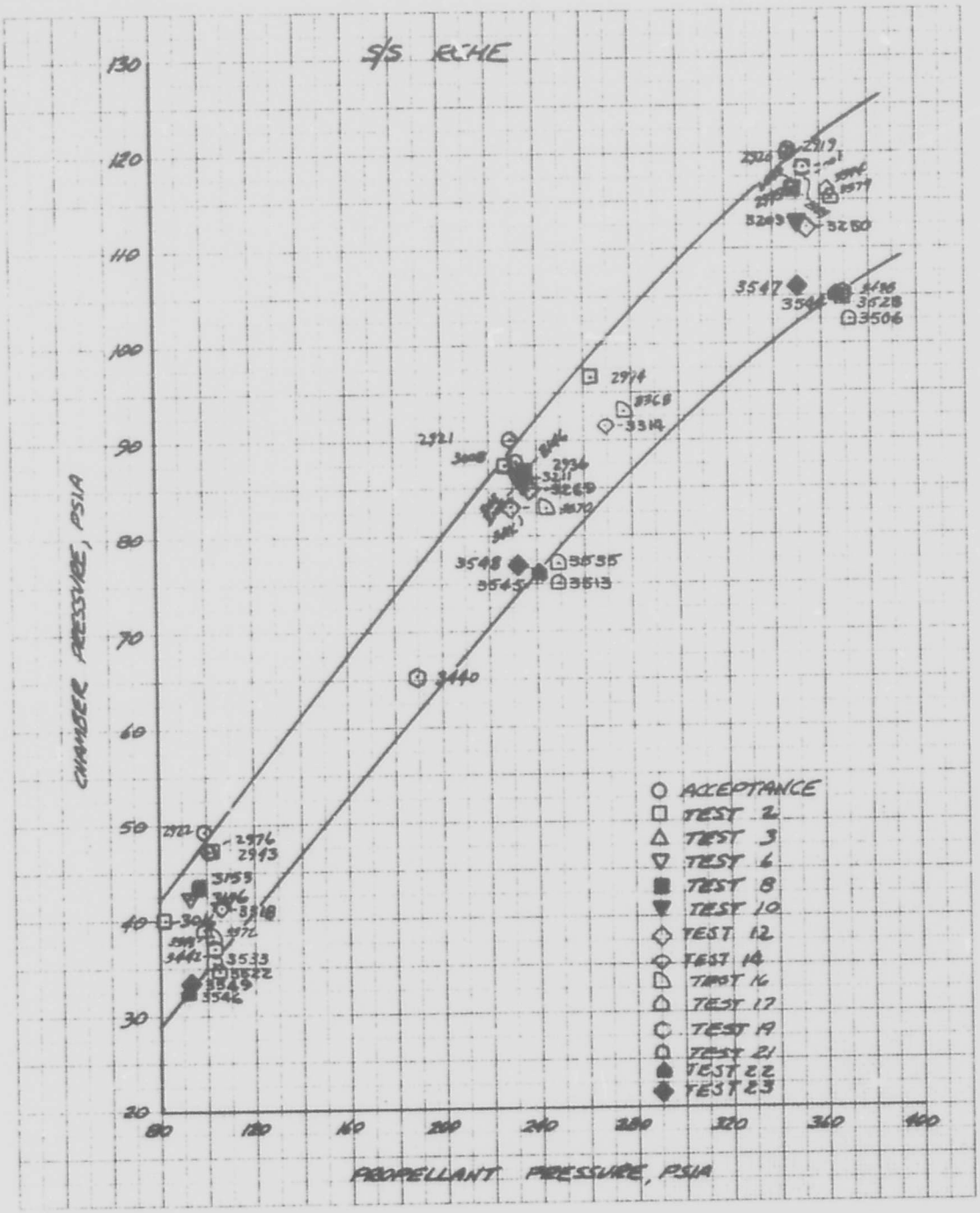
S/S ECHE
CHAMBER PRESSURE, PSIA
PROPELLANT PRESSURE, PSIA
130
120
110
100
90
80
70
60
50
40
30
20
80
120
160
200
240
280
320
360
400
ACCEPTANCE
TEST 2
TEST 3
TEST 6
TEST 8
TEST 10
TEST 12
TEST 14
TEST 16
TEST 17
TEST 19
TEST 21
TEST 22
TEST 23

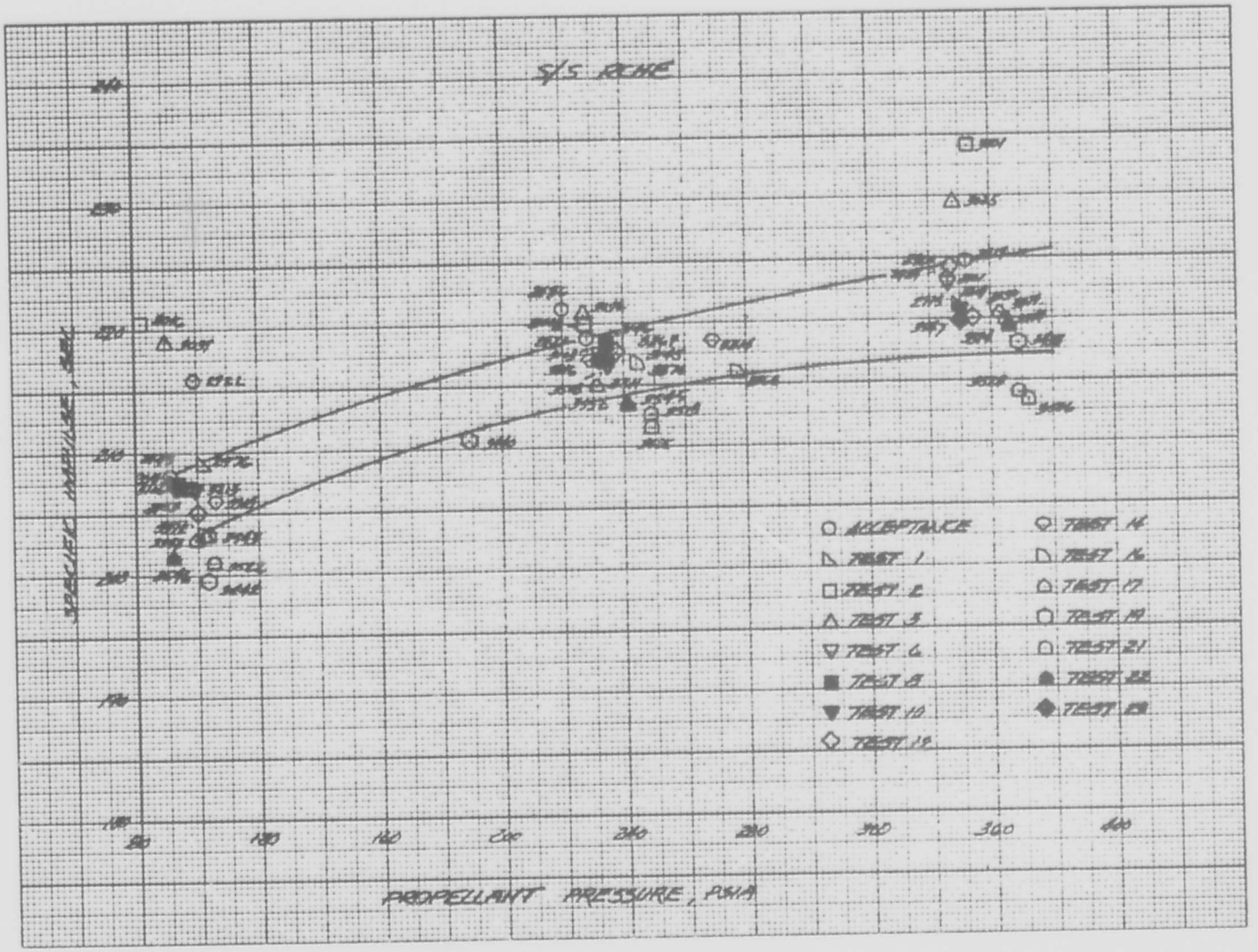
S/S ARCAIR
PROPELLANT PRESSURE, PSIA
ACCEPTANCE
TEST 1
TEST 2
TEST 3
TEST 4
TEST 5
TEST 10
TEST 12
TEST 14
TEST 16
TEST 17
TEST 19
TEST 21
TEST 22
TEST 23

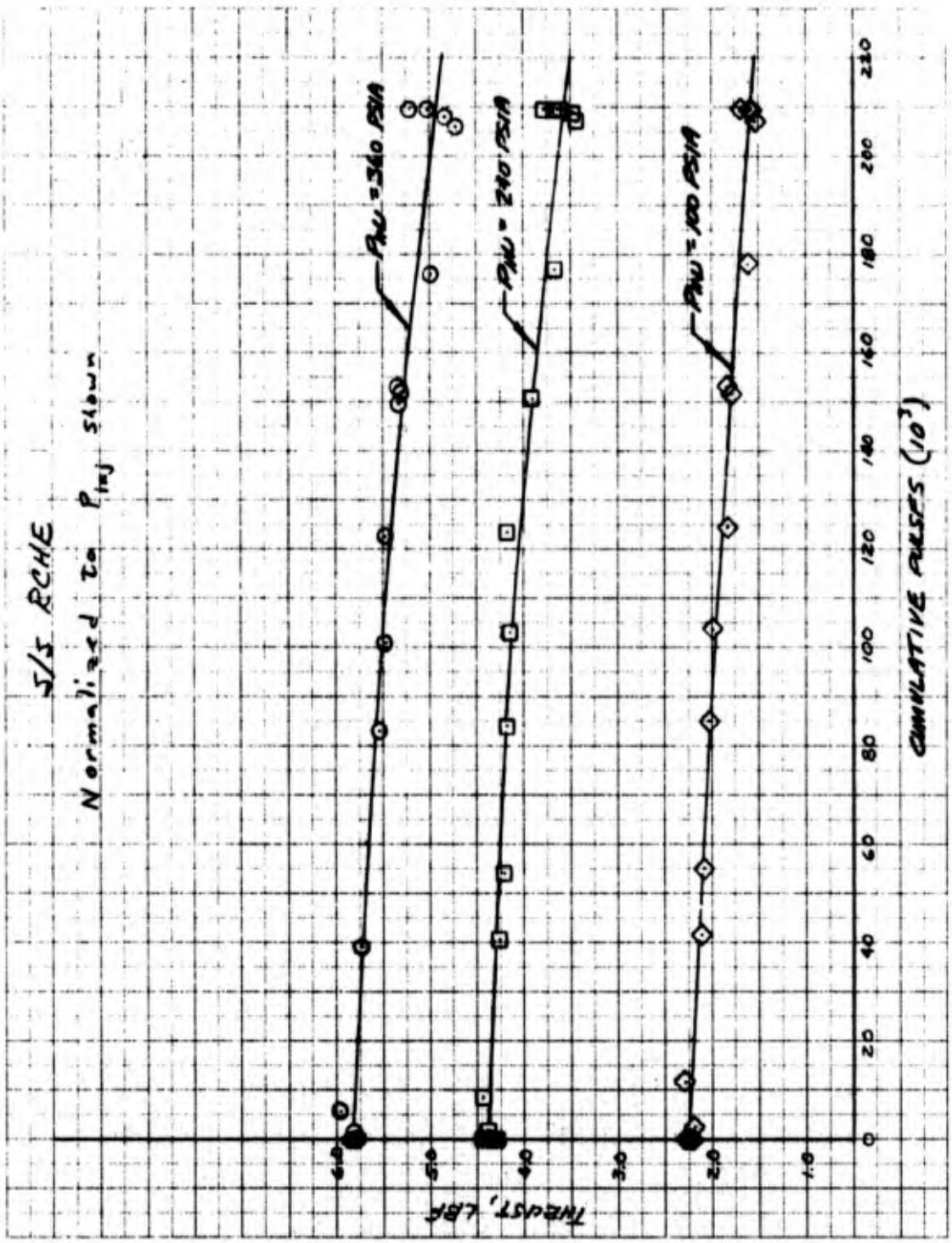
S/S RCHE
Normalized to P_{inj} shown
P_{INJ} = 340 PSIA
P_{INJ} = 240 PSIA
P_{INJ} = 100 PSIA
THRUST, LBF
CUMULATIVE PULSES (10^3)
0
20
40
60
80
100
120
140
160
180
200
220
1.0
2.0
3.0
4.0
5.0

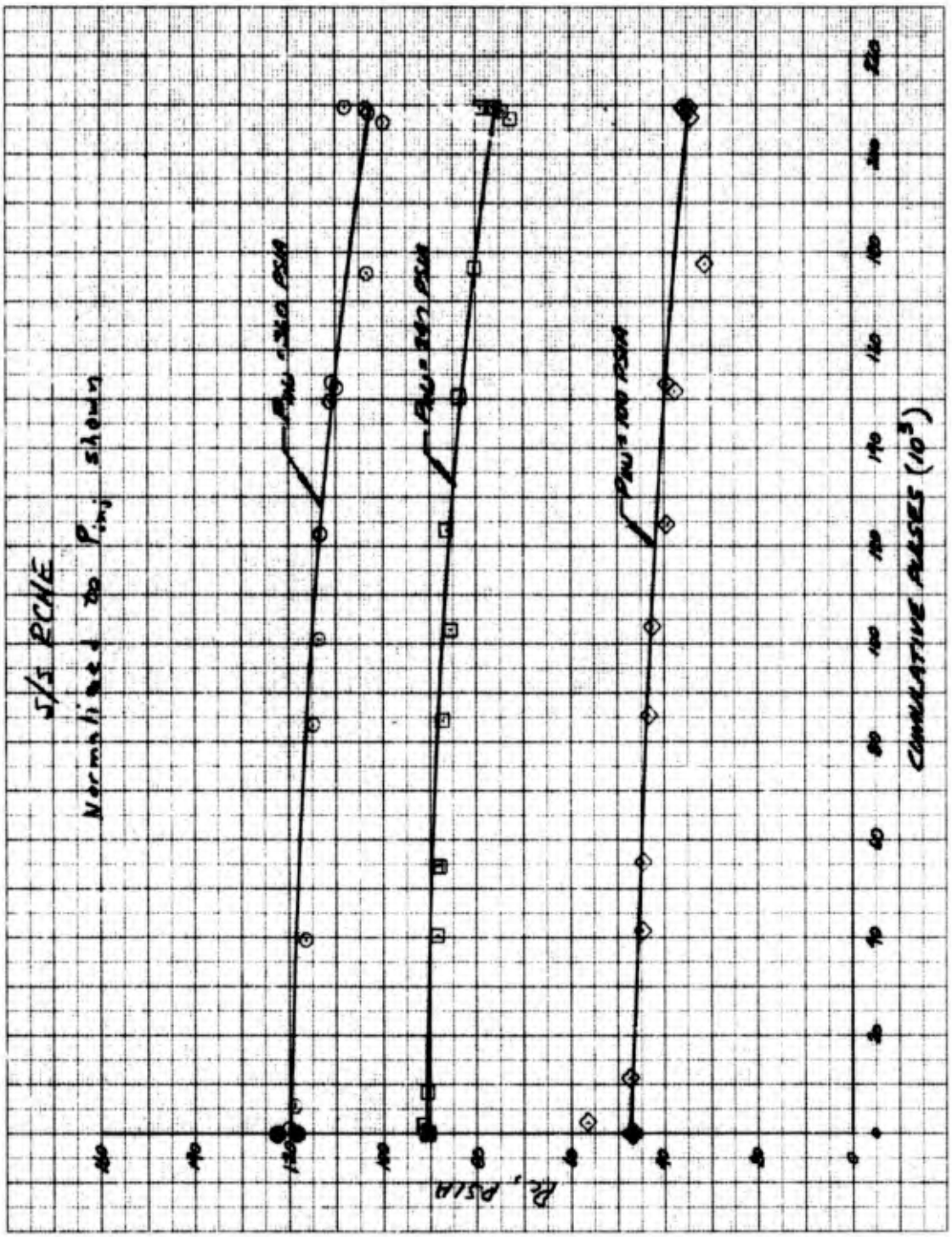
S/S ECME
Normalized to P_{inj} shown
R_c, PSIA
CUMULATIVE PULSES (10^3)

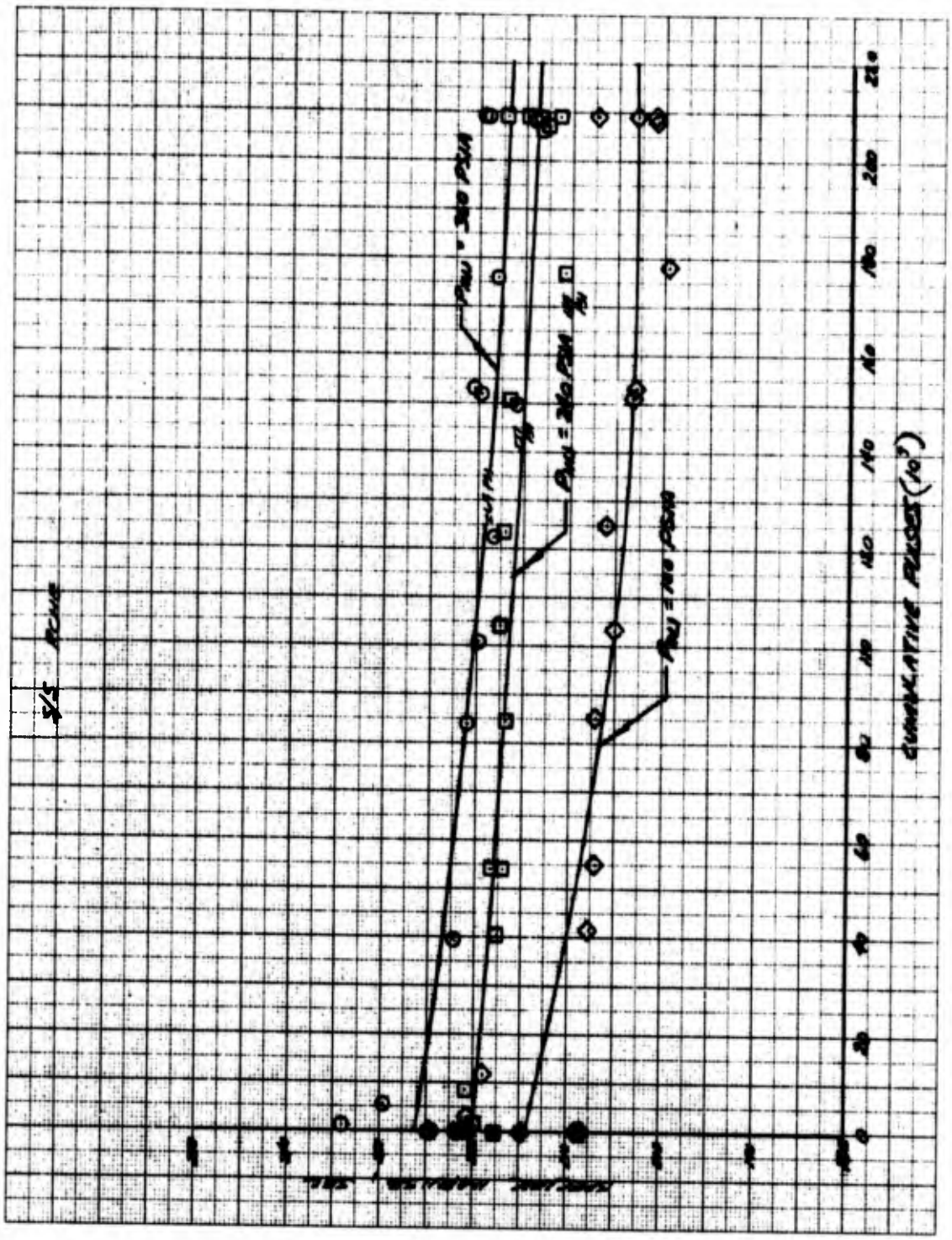

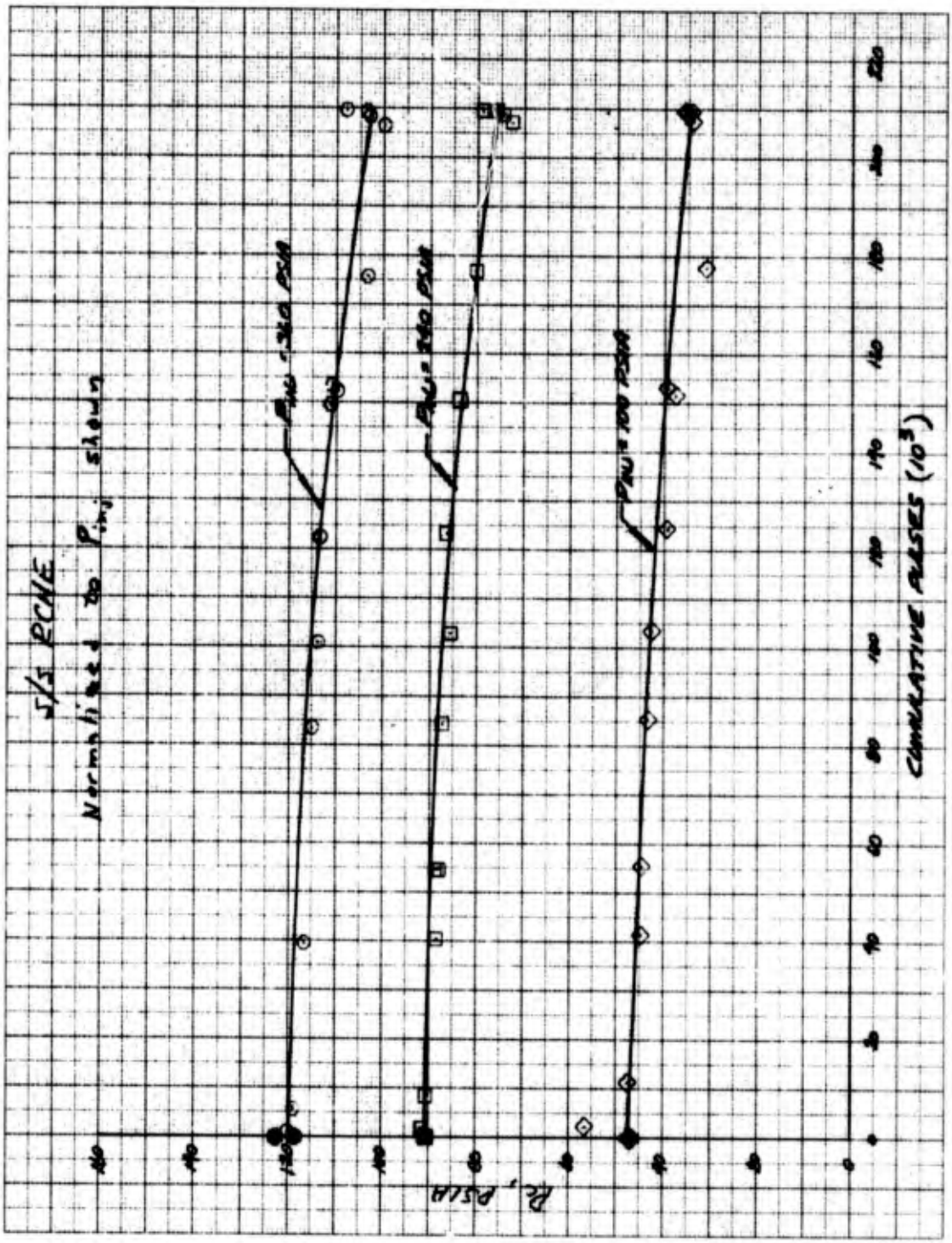
S/S PCNE
Normalized to P_{inj} shown
CUMULATIVE PULSES (10^3)
R_c, PSIA

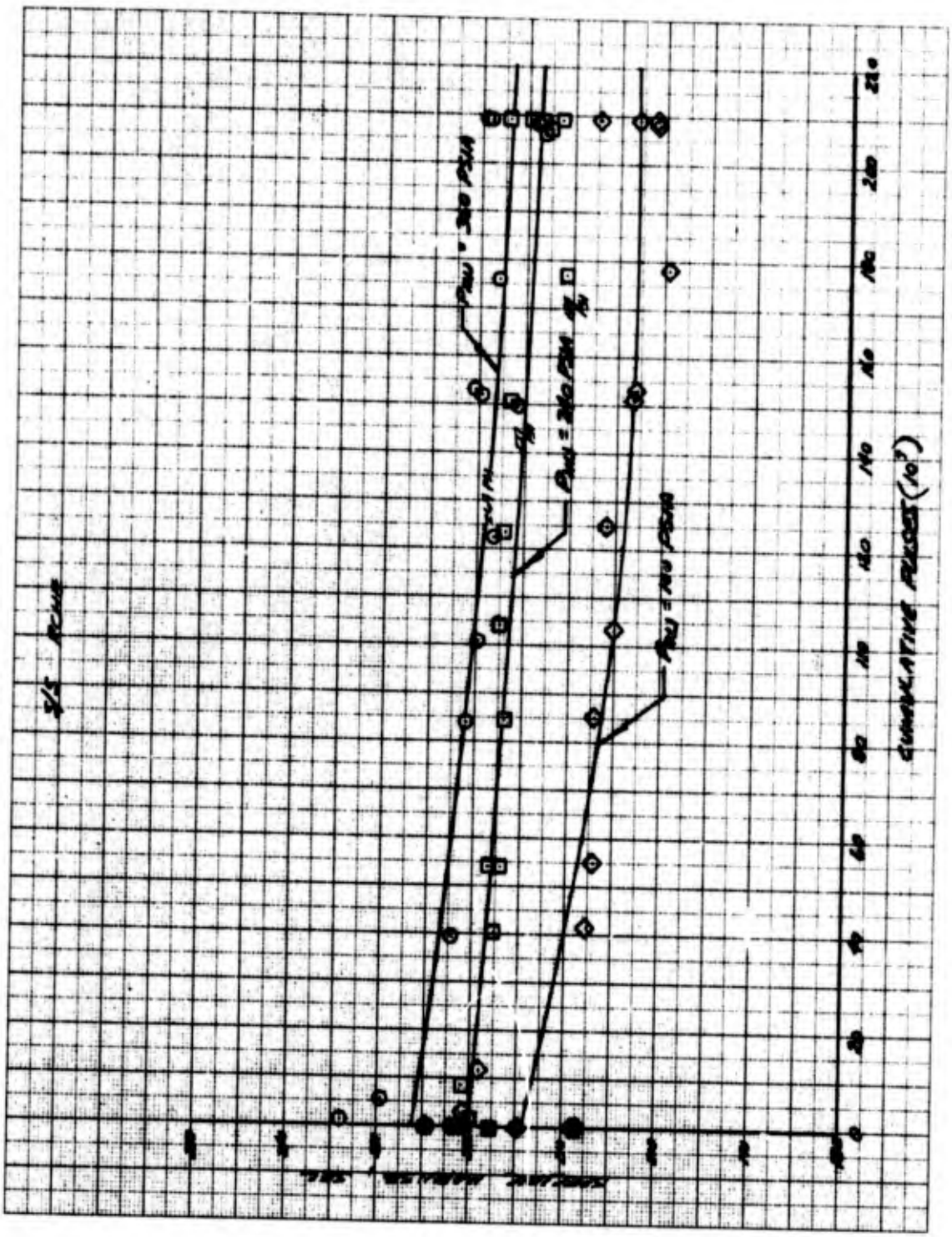

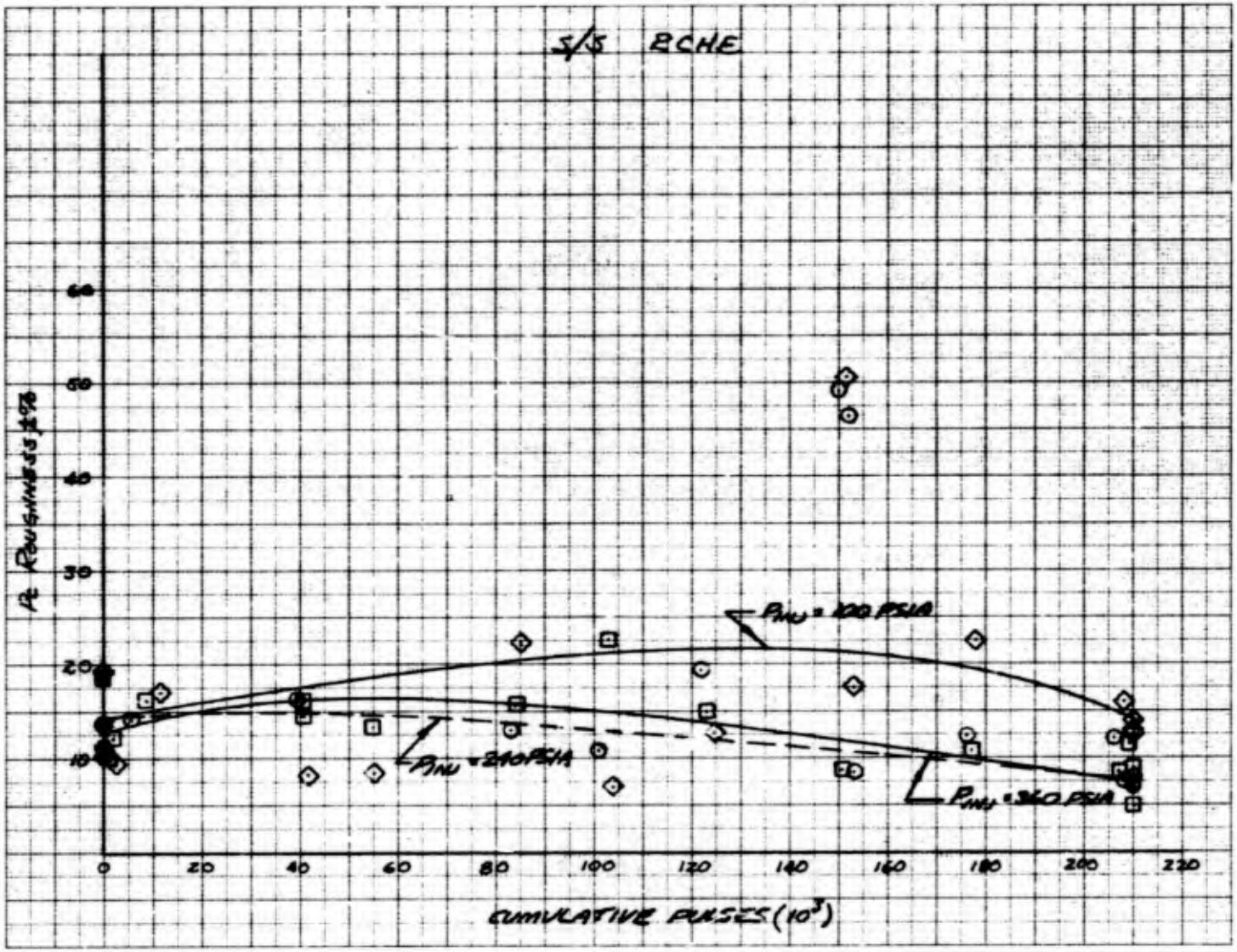
S/S 2CHE
Ra ROUGHNESS μIN
60
50
40
30
20
10
0
20
40
60
80
100
120
140
160
180
200
220
CUMULATIVE PULSES (10^3)
P_{INJ} = 100 PSIA
P_{INJ} = 240 PSIA
P_{INJ} = 360 PSIA

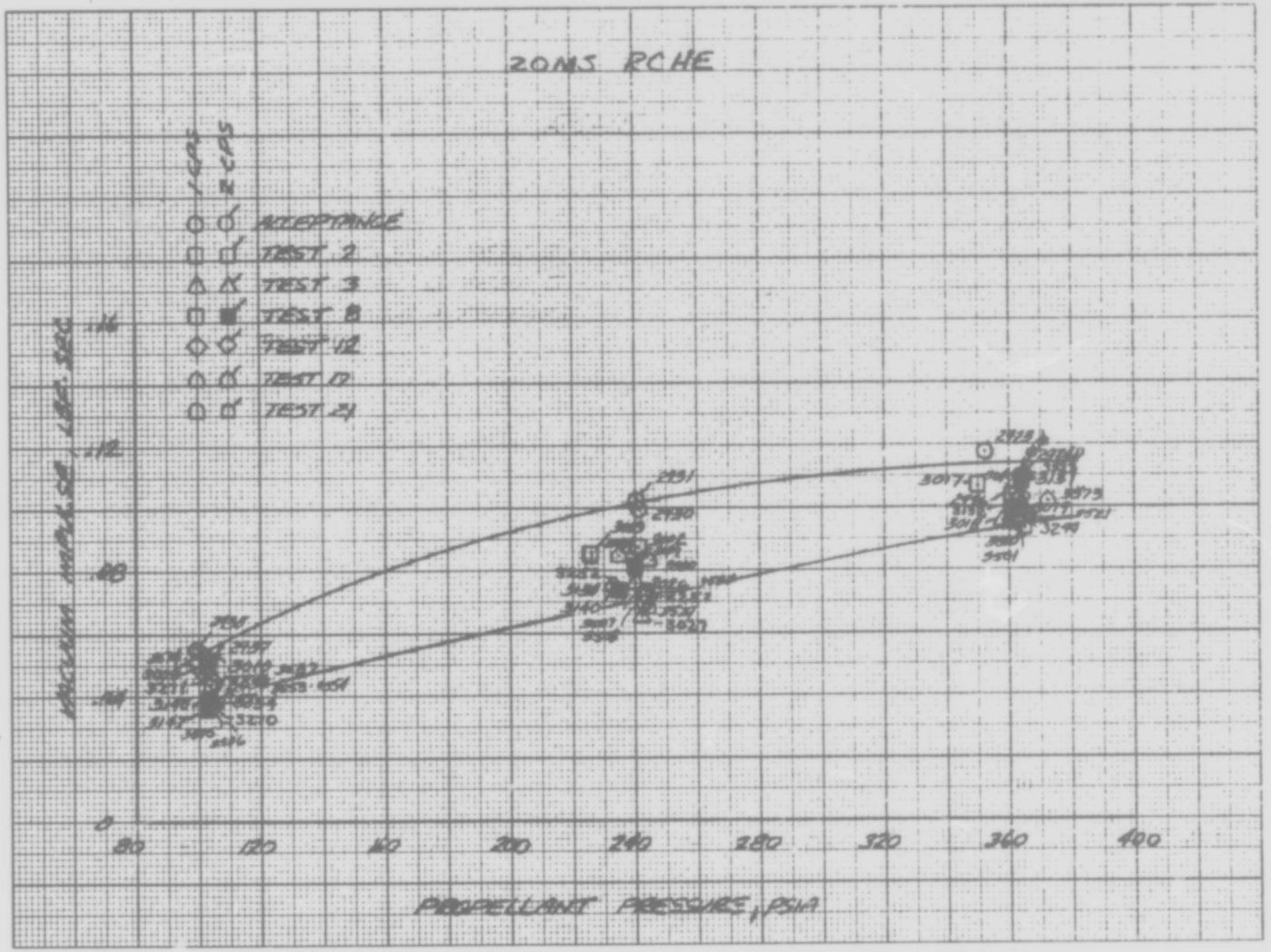
ZONES RCHE
ACCEPTANCE
TEST 2
TEST 3
TEST 8
TEST 12
TEST 17
TEST 24
.16
.12
.08
.04
0
80
120
160
200
240
280
320
360
400
PROPELLANT PRESSURE, PSIA

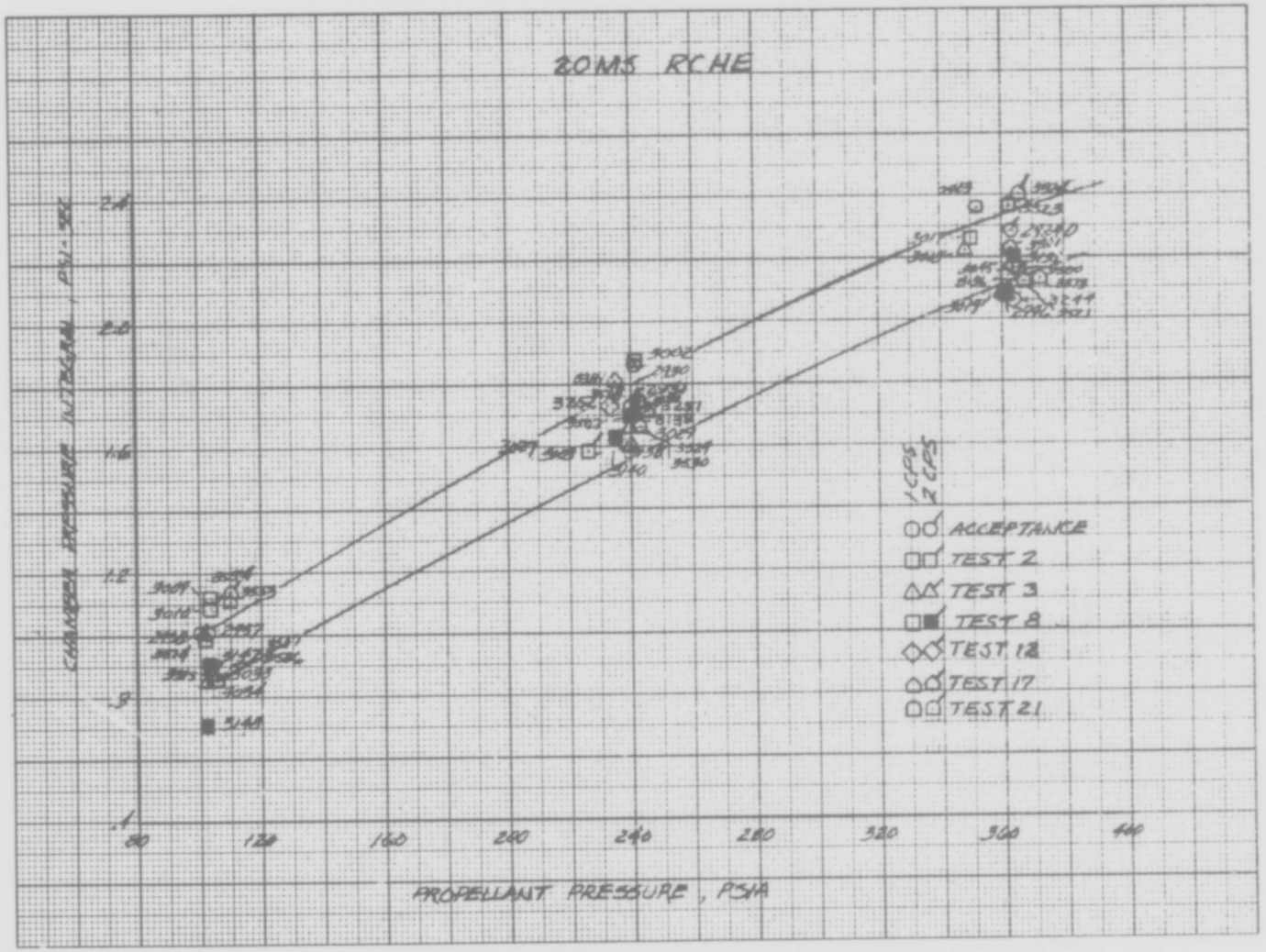
20MS RCHE
CHAMBER PRESSURE INTEGRAL, PSI-SEC
2.4
2.0
1.6
1.2
.8
.4
80
120
160
200
240
280
320
360
440
PROPELLANT PRESSURE, PSIA
LOT
1 CPS
2 CPS
ACCEPTANCE
TEST 2
TEST 3
TEST 8
TEST 12
TEST 17
TEST 21

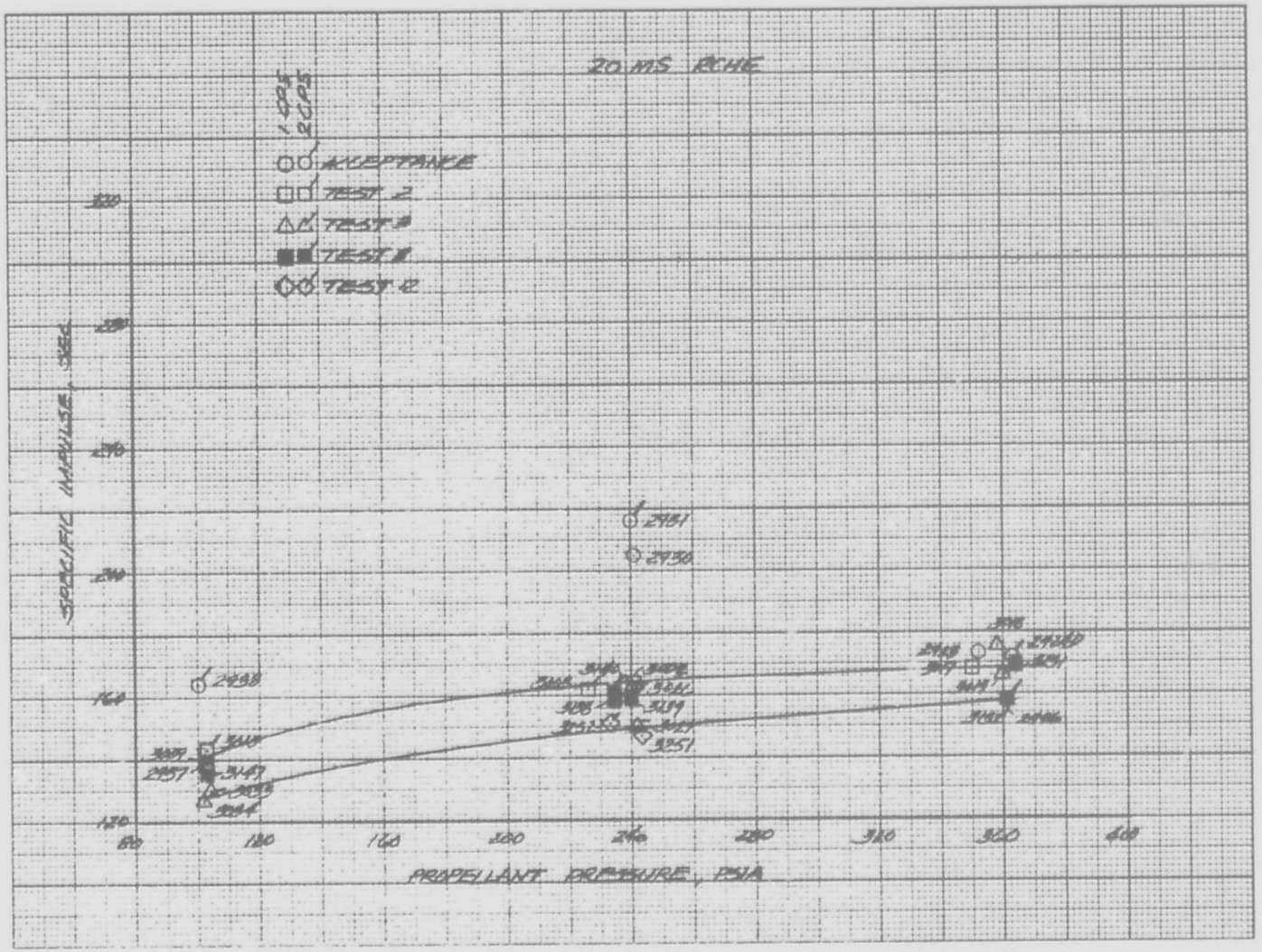
20 MS ISHE
ACCEPTANCE
TEST 2
TEST 3
TEST 4
TEST 5
SPECIFIC IMPULSE, LBSEC
PROPELLANT PRESSURE, PSIA

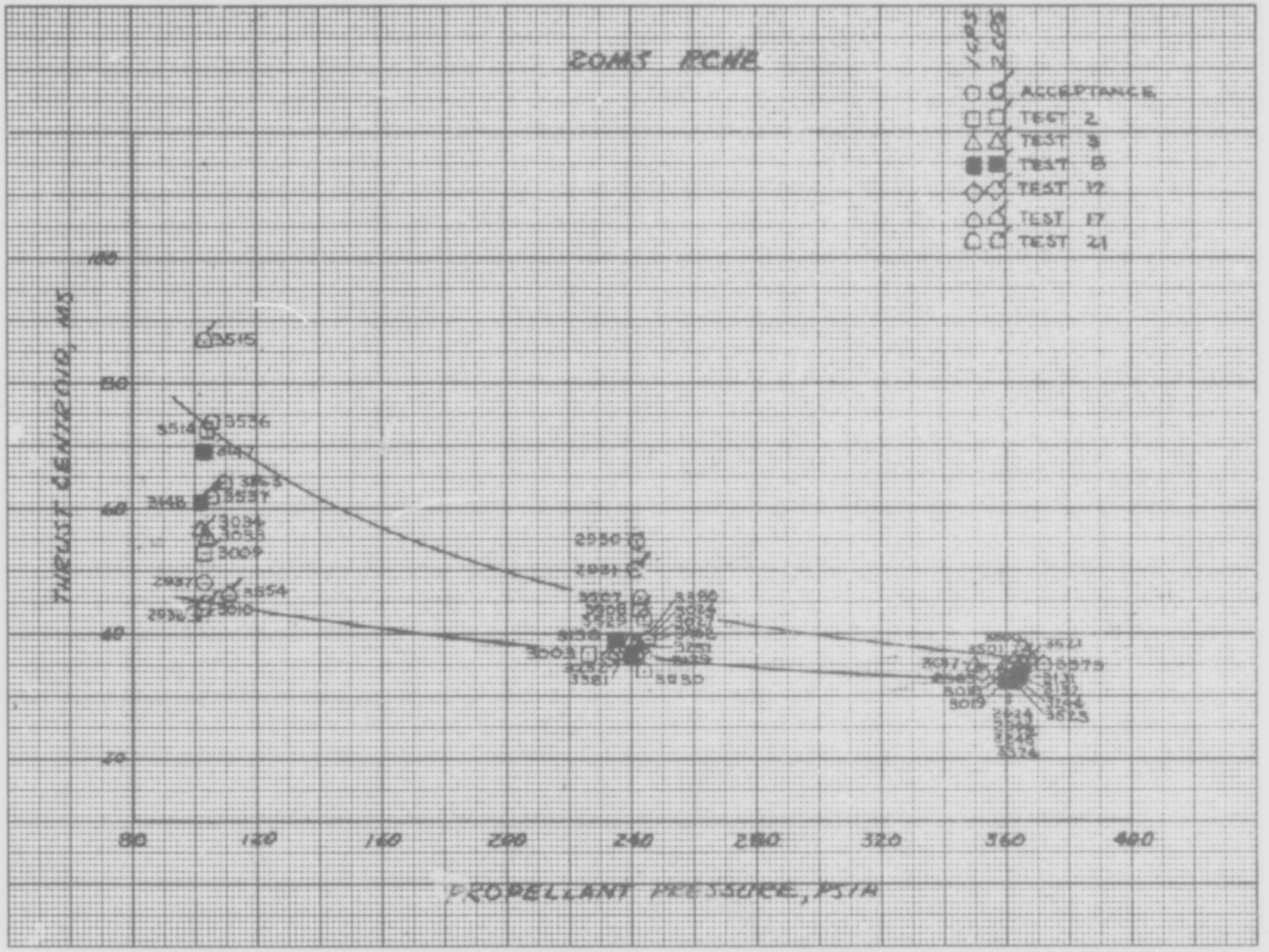
20MS RCNE
ACCEPTANCE
TEST 2
TEST 5
TEST 8
TEST 12
TEST 17
TEST 21
THRUST DENSITY, MS
PROPELLANT PRESSURE, PSIA
80
120
160
200
240
280
320
360
400
40
60
80
100

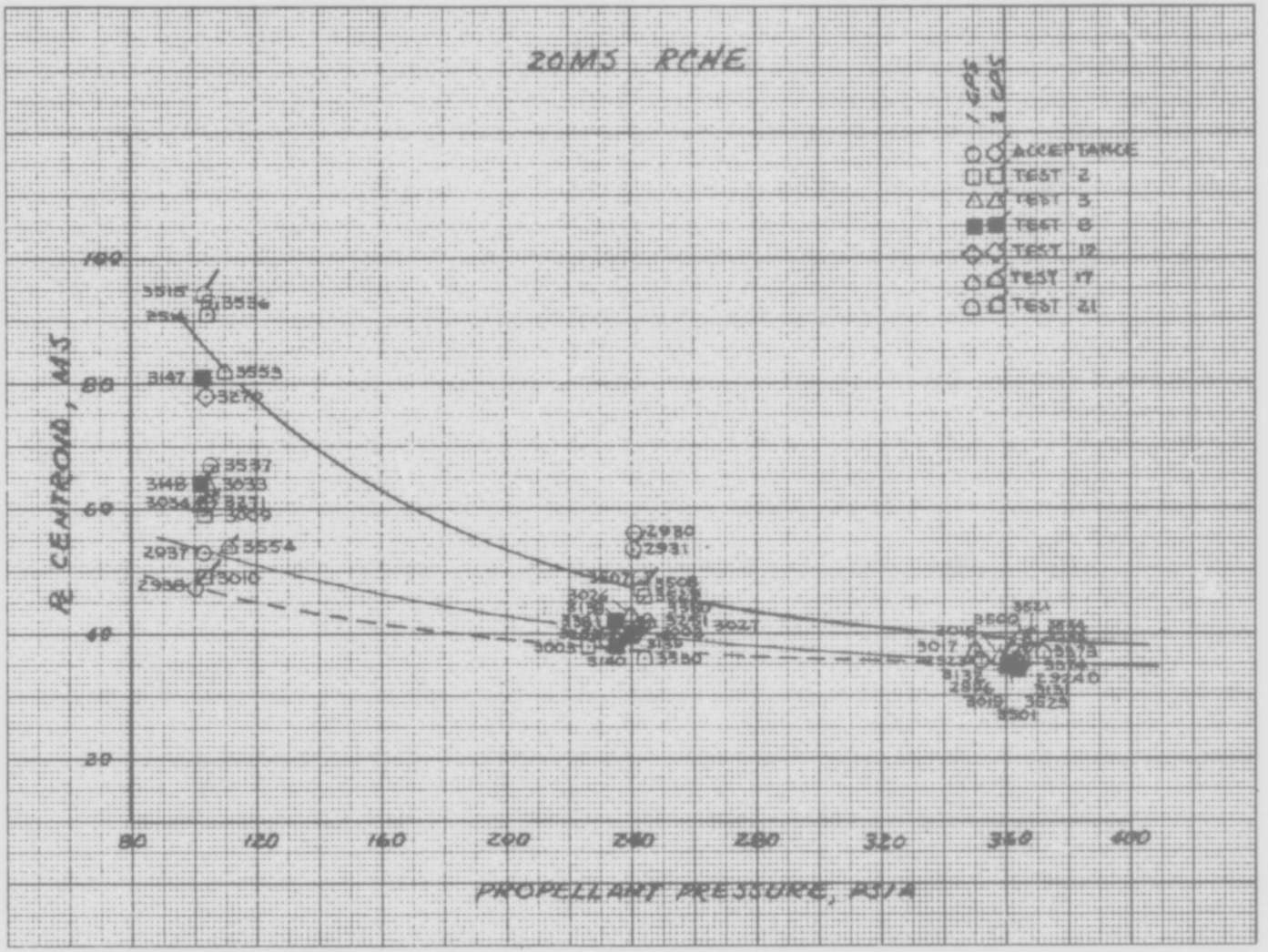
20MS RCNE
ACCEPTANCE
TEST 2
TEST 5
TEST 8
TEST 12
TEST 17
TEST 21
RE CENTROID, MS
PROPELLANT PRESSURE, PSIA
100
80
60
40
20
80
120
160
200
240
280
320
360
400

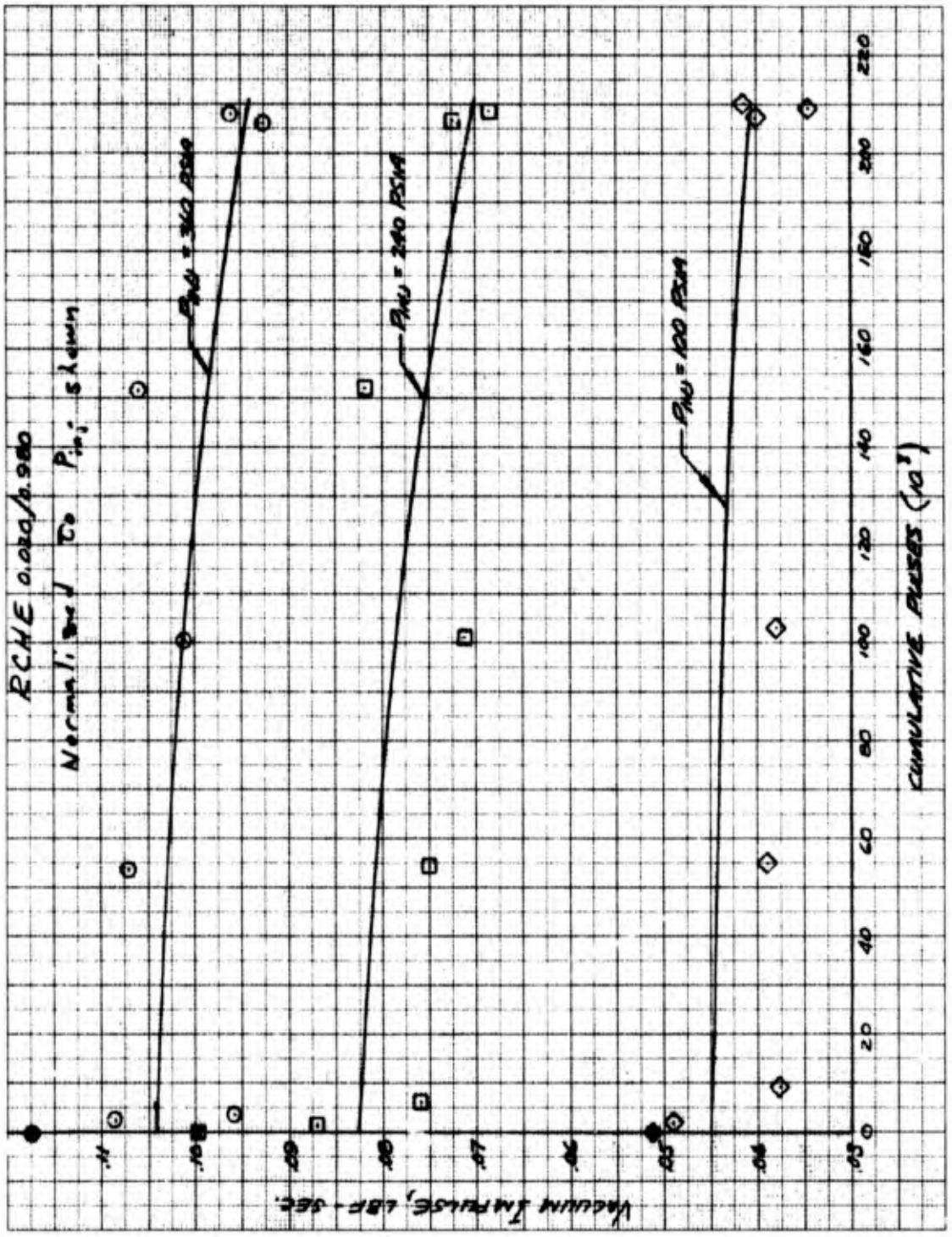
RCHE 0.080/0.980
Normalized To P_{inj} Shown
P_{inj} = 340 PSIA
P_{inj} = 240 PSIA
P_{inj} = 100 PSIA
Vacuum Impulse, LBF-SEC.
Cumulative Pulses ($\times 10^3$)
0
20
40
60
80
100
120
140
160
180
200
220

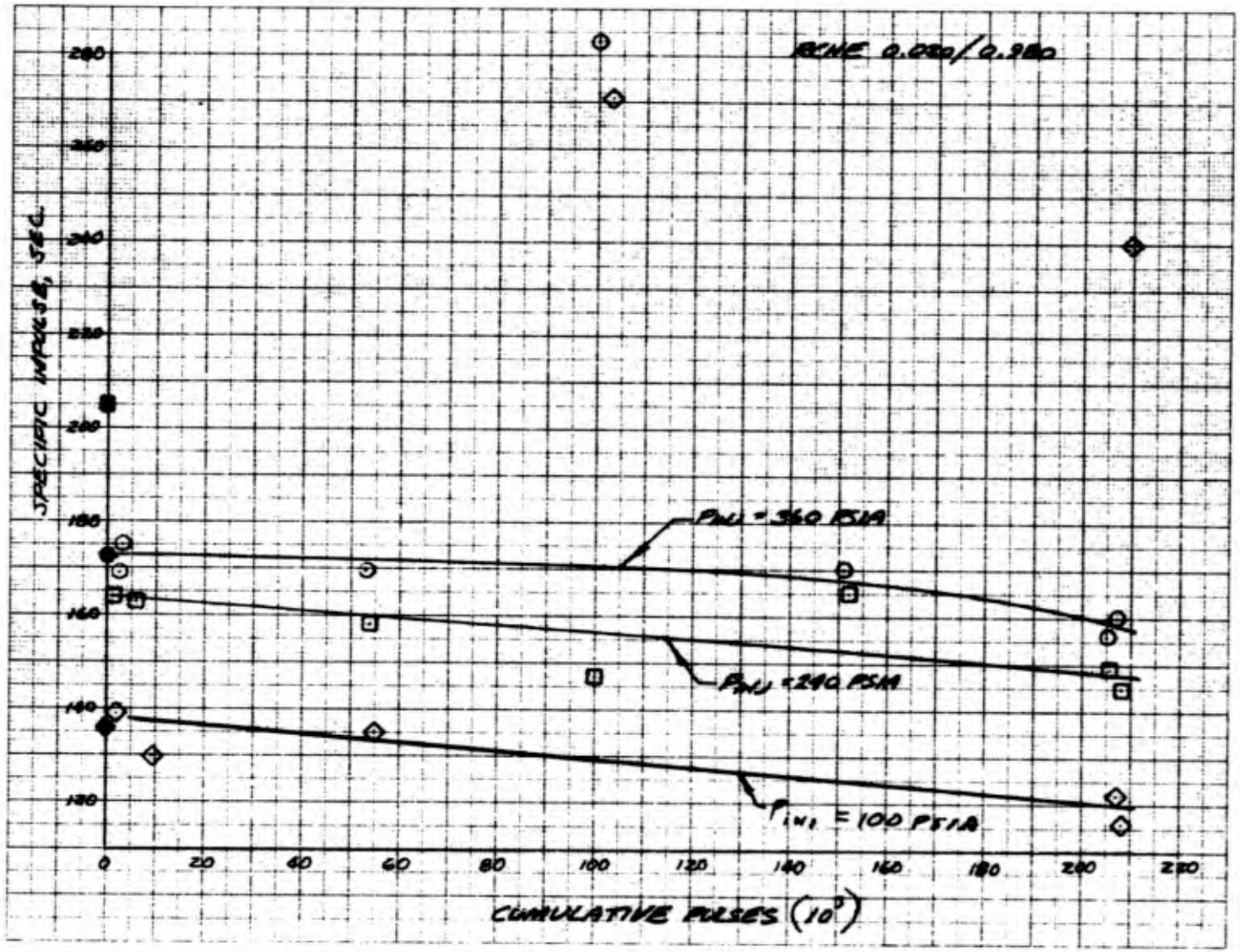
RCHE 0.280/0.980
P_{INJ} = 360 PSIA
P_{INJ} = 240 PSIA
P_{INJ} = 100 PSIA
SPECIFIC IMPULSE, SEC.
CUMULATIVE PULSES (10^5)
0
20
40
60
80
100
120
140
160
180
200
220

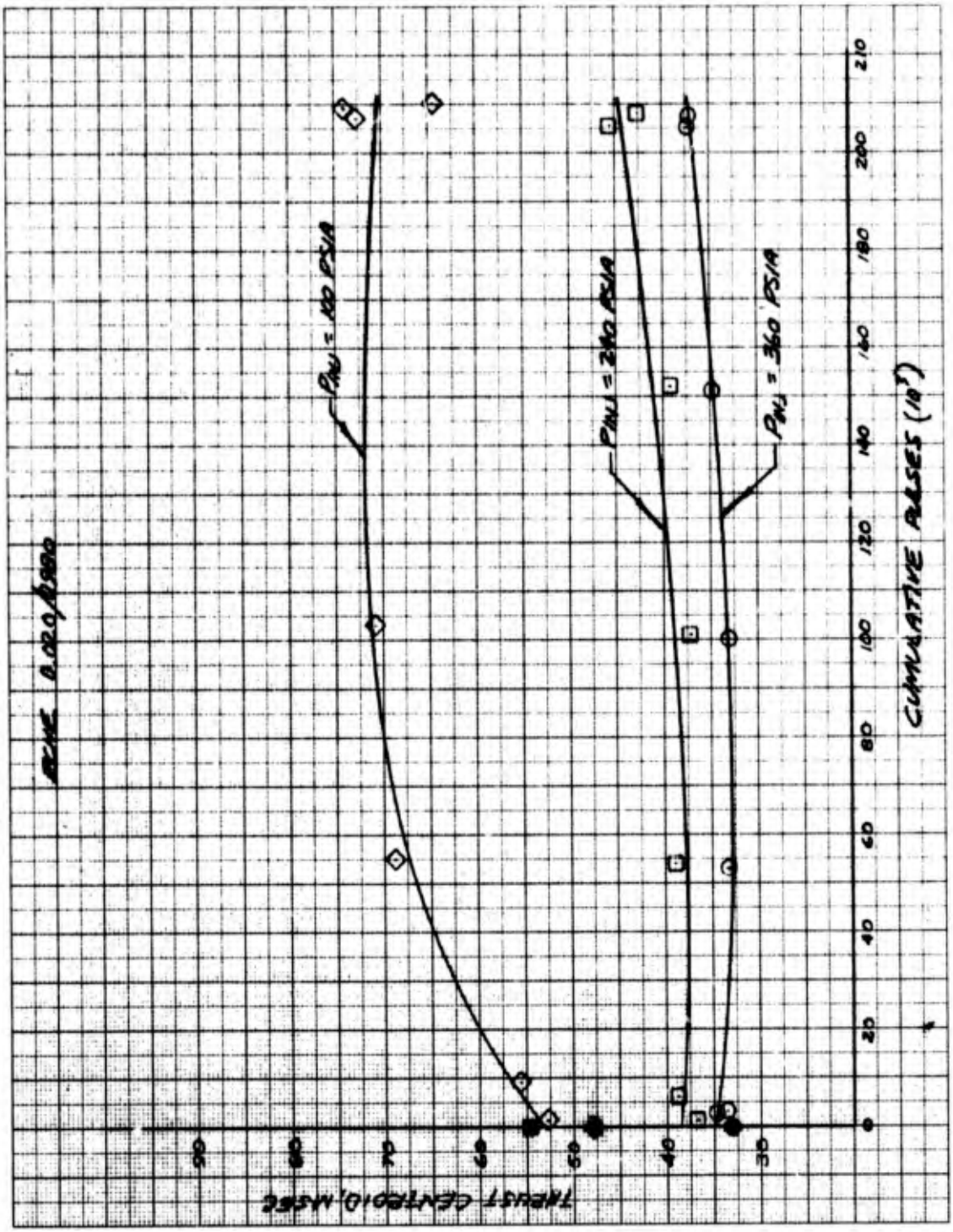
ARC-JET 0.020/0.090
P_{INJ} = 100 PSIA
P_{INJ} = 240 PSIA
P_{INJ} = 360 PSIA
THRUST COEFFICIENT, MSEC
CUMULATIVE PULSES (10^3)
0
20
40
60
80
100
120
140
160
180
200
210
30
40
50
60
70
80
90

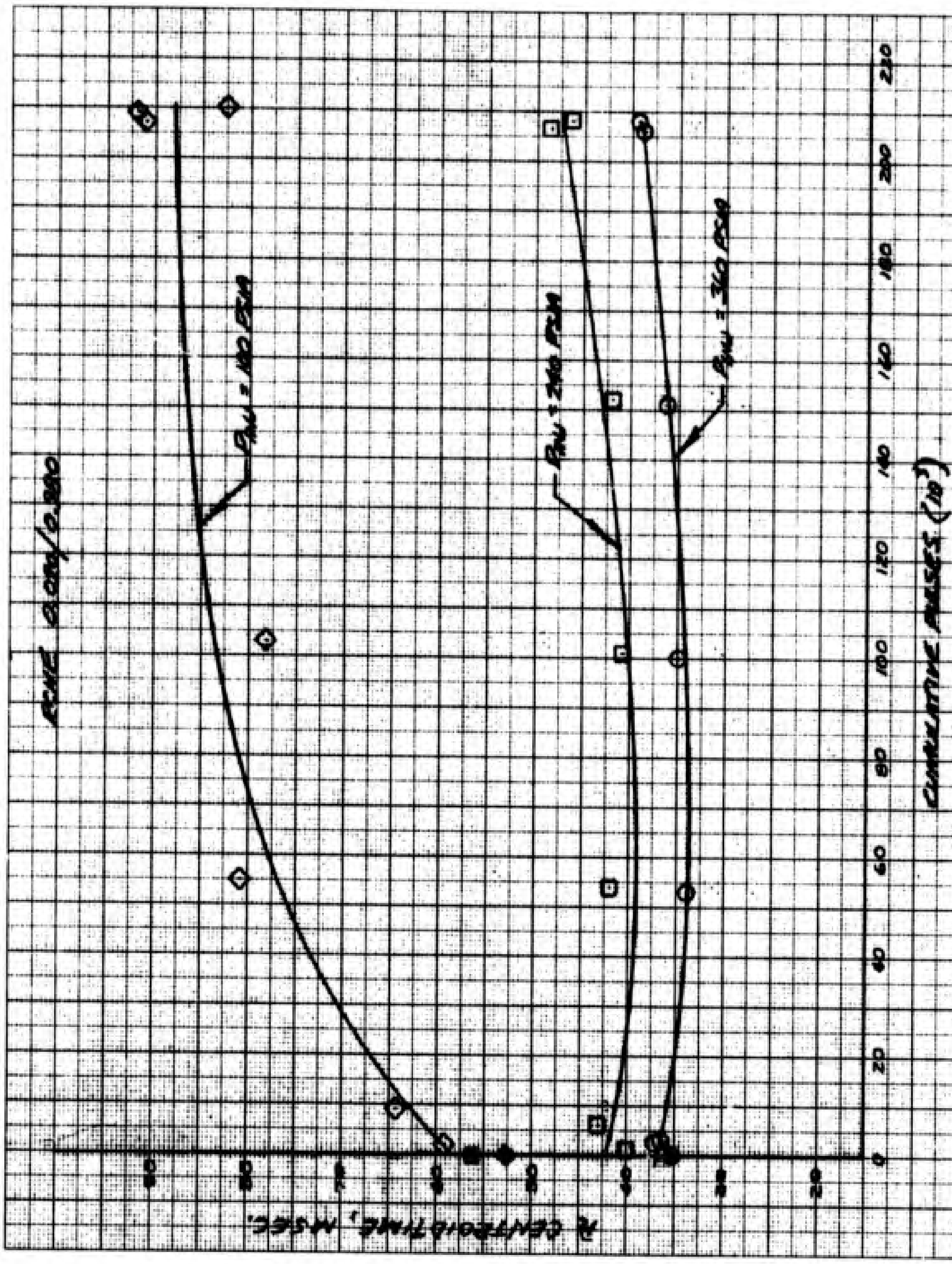

CUMULATIVE PULSES (10³)
0
20
40
60
80
100
120
140
160
180
200
220

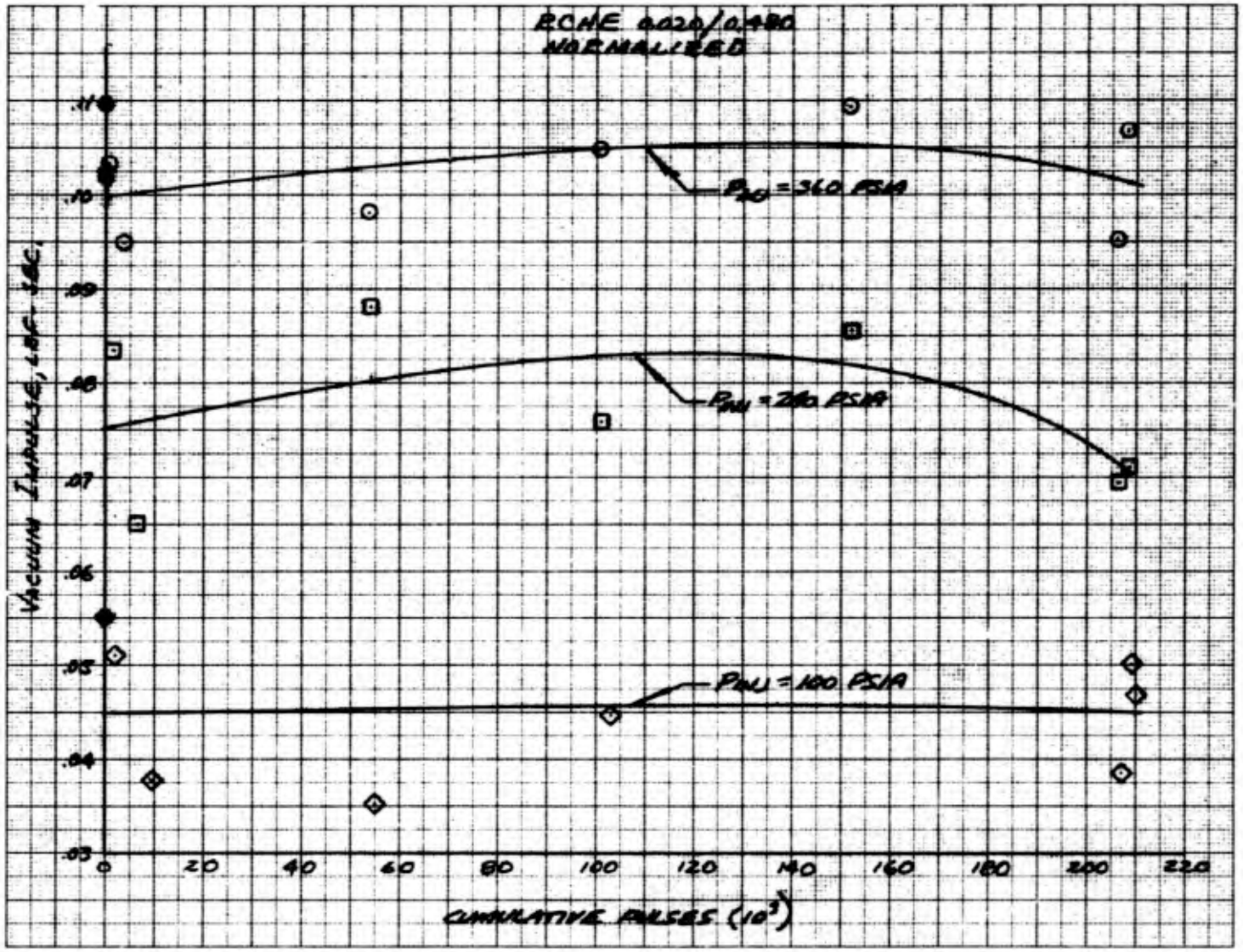
RCHE 0020/0480
NORMALIZED
P_{INJ} = 360 PSIA
P_{INJ} = 280 PSIA
P_{INJ} = 100 PSIA
VACUUM IMPULSE, LBF-SEC
.11
.10
.09
.08
.07
.06
.05
.04
.03
0
20
40
60
80
100
120
140
160
180
200
220
CUMULATIVE PULSES (10^3)

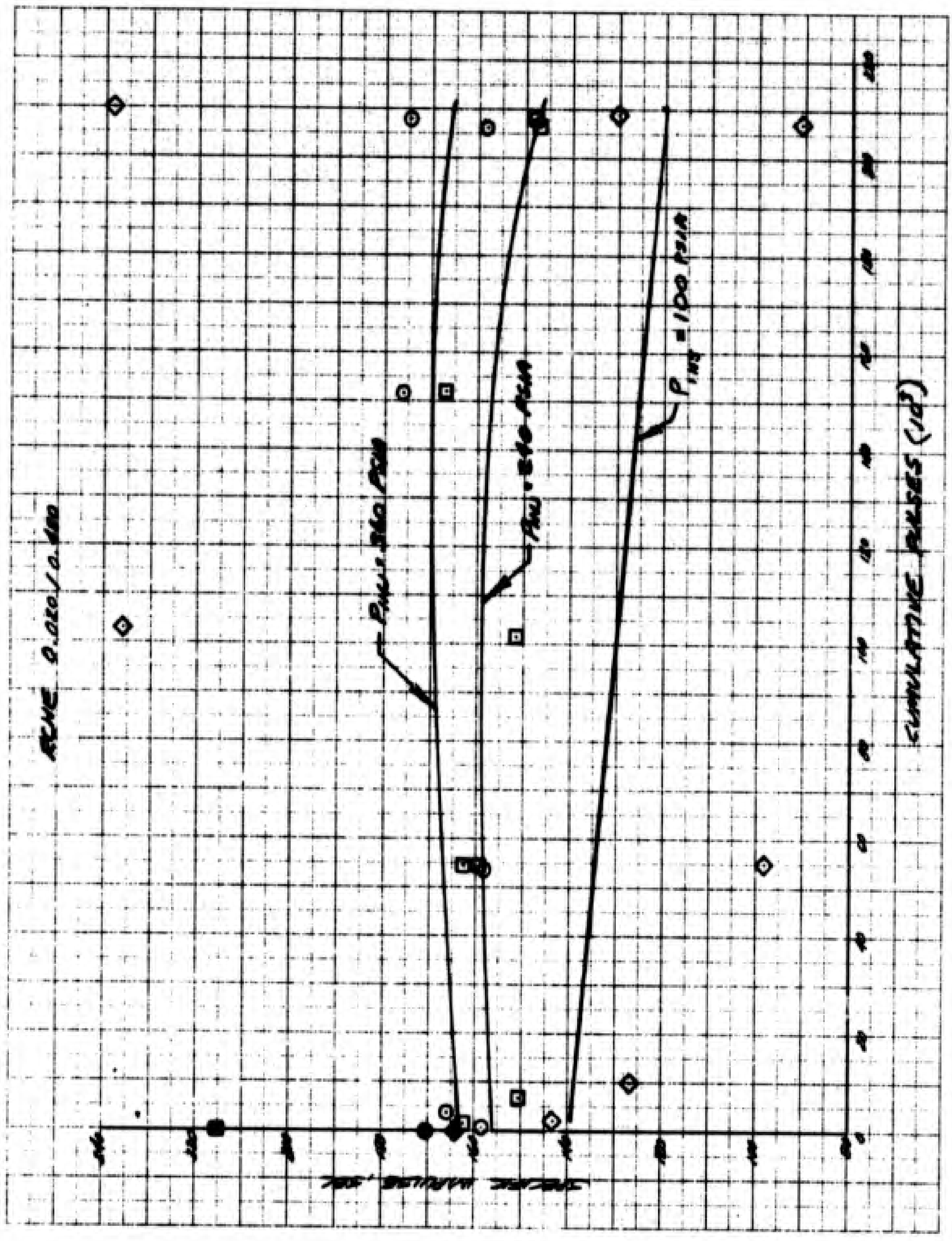

PINJ = 360 PSIA
PINJ = 240 PSIA
PINJ = 100 PSIA
CUMULATIVE PULSES (10³)

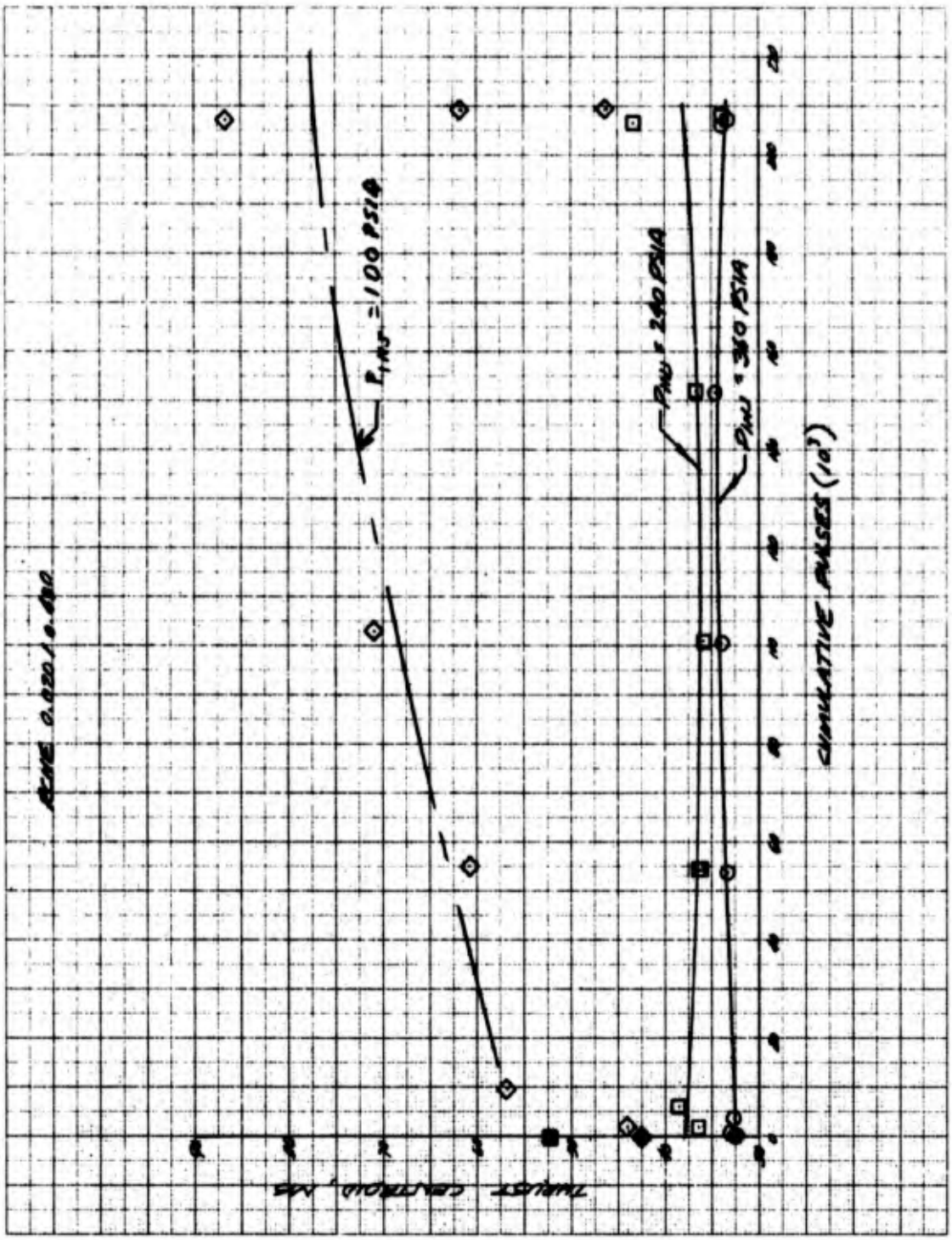
P_{LINE} = 100 PSIA
P_{INJ} = 240 PSIA
P_{INJ} = 350 PSIA
CUMULATIVE PULSES (10^3)

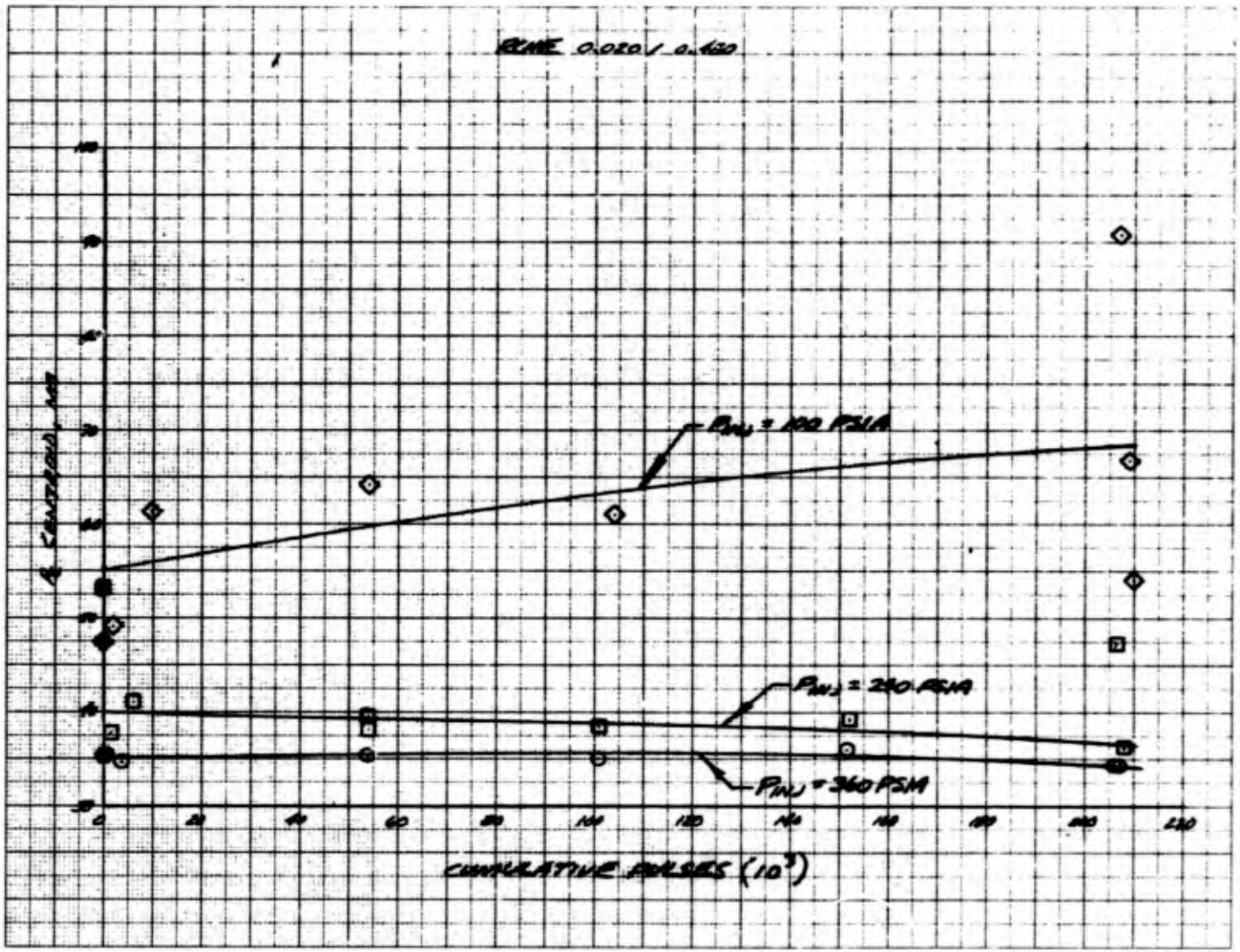
RUN 0.020 / 0.420
P_{INJ} = 100 PSIA
P_{INJ} = 230 PSIA
P_{INJ} = 360 PSIA
CUMULATIVE PULSES (10^3)

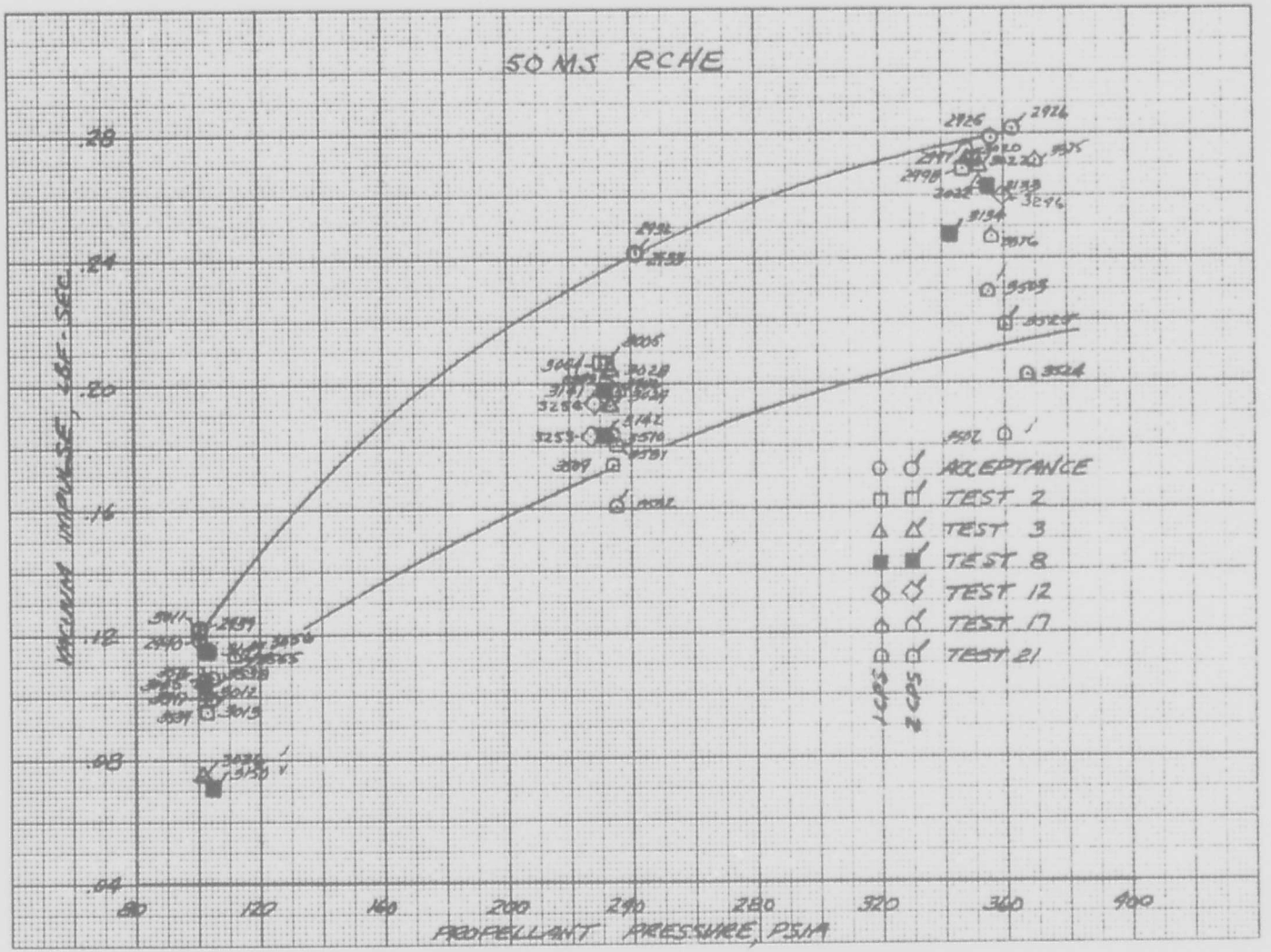
50 MS RCHE
VACUUM IMPULSE, LBF-SEC
PROPELLANT PRESSURE, PSIA
.08
.12
.16
.20
.24
.28
80
120
160
200
240
280
320
360
400
ACCEPTANCE
TEST 2
TEST 3
TEST 8
TEST 12
TEST 17
TEST 21
1 CPS
2 CPS

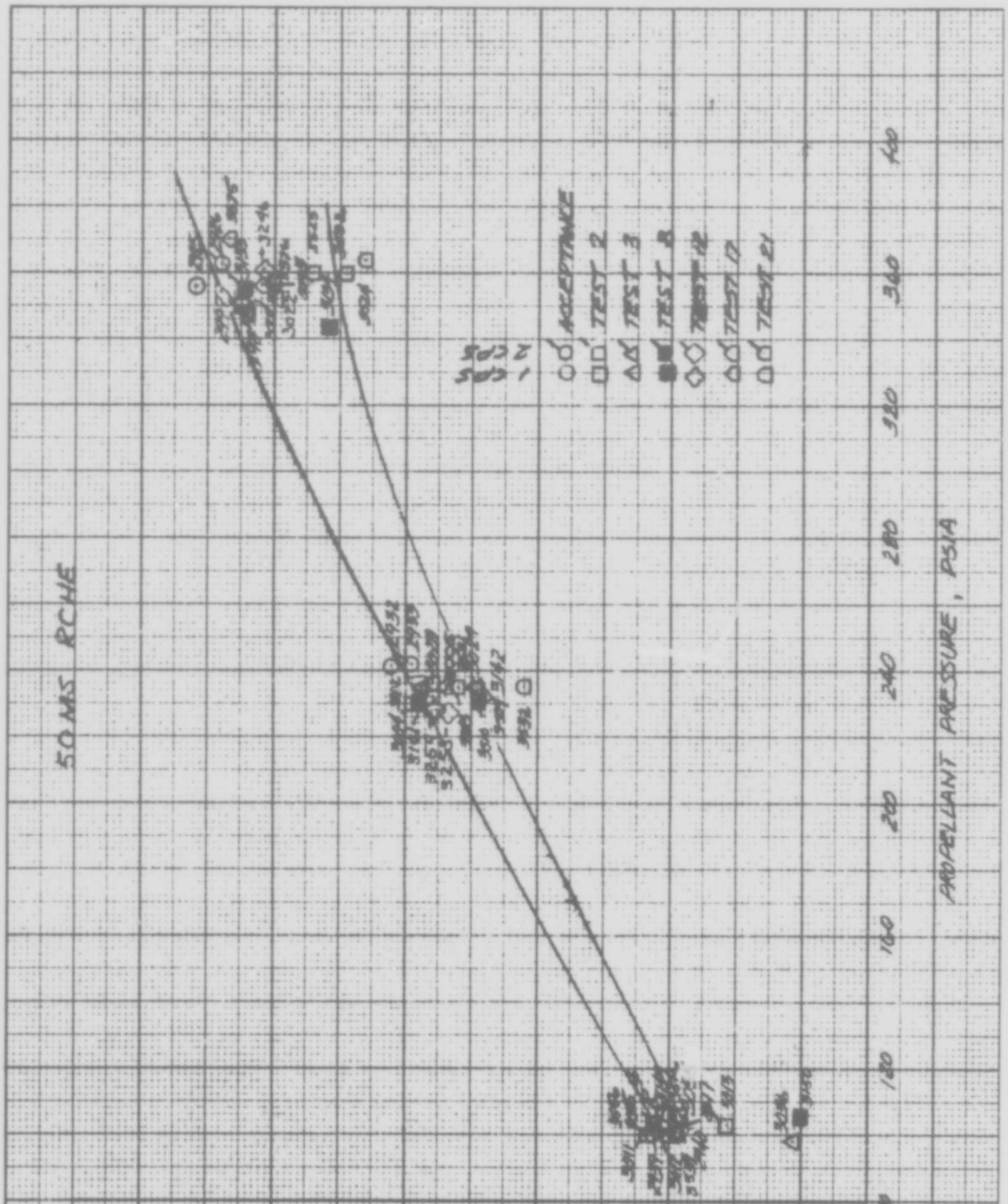
50 MS RCHE
CHAMBER PRESSURE INTEGRAL, PSI-SEC
PROPELLANT PRESSURE, PSIA
1 CPS
2 CPS
ACCEPTANCE
TEST 2
TEST 3
TEST 8
TEST 12
TEST 17
TEST 21
80
120
160
200
240
280
320
360
400
1
2
3
4
5
6
7

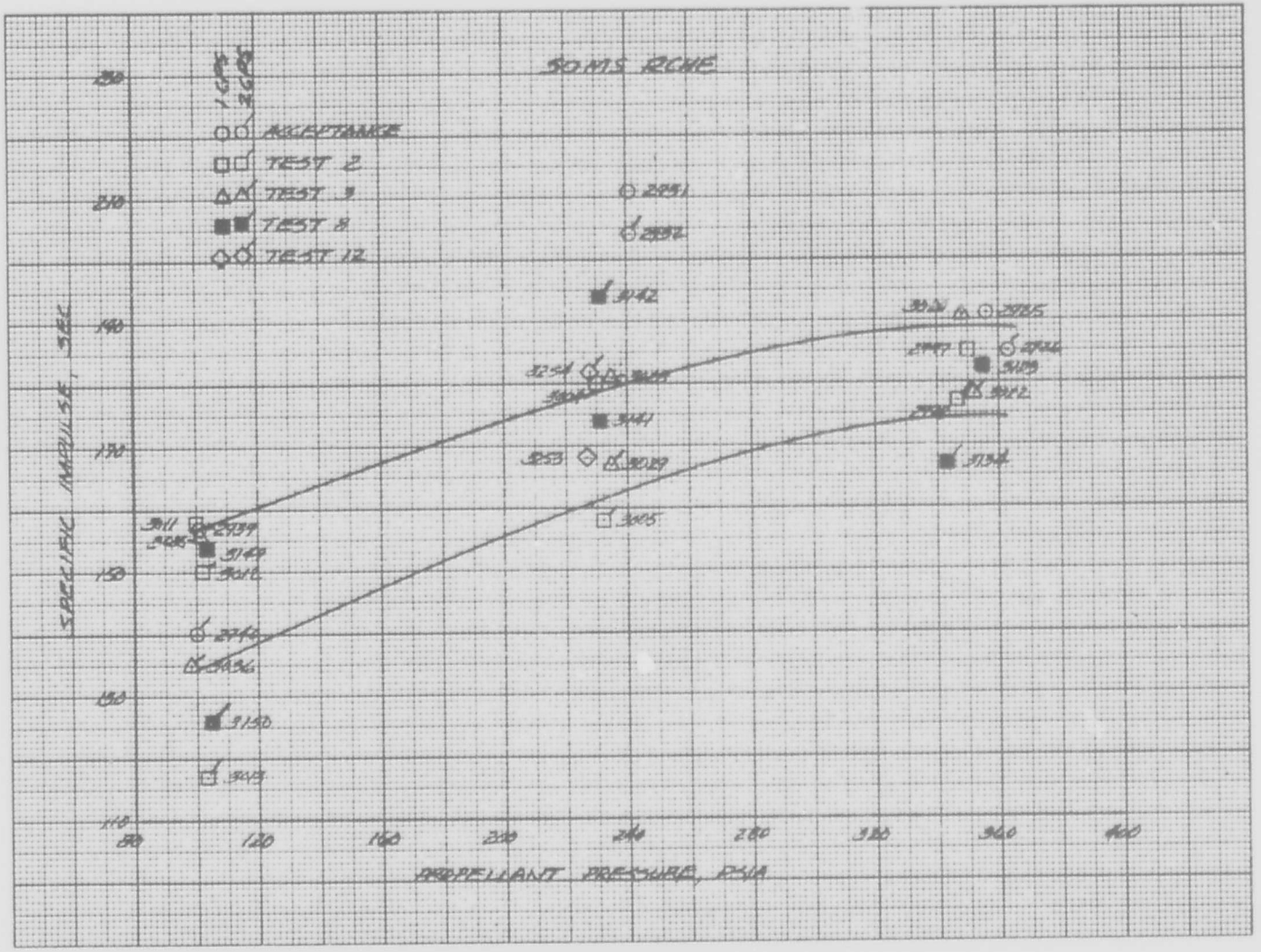
SOMS RICHE
ACCEPTANCE
TEST 2
TEST 3
TEST 8
TEST 12
SPECIFIC IMPULSE, SEC
PROPELLANT PRESSURE, PSIA
110
130
150
170
190
210
80
120
160
200
240
280
320
360
400

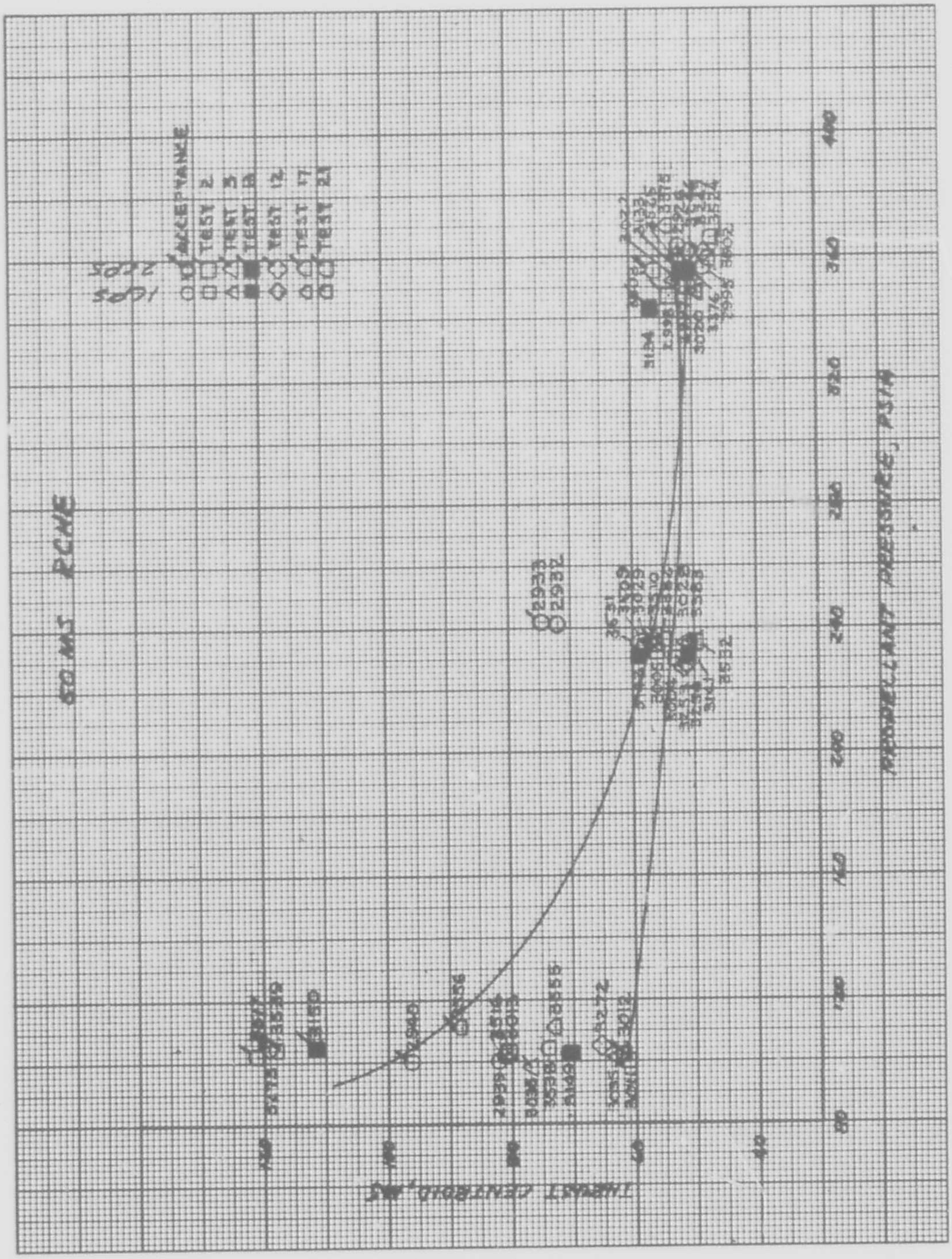
50 MS RCME
1605
2205
ACCEPTANCE
TEST 2
TEST 5
TEST 8
TEST 12
TEST 17
TEST 21
THRUST CENTROID, MS
PROPELLANT PRESSURE, PSIA

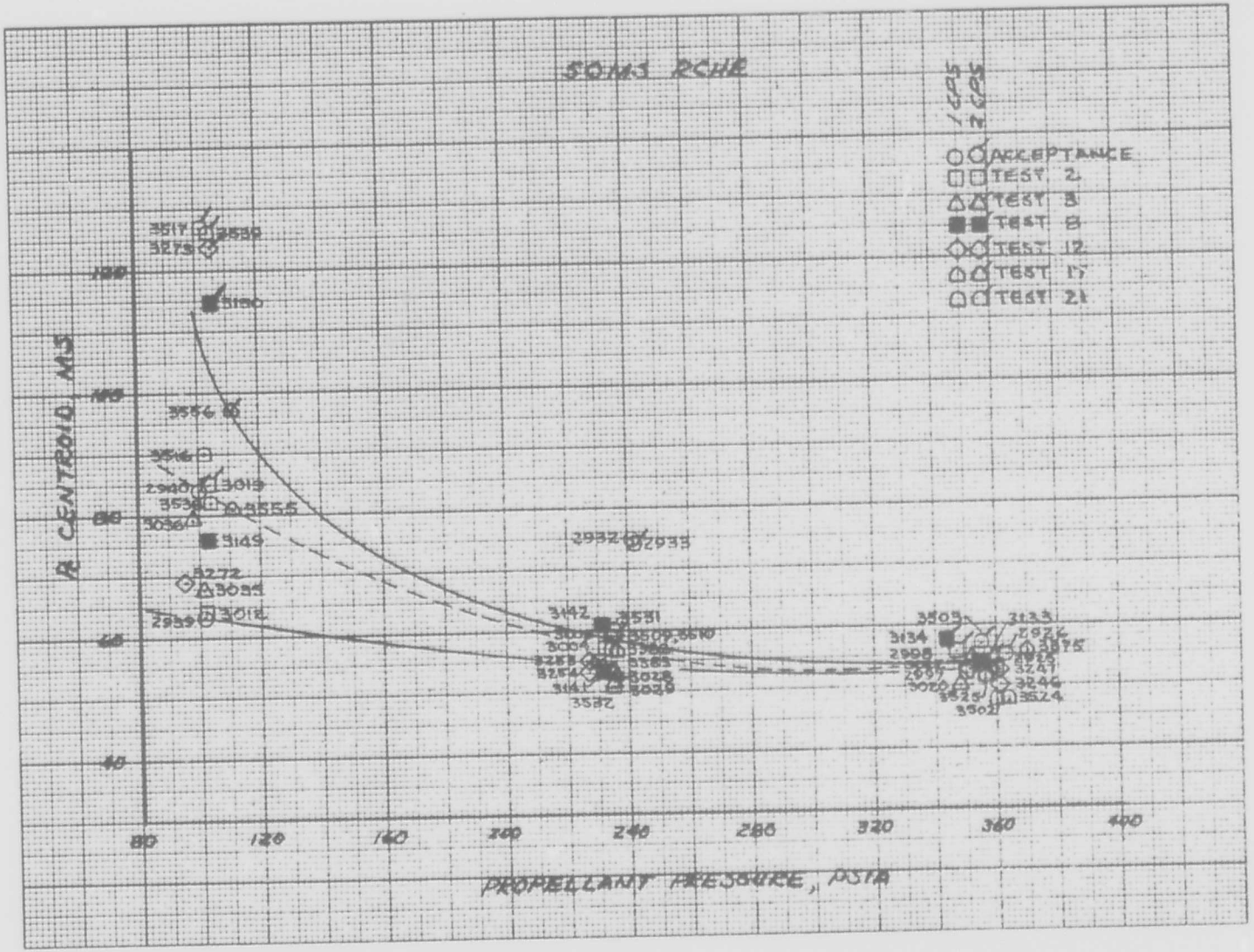
VON MISES
SET 2
ACCEPTANCE
TEST 2
TEST 8
TEST 8
TEST 12
TEST 17
TEST 21
R CENTROID, MM
PROPELLANT PRESSURE, PSIA
80
120
140
200
240
280
320
360
400

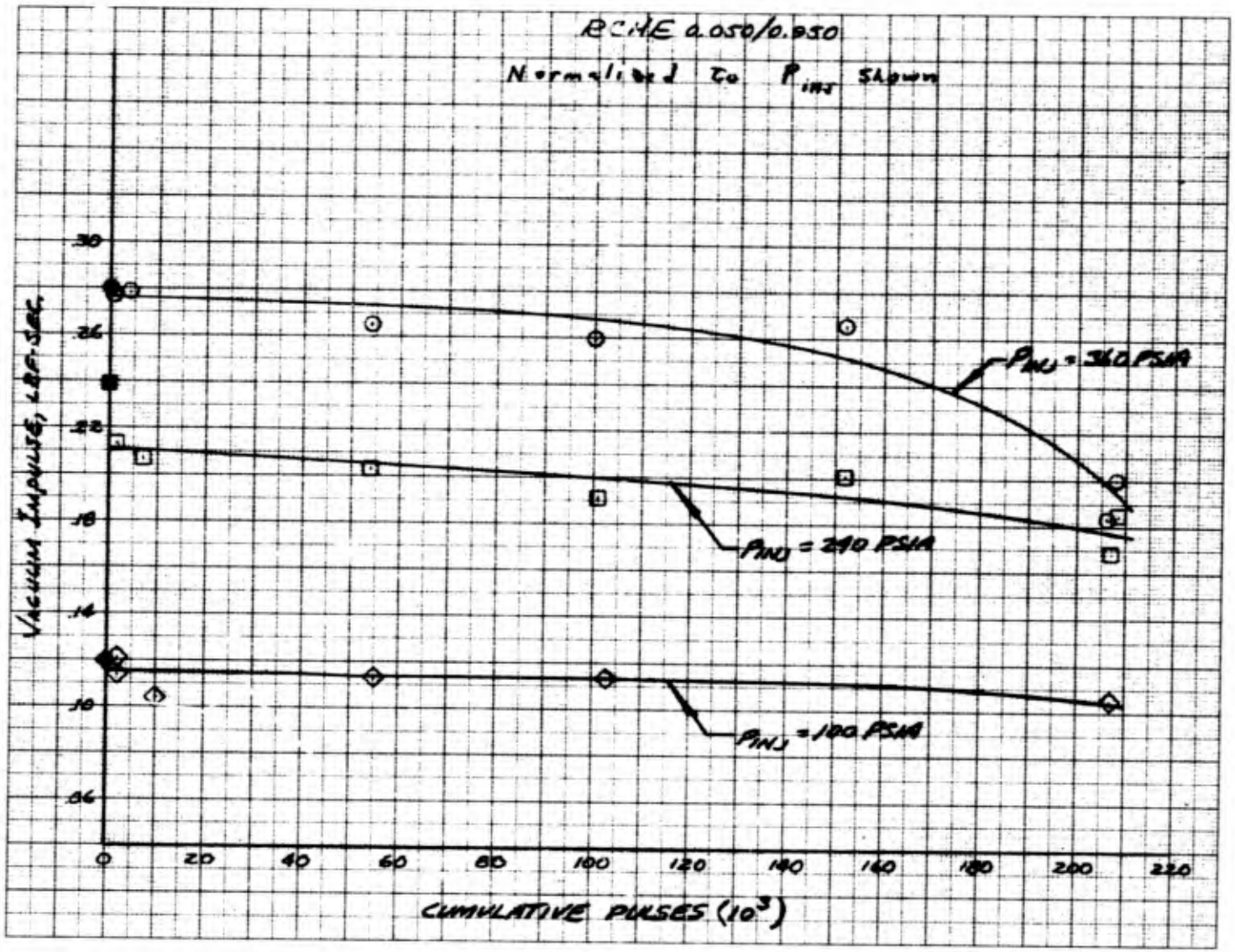
RCHE 0.050/0.950
Normalized to P_{INJ} Shown
VACUUM IMPULSE, LBF-SEC
30
26
22
18
14
10
.06
0
20
40
60
80
100
120
140
160
180
200
220
CUMULATIVE PULSES (10^3)
P_{INJ} = 360 PSIA
P_{INJ} = 240 PSIA
P_{INJ} = 100 PSIA

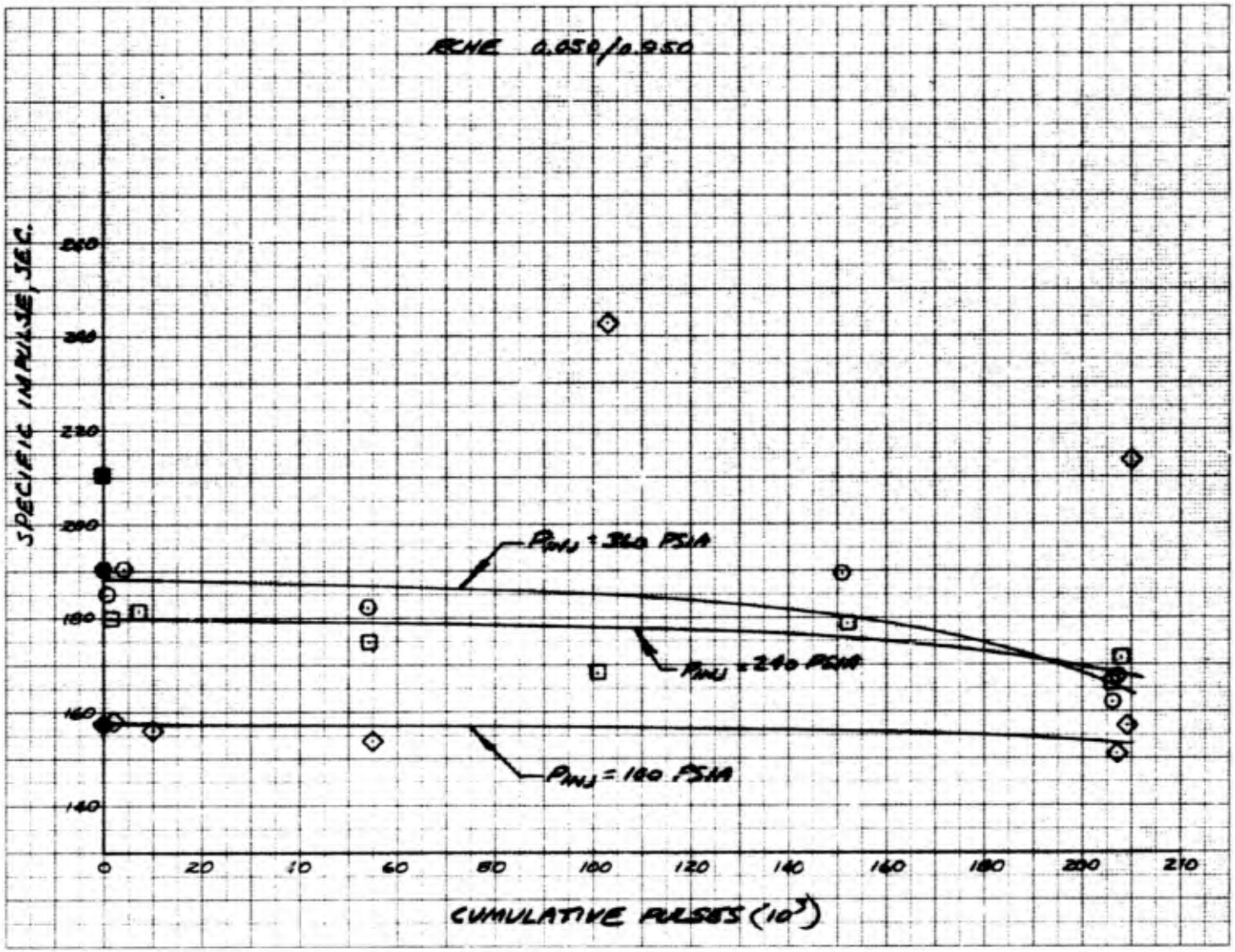
RCHE 0.650/0.350
SPECIFIC IMPULSE, SEC.
280
260
240
220
200
180
160
140
P_{INJ} = 360 PSIA
P_{INJ} = 240 PSIA
P_{INJ} = 180 PSIA
0
20
40
60
80
100
120
140
160
180
200
210
CUMULATIVE PULSES (10^3)

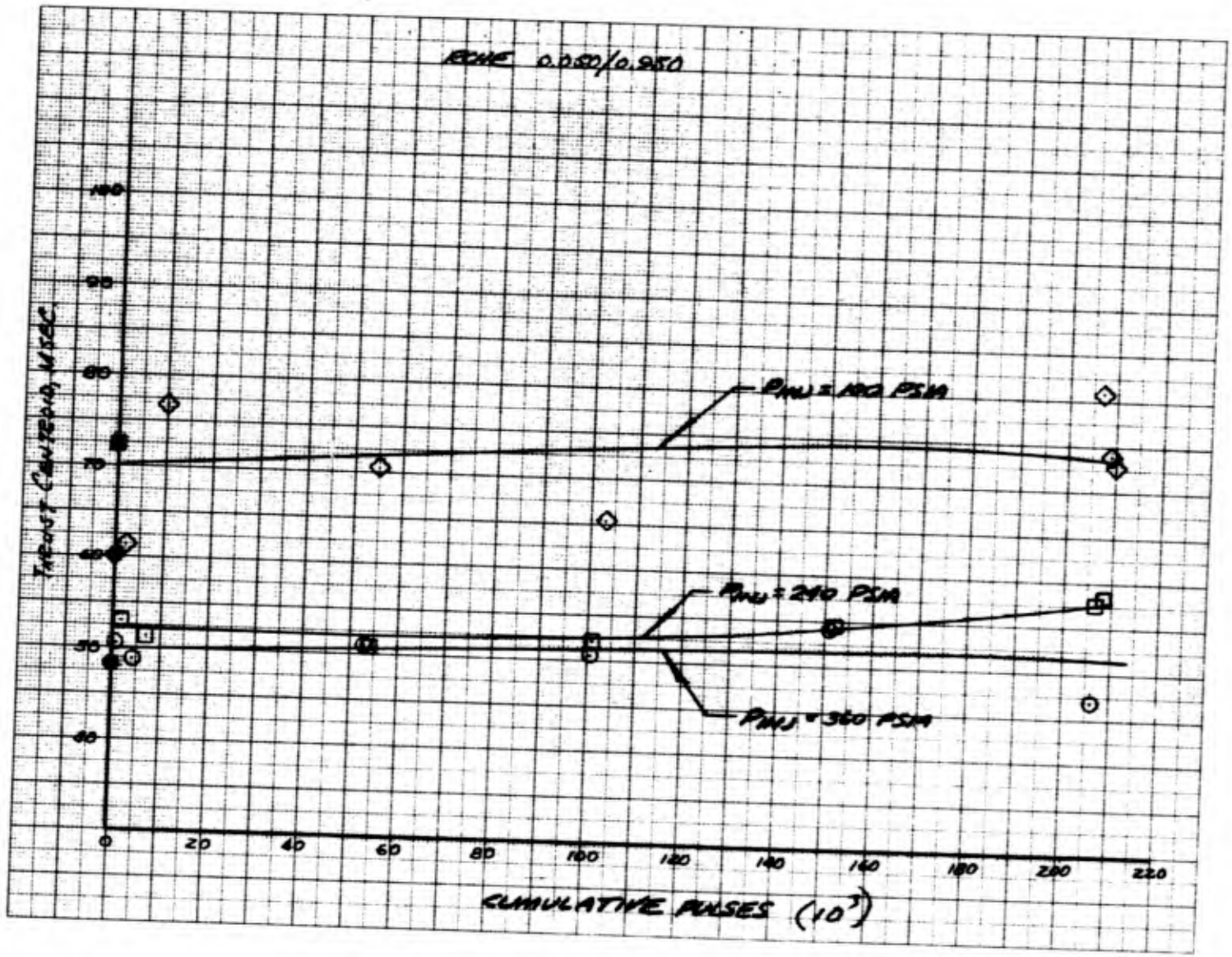
RCHE 0.050/0.950
P_{INJ} = 180 PSIA
P_{INJ} = 240 PSIA
P_{INJ} = 360 PSIA
TRACER CONCENTRATION, MG/SEC
CUMULATIVE PULSES (10^3)
0
20
40
60
80
100
120
140
160
180
200
220

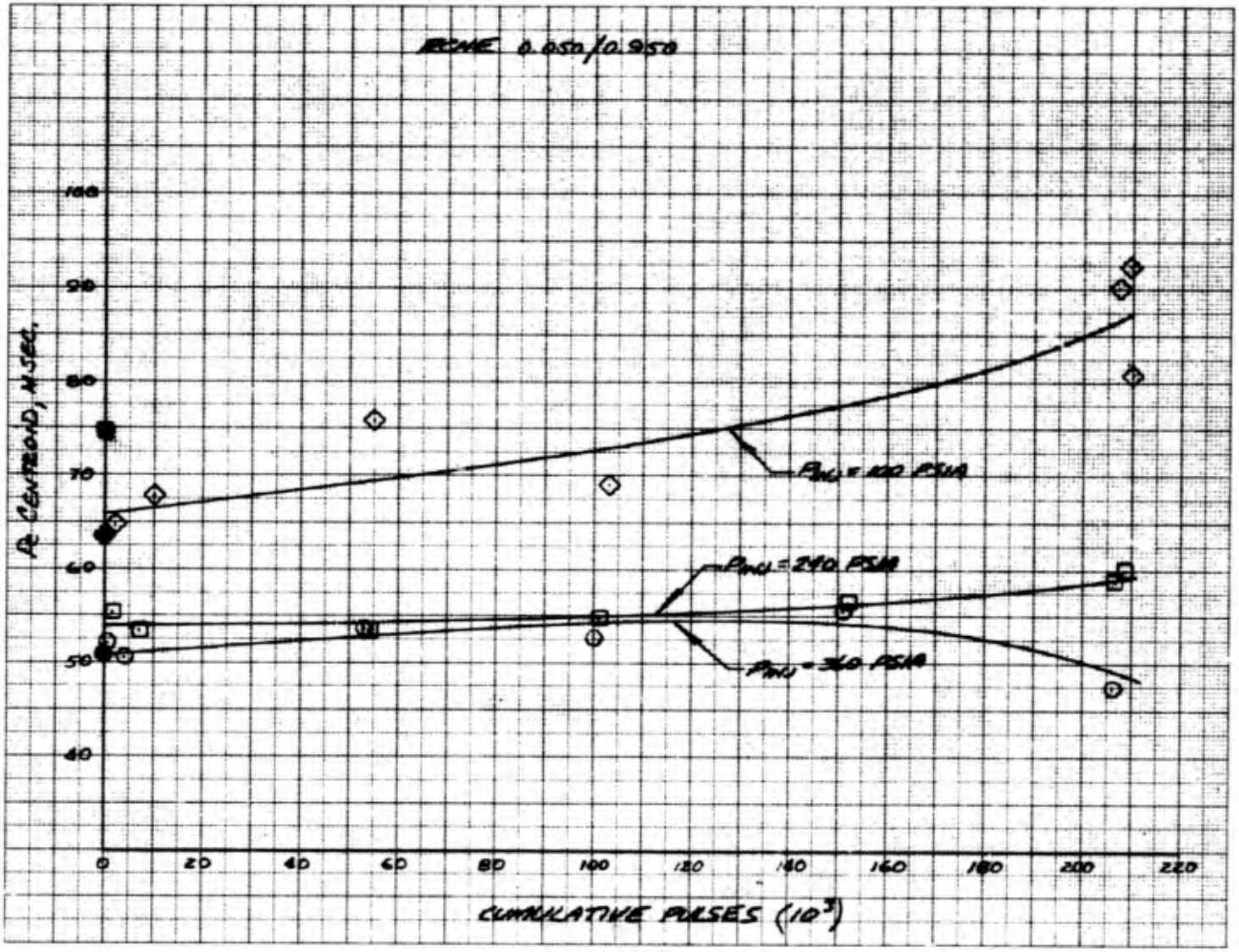
BOME 0.050/0.950
P_{INJ} = 420 PSIA
P_{INJ} = 290 PSIA
P_{INJ} = 340 PSIA
$\bar{R}$ CENTROID, MSEC.
CUMULATIVE PULSES (10^3)
0
20
40
60
80
100
120
140
160
180
200
220
40
50
60
70
80
90
100

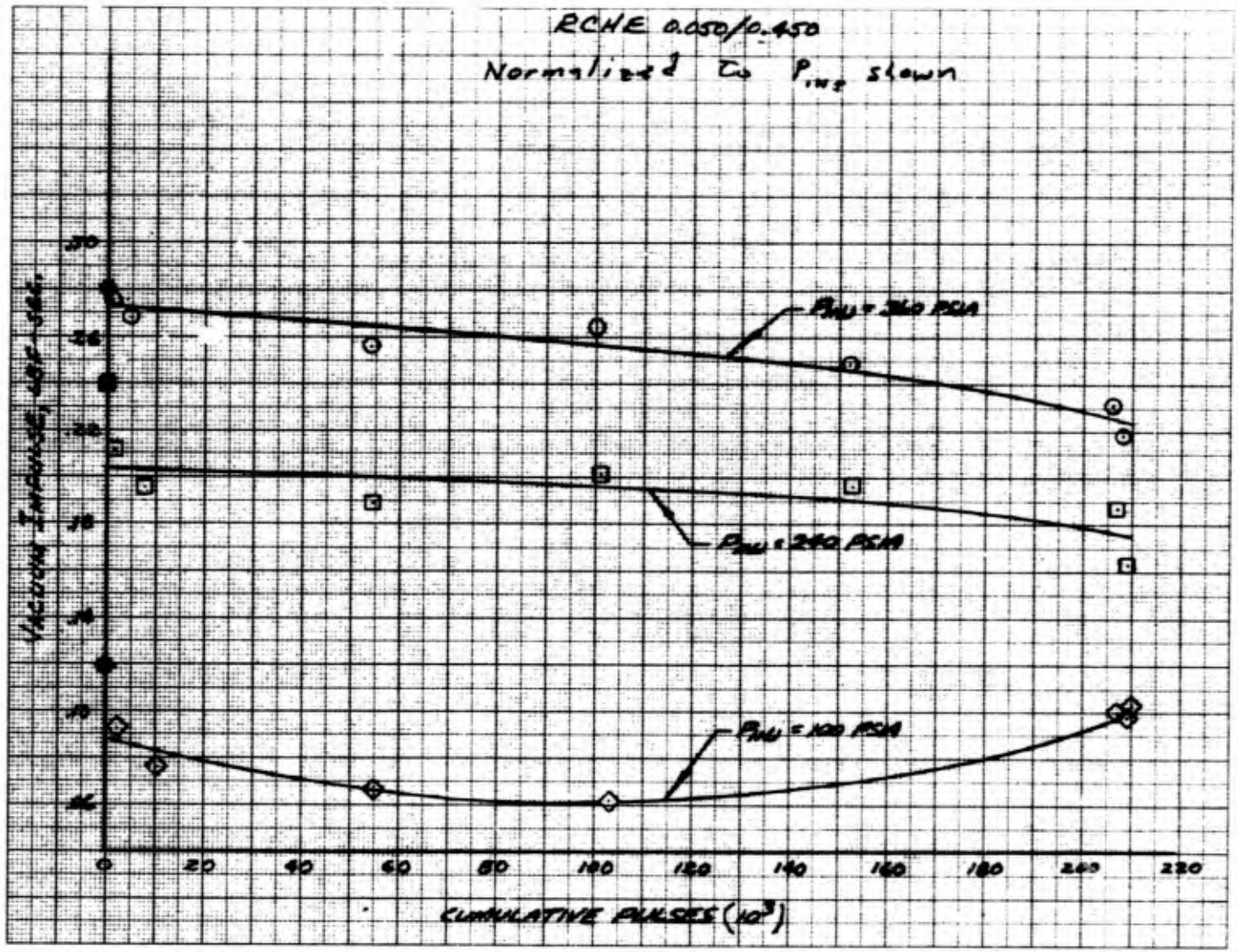
RCHE 0.050/0.450
Normalized to P_INI shown
P_INJ = 360 PSIA
P_INJ = 240 PSIA
P_INJ = 100 PSIA
CUMULATIVE PULSES (10^3)
0
20
40
60
80
100
120
140
160
180
200
220

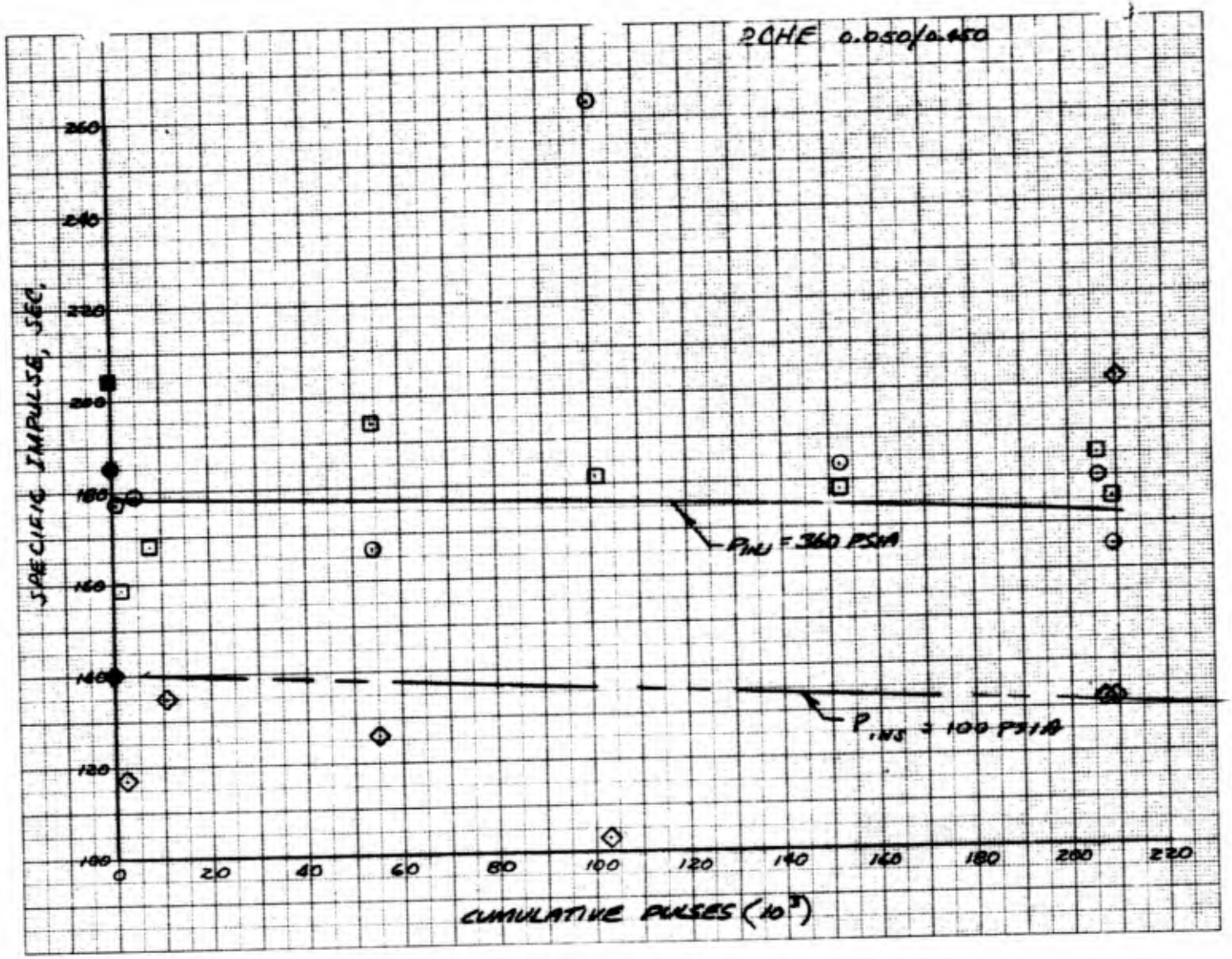
2CHE 0.050/0.450
SPECIFIC IMPULSE, SEC.
260
240
220
200
180
160
140
120
100
0
20
40
60
80
100
120
140
160
180
200
220
CUMULATIVE PULSES (10³)
P_INJ = 360 PSIA
P_INJ = 100 PSIA

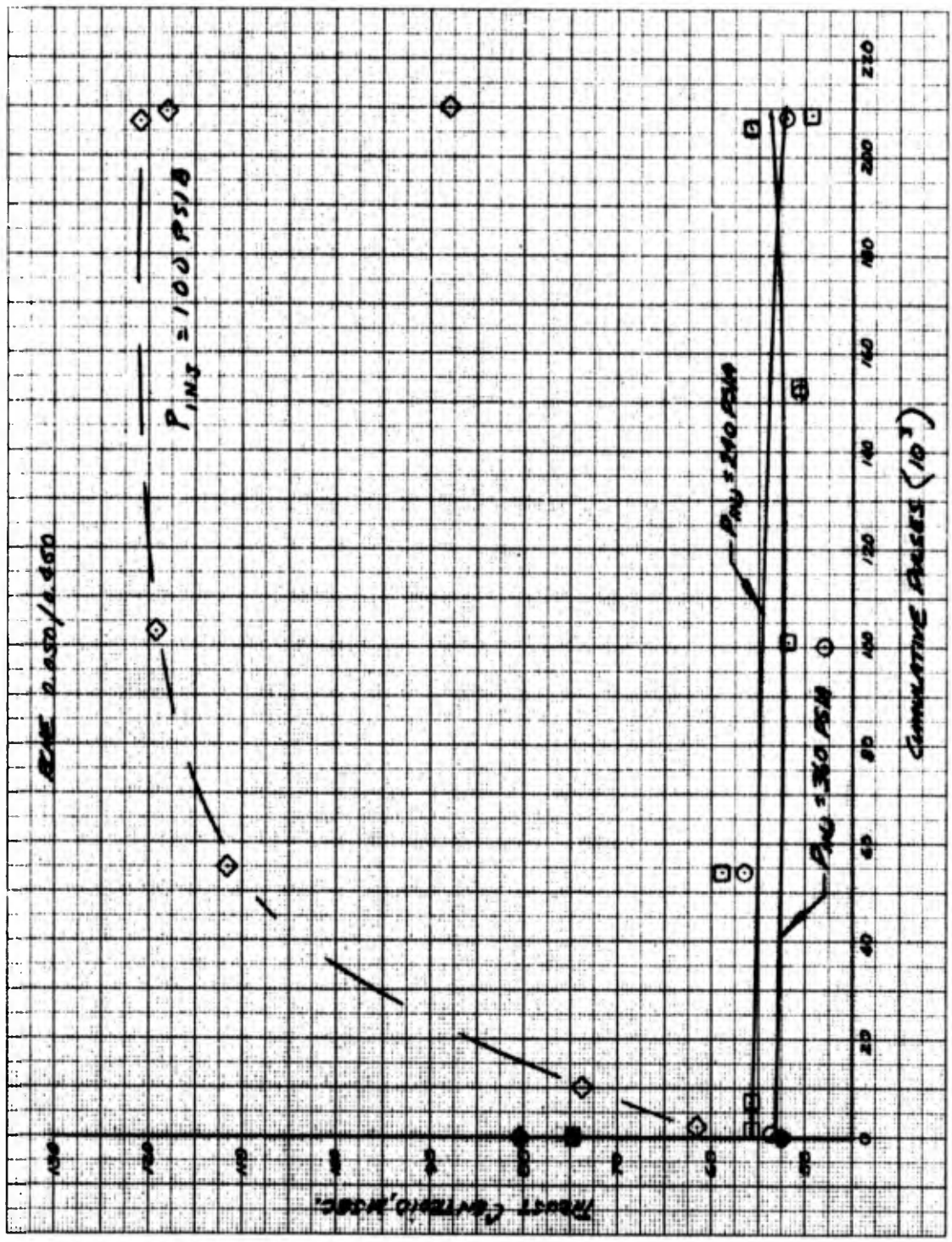
P_{INJ} = 1050 PSIG
P_{INJ} = 1040 PSIG
P_{INJ} = 1030 PSIG
Cumulative Pulses (10^3)

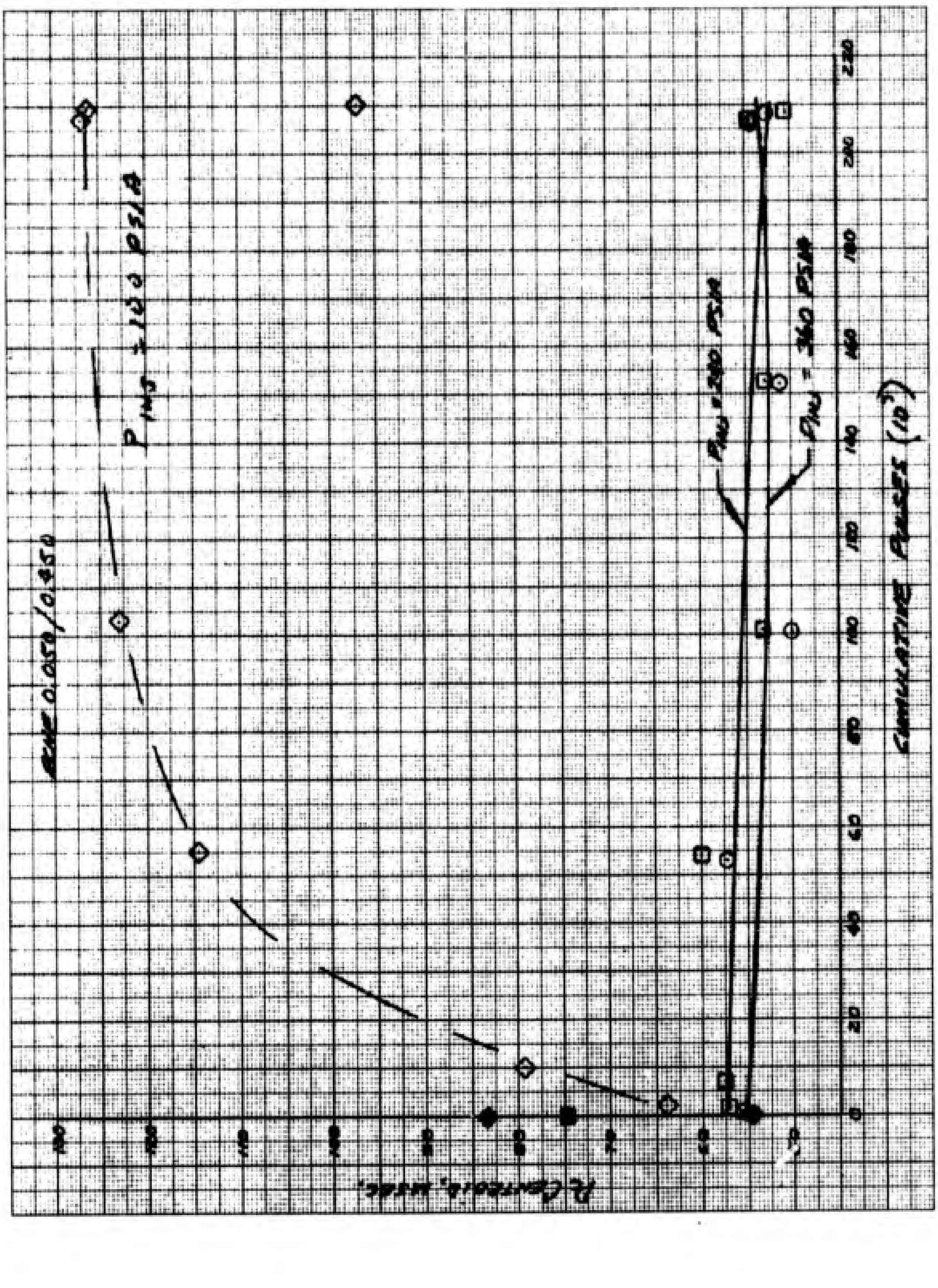
P INJ = 100 PSIA
P INJ = 280 PSIA
P INJ = 360 PSIA
CUMULATIVE PULSES (10^3)

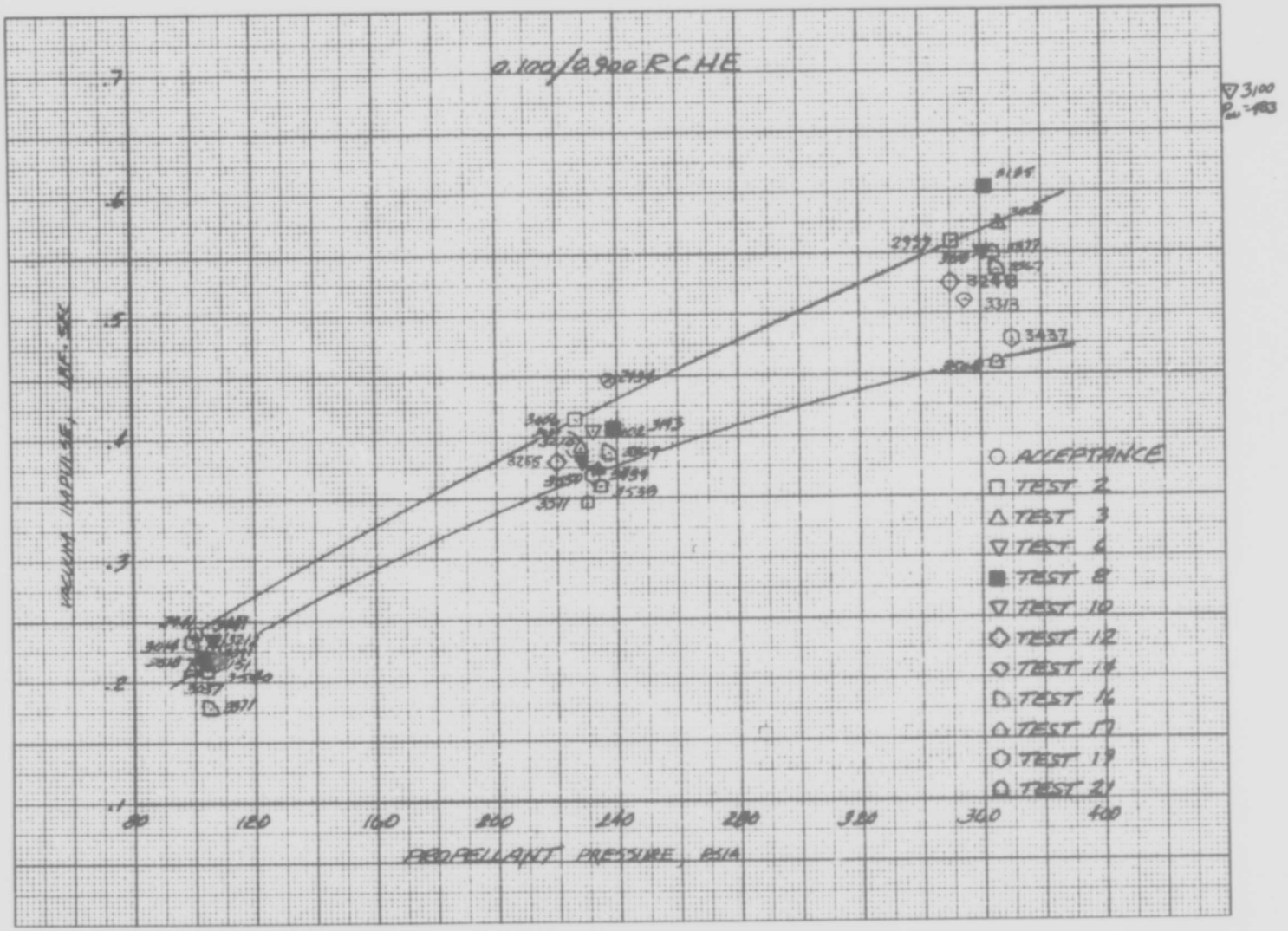
0.100/0.900 RCHE
VACUUM IMPULSE, LBF-SEC
PROPELLANT PRESSURE, PSIA
.1
.2
.3
.4
.5
.6
.7
80
120
160
200
240
280
320
360
400
ACCEPTANCE
TEST 2
TEST 3
TEST 6
TEST 8
TEST 10
TEST 12
TEST 14
TEST 16
TEST 17
TEST 19
TEST 21

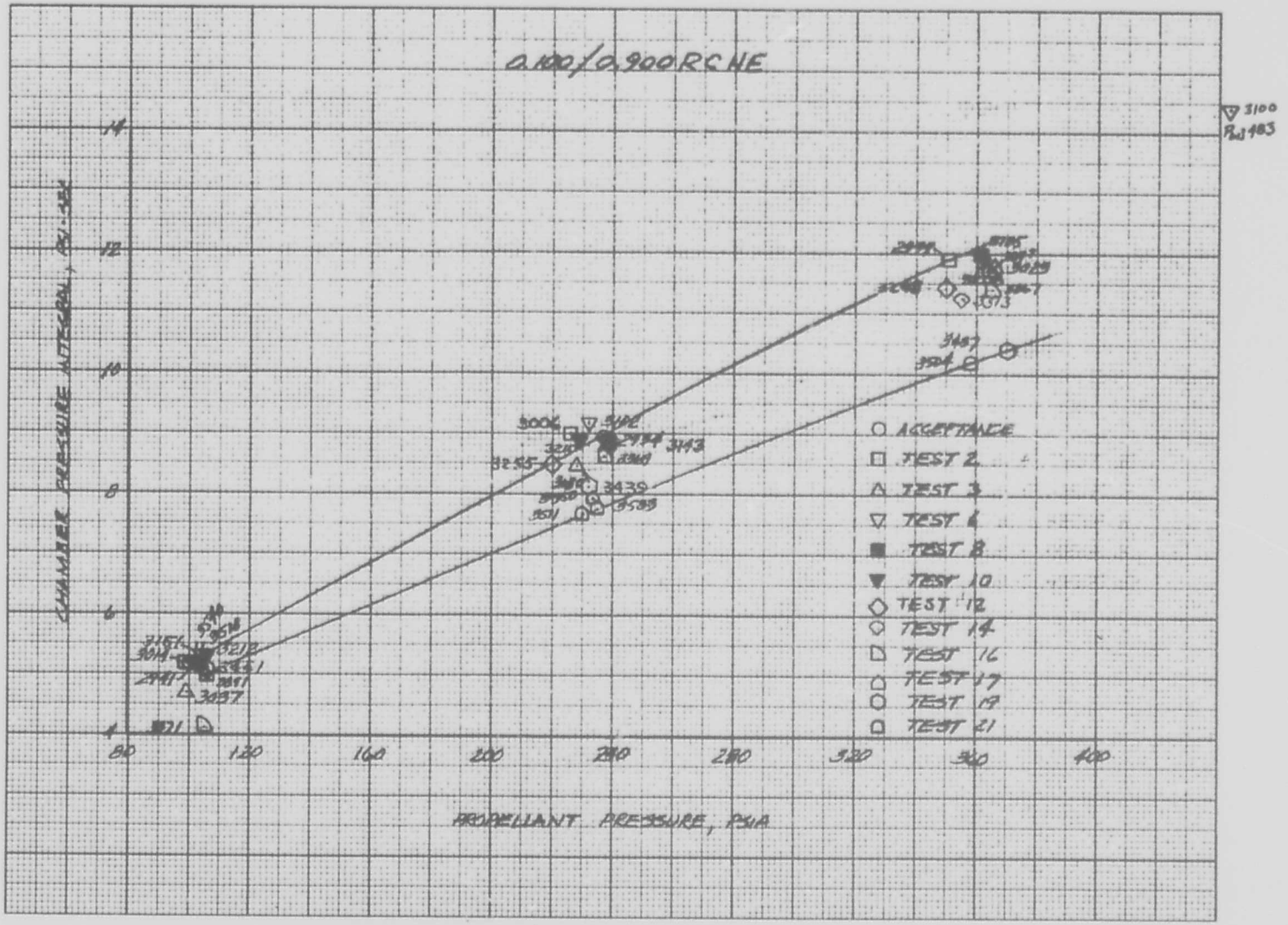
0.100/0.900RCHE
CHAMBER PRESSURE INTEGRAL, PSI-SEC
PROPELLANT PRESSURE, PSIA
ACCEPTANCE
TEST 2
TEST 3
TEST 4
TEST 8
TEST 10
TEST 12
TEST 14
TEST 16
TEST 17
TEST 19
TEST 21
80
120
160
200
240
280
320
360
400
4
6
8
10
12
14

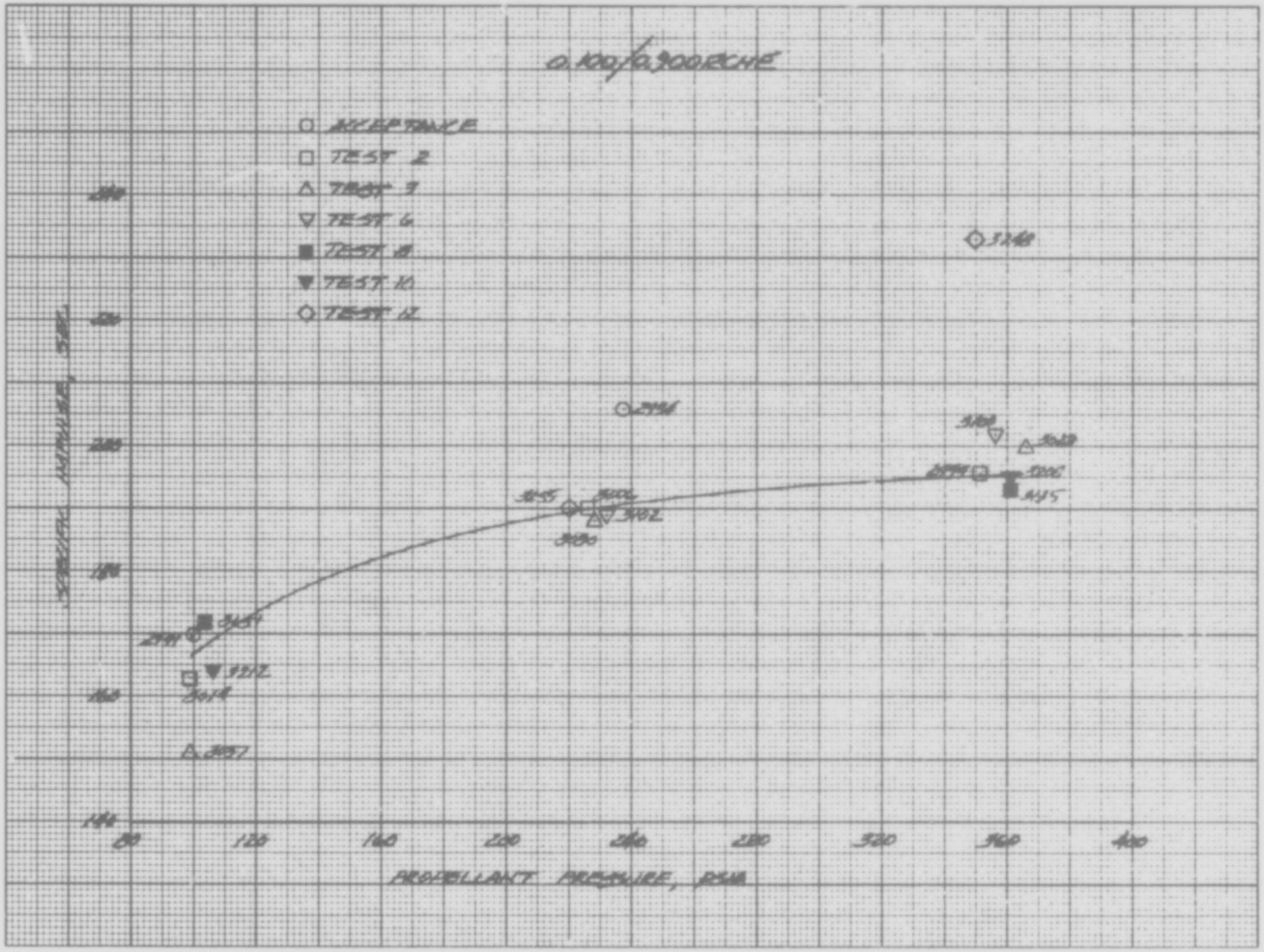
0.100 to 300 RCHE
ACCEPTANCE
TEST 2
TEST 4
TEST 6
TEST 8
TEST 10
TEST 12
THRUST, PRIMARY, POUNDS
PROPELLANT PRESSURE, PSIA
80
120
160
200
240
280
320
360
400

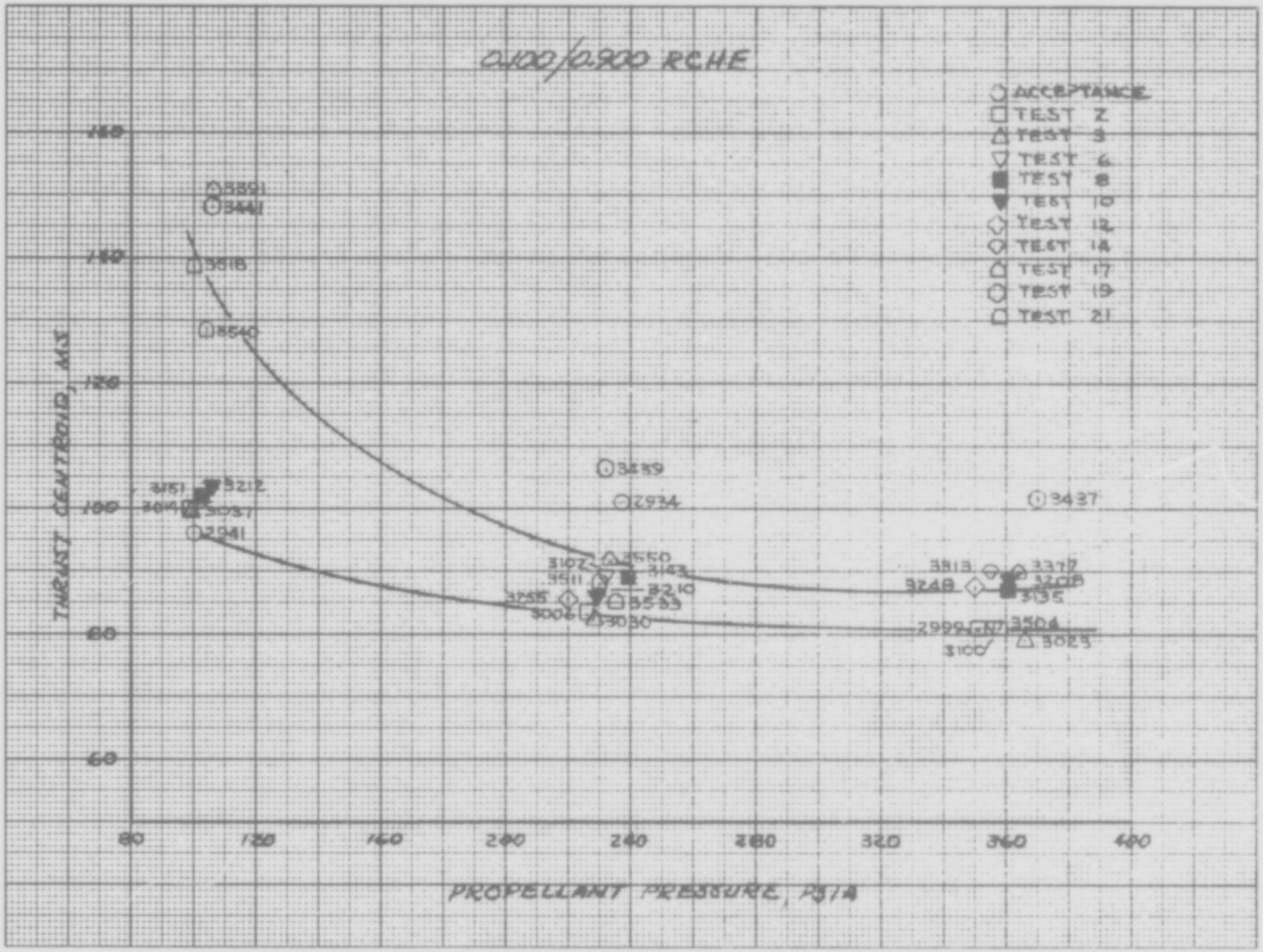
0.400/0.900 RCHE
ACCEPTANCE
TEST 2
TEST 4
TEST 6
TEST 8
TEST 10
TEST 12
TEST 14
TEST 17
TEST 19
TEST 21
THRUST CENTROID, MM
PROPELLANT PRESSURE, PSIA
160
140
120
100
80
60
80
120
160
200
240
280
320
360
400
3891
3441
3618
3540
3212
3451
3037
2941
3489
2934
3437
3550
3143
3210
3583
3030
3748
3135
3504
3025
3100

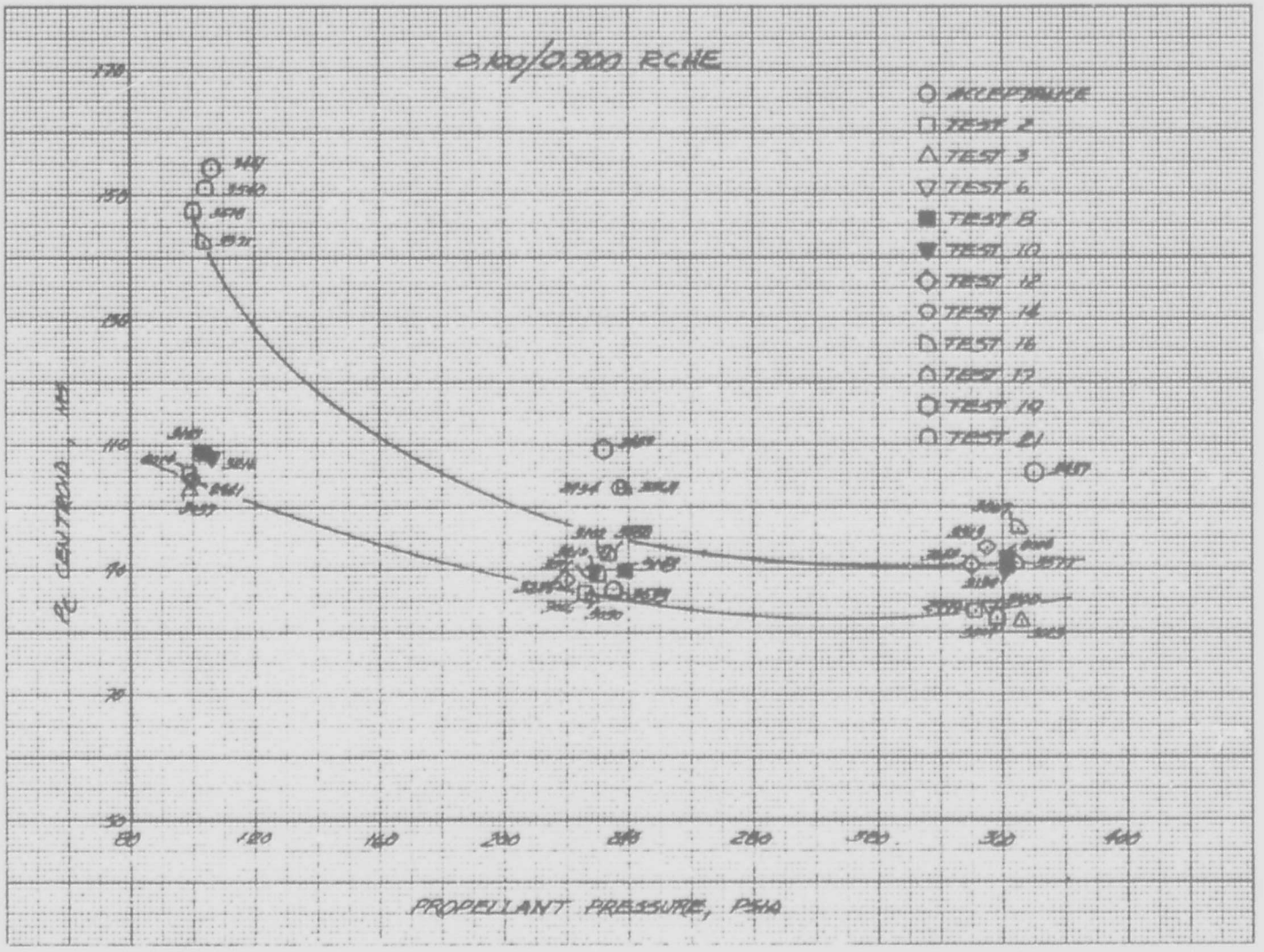
0.100/0.300 RCHE
ACCEPTANCE
TEST 2
TEST 3
TEST 6
TEST 8
TEST 10
TEST 12
TEST 14
TEST 16
TEST 17
TEST 19
TEST 21
PROPELLANT PRESSURE, PSIA

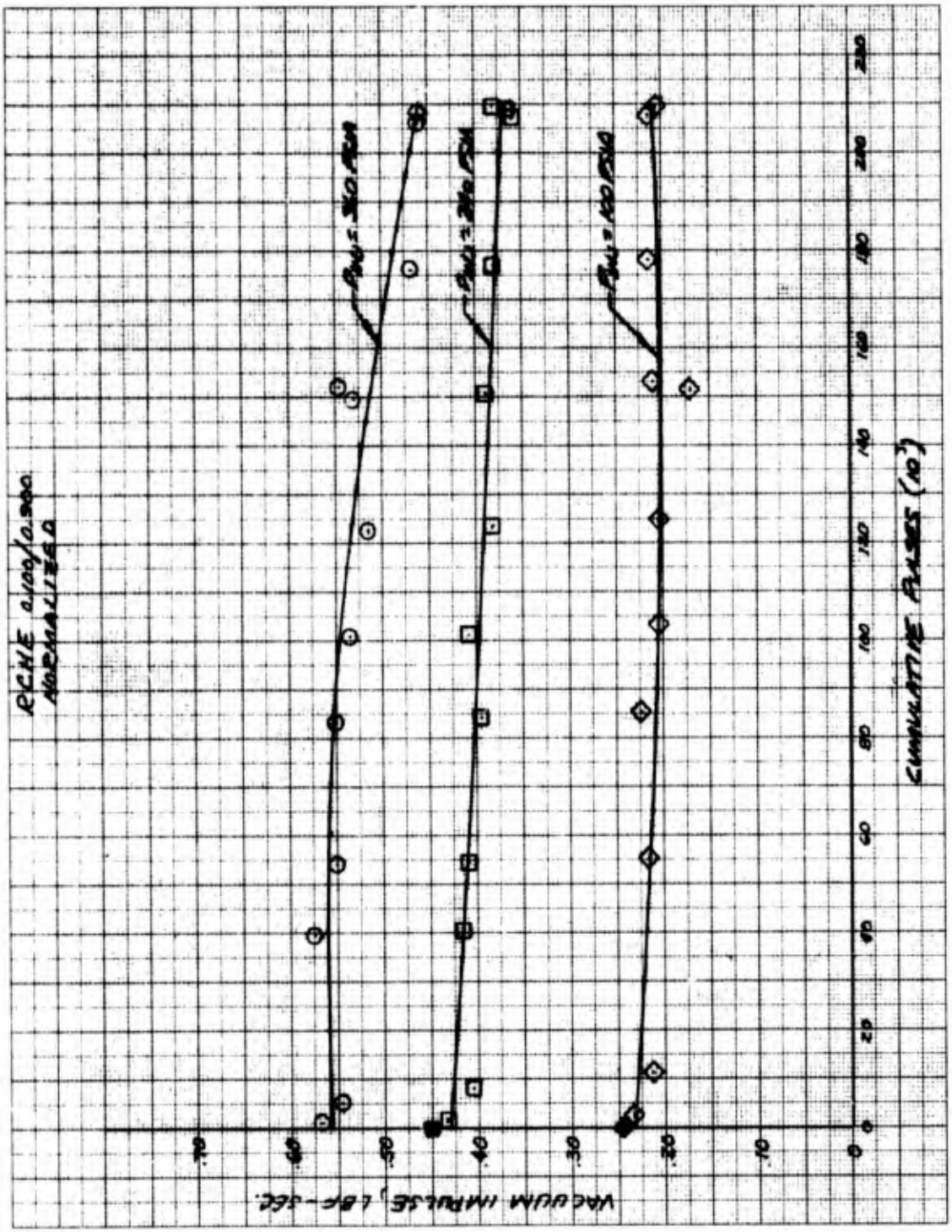
PICKLE area/a.900
MECHANICIZED
CUMULATIVE PULSES (10³)
VACUUM IMPULSE, LBF-SEC.

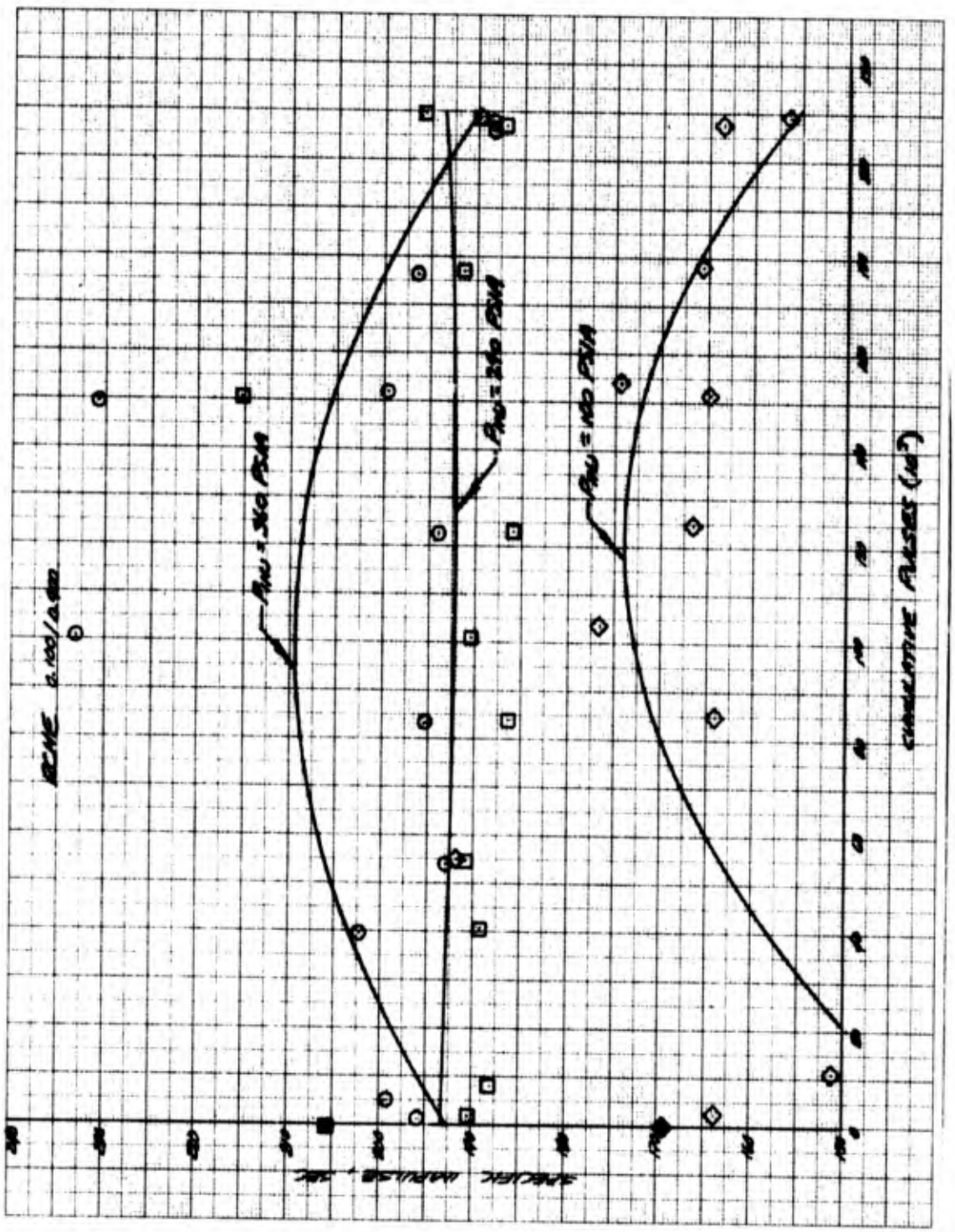

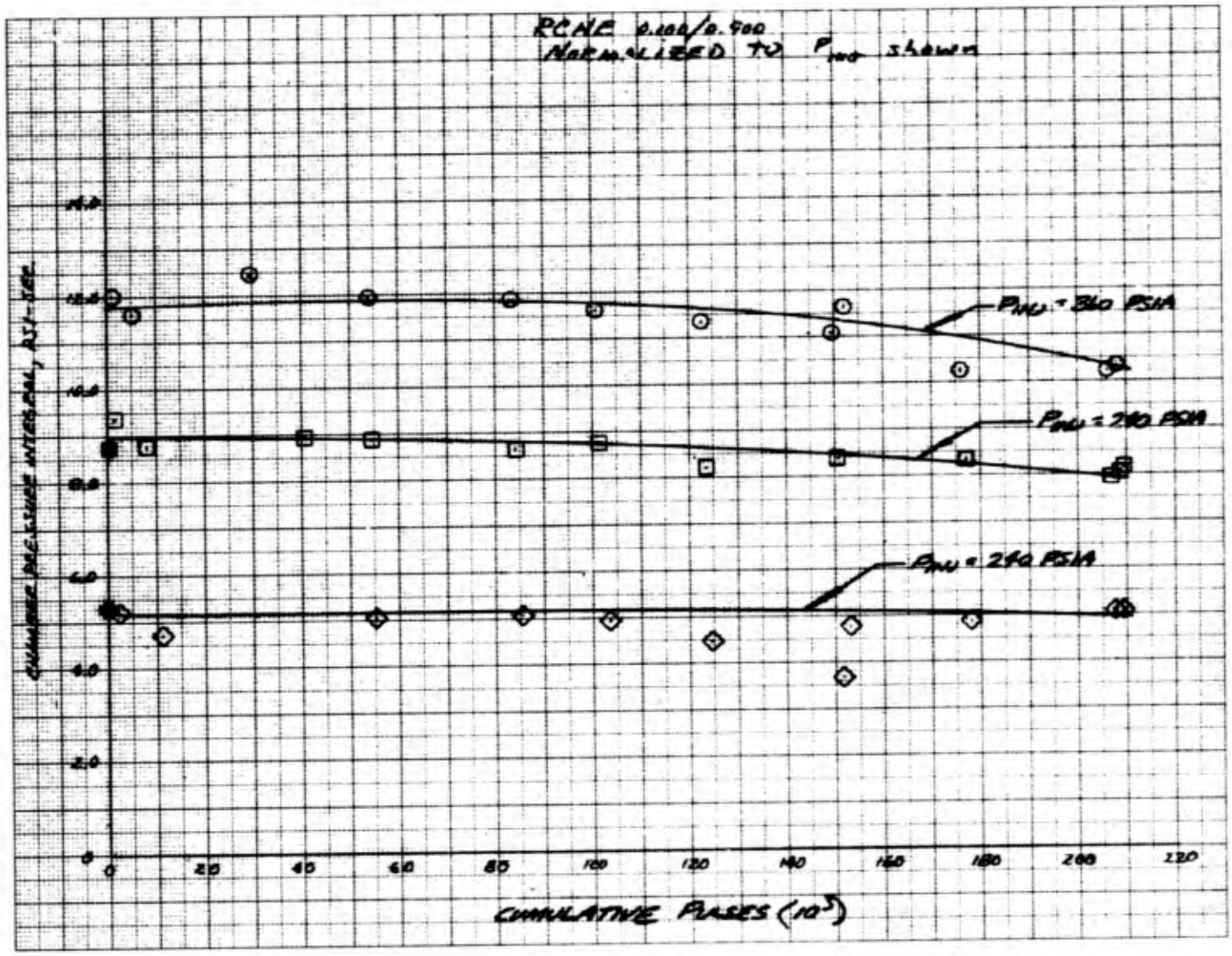
RCNC 0.100/0.900
NORMALIZED TO P_{INJ} shown
P_{INJ} = 360 PSIA
P_{INJ} = 280 PSIA
P_{INJ} = 240 PSIA
CUMULATIVE PRESSURE INTEGRAL, PSI-SEC
CUMULATIVE PULSES (10^3)
0
20
40
60
80
100
120
140
160
180
200
220

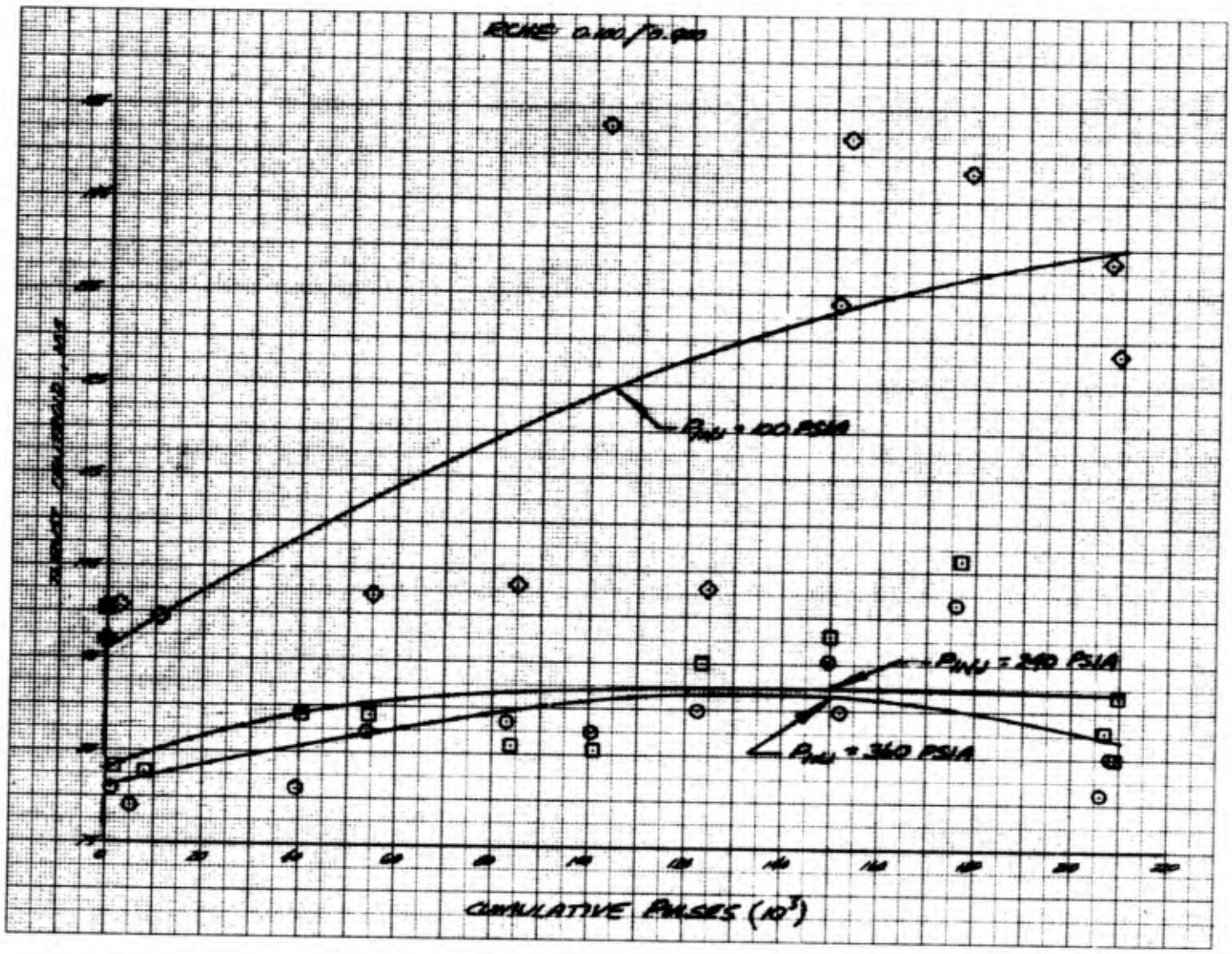
P_{INJ} = 100 PSIA
P_{INJ} = 250 PSIA
P_{INJ} = 360 PSIA
CUMULATIVE PULSES (10^3)

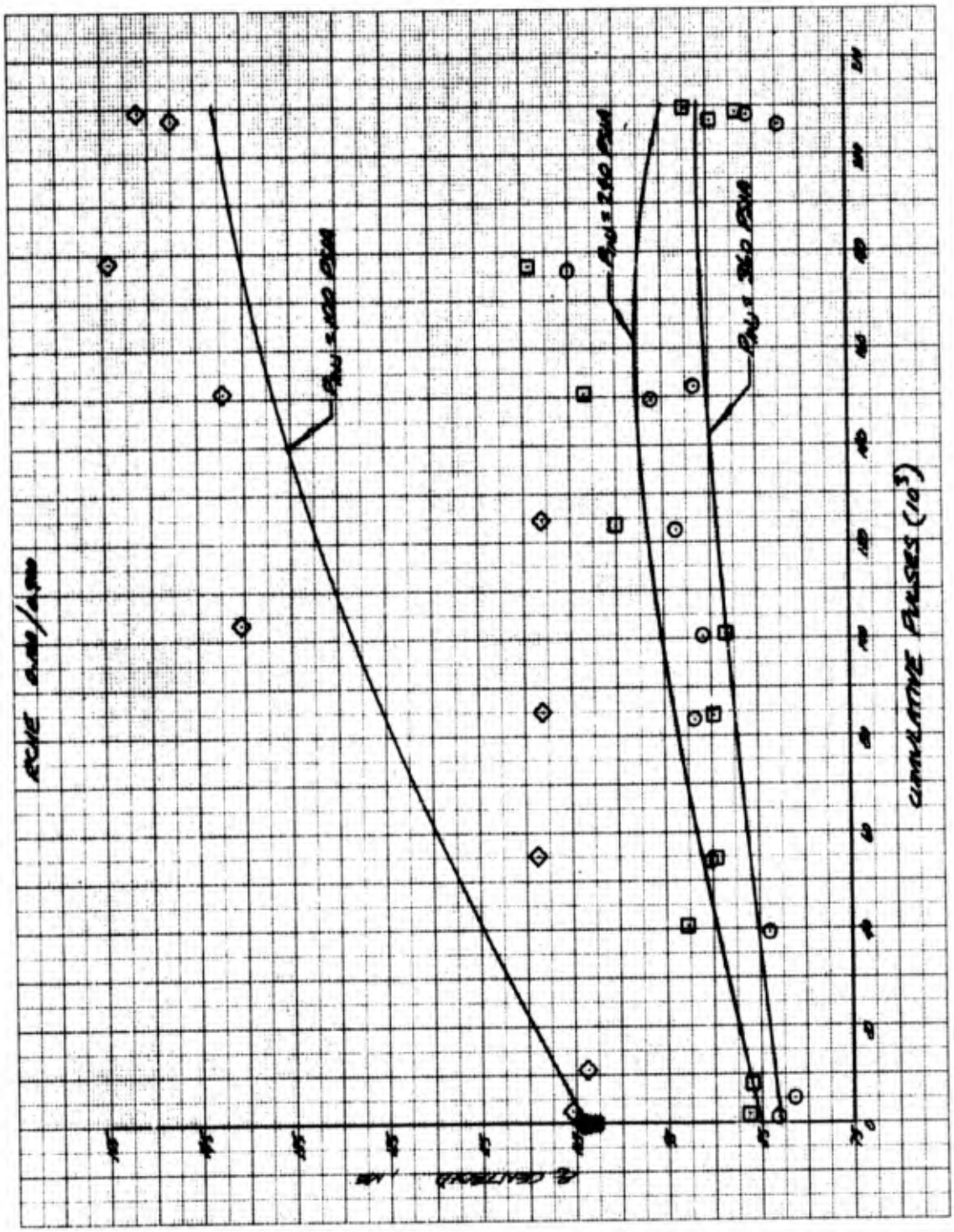

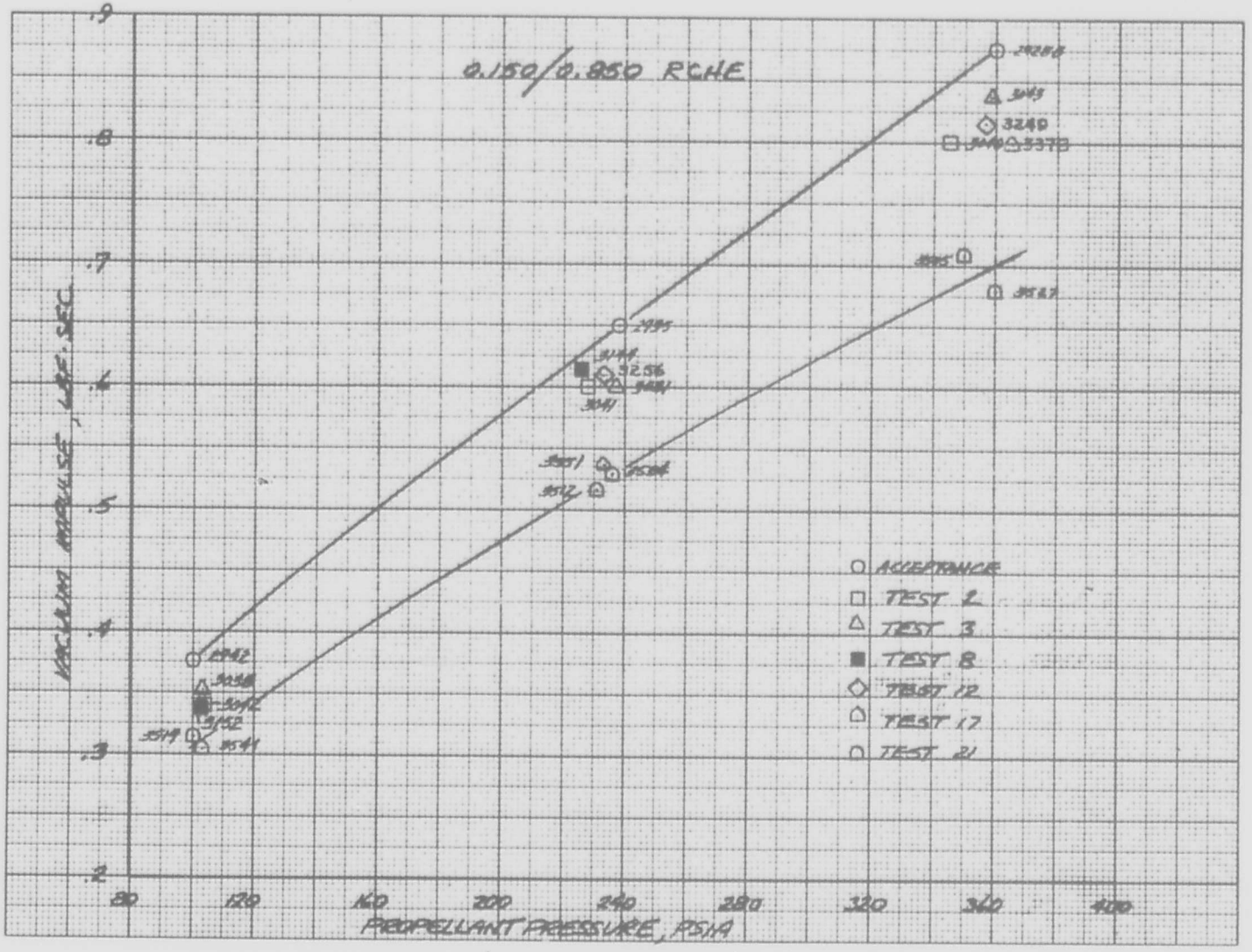
0.150/0.850 RCHE
ACCEPTANCE
TEST 2
TEST 3
TEST 8
TEST 12
TEST 17
TEST 21
MACH NUMBER AT THROAT, SEC.
PROPELLANT PRESSURE, PSIA
.9
.8
.7
.6
.5
.4
.3
.2
80
120
160
200
240
280
320
360
400

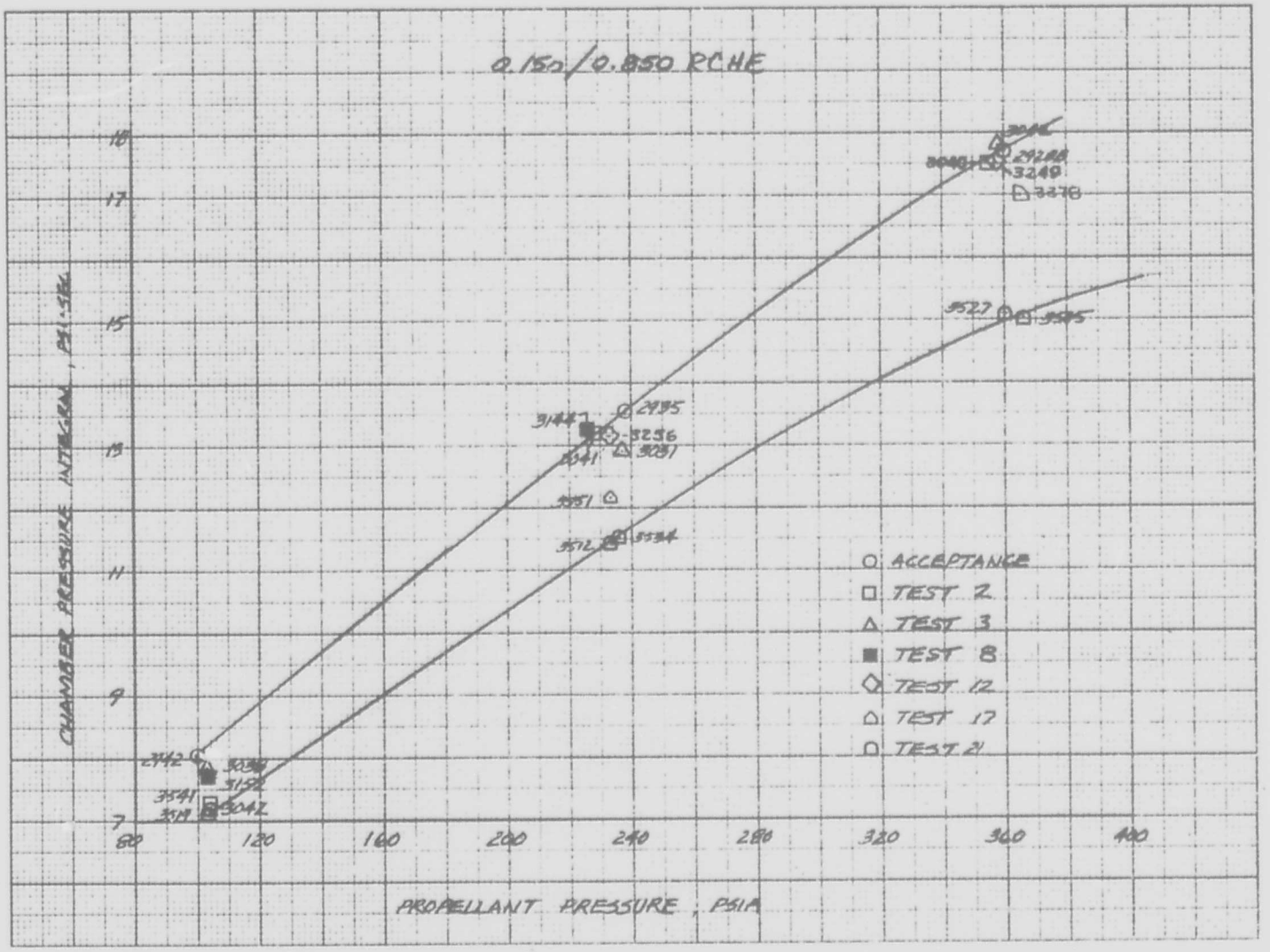
0.150/0.850 RCHE
CHAMBER PRESSURE INTEGRAL, PSI-SEC
PROPELLANT PRESSURE, PSIA
7
9
11
13
15
17
80
120
160
200
240
280
320
360
400
ACCEPTANCE
TEST 2
TEST 3
TEST 8
TEST 12
TEST 17
TEST 21

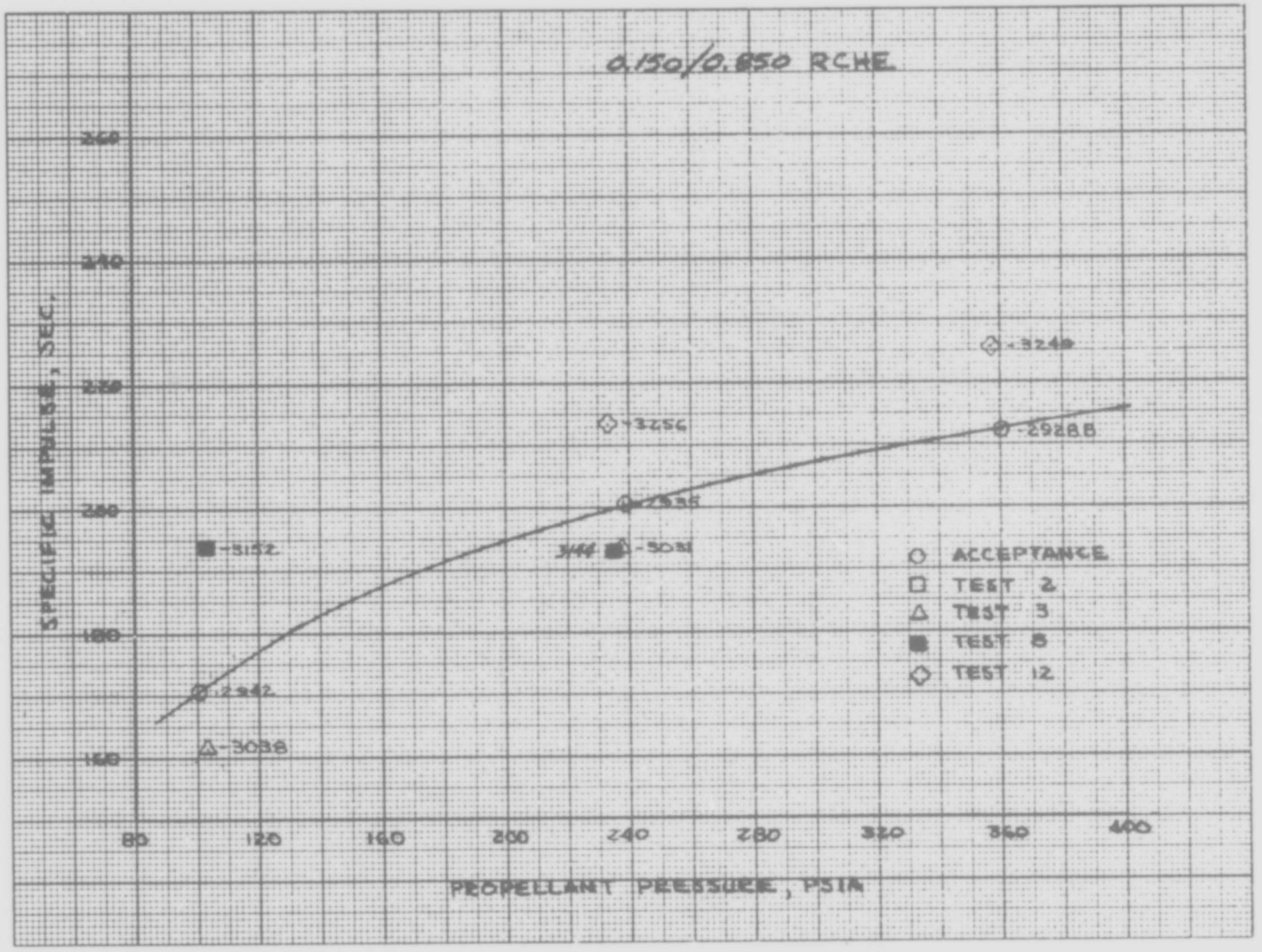
0.150/0.850 RCHE
SPECIFIC IMPULSE, SEC.
260
240
220
200
180
160
80
120
160
200
240
280
320
360
400
PROPELLANT PRESSURE, PSIA
-3248
-3256
-2928B
-2958
-3152
-3031
-2942
-3038
ACCEPTANCE
TEST 2
TEST 3
TEST 8
TEST 12

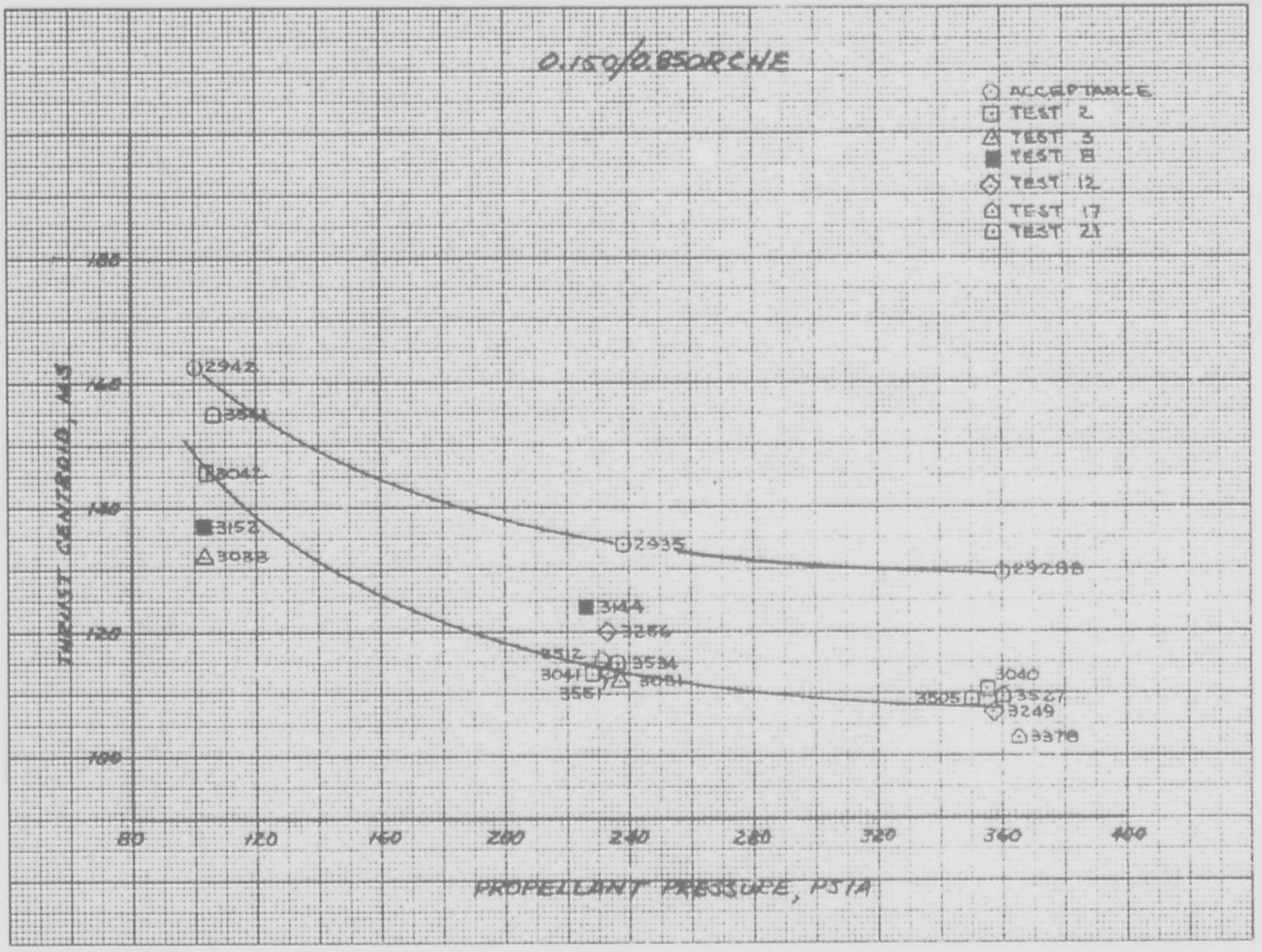
0.150/0.850RCHE
ACCEPTANCE
TEST 2
TEST 5
TEST 8
TEST 12
TEST 17
TEST 21
THRUST CENTROID, MS
PROPELLANT PRESSURE, PSIA
100
140
180
80
120
160
200
240
280
320
360
400
2942
3044
3042
3152
3088
2935
2928B
3144
3256
3512
3534
3041
3081
3561
3505
3040
3527
3249
3378

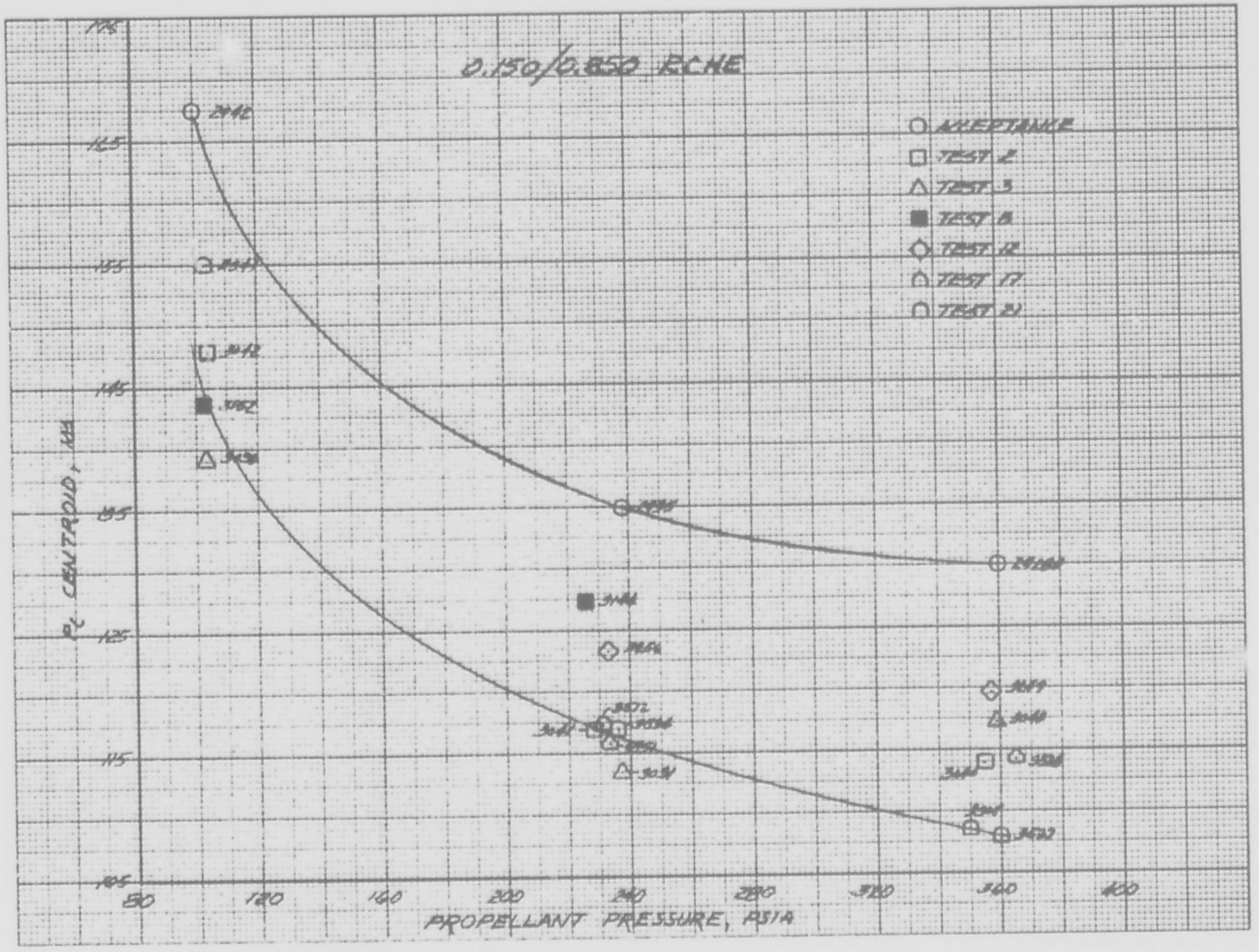
0.150/0.850 RCHE
ACCEPTANCE
TEST 2
TEST 5
TEST 8
TEST 12
TEST 17
TEST 21
PROPELLANT PRESSURE, PSIA
50
120
160
200
240
280
320
360
400
105
115
125
135
145
155
165

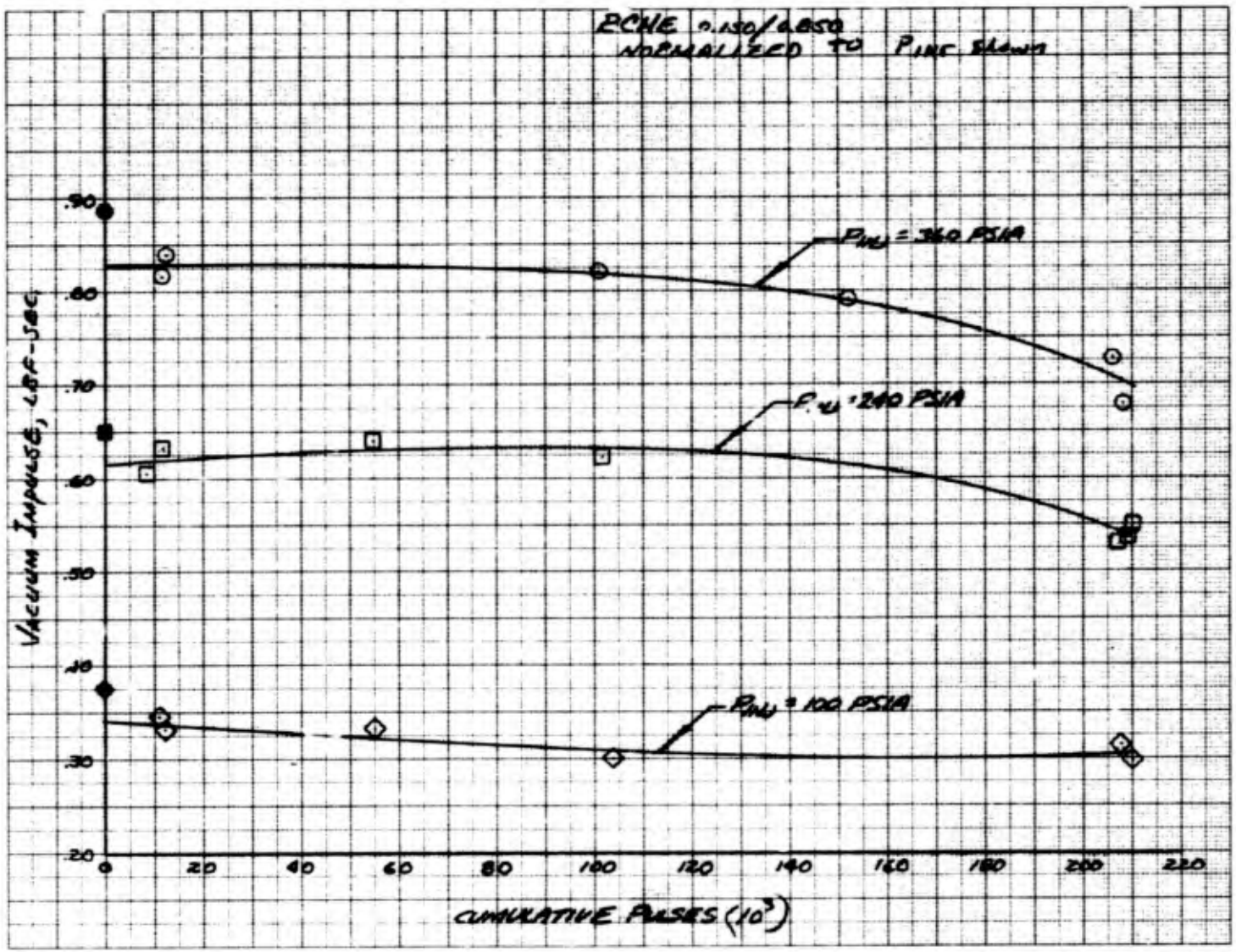
RCHE 0.150/0.850
NORMALIZED TO PINJ SHOWN
P_{INJ} = 360 PSIA
P_{INJ} = 240 PSIA
P_{INJ} = 100 PSIA
VACUUM IMPULSE, LBF-SEC
.90
.80
.70
.60
.50
.40
.30
.20
0
20
40
60
80
100
120
140
160
180
200
220
CUMULATIVE PULSES (10^3)

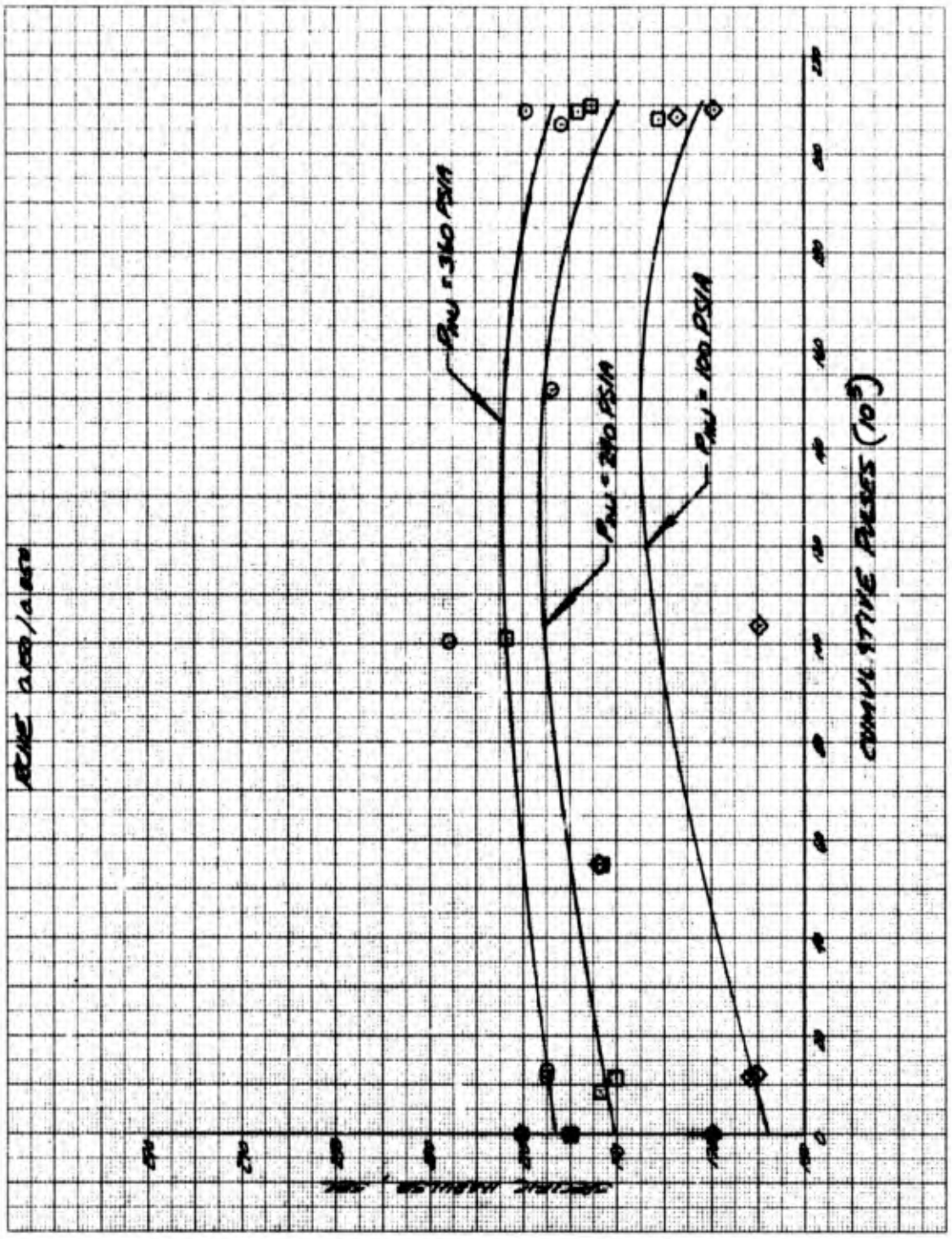

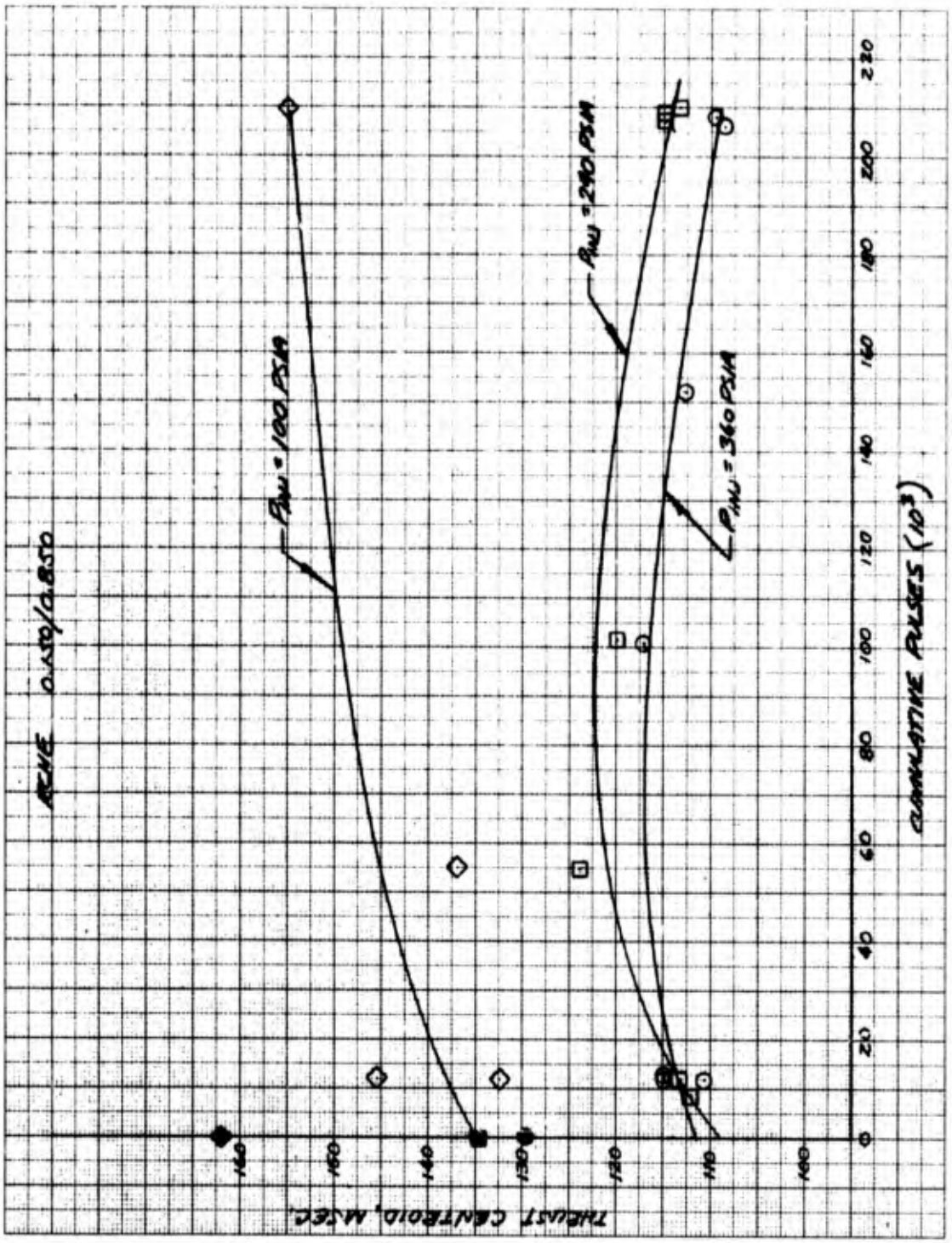
ARENE 0.45TQ/0.85D
P_{HU} = 100 PSIA
P_{HU} = 240 PSIA
P_{HU} = 360 PSIA
THRUST CENTROID, M SEC.
CUMULATIVE PULSES (10^3)

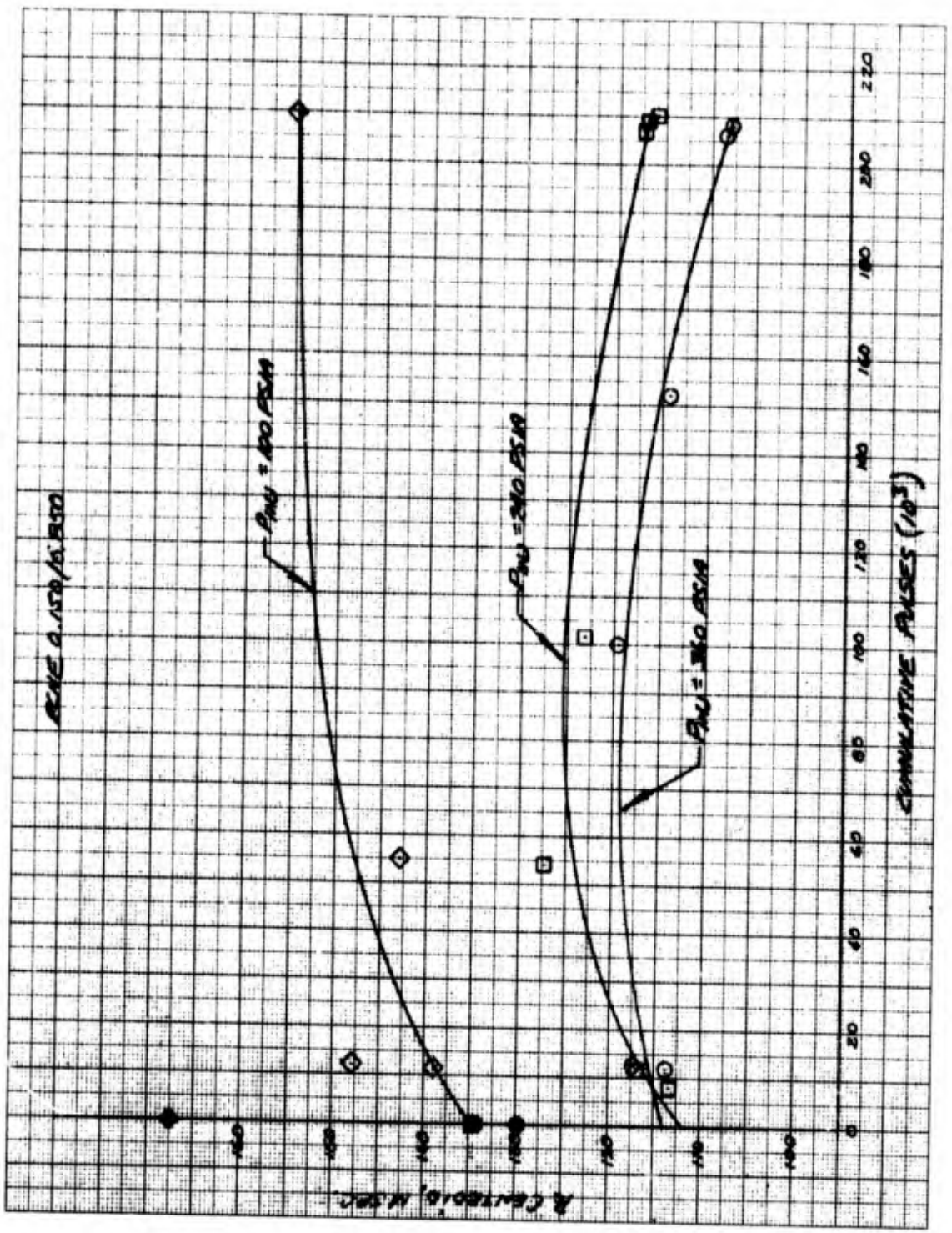
CUMULATIVE PULSES (10^3)
P_{INJ} = 400 PSIG
P_{INJ} = 340 PSIG
P_{INJ} = 300 PSIG

APPENDIX B

ENGINE TEST LOG

ENGINE TEST SUMMARY

RCHE S/N X001

ACCEPTANCE

DATE	TEST NO.	TANK PRESS (PSIA)	INJ. PRESS (PSIA)	PULSE MODE CHARACTERISTICS: NO. PULSES	CYCLE ON/OFF	CHAMBER PRESSURE INTEGRAL: PULSE 1-5	CHAMBER PRESSURE INTEGRAL: PULSE 90-100	CHAMBER PRESSURE INTEGRAL: LAST 10 PULSES	VACUUM IMPULSE: PULSE 1-5	VACUUM IMPULSE: PULSE 90-100	VACUUM IMPULSE: LAST 10 PULSES	IMPULSE SHIFT (%)	P_c SHIFT (%)	SPECIFIC IMPULSE (SEC)	AVE. CENTROID TIME (MSEC): P_c (MSEC)	AVE. CENTROID TIME (MSEC): THRUST (MSEC)	START TEMP. (°F)	SUMMATION OF PULSES	STEADY STATE CHARACTERISTICS: DURATION (SEC)	THRUST (LBF)	P_c (PSIA)	FLOW RATE (LBM/SEC)	SPECIFIC IMPULSE (SEC)	EPC EPV SHIFT	^1T_c ROUGHNESS (±)	^1T_c TRANSITION BURN TIME (SEC)	SUMMATION OF ON TIME (SEC)	SUMMATION OF PROPELLANT USAGE (LBM)	SUMMATION OF AMBIENT STARTS
6-15	2014	495	347.2	—	—	—	—		—	—				—	—	—	262	—	10.1	5.71	120.3	.02980	224.2		11.5	10.1	10.1	.2605	1
6-15	2020	497	346.5	—	—	—	—		—	—				—	—	—	211.1	—	10.9	5.71	119.9	.02979	228.8		13.6	21.0	21.0	.5416	2
6-15	2021	320	228.6	—	—	—	—		—	—				—	—	—	208.1	—	11.8	6.04	90.1	.01920	215.8		18.8	32.5	32.9	.7481	3
6-15	2022	128	99.3	—	—	—	—		—	—				—	—	—	214.4	—	14.8	2.31	44.3	.01060	215.8		10.1	49.9	49.9	.9462	4
6-15	2023	496	352.0	100	20/980	1.297	2.360		.0250	.1176				173.9	35.96	99.5	185.1	100	—	—	—	—	—		—	—	51.8	1.0141	5
6-15	2024	347	248.6	14	20/480	—	—		—	—				—	—	—	221	114	—	—	—	—	—		—	—	51.6	1.0230	6
6-15	2025	347	248.6	13	20/480	—	—		—	—				—	—	—	216	127	—	—	—	—	—		—	—	51.9	1.0419	7
6-15	2026	347	248.6	20	20/480	—	—		—	—				—	—	—	216	147	—	—	—	—	—		—	—	52.8	1.0441	8
6-15	2028	347	248.6	100	20/480	1.327	2.384		.0236	.1098				171.6	35.30	98.0	196.6	247	—	—	—	—	—		—	—	58.3	1.1081	9
6-15	2029	348	250.0	100	20/480	1.420	2.081		.0254	.2386				181.6	37.32	98.0	198.5	347	—	—	—	—	—		—	—	59.9	1.2535	10
6-15	2030	348	249.0	100	20/480	1.420	2.090		.0252	.2819				185.3	38.62	97.0	200.5	447	—	—	—	—	—		—	—	64.3	1.4053	11
6-15	2031	348	250.0	100	20/480	—	—		—	—				—	—	—	208	547	—	—	—	—	—		—	—	74.3	1.6019	12
6-15	2032	348	250.0	100	20/480	—	—		—	—				—	—	—	197	562	—	—	—	—	—		—	—	87.1	1.7541	13
6-15	2033	350	250.0	15	850/450	—	—		—	—				—	—	—	211.3	761	—	—	—	—	—		—	—	101.9	2.1648	14
6-15	2034	350	250.0	99	20/2250	15.090	17.216		.1896	.8754				211.13	50.00	129.6	197	761	—	—	—	—	—		—	—	102.9	2.1648	14
6-15	2035	499	352.7	—	—	—	—		—	—				—	—	—	201.5	—	10.1	5.79	118.8	.02537	229.7		10.2	99.4	112.0	2.4211	15
6-15	2036	241	248.8	100	20/480	1.078	1.862		.0248	.0998				205.9	36.24	91.6	230	761	—	—	—	—	—		—	—	114.0	2.4697	16
6-15	2037	241	248.6	101	20/480	.8920	1.729		.0498	.1087				214.7	39.44	90.2	216	862	—	—	—	—	—		—	—	116.0	2.5125	17
6-15	2038	242	248.6	100	20/480	3.062	4.602		.1582	.2614				211.8	74.32	72.2	207	962	—	—	—	—	—		—	—	121.2	2.6415	18
6-15	2039	244	249.8	100	20/480	2.908	8.160		.1410	.2622				204.4	74.38	74.5	216	1062	—	—	—	—	—		—	—	126.2	2.7400	19
6-15	2040	245	249.6	100	20/480	7.052	8.966		.3482	.4876				206.1	89.2	101.8	216	1162	—	—	—	—	—		—	—	136.2	2.9772	20
6-15	2041	246	250.0	100	20/480	11.442	13.552		.3470	.6495				200.9	96.9	134.0	226	1262	—	—	—	—	—		—	—	151.2	3.3614	21
6-15	2042	320	230.0	—	—	—	—		—	—				—	—	—	211.3	—	10.8	4.26	81.8	.01903	221.2		7.1	70.2	162.0	3.5129	22
6-15	2043	104	105.0	100	20/480	.5760	1.062		.0258	.0514				197.0	52.96	68.1	216	1962	—	—	—	—	—		—	—	169.0	3.5492	23
6-15	2044	101	99.8	101	20/480	.5860	1.082		.0272	.0498				164.2	47.96	68.8	197	1869	—	—	—	—	—		—	—	166.0	3.5842	24
6-15	2045	104	104.8	100	20/480	.6420	2.625		.0270	.1220				157.6	63.28	60.6	216	1968	—	—	—	—	—		—	—	171.0	3.6616	25
6-15	2046	102	100.0	100	20/480	1.560	2.438		.0746	.1186				146.3	89.92	89.8	221	1469	—	—	—	—	—		—	—	176.0	3.7461	26
6-15	2047	104	100.1	100	20/480	3.8660	5.140		.1722	.2608				168.8	94.56	96.2	216	1768	—	—	—	—	—		—	—	186.0	3.8079	27
6-15	2048	102	100.2	100	20/480	5.1890	8.050		.2669	.3762				170.6	127.5	162.8	218	1869	—	—	—	—	—		—	—	201.0	4.1284	28
6-15	2049	129	101.3	—	—	—	—		—	—				—	—	—	227.2	—	10.7	2.73	42.6	.01072	208.1		9.5	89.9	211.7	4.2291	29

1 Pc ROUGHNESS DETERMINED FROM DATA BETWEEN 8 AND 10 SECONDS

2 40.4% OVERSHOOT AT APPROX. 15 SECONDS

ENGINE TEST SUMMARY

DATE	TEST NO.	TANK PRESS. (PSIA)	INJ. PRESS. (PSIA)	PULSE MODE CHARACTERISTICS																STEADY STATE CHARACTERISTICS								SUMMATION OF ON TIME (SEC)	SUMMATION OF PROPELLANT USAGE (LBM)	SUMMATION OF AMBIENT STARTS
				NO. PULSES	CYCLE ON/OFF	CHAMBER PRESSURE INTEGRAL PULSE 1-5	CHAMBER PRESSURE INTEGRAL PULSE 90-100	CHAMBER PRESSURE INTEGRAL LAST 10 PULSES	VACUUM IMPULSE PULSE 1-5	VACUUM IMPULSE PULSE 90-100	VACUUM IMPULSE LAST 10 PULSES	IMPULSE SHIFT (%)	P_C SHIFT (%)	SPECIFIC IMPULSE (SEC)	AVE. CENTROID TIME (MSEC) P_C (MSEC)	AVE. CENTROID TIME (MSEC) THRUST (MSEC)	START TEMP. (°F)	SUMMATION OF PULSES	DURATION (SEC)	THRUST (LBF)	P_C (PSIA)	FLOW RATE (LBM/SEC)	SPECIFIC IMPULSE (SEC)	$\frac{\text{IPC}}{\text{IFV}}$ SHIFT	P_C ROUGHNESS (±)	STEADY-STATE BURN TIME (SEC)				
7-10	9979	365	—	—	—	—	—		—	—	—	—	—	—	—	—	—	—	—	—	—	—	—	—	—	—	—	0	0	—
7-11	9980	362	263	—	—	—	—		—	—	—	—	—	—	—	—	214	—	10.0	4461	94.6	—	—	18/5A	10.7	10.0	10.0	.2000	1
7-11	9981	495	349	—	—	—	—		—	—	—	—	—	—	—	—	210	—	10.0	5453	116.9	.02557	221.1	19/9	13.7	20.0	20.0	.4457	2
7-11	9982	127	101	—	—	—	—		—	—	—	—	—	—	—	—	209	—	10.0	2.237	47.1	.01068	209.0	23/22	19.2	40.0	40.0	.5625	3
7-12	9991	285	—	111	SHEEP	—	—		—	—	—	—	—	—	—	—	320	111	10.0	—	—	—	—	—	—	40.0	52.9	—	—
7-12	9992	115	—	187	SHEEP	—	—		—	—	—	—	—	—	—	—	358	298	10.0	—	—	—	—	—	—	50.0	77.8	—	—
7-12	9993	100	—	168	SHEEP	—	—		—	—	—	—	—	—	—	—	645	406	10.0	—	—	—	—	—	—	60.0	56.5	1.4482	—
7-13	9994	365		100	20/480												210	506	—	—	—	—	—	—	—	—	98.5	1.5535	4
7-13	9995	365	—	100	20/480	—	—		—	—	—	—	—	—	—	—	210	606	—	—	—	—	—	—	—	—	100.5	1.6188	5
7-16	9996	362	241	100	20/480	1.385	2.192		.0781	.1094	—			158.9	35.98	39.16	208	706	—	—	—	—	—	—	—	—	162.5	1.6841	6
7-16	9997	362	350	100	50/450	4.009	5.242		.1806	.2219	—			185.2	52.16	50.48	207	806	—	—	—	—	—	—	—	—	107.5	1.8809	7
7-16	9998	361	347	100	50/450	3.821	5.690		.1846	.2698	—			177.6	53.64	53.69	209	906	—	—	—	—	—	—	—	—	112.5	1.9822	8
7-16	9999	360	351	100	100/400	9.305	11.89		.4997	.3588	—			195.7	80.20	80.90	215	1006	—	—	—	—	—	—	—	—	122.5	2.2677	9
7-16	9000	365	—	100	150/850	—	—		—	—	—	—	—	—	—	—	210	1106	—	—	—	—	—	—	—	—	137.5	2.4190	10
7-16	9001	364	353	—	—	—	—		—	—	—	—	—	—	—	—	218	—	10.0	5.747	118.1	.02456	234.1	17/0	16.0	70.0	149.5	2.6446	11
7-16	9002	241	24	100	20/480	1.084	1.872		.0513	.0875	—			163.9	40.00	36.88	216	1206	—	—	—	—	—	—	—	—	49.5	2.7178	12
7-16	9003	291	226	100	20/480	.8979	1.585		.0478	.0855	—			162.6	37.78	36.44	214	1306	—	—	—	—	—	—	—	—	151.5	2.7623	13
7-16	9004	297	230	100	50/450	2.968	4.454		.1376	.2068	—			180.2	55.20	53.00	210	1406	—	—	—	—	—	—	—	—	156.5	2.8626	14
7-16	9005	299	232	100	50/450	2.895	4.286		.1388	.2068	—			158.7	57.07	55.87	216	1506	—	—	—	—	—	—	—	—	161.5	3.0129	15
7-16	9006	297	226	100	100/400	7.137	9.000		.3279	.4153	—			190.9	86.27	85.83	219	1606	—	—	—	—	—	—	—	—	171.5	3.2906	16
7-16	9007	297	—	100	150/850	—	—		—	—	—	—	—	—	—	—	210	1706	—	—	—	—	—	—	—	—	176.5	3.4665	17
7-16	9008	318	227	—	—	—	—		—	—	—	—	—	—	—	—	206	—	9.9	9.770	87.4	.01919	219.9	10/3	12.1	79.9	110.4	3.4564	18
7-17	9009	109	103	100	20/480	.6727	1.095		.0284	.0490	—			138.7	33.16	32.88	206	1806	—	—	—	—	—	—	—	—	112.4	3.4673	19
7-17	9010	105	109	100	20/480	.4534	1.123		.0270	.0590	—			149.2	49.16	44.00	211	1906	—	—	—	—	—	—	—	—	114.4	3.5285	20
7-17	9011	104	100	100	50/450	1.285	2.649		.0769	.1213	—			158.6	64.89	61.36	220	2006	—	—	—	—	—	—	—	—	119.4	3.6049	21
7-17	9012	104	102	100	50/450	1.341	2.484		.0625	.1159	—			150.1	64.99	61.68	202	2106	—	—	—	—	—	—	—	—	124.4	3.6817	22
7-17	9013	105	103	100	50/450	1.389	2.066		.0536	.0950	—			117.0	85.16	80.53	213	2206	—	—	—	—	—	—	—	—	129.4	3.7629	23
7-17	9014	103	98	100	100/400	3.688	5.182		.1604	.2320	—			163.8	106.3	100.6	216	2306	—	—	—	—	—	—	—	—	134.4	3.9045	24
7-17	9015	105	—	100	150/850	—	—		—	—	—	—	—	—	—	—	210	2406	—	—	—	—	—	—	—	—	156.4	4.1461	25
7-17	9016	102	82	—	—	—	—		—	—	—	—	—	—	—	—	216	—	9.9	1.880	40.0	.00857	220.5	3.8/3.1	9.3	89.8	166.4	4.1309	26

ENGINE TEST SUMMARY

DATE	TEST NO.	TANK PRESS. (PSIA)	INJ. PRESS. (PSIA)	PULSE MODE CHARACTERISTICS: NO. PULSES	CYCLE ON/OFF	CHAMBER PRESSURE INTEGRAL: PULSE 1-5	PULSE 90-100	LAST 10 PULSES	VACUUM IMPULSE: PULSE 1-5	PULSE 90-100	LAST 10 PULSES	IMPULSE SHIFT (%)	P_C SHIFT (%)	SPECIFIC IMPULSE (SEC)	AVE. CENTROID TIME (MSEC): P_C (MSEC)	THRUST (MSEC)	START TEMP. (°F)	SUMMATION OF PULSES	STEADY STATE CHARACTERISTICS: DURATION (SEC)	THRUST (LBF)	P_C (PSIA)	FLOW RATE (LBM/SEC)	SPECIFIC IMPULSE (SEC)	$\frac{\Delta P_C}{\Delta P_V}$ SHIFT	P_C ROUGHNESS (%)	SUMMATION BURN TIME (SEC)	SUMMATION OF ON TIME (SEC)	SUMMATION OF PROPELLANT USAGE (LBM)	SUMMATION OF AMBIENT STARTS
2-27	3007	341	350	100	20/180	1.395	2.262	—	.06410	.10615	—			168.9	97.12	94.72	219	25506	—	—	—	—	—		—	—	156.4	9.1939	27
7-17	3008	338	338	500	20/90	1.248	2.220	2.911	.05515	.09598	.1109			175.2	94.40	89.69	218	9006	—	—	—	—	—		—	—	166.4	9.1666	28
7-17	3009	340	340	500	20/680	1.195	2.084	2.749	.05368	.09699	.1025			166.1	94.78	92.53	218	9506	—	—	—	—	—		—	—	176.4	9.7520	29
7-17	3010	342	348	500	20/490	4.087	3.207	5.875	.1880	.2709	.2749			190.5	57.67	48.80	218	4006	—	—	—	—	—		—	—	201.4	5.9654	30
7-17	3011	341	—	100	20/450	—	—	—	—	—	—			—	—	—	220	4118	—	—	—	—	—		—	—	206.8	5.6185	31
7-17	3012	341	—	100	20/450	—	—	—	—	—	—			—	—	—	216	4618	—	—	—	—	—		—	—	211.8	6.3628	32
7-17	3013	346	352	500	20/450	3.289	3.495	5.252	.1844	.2689	.2728			178.9	59.46	52.85	216	4618	—	—	—	—	—		—	—	216.8	7.7447	33
7-17	3014	372	346	500	20/900	2.166	11.75	12.28	.4476	.6519	.5723			199.6	81.91	79.11	200	9018	—	—	—	—	—		—	—	256.8	9.1506	34
7-17	3015	345	—	500	20/850	—	—	—	—	—	—			—	—	—	210	7669	—	—	—	—	—		—	—	276.8	10.675	35
7-17	3016	336	344	—	—	—	—	—	—	—	—			—	—	—	200	—	60.0	5.829	44.2	0254	229.5	23/23	14.2	144.8	416.8	10.907	36
7-17	3017	260	290	500	20/480	.8490	1.660	1.867	.04162	.07602	.08895			162.9	93.03	88.86	209	6618	—	—	—	—	—		—	—	426.8	11.169	37
7-17	3018	268	262	500	20/480	1.452	1.472	1.601	.06440	.06589	.07702			150.5	91.11	86.62	198	6618	—	—	—	—	—		—	—	441.8	11.724	38
7-17	3019	241	295	500	20/950	2.879	4.571	4.956	.1361	.2048	.2105			167.4	57.36	51.97	206	7118	—	—	—	—	—		—	—	456.8	12.301	39
7-17	3020	294	285	500	20/450	2.694	3.965	3.999	.1394	.1928	.2454			167.9	77.36	75.78	211	7618	—	—	—	—	—		—	—	536.8	13.338	40
7-18	3021	241	228	500	20/900	.4955	8.961	8.844	.2124	.3902	.4069			128.1	26.09	26.60	208	8108	—	—	—	—	—		—	—	611.8	14.830	41
7-18	3022	241	237	500	20/850	12.98	12.98	13.66	.5059	.6009	.6463			199.5	118.4	112.0	210	8618	—	—	—	—	—		—	—	671.8	16.098	42
7-18	3023	314	287	—	—	—	—	—	—	—	—			—	—	—	210	—	60.0	7.263	36.8	04730	220.8	15/60	11.2	209.8	681.8	16.211	43
7-18	3024	105	104	500	20/480	.5160	.8245	.9497	.02564	.03882	.04246			130.2	64.3	55.62	218	9118	—	—	—	—	—		—	—	691.8	16.3726	44
7-18	3025	105	102	499	20/480	.4060	.8457	.5246	.02473	.03821	.04097			120.5	61.29	56.71	205	9617	—	—	—	—	—		—	—	716.7	16.7499	45
7-18	3026	104	101	500	20/450	1.505	2.461	2.651	.06224	.10147	.11178			156.1	67.30	62.96	217	10117	—	—	—	—	—		—	—	741.7	17.1542	46
7-18	3027	101	98	500	20/450	1.286	1.563	2.189	.04992	.07470	.10140			145.3	79.30	76.80	203	10617	—	—	—	—	—		—	—	791.7	17.9342	47
7-18	3028	102	99	500	20/900	3.529	4.695	4.652	.1449	.2118	.2104			151.1	108.6	99.50	207	11117	—	—	—	—	—		—	—	846.7	19.2762	48
7-18	3029	106	105	500	20/850	5.549	7.850	7.260	.2213	.3529	.3164			161.4	119.0	132.9	212	11617	—	—	—	—	—		—	—	926.7	19.3282	49
7-18	3030	113	90	—	—	—	—	—	—	—	—			—	—	—	210	—	60.0	7.123	43.8	00970	218.9	9/60	12.1	269.8	986.7	19.5282	49
7-18	3031	344	355	100	20/850	14.81	12.509	—	.6563	.8072	—			175	118.8	110.7	207	11717	—	—	—	—	—		—	—	941.7	19.7719	50
7-18	3032	344	355	100	20/850	16.87	13.19	—	.6992	.6095	—			170	116.8	113.9	214	11817	—	—	—	—	—		—	—	956.7	20.0226	51
7-18	3033	240	228	100	20/850	16.87	13.19	—	.6992	.6095	—			160	147.8	145.4	210	11917	—	—	—	—	—		—	—	1031.7	20.1052	52
7-18	3034	168	169	100	150/850	5.501	7.261	—	.2551	.3403	—			205	117.3	114.8	216	12417	—	—	—	—	—		—	—	1106.7	22.3986	53
7-18	3035	370	359	500	20/850	14.92	17.82	18.25	.6904	.8939	.9495						210	13416	—	—	—	—	—		—	—	1246.6	24.2676	54
7-18	3044	346	—	999	100/500	—	—	—	—	—	—			—	—	—	210	—	10.0	—	—	—	—		—	279.8	1246.6	24.4336	55
7-18	3045	345	—	—	—	—	—	—	—	—	—			—	—	—	210	14415	—	—	—	—	—		—	—	1346.5	26.3536	56
7-18	3046	236	—	999	100/500	—	—	—	—	—	—			—	—	—	210	—	10.0	—	—	—	—		—	289.8	1326.5	26.5186	57
7-18	3047	236	—	—	—	—	—	—	—	—	—			—	—	—	210	14415	—	—	—	—	—		—	—	1426.4	28.4167	58
7-18	3048	103	—	999	100/500	—	—	—	—	—	—			—	—	—													

* MALFUNCTION

ENGINE TEST SUMMARY

DATE	TEST NO.	TANK PRESS. (PSIA)	INJ. PRESS. (PSIA)	PULSE MODE CHARACTERISTICS: NO. PULSES	CYCLE ON/OFF	CHAMBER PRESSURE INTEGRAL: PULSE 1-5	PULSE 90-100	LAST 10 PULSES	VACUUM IMPULSE: PULSE 1-5	PULSE 90-100	LAST 10 PULSES	IMPULSE SHIFT (%)	P_c SHIFT (%)	SPECIFIC IMPULSE (SEC)	AVE. CENTROID TIME (MSEC): P_c (MSEC)	THRUST (MSEC)	START TEMP. (°F)	SUMMATION OF PULSES	STEADY STATE CHARACTERISTICS: DURATION (SEC)	THRUST (LBF)	P_c (PSIA)	FLOW RATE (LBM/SEC)	SPECIFIC IMPULSE (SEC)	ΔPC ΔFV SHIFT	P_c ROUGHNESS (±)	TERMINATION BURN TIME (SEC)	SUMMATION OF ON TIME (SEC)	SUMMATION OF PROPELLANT USAGE (LBM)	SUMMATION OF AMBIENT STARTS
7-18	3049	105	—	—	—												210	—	10.0	—	—				—	279.8	1936.4	28.58	59
7-18	3050	345	—	15	100/300												210	14450	21.0	—	—				—	320.8	1957.8	28.93	60
7-18	3051	345	—	999	100/300												210	15449	—	—	—				—	—	1587.3	30.83	61
7-18	3052	345	—	—	—												210	—	3.0	—	—				—	323.8	1560.3	30.88	62
7-18	3053	345	—	—	—												210	—	10.0	—	—				—	333.8	1570.3	31.05	63
7-20	3054	235	—	999	100/300												210	16448	—	—	—				—	—	1670.2	32.99	64
7-20	3055	235	—	—	—												210	—	10.0	—	—				—	343.8	1620.2	33.11	65
7-20	3056	108	—	999	100/300												210	17497	—	—	—				—	—	1790.1	35.01	66
7-23	3057	105	—	—	—												210	—	10.0	—	—				—	363.8	1790.1	35.17	67
7-23	3058	363	—	999	100/300												210	18446	—	—	—				—	—	1890.0	37.07	68
7-23	3059	363	—	—	—												210	—	10.0	—	—				—	363.8	1900.0	37.24	69
7-23	3060	235	—	999	100/300												210	19445	—	—	—				—	—	1999.9	39.13	70
7-23	3061	233	—	—	—												210	—	10.0	—	—				—	373.8	2009.9	39.30	71
7-24	3062	103	—	999	100/300												210	20444	—	—	—				—	—	2109.8	41.20	72
7-24	3063	107	—	—	—												210	—	10.0	—	—				—	383.8	2119.8	41.37	73
7-24	3064	362	—	999	100/300												210	21443	—	—	—				—	—	2229.7	43.26	74
7-24	3065	345	—	—	—												210	—	10.0	—	—				—	393.8	2229.7	43.43	75
7-24	3066	240	—	999	100/300												210	22442	—	—	—				—	—	2329.6	45.33	76
7-24	3067	240	—	—	—												210	—	10.0	—	—				—	403.8	2339.6	45.49	77
7-24	3068	105	—	999	100/300												210	23441	—	—	—				—	—	2435.5	47.39	78
7-24	3069	105	—	—	—												210	—	10.0	—	—				—	413.8	2445.5	47.56	79
7-24	3070	365	—	999	100/300												210	24440	—	—	—				—	—	2545.4	49.45	80
7-25	3071	365	—	—	—												210	—	10.0	—	—				—	423.8	2555.4	49.62	81
7-25	3072	240	—	999	100/300												210	25439	—	—	—				—	—	2655.3	51.52	82
7-25	3073	235	—	—	—												210	—	10.0	—	—				—	433.8	2665.3	51.68	83
7-29	3074	107	—	999	100/300												210	26438	—	—	—				—	—	2765.2	53.58	84
7-29	3075	106	—	—	—												210	—	10.0	—	—				—	443.8	2775.2	53.75	85
7-29	3076	363	—	999	100/300												210	27437	—	—	—				—	—	2875.1	55.65	86
7-29	3077	362	—	—	—												210	—	10.0	—	—				—	453.8	2885.1	55.81	87
7-29	3078	235	—	999	100/300												210	28436	—	—	—				—	—	2985.0	57.71	88
7-29	3079	235	—	—	—												210	—	10.0	—	—				—	463.8	2995.0	57.88	89
7-29	3080	105	—	999	100/300												210	29435	—	—	—				—	—	3094.9	59.78	90

* 5 S/S STARTS AND 4 PULSE STARTS

DATE	TEST NO	TANK PRESS. (PSIA)	INJ. PRESS. (PSIA)	PULSE MODE CHARACTERISTICS														STEADY STATE CHARACTERISTICS								SUMMATION OF ON TIME (SEC)	SUMMATION OF PROPELLANT USAGE (LBM)	SUMMATION OF AMBIENT STARTS
				NO. PULSES	CYCLE ON-OFF	CHAMBER PRESSURE INTEGRAL PULSE 1-5	CHAMBER PRESSURE INTEGRAL PULSE 90-100	CHAMBER PRESSURE INTEGRAL LAST 10 PULSES	VACUUM IMPULSE PULSE 1-5	VACUUM IMPULSE PULSE 90-100	VACUUM IMPULSE LAST 10 PULSES	IMPULSE SHIFT (%)	P_C SHIFT (%)	SPECIFIC IMPULSE (SEC)	AVE. CENTROID TIME (MSEC) P_C (MSEC)	AVE. CENTROID TIME (MSEC) THRUST (MSEC)	START TEMP. (°F)	SUMMATION OF PULSES	DURATION (SEC)	THRUST (LBF)	P_C (PSIA)	FLOW RATE (LBM/SEC)	SPECIFIC IMPULSE (SEC)	$\frac{\Delta P_C}{\Delta F_V}$ SHIFT	P_C ROUGHNESS (±%)	SUMMATION BURN TIME (SEC)			
7-24	3081	105	—	—	—												Z10		10.0		—				—	473.8	3104.9	54.99	91
7-24	3082	365	—	999	100/300												Z10	30434	—		—				—	—	3209.8	61.67	92
7-24	3083	365	—	—	—												Z10	—	10.0		—				—	483.8	3219.8	61.84	93
7-24	3084	240	—	999	100/300												Z10	31433	—		—				—	—	3314.7	63.79	94
7-24	3085	240	—	—	—												Z10	—	10.0		—				—	493.8	3324.7	63.90	95
7-24	3086	105	—	999	100/300												Z10	32432	—		—				—	—	3424.6	65.80	96
7-24	3087	105	—	—	—												Z10	—	10.0		—				—	503.8	3434.6	65.97	97
7-24	3088	365	—	999	100/300												Z10	33431	—		—				—	—	3534.5	67.87	98
7-24	3089	365	—	—	—												Z10	—	10.0		—				—	513.8	3544.5	68.03	99
7-24	3090	240	—	999	100/300												Z10	34430	—		—				—	—	3644.4	69.93	100
7-25	3091	238	—	—	—												Z10	—	10.0		—				—	523.8	3654.4	70.10	101
7-25	3092	108	—	999	100/300												Z10	35429	—		—				—	—	3754.3	71.99	102
7-25	3093	108	—	—	—												Z10	—	10.0		—				—	533.8	3764.3	72.16	103
7-25	3094	367	—	999	100/300												Z10	36428	—		—				—	—	3864.2	74.06	104
7-25	3095	364	—	—	—												Z10	—	10.0		—				—	543.8	3874.2	74.22	105
7-25	3096	240	—	999	100/300												Z10	37427	—		—				—	—	3974.1	76.12	106
7-25	3097	240	—	—	—												Z10	—	10.0		—				—	553.8	3984.1	76.29	107
7-25	3098	105	—	999	100/300												Z10	38426	—		—				—	—	4084.0	78.19	108
7-25	3099	105	—	—	—												Z10	—	10.0		—				—	563.8	4094.0	78.35	109
7-25	3100	489	483	119	100/300	10.76	14.99	14.721	.4918	.6864	.6849			202.3	84.6	81.0	Z2	39425	—	—	—	—	—	—	—	—	41939	80.25	110
7-25	3101	482	346	—	—	—	—	—	—	—	—			—	—	—	Z14	—	10	5.579	113.4	.02503	222.9	49%	16.2	573.8	4203.9	82.56	111
7-25	3102	238	232	999	100/300	6.662	8.706	7.185	.3633	.4059	.4191			189.2	92.8	89.26	Z14	40428	—	—	—	—	—	—	—	—	43038	82.71	112
7-25	3103	319	232	—	—	—	—	—	—	—	—			—	—	—	Z09	—	9.9	4.154	84.2	.01908	217.6	38%	14.6	583.7	43137	82.90	113
7-25	3104	318	232	—	—	—	—	—	—	—	—			—	—	—	Z07	—	9.9	4.157	86.1	.01909	217.8	39%	16.1	593.6	43236	83.09	114
7-26	3105	107	—	999	100/300	—	—	—	—	—	—			—	—	—		41423	—	—	—	—	—	—	—	—	44235	84.99	115
7-26	3106	115	93	—	—	—	—	—	—	—	—			—	—	—	Z12	—	10.0	2.000	42.4	.00963	207.7	69%	8.2	603.6	44335	85.09	116
7-26	3107	367	—	999	100/300												Z10	42422	—	—	—	—	—	—	—	—	45334	86.99	117
7-26	3108	365	—	—	—												Z10	—	10.0		—				—	613.6	45434	87.15	118
7-26	3109	236	—	999	100/300												Z10	43421	—		—				—	—	46433	89.05	119
7-26	3110	240	—	—	—												Z10	—	10.0		—				—	623.6	46533	89.21	120
7-26	3111	105	—	999	100/300												Z10	44420	—		—				—	—	47532	91.11	121
7-26	3112	105	—	—	—												Z10	—	10.0		—				—	633.6	47632	91.28	122

DATE	TEST NO.	TANK PRESS. (PSIA)	INJ. PRESS. (PSIA)	PULSE MODE CHARACTERISTICS															STEADY STATE CHARACTERISTICS								SUMMATION OF ON TIME (SEC)	SUMMATION OF PROPELLANT USAGE (LBM)	SUMMATION OF AMBIENT STARTS
				NO. PULSES	CYCLE ON/OFF	CHAMBER PRESSURE INTEGRAL PULSE 1-5	CHAMBER PRESSURE INTEGRAL PULSE 90-100	CHAMBER PRESSURE INTEGRAL LAST 10 PULSES	VACUUM IMPULSE PULSE 1-5	VACUUM IMPULSE PULSE 90-100	VACUUM IMPULSE LAST 10 PULSES	IMPULSE SHIFT (%)	P_C SHIFT (%)	SPECIFIC IMPULSE (SEC)	AVE. CENTROID TIME (MSEC) P_C (MSEC)	AVE. CENTROID TIME (MSEC) THRUST (MSEC)	START TEMP. (°F)	SUMMATION OF PULSES	DURATION (SEC)	THRUST (LBF)	P_C (PSIA)	FLOW RATE (LBM/SEC)	SPECIFIC IMPULSE (SEC)	$\frac{\Sigma PC}{\Sigma FV}$ SHIFT	P_C ROUGHNESS (±3)	SUMMATION BURN TIME (SEC)				
7-26	3/18	365	—	999	100/300												210	45419	—		—				—	—	48631	93.18	123
7-26	3/14	345	—	—	—												210	—	10.0		—				—	6436	48731	93.34	124
7-26	3/15	240	—	999	100/300												210	46418	—		—				—	—	49730	95.24	125
7-26	3/16	240	—	—	—												210	—	10.0		—				—	6536	49830	95.41	126
7-26	3/17	105	—	999	100/300												210	47417	—		—				—	—	50829	97.30	127
7-26	3/18	105	—	—	—												210	—	10.0		—				—	6636	50929	97.47	128
7-26	3/19	365	—	999	100/300												210	48416	—		—				—	—	51928	99.37	129
7-26	3/20	365	—	—	—												210	—	10.0		—				—	6736	52028	99.53	130
7-26	3/21	238	—	999	100/300												210	49415	—		—				—	—	53027	101.43	131
7-27	3/22	242	—	—	—												210	—	10.0		—				—	6836	53127	101.60	132
7-27	3/23	107	—	999	100/300												210	50414	—		—				—	—	54126	103.50	133
7-27	3/24	106	—	—	—												210	—	10.0		—				—	6936	54226	103.66	134
7-27	3/25	348	—	999	100/300												210	51413	—		—				—	—	55225	105.56	135
7-27	3/26	365	—	—	—												210	—	10.0		—				—	7036	55325	105.73	136
7-27	3/27	237	—	999	100/300												210	52412	—		—				—	—	56324	107.62	137
7-27	3/28	233	—	—	—												210	—	10.0		—				—	7136	56424	107.79	138
7-27	3/29	106	—	999	100/300												210	53411	—		—				—	—	57423	109.69	139
7-27	3/30	105	—	—	—												210	—	10.0		—				—	7236	57523	109.85	140
7-27	3/31	364	364	100	20/380	1.260	2.264		.05553	.1079				169.4	99.1	99.20	206	53511	—		—				—	—	57593	109.92	141
7-27	3/32	365	361	100	20/480	1.174	2.681		.05918	.09821				169.1	95.79	98.93	210	53611	—		—				—	—	57613	109.98	142
7-27	3/33	374	370	100	50/750	4.627	5.759		.1053	.2628				182.4	59.62	57.00	210	53711	—		—				—	—	57663	110.12	143
7-27	3/34	369	369	100	50/450	9.650	5.096		.1203	.2473				166.8	57.30	56.66	202	53811	—		—				—	—	57763	110.27	144
7-27	3/35	369	361	100	100/930	4.245	11.969		.1492	.5521				193.0	70.26	82.20	209	53911	—		—				—	—	57763	110.56	145
7-27	3/36	365	—	100	150/850	—	—		—	—				—	—	—	210	54011	—		—				—	—	57913	110.75	146
7-27	3/37	490	—	—	—												210	—	10.0		—				—	7336	58013	110.92	147
7-27	3/38	285	285	100	20/380	.9955	1.634		.03565	.07300				158.3	92.24	99.96	208	54111	—		—				—	—	58033	110.96	148
7-27	3/39	240	240	100	20/480	.8512	1.772		.03780	.06072				159.0	94.66	96.24	210	54211	—		—				—	—	58053	111.01	149
7-27	3/40	240	235	100	20/480	.8859	1.632		.04638	.07976				162.6	94.22	96.09	210	54311	—		—				—	—	58073	111.06	150
7-27	3/41	241	231	100	50/750	2.867	4.402		.1260	.1978				178.9	59.32	56.80	218	54411	—		—				—	—	58123	111.17	151
7-27	3/42	239	231	100	50/450	2.776	3.946		.1011	.1185				196.1	60.09	52.84	209	54511	—		—				—	—	58173	111.27	152
7-27	3/43	233	229	100	100/300	6.592	8.850		.2978	.4077				164.8	89.6	89.0	202	54611	—		—				—	—	58223	111.38	153
7-27	3/44	243	226	100	150/850	10.67	13.24		.4992	.6131				193.1	127.2	128.8	210	54711	—		—				—	—	58423	111.60	154

ENGINE TEST SUMMARY

#9 (tests 3145–3153)

DATE	TEST NO.	TANK PRESS. (PSIA)	INJ. PRESS. (PSIA)	PULSE MODE: NO. PULSES	CYCLE ON/OFF	CHAMBER PRESSURE INTEGRAL: PULSE 1-5	CHAMBER PRESSURE INTEGRAL: PULSE 90-100	CHAMBER PRESSURE INTEGRAL: LAST 10 PULSES	VACUUM IMPULSE: PULSE 1-5	VACUUM IMPULSE: PULSE 90-100	VACUUM IMPULSE: LAST 10 PULSES	IMPULSE SHIFT (%)	P_C SHIFT (%)	SPECIFIC IMPULSE (SEC)	AVE. CENTROID TIME (MSEC): P_C (MSEC)	AVE. CENTROID TIME (MSEC): THRUST (MSEC)	START TEMP. (°F)	SUMMATION OF PULSES	STEADY STATE: DURATION (SEC)	THRUST (LBF)	P_C (PSIA)	FLOW RATE (LBM/SEC)	SPECIFIC IMPULSE (SEC)	$\Delta PC/\Delta FV$ SHIFT	P_C ROUGHNESS (±%)	SUMMATION BURN TIME (SEC)	SUMMATION OF ON TIME (SEC)	SUMMATION OF PROPELLANT USAGE (LBM)	SUMMATION OF AMBIENT STARTS
7-20	3145	319	235	—	—	—	—		—	—				—	—	—	209	—	10.0	4.149	86.9	.01911	217.1	3.0/3.8	13.3	793.6	5852.3	111.80	155
7-20	3146	319	235	—	—	—	—		—	—				—	—	—	208	—	10.0	4.173	86.7	.01911	218.4	3.2/3.3	13.3	753.6	5862.3	111.99	156
7-20	3147	103	103	100	20/980	.5240	.9117		.02716	.09985				195.2	80.48	68.88	206	54811	—	—	—	—	—		—	—	5869.3	112.02	157
7-20	3148	105	102	100	20/950	.9490	1.265		.01796	.09575				[illegible]	4.24	60.88	204	54911	—	—	—	—	—		—	—	5866.3	112.05	158
7-20	3149	106	103	75	50/950	1.464	2.614		.02528	.1150				153.8	76.80	76.60	207	55006	—	—	—	—	—		—	—	5871.1	112.12	159
7-20	3150	106	105	100	50/450	1.432	1.506		.04212	.01032				126.1	114.5	111.6	210	55106	—	—	—	—	—		—	—	5876.1	112.18	160
7-20	3151	105	103	100	100/900	3.669	3.163		.1518	.2207				191.8	108.7	102.1	216	55206	—	—	—	—	—		—	—	5880.1	112.30	161
7-20	3152	105	103	100	150/850	5.633	7.219		.2422	.3346				193.8	141.6	136.9	215	55306	—	—	—	—	—		—	—	5901.1	112.47	162
7-20	3153	121	97	—	—	—	—		—	—				—	—	—	202	—	10.0	2.046	43.5	.00988	207.1	7.5/7.5	8.5	763.6	5911.1	112.57	163
7-20	3154	363	—	999	100/900												210	56305	—		—				—	—	6011.0	119.47	164
7-20	3155	367	—	—	—												210	—	10.0		—				—	773.6	6021.0	119.63	165
7-20	3156	236	—	999	100/900												210	57304	—		—				—	—	6120.9	116.53	166
7-20	3157	234	—	—	—												210	—	10.0		—				—	783.6	6130.9	116.70	167
7-20	3158	106	—	999	100/900												210	58303	—		—				—	—	6230.8	118.59	168
7-20	3159	107	—	—	—												210	—	10.0		—				—	793.6	6240.8	118.76	169
7-20	3160	365	—	999	100/900												210	59302	—		—				—		6340.7	120.66	170
7-20	3161	364	—	—	—												210	—	10.0		—				—	803.6	6350.7	120.82	171
7-20	3162	238	—	999	100/900												210	60301	—		—				—		6450.6	122.72	172
7-20	3163	236	—	—	—												210	—	10.0		—				—	813.6	6460.6	122.89	173
7-31	3164	105	—	999	100/900												210	61300	—		—				—	—	6560.5	124.79	174
7-31	3165	105	—	—	—												210	—	10.0		—				—	823.6	6570.5	124.95	175
7-31	3166	365	—	999	100/900												210	62299	—		—				—	—	6670.4	126.85	176
7-31	3167	365	—	—	—												210	—	10.0		—				—	833.6	6680.4	127.02	177
7-31	3168	240	—	999	100/900												210	63298	—		—				—	—	6780.3	128.92	178
7-31	3169	240	—	—	—												210	—	10.0		—				—	843.6	6790.3	129.08	179
7-31	3170	105	—	999	100/900												210	64297	—		—				—	—	6890.2	130.98	180
7-31	3171	105	—	—	—												210	—	10.0		—				—	853.6	6900.2	131.15	181
7-31	3172	369	—	999	100/900												210	65296	—		—				—	—	7000.1	133.04	182
7-31	3173	362	—	—	—												210	—	10.0		—				—	863.6	7010.1	133.21	183
7-31	3174	238	—	999	100/900												210	66295	—		—				—	—	7110.0	135.11	184
7-31	3175	237	—	—	—												210	—	10.0		—				—	873.6	7120.0	135.27	185
7-31	3176	108	—	999	100/900												210	67294	—		—				—	—	7219.9	137.17	186

ENGINE TEST SUMMARY

DATE	TEST NO	TANK PRESS. (PSIA)	INJ. PRESS (PSIA)	PULSE MODE CHARACTERISTICS																STEADY STATE CHARACTERISTICS								SUMMATION OF ON TIME (SEC)	SUMMATION OF PROPELLANT USAGE (LBM)	SUMMATION OF AMBIENT STARTS
				NO. PULSES	CYCLE ON/OFF	CHAMBER PRESSURE INTEGRAL PULSE 1-5	CHAMBER PRESSURE INTEGRAL PULSE 90-100	CHAMBER PRESSURE INTEGRAL LAST 10 PULSES	VACUUM IMPULSE PULSE 1-5	VACUUM IMPULSE PULSE 90-100	VACUUM IMPULSE LAST 10 PULSES	IMPULSE SHIFT (%)	P_C SHIFT (%)	SPECIFIC IMPULSE (SEC)	AVE. CENTROID TIME (MSEC) P_C (MSEC)	AVE. CENTROID TIME (MSEC) THRUST (MSEC)	START TEMP. (°F)	SUMMATION OF PULSES	DURATION (SEC)	THRUST (LBF)	P_C (PSIA)	FLOW RATE (LBM/SEC)	SPECIFIC IMPULSE (SEC)	ΣPC ΣFV SHIFT	P_C ROUGHNESS (±)	SUMMATION BURN TIME (SEC)					
7-31	3177	108	—	—	—												210	—	10.0		—				—	8836	7229.9	137.34	187
7-31	3178	369	—	999	100/300												210	68293	—		—				—		7329.8	139.24	188
7-31	3179	367	—	—	—												210	—	10.0		—				—	8936	7339.8	139.40	189
7-31	3180	237	—	999	100/300												210	69292	—		—				—	—	7439.7	141.30	190
7-31	3181	237	—	—	—												210	—	10.0		—				—	9036	7449.7	141.47	191
8-1	3182	106	—	999	100/300												210	70291	—		—				—	—	7549.6	143.36	192
8-1	3183	106	—	—	—												210	—	10.0		—				—	9136	7559.6	143.53	193
8-1	3184	166	—	—	—												210	71290	—		—				—	—	7659.5	145.43	194
8-1	3185	365	—	999	100/300												210	—	10.0		—				—	9236	7669.5	145.59	195
8-1	3186	365	—	—	—												210	72289	—		—				—	—	7769.4	147.49	196
8-1	3187	240	—	999	100/300												210	—	10.0		—				—	9336	7779.4	147.66	197
8-1	3188	240	—	—	—												210	73288	—		—				—	—	7879.3	149.56	198
8-1	3189	105	—	999	100/300												210	—	10.0		—				—	9436	7889.3	149.72	199
8-1	3190	105	—	—	—												210	74287	—		—				—	—	7989.2	151.62	200
8-1	3191	369	—	999	100/300												210	—	10.0		—				—	9536	7999.2	151.79	201
8-1	3192	370	—	—	—												210	75286	—		—				—	—	8099.1	153.68	202
8-1	3193	236	—	999	100/300												210	—	10.0		—				—	9636	8109.1	153.85	203
8-1	3194	236	—	—	—												210	76285	—		—				—	—	8209.0	155.75	204
8-1	3195	105	—	999	100/300												210	—	10.0		—				—	9736	8219.0	155.91	205
8-1	3196	105	—	—	—												210	77284	—		—				—	—	8318.9	157.91	206
8-1	3196	366	—	999	100/300												210	—	10.0		—				—	9836	8328.9	157.98	207
8-1	3197	365	—	—	—												210	78283	—		—				—	—	8428.8	159.88	208
8-1	3198	236	—	999	100/300												210	—	10.0		—				—	9936	8438.8	160.09	209
8-1	3199	236	—	—	—												210	79282	—		—				—	—	8538.7	161.98	210
8-1	3200	106	—	999	100/300												210	—	10.0		—				—	10036	8548.7	162.11	211
8-1	3201	106	—	—	—												210	80281	—		—				—	—	8648.6	164.01	212
8-1	3202	365	—	999	100/300												210	—	10.0		—				—	10136	8658.6	164.17	213
8-1	3203	365	—	—	—												210	81280	—		—				—	—	8758.5	165.90	214
8-2	3204	240	—	999	100/300												210	—	10.0		—				—	10236	8768.5	166.07	215
8-2	3205	240	—	—	—												210	82279	—		—				—	—	8868.4	167.97	216
8-2	3206	105	—	999	100/300												210	—	10.0		—				—	10336	8878.4	168.13	217
8-2	3207	105	—	—	—												210	—	—		—				—	—	8978.4	170.03	218
#10 8-2	3209	365	361	1000	100/300	8.968	11.88	12.10	.4187	.5512	.5799			195.9	91.7	RR.48	210	83279	—		—				—				

ENGINE TEST SUMMARY

DATE	TEST NO	TANK PRESS (PSIA)	INJ. PRESS (PSIA)	PULSE MODE CHARACTERISTICS: NO PULSES	CYCLE ON/OFF	CHAMBER PRESSURE INTEGRAL: PULSE 1-5	PULSE 90-100	LAST 10 PULSES	VACUUM IMPULSE: PULSE 1-5	PULSE 90-100	LAST 10 PULSES	IMPULSE SHIFT (%)	P_c SHIFT (%)	SPECIFIC IMPULSE (SEC)	AVE. CENTROID TIME (MSEC): P_c (MSEC)	THRUST (MSEC)	START TEMP. (°F)	SUMMATION OF PULSES
8-2	3209	407	350	—	—	—	—	—	—	—	—			—	—	—	215	
8-2	3210	298	229	1000	100/300	6.466	8.370	8.873	.2649	.3418	.4011			176.3	171.8	176.1	208	84279
8-2	3211	321	235	—	—	—	—	—	—	—	—			—	—	—	214	—
8-2	3212	169	186	999	100/300	5.121	5.282	5.896	.1954	.2240	.2250			164.0	168.2	168.9	209	85218
8-2	3213	121	98.9	—	—	—	—	—	—	—	—			—	—	—	210	—
8-2	3214	368	—	999	100/300												210	86277
8-2	3215	368	—	—	—												210	—
8-2	3216	290	—	999	100/300												210	87270
8-2	3217	227	—	—	—												210	—
8-2	3218	107	—	999	100/300												210	88275
8-2	3219	109	—	—	—												210	—
8-2	3220	368	—	999	100/300												210	89274
8-2	3221	369	—	—	—												210	—
8-2	3222	226	—	999	100/300												210	90273
8-2	3223	236	—	—	—												210	—
8-2	3224	102	—	999	100/300												210	91272
8-2	3225	105	—	—	—												210	—
8-2	3226	365	—	999	100/300												210	92271
8-2	3227	365	—	—	—												210	—
8-2	3228	290	—	999	100/300												210	93270
8-2	3229	240	—	—	—												210	—
8-2	3230	102	—	999	100/300												210	94269
8-2	3231	109	—	—	—												210	—
8-2	3232	366	—	999	100/300												210	95268
8-2	3233	362	—	—	—												210	—
8-2	3234	229	—	999	100/300												210	96267
8-2	3235	238	—	—	—												210	—
8-2	3236	110	—	999	100/300												210	97266
8-2	3237	107	—	—	—												210	—
8-2	3238	363	—	999	100/300												210	98265
8-2	3239	365	—	—	—												210	—
8-2	3240	239	—	999	100/300												210	99264

STEADY STATE CHARACTERISTICS: DURATION (SEC)	THRUST (LBF)	P_c (PSIA)	FLOW RATE (LBM/SEC)	SPECIFIC IMPULSE (SEC)	%PC EFV SHIFT	P_c ROUGHNESS (±%)	TERMINATION BURN TIME DEC)	SUMMATION OF ON TIME (SEC)	SUMMATION OF PROPELLANT USAGE (LBM)	SUMMATION OF AMBIENT STARTS
9.9	5.434	12.6	.02460	220.9	5.8/6.9	3.0	.043.2	8988.3	178.27	219
—	—	—	—	—	—	—	—	9088.3	178.93	220
9.9	4.105	85.7	.01893	216.8	5.3/6.0	15.8	1053.1	9098.2	179.61	221
—	—	—	—	—	—	—	—	9198.1	179.99	222
9.9	2.009	42.9	.00970	207.1	10/10.5	22.4	1063.0	9208.0	180.08	223
—	—	—	—	—	—	—	—	9307.9	180.93	224
—	—	—	—	—	—	—	1073	9317.9	181.15	225
10.0	—	—	—	—	—	—	—	9417.8	181.09	226
—	—	—	—	—	—	—	1083	9427.8	181.21	227
10.0	—	—	—	—	—	—	—	9527.7	181.11	228
—	—	—	—	—	—	—	1093	9537.7	181.27	229
10.0	—	—	—	—	—	—	—	9637.6	181.17	230
—	—	—	—	—	—	—	1103	9647.6	181.34	231
10.0	—	—	—	—	—	—	—	9747.5	181.24	232
—	—	—	—	—	—	—	1113	9757.5	181.40	233
10.0	—	—	—	—	—	—	—	9857.4	181.30	234
—	—	—	—	—	—	—	1123	9867.4	181.47	235
10.0	—	—	—	—	—	—	—	9967.3	181.36	236
—	—	—	—	—	—	—	1133	9977.3	181.53	237
10.0	—	—	—	—	—	—	—	10077.2	181.43	238
—	—	—	—	—	—	—	1143	10087.2	181.54	239
10.0	—	—	—	—	—	—	—	10187.1	181.49	240
—	—	—	—	—	—	—	1153	10197.1	181.66	241
10.0	—	—	—	—	—	—	—	10297.0	181.56	242
—	—	—	—	—	—	—	1163	10307.0	181.76	243
10.0	—	—	—	—	—	—	—	10406.9	181.62	244
—	—	—	—	—	—	—	1173	10416.9	181.79	245
10.0	—	—	—	—	—	—	—	10516.8	181.68	246
—	—	—	—	—	—	—	1183	10526.8	181.83	247
10.0	—	—	—	—	—	—	—	10626.7	181.75	248
—	—	—	—	—	—	—	1193	10636.7	181.91	249
10.0	—	—	—	—	—	—	—	10736.6	181.81	250

ENGINE TEST SUMMARY

DATE	TEST NO.	TANK PRESS. (PSIA)	INJ. PRESS. (PSIA)	PULSE MODE CHARACTERISTICS: NO. PULSES	CYCLE ON/OFF	CHAMBER PRESSURE INTEGRAL: PULSE 1-5	PULSE 90-100	LAST 10 PULSES	VACUUM IMPULSE: PULSE 1-5	PULSE 90-100	LAST 10 PULSES	IMPULSE SHIFT (%)	P_C SHIFT (%)	SPECIFIC IMPULSE (SEC)	AVE. CENTROID TIME (MSEC): P_C (MSEC)	THRUST (MSEC)	START TEMP. (°F)	SUMMATION OF PULSES	STEADY STATE CHARACTERISTICS: DURATION (SEC)	THRUST (LBF)	P_C (PSIA)	FLOW RATE (LBM/SEC)	SPECIFIC IMPULSE (SEC)	RPC RPV SHIFT	P_C ROUGHNESS (±)	TERMINATION BURN TIME (SEC)	SUMMATION OF CYN TIME (SEC)	SUMMATION OF PROPELLANT USAGE (LBM)	SUMMATION OF AMBIENT STARTS
8-2	3241	329	—	—	—												210	—	10.0	—	—	—	—		—	1203	10746.6	202.98	251
8-2	3242	106	—	320	20/480												210	10263	—	—	—	—	—		—	—	10846.5	204.88	252
8-2	3243	110	—	—	—												210	—	10.0	—	—	—	—		—	1213	10856.5	205.09	253
8-6	3244	365	368	100	20/480	1.963	2.161		.0646	.1088				285.5	34.9	39.1	209	10263	—	—	—	—	—		—	—	10852.5	205.68	254
8-6	3245	365	369	100	20/480	1.119	2.172		.0660	.1054				290	31.8	33.8	220	10263	—	—	—	—	—		—	—	10860.5	205.12	255
8-6	3246	364	361	100	20/480	3.845	5.581		.1796	.2600				—	52.6	58.6	260	10263	—	—	—	—	—		—	—	10865.5	205.17	256
8-6	3247	368	361	100	20/480	3.585	5.218		.1765	.2649				268.1	50.0	48.0	246	10263	—	—	—	—	—		—	—	10870.5	205.27	257
8-6	3248	363	350	100	20/480	9.990	11.424		.3914	.5252				233.0	60.8	67.4	225	10263	—	—	—	—	—		—	—	10880.5	205.49	258
8-6	3249	362	357	100	20/480	15.06	17.52		.6866	.8457				225.7	114.6	117.0	219	10263	—	—	—	—	—		—	—	10895.5	205.75	259
8-6	3250	372	354	—	—	—	—		—	—				—	—	—	219	—	10.0	5.412	112.4	.10462	217.8	7%/6.0	10.8	1223	10905.5	206.10	260
8-6	3251	243	249	100	20/480	.9976	1.781		.0382	.0720				147.3	46.72	37.12	214	10263	—	—	—	—	—		—	—	10910.5	206.15	261
8-6	3252	244	253	100	20/480	.8721	1.226		.0439	.0745				151.4	38.5	35.8	211	10263	—	—	—	—	—		—	—	10915.5	206.20	262
8-6	3253	240	227	100	20/480	2.894	4.173		.1126	.1832				160.9	54.72	52.16	204	10263	—	—	—	—	—		—	—	10919.5	206.31	263
8-6	3254	238	228	100	20/480	2.607	4.246		.1009	.1987				181.7	53.2	56.7	203	10263	—	—	—	—	—		—	—	10924.5	206.41	264
8-6	3255	240	220	100	20/480	6.280	8.241		.2911	.3816				140.4	88.4	85.6	206	10263	—	—	—	—	—		—	—	10929.5	206.61	265
8-6	3256	241	233	100	20/480	9.807	13.15		.4499	.6095				218.4	123.2	119.9	207	10263	—	—	—	—	—		—	—	10934.5	206.90	266
8-6	3257	321	—	—	—	—	—		—	—				—	—	—	210	—	10.0	—	—	—	—		—	1233	10939.5	207.07	267
8-6	3258	108	—	100	20/480	—	—		—	—				—	—	—	210	10263	—	—	—	—	—		—	—	10796.5	207.26	268
8-6	3259	108	—	100	20/480	—	—		—	—				—	—	—	210	10263	—	—	—	—	—		—	—	10868.5	207.45	269
8-6	3260	104	—	100	20/480	—	—		—	—				—	—	—	210	10263	—	—	—	—	—		—	—	10868.5	207.64	270
8-6	3261	104	—	100	20/480	—	—		—	—				—	—	—	210	10263	—	—	—	—	—		—	—	10868.5	207.83	271
8-6	3262	108	—	100	20/480	—	—		—	—				—	—	—	210	10263	—	—	—	—	—		—	—	10930.5	208.02	272
8-6	3263	106	—	100	20/480	—	—		—	—				—	—	—	210	10263	—	—	—	—	—		—	—	10980.5	208.21	273
8-6	3264A	108	—	—	—	—	—		—	—				—	—	—	—	—	—	—	—	—	—		—	—	—	—	—
8-6	3264B	106	—	100	20/480	—	—		—	—				—	—	—	210	10263	—	—	—	—	—		—	—	10995.5	208.40	274
8-6	3265	106	—	—	—	—	—		—	—				—	—	—	210	—	10.0	—	—	—	—		—	1243	12005.5	208.56	275
8-7	3266	365	—	315	SWEEP	—	—		—	—				—	—	—	210	10263	10.0	—	—	—	—		—	1253	12015.5	209.33	276
8-7	3267	230	—	204	SWEEP	—	—		—	—				—	—	—	210	10263	10.0	—	—	—	—		—	1263	12025.5	209.98	277
8-7	3268	100	—	253	SWEEP	—	—		—	—				—	—	—	210	10263	10.0	—	—	—	—		—	1273	12035.5	210.53	278
8-7	3269	312	237	—	—	—	—		—	—				—	—	—	205	—	10.0	4.111	84.7	.01889	217.6	7%/3.0	22.6	1283	12045.5	210.72	279
8-7	3270	106	104	120	20/480	.6092	.8642		.0317	.0391				270.9	78.2	70.9	216	10303.5	—	—	—	—	—		—	—	12047.5	210.73	280
8-12	3271	104	104	100	20/480	.4002	.5801		.02669	.04574				285.9	61.0	58.0	218	10313.5	—	—	—	—	—		—	—	12049.5	210.75	281

ENGINE TEST SUMMARY

DATE	TEST NO.	TANK PRESS. (PSIA)	INJ. PRESS. (PSIA)	PULSE MODE CHARACTERISTICS: NO. PULSES	CYCLE ON/OFF	CHAMBER PRESSURE INTEGRAL: PULSE 1-5	PULSE 90-100	LAST 10 PULSES	VACUUM IMPULSE: PULSE 1-5	PULSE 90-100	LAST 10 PULSES	IMPULSE SHIFT (%)	P_C SHIFT (%)	SPECIFIC IMPULSE (SEC)	AVE. CENTROID TIME (MSEC): P_C (MSEC)	THRUST (MSEC)	START TEMP. (°F)	SUMMATION OF PULSES	STEADY STATE CHARACTERISTICS: DURATION (SEC)	THRUST (LBF)	P_C (PSIA)	FLOW RATE (LBM/SEC)	SPECIFIC IMPULSE (SEC)	$\frac{\Sigma PC}{\Sigma TV}$ SHIFT	P_C ROUGHNESS (±%)	SUMMATION (LBM) TIME (SEC)	SUMMATION OF ON TIME (SEC)	SUMMATION OF PROPELLANT USAGE (LBM)	SUMMATION OF AMBIENT STARTS
8-1	[illegible]	106	105	99	50/350	1.5272	2.600		.0700	.1172				262.9	69.0	65.4	210	103234	—	—	—	—	—	—	—	—	12094.925	210.90	282
8-1	[illegible]	107	105	100	50/400	1.366	1.268		.0468	.0657				263.0	129.7	119.3	208	103354	—	—	—	—	—	—	—	—	12059.5	210.85	283
8-7	[illegible]	107	103	100	100/300	8.629	5.040		.1596	.2102				176.5	190.3	153.1	205	104280	—	—	—	—	—	—	—	—	12069.5	210.97	284
8-1	[illegible]	109	99	100	300/1500	5.300	7.078		.2205	.2492				159.6			220	105514	—	—	—	—	—	—	—	—	12094.3	211.16	285
8-1	[illegible]	124	100	—	—												220	—	10.0	1.998	42.6	.00974	205.1	"S/LB	6.9	293	12094.5	211.26	286
8-7	[illegible]	[illegible]		999	100/300												210	104533	—	—	—	—	—	—	—	—	12194.4	213.16	287
8-7	[illegible]	[illegible]		—	—												210	—	10.0							303	12204.9	213.32	288
8-7	[illegible]	[illegible]		999	100/300												210	105532	—							—	12304.3	215.22	289
8-8	[illegible]	[illegible]		—	—												210	—	10.0							1313	12369.3	215.39	290
8-8	[illegible]	[illegible]		999	100/300												210	106981	—							—	12414.2	217.28	291
8-8	[illegible]	[illegible]		—	—												210	—	10.0							1323	12424.2	217.45	292
8-8	[illegible]	[illegible]		999	100/300												210	107530	—							—	12524.1	219.35	293
8-8	[illegible]	[illegible]		—	—												210	—	10.0							1333	12534.1	219.51	294
8-8	[illegible]	[illegible]		999	100/300												210	108526	—							—	12634.0	221.41	295
8-8	[illegible]	[illegible]		—	—												210	—	10.0							1343	12644.0	221.58	296
8-8	[illegible]	[illegible]		999	100/300												210	109528	—							—	12743.9	223.48	297
8-8	[illegible]	[illegible]		—	—												210	—	10.0							1353	12753.9	223.64	298
8-8	[illegible]	[illegible]		999	100/300												210	110527	—							—	12853.9	225.54	299
8-8	[illegible]	[illegible]		—	—												210	—	10.0							1363	12863.8	225.71	308
8-8	[illegible]	[illegible]		999	100/300												210	111526	—							—	12963.7	227.61	301
8-8	[illegible]	[illegible]		—	—												210	—	10.0							1373	12973.7	227.77	302
8-8	[illegible]	[illegible]		999	100/300												210	112525	—							—	13073.6	229.67	303
8-8	[illegible]	[illegible]		—	—												210	—	10.0							1383	13083.6	229.73	304
8-8	[illegible]	[illegible]		999	100/300												210	113524	—							—	13183.5	231.73	305
8-8	[illegible]	[illegible]		—	—												210	—	10.0							1393	13193.5	231.90	306
8-8	[illegible]	[illegible]		999	100/300												210	114523	—							—	13293.4	232.07	307
8-8	[illegible]	[illegible]		—	—												210	—	10.0							1403	13303.4	232.23	308
8-8	[illegible]	[illegible]		999	100/300												210	115522	—							—	13403.3	234.13	309
8-8	[illegible]	[illegible]		—	—												210	—	10.0							1413	13413.3	234.30	310
8-8	[illegible]	[illegible]		999	100/300												210	116521	—							—	13513.2	236.19	311
8-8	[illegible]	[illegible]		—	—												210	—	10.0							1423	13523.2	236.36	312
8-9	[illegible]	[illegible]																											

ENGINE TEST SUMMARY

DATE	TEST NO.	TANK PRESS. (PSIA)	INJ. PRESS. (PSIA)	PULSE MODE CHARACTERISTICS															STEADY STATE CHARACTERISTICS									SUMMATION OF ON TIME (SEC)	SUMMATION OF PROPELLANT USAGE (LBM)	SUMMATION OF AMBIENT STARTS
				NO. PULSES	CYCLE ON/OFF	CHAMBER PRESSURE INTEGRAL PULSE 1-5	CHAMBER PRESSURE INTEGRAL PULSE 90-100	CHAMBER PRESSURE INTEGRAL LAST 10 PULSES	VACUUM IMPULSE PULSE 1-5	VACUUM IMPULSE PULSE 90-100	VACUUM IMPULSE LAST 10 PULSES	IMPULSE SHIFT (%)	P_C SHIFT (%)	SPECIFIC IMPULSE (SEC)	AVE. CENTROID TIME (MSEC) P_C (MSEC)	AVE. CENTROID TIME (MSEC) THRUST (MSEC)	START TEMP. (°F)	SUMMATION OF PULSES	DURATION (SEC)	THRUST (LBF)	P_C (PSIA)	FLOW RATE (LBM/SEC)	SPECIFIC IMPULSE (SEC)	ΣPC ΣPV SHIFT	P_C ROUGHNESS (±)	SUMMATION BURN TIME (SEC)				
8-9	3305	293	—	999	100/100												210	117520	—								13623.1	238.26	313
8-9	3306	290	—	—	—												210	—	10.0								13633.1	238.92	314
8-9	3307	109	—	999	100/100												210	118519	—								13733.0	240.32	315
8-9	3308	109	—	—	—												210	—	10.0							1493	13743.0	240.99	316
8-9	3309	365	—	999	100/200												210	119518	—								13842.9	242.39	317
8-9	3310	366	—	—	—												210	—	10.0							1453	13852.9	242.55	318
8-9	3311	237	—	999	100/200												210	120517	—								13952.8	244.45	319
8-9	3312	236	—	—	—												210	—	10.0							1463	13962.8	244.62	320
8-9	3313	107	—	999	100/200												210	21716	—								14062.7	246.51	321
8-9	3314	107	—	—	—												210	—	10.0							1473	14072.7	246.68	322
8-9	3315	368	955	1000	100/200	11.01	11.25	11.56	.5088	.5119	.5249			144.1	93.6	89.8	382	122516	—	—	—	—	—	—	—	—	14172.7	248.38	323
8-9	3316	363	269	—	—	—	—	—	—	—	—			—	—	—	216	—	10.0	1.416	91.5	.02022	218.4	6.8/6.0	18.4	1483	14182.7	248.53	324
8-9	3317	241	232	1000	100/200	6.196	5.008	9.032	2874	3721	.4034			186.0	100.0	95.1	214	123516	—	—	—	—	—	—	—	—	14282.7	251.76	325
8-10	3318	320	229	—	—	—	—	—	—	—	—			—	—	—	206	—	10.0	1.028	83.1	.01855	217.1	6.9/6.7	10.0	1493	14292.7	251.94	326
8-10	3319	106	102	999	100/200	3.046	4.540	4.722	.1360	.2074	.2101			155.6	107.9	102.8	202	124516	—	—	—	—	—	—	—	—	14392.7	253.32	327
8-10	3320	119	106	—	—	—	—	—	—	—	—			—	—	—	211	—	10.0	1.317	91.3	.00930	206.1	18.5/20.8	12.7	1503	14402.7	253.31	328
8-10	3321	365	—	999	100/200												210	125515	—								14502.6	255.21	329
8-10	3322	365	—	—	—												210	—	10.0							1513	14512.6	255.38	330
8-10	3323	240	—	999	100/200												210	126514	—								14612.5	257.27	331
8-10	3324	240	—	—	—												210	—	10.0							1523	14622.5	257.44	332
8-10	3325	105	—	999	100/200												210	127513	—								14722.4	259.34	333
8-10	3326	105	—	—	—												210	—	10.0							1533	14732.4	259.50	334
8-10	3327	365	—	999	100/200												210	128512	—								14832.3	261.40	335
8-10	3328	365	—	—	—												210	—	10.0							1543	14842.3	261.57	336
8-10	3329	240	—	999	100/200												210	129511	—								14942.2	263.47	337
8-10	3330	237	—	—	—												210	—	10.0							1553	14952.2	263.63	338
8-10	3331	105	—	999	100/200												210	130510	—								15052.1	265.53	339
8-10	3332	105	—	—	—												210	—	10.0							1563	15062.1	265.70	340
8-10	3333	364	—	999	100/200												210	131509	—								15162.0	267.60	341
8-10	3334	368	—	—	—												210	—	10.0							1573	15172.0	267.76	342
8-10	3335	239	—	999	100/200												210	132508	—								15271.9	269.66	343
8-10	3336	239	—	—	—												210	—	10.0							1583	15281.9	269.83	344

ENGINE TEST SUMMARY

DATE	TEST NO.	TANK PRESS. (PSIA)	INJ PRESS. (PSIA)	PULSE MODE CHARACTERISTICS: NO. PULSES	CYCLE ON/OFF	CHAMBER PRESSURE INTEGRAL: PULSE 1-5	PULSE 90-100	LAST 10 PULSES	VACUUM IMPULSE: PULSE 1-5	PULSE 90-100	LAST 10 PULSES	IMPULSE SHIFT (%)	P_C SHIFT (%)	SPECIFIC IMPULSE	[illegible] P_C	[illegible] THRUST	START TEMP. (°F)	SUMMATION OF PULSES	STEADY STATE CHARACTERISTICS: DURATION (SEC)	THRUST (LBF)	P_V (PSIA)	FLOW RATE (LBM/SEC)	SPECIFIC IMPULSE (SEC)	$\Sigma PC / \Sigma PV$ SHIFT	P_C ROUGHNESS	SUMMATION BURN TIME (SEC)	SUMMATION OF ON TIME (SEC)	SUMMATION OF PROPELLANT USAGE (LBM)	SUMMATION OF AMBIENT STARTS
8-10	[illegible]	105	—	999	[illegible]												210	135507	—		...				—	—	15381.8	271.56	345
8-10	[illegible]	103	—	—	—												210	—	10.0		—				—	1593	15391.8	271.72	346
8-10	[illegible]	365	—	999	[illegible]												210	134506	—		—				—	—	15491.7	273.62	347
8-10	[illegible]	365	—	—	—												210	—	10.0		—				—	1603	15501.7	273.79	348
8-10	[illegible]	295	—	999	[illegible]												210	135505	—		—				—	—	15601.6	275.65	349
8-10	[illegible]	296	—	—	—												210	—	10.0		—				—	1613	15611.6	275.85	350
8-10	[illegible]	105	—	999	[illegible]												210	136504	—		—				—	—	15711.5	277.75	351
8-10	[illegible]	105	—	—	—												210	—	10.0		—				—	1623	15721.5	277.92	352
8-19	[illegible]	371	—	999	[illegible]												210	137503	—		—				—	—	15821.4	279.81	353
8-19	[illegible]	366	—	—	—												210	—	10.0		—				—	1633	15831.4	279.98	354
8-19	[illegible]	296	—	999	[illegible]												210	138502	—		—				—	—	15931.3	281.88	355
8-19	[illegible]	234	—	—	—												210	—	10.0		—				—	1643	15941.3	282.04	356
8-19	[illegible]	108	—	999	[illegible]												210	139501	—		—				—	—	16041.2	283.94	357
8-19	[illegible]	106	—	—	—												210	—	10.0		—				—	1653	16051.2	284.11	358
8-19	[illegible]	365	—	999	[illegible]												210	140500	—		—				—	—	16151.1	286.01	359
8-19	[illegible]	365	—	—	—												210	—	10.0		—				—	1663	16161.1	286.17	360
8-19	[illegible]	296	—	999	[illegible]												210	141499	—		—				—	—	16261.0	288.07	361
8-19	[illegible]	295	—	—	—												210	—	10.0		—				—	1673	16271.0	288.24	362
8-19	[illegible]	105	—	999	[illegible]												210	142498	—		—				—	—	16370.9	290.13	363
8-19	[illegible]	105	—	—	—												210	—	10.0		—				—	1683	16380.9	[illegible]	364
8-19	[illegible]	365	—	999	[illegible]												210	143497	—		—				—	—	16480.8	[illegible]	365
8-19	[illegible]	365	—	—	—												210	—	10.0		—				—	1693	16490.8	292.36	366
8-19	[illegible]	240	—	999	[illegible]												210	144496	—		—				—	—	16550.7	294.26	367
8-19	[illegible]	240	—	—	—												210	—	10.0		—				—	1703	16600.7	294.43	368
8-19	[illegible]	105	—	999	[illegible]												210	145495	—		—				—	—	16700.6	296.33	369
8-19	[illegible]	105	—	—	—												210	—	10.0		—				—	1713	16710.6	296.49	370
8-19	[illegible]	365	—	999	[illegible]												210	146494	—		—				—	—	16810.5	298.39	371
8-19	[illegible]	365	—	—	—												210	—	10.0		—				—	1723	16820.5	298.56	372
8-19	[illegible]	240	—	999	[illegible]												210	147493	—		—				—	—	16920.4	300.45	373
8-19	[illegible]	240	—	—	—												210	—	10.0		—				—	1733	16930.4	300.62	374
8-19	[illegible]	105	—	999	[illegible]												210	148492	—		—				—	—	17030.3	302.52	375
8-19	[illegible]	105	—	—	—												210	—	10.0		—				—	1743	17040.3	302.68	376

ENGINE TEST SUMMARY

DATE	TEST NO.	TANK PRESS. (PSIA)	INJ. PRESS. (P' A)	PULSE MODE CHARACTERISTICS: NO. PULSES	CYCLE ON-OFF	CHAMBER PRESSURE INTEGRAL: PULSE 1-5	PULSE 90-100	LAST 10 PULSES	VACUUM IMPULSE: PULSE 1-5	PULSE 90-100	LAST 10 PULSES	IMPULSE SHIFT (%)	P_C SHIFT (%)	SPECIFIC IMPULSE (SEC)	AVE. CENTROID TIME (MSEC): P_C (MSEC)	THRUST (MSEC)	START TEMP. (°F)	SUMMATION OF PULSES	STEADY STATE CHARACTERISTICS: DURATION (SEC)	THRUST (LBF)	P_C (PSIA)	FLOW RATE (LBM/SEC)	SPECIFIC IMPULSE (SEC)	EPC TPV SHIFT	P_C ROUGHNESS (±)	IGNITION TIME (SEC)	SUMMATION OF ON TIME (SEC)	SUMMATION OF PROPELLANT USAGE (LBM)	SUMMATION OF AMBIENT STARTS
8-14	8267	321	345	999	100/100	8.528	11.48	11.82	.4197	.5365	.5997			220.8	96.2	96.3	219	49491	—	—	—	—	—	—	—	—	17140.2	305.24	377
8-14	8268	324	347	—	—	—	—	—	—	—	—			—	—	—	218		4.1	4.340	91.2	.0808	215.8	88/76.3	49.1	1752.9	17149.4	305.42	378
8-14	8269	242	287	1000	100/900	5.864	8.259	8.280	.2750	.3961	.3958			215.3	107.2	98.1	208	150491	—	—	—	—	—	—	—	—	17249.4	307.25	379
8-14	8270	326	346	—	—	—	—	—	—	—	—			—	—	—	214		9.2	3.345	92.0	0.0188	214.7	113/108	8.7	1762.1	17258.6	307.92	380
8-14	8271	107	105	999	100/900	9.616	9.695	9.982	.1582	.1781	.1936			164.1	142.2	144.0	216	151490	—	—	—	—	—	—	—	—	17356.5	308.34	381
8-14	8272	121	108	—	—	—	—	—	—	—	—			—	—	—	211		9.2	1.817	39.1	0.0088	203.3	227/61	50.6	1771.3	17367.7	308.92	382
8-14	8273	322	342	100	2/491	1.830	2.387	—	.0608	.1086	—			130.2	96.7	94.8	222	151590	—	—	—	—	—	—	—	—	17369.7	308.98	383
8-14	8274	328	345	100	2/489	1.311	2.399	—	.03524	.1130	—			126.4	96.0	94.6	222	151690	—	—	—	—	—	—	—	—	17311.7	309.05	384
8-14	8275	322	320	100	10/490	8.874	5.848	—	.1811	.2707	—			129.9	99.6	94.0	219	151790	—	—	—	—	—	—	—	—	17336.7	309.19	385
8-14	8276	323	336	100	20/490	8.730	5.608	—	.1772	.2472	—			133.6	91.2	90.5	220	151890	—	—	—	—	—	—	—	—	17381.7	309.32	386
8-14	8277	325	346	100	20/490	8.856	11.76	—	.4051	.5819	—			129.8	91.6	89.8	217	151990	—	—	—	—	—	—	—	—	17391.7	309.60	387
8-14	8278	328	345	100	20/490	14.19	16.41	—	.6430	.7997	—			103.5	114.3	112.7	222	152090	—	—	—	—	—	—	—	—	17406.7	309.99	388
8-14	8279	501	345	—	—	—	—	—	—	—	—			—	—	—	229		9.2	5.363	101.8	0.0244	219.8	10/8.8	46.3	1780.5	17415.9	310.22	389
8-14	8280	245	245	100	20/490	.9869	1.382	—	.04177	.04916	—			165.0	41.8	39.2	219	152190	—	—	—	—	—	—	—	—	17419.9	310.27	390
8-14	8281	244	295	100	20/490	.9928	1.409	—	.03961	.04645	—			167.9	39.2	36.6	216	152290	—	—	—	—	—	—	—	—	17429.9	310.32	391
8-14	8282	243	286	100	11/490	2.812	4.304	—	.1270	.1692	—			138.9	56.5	58.4	207	152390	—	—	—	—	—	—	—	—	17439.5	310.93	392
8-14	8283	249	295	100	20/490	2.624	4.201	—	.1215	.1936	—			138.8	52.8	50.6	221	152490	—	—	—	—	—	—	—	—	17449.9	310.54	393
8-15	8284	241	—	100	20/490	—	—	—	—	—	—			—	—	—	210	152590	—	—	—	—	—	—	—	—	17459.9	310.73	394
8-15	8285	249	—	100	20/490	—	—	—	—	—	—			—	—	—	210	152690	—	—	—	—	—	—	—	—	17469.9	310.92	395
8-15	8286	320	—	—	—	—	—	—	—	—	—			—	—	—	220	—	10.0	—	—	—	—	—	—	1790.5	17479.9	311.08	396
8-15	8287	107	—	100	20/490	—	—	—	—	—	—			—	—	—	210	152790	—	—	—	—	—	—	—	—	17489.9	311.27	397
8-15	8288	106	—	100	20/490	—	—	—	—	—	—			—	—	—	210	152890	—	—	—	—	—	—	—	—	17499.9	311.47	398
8-15	8289	107	—	100	20/490	—	—	—	—	—	—			—	—	—	210	152990	—	—	—	—	—	—	—	—	17509.9	311.66	399
8-15	8290	107	—	100	20/490	—	—	—	—	—	—			—	—	—	210	153090	—	—	—	—	—	—	—	—	17519.9	311.86	400
8-15	8291	108	106	100	20/490	9.997	9.987	—	.1586	.2199	—			134.5	—	151.9	200	153190	—	—	—	—	—	—	—	—	17529.9	311.99	401
8-15	8292			100	20/490													153290	—	—	—	—	—	—	—	—	17539.9	312.18	402
8-15	8293	118	99	—	—	—	—	—	—	—	—			—	—	—	190.1	—	9.8	1.808	39.0	0.0091	202.9	10/9	12.5	1800.3	17548.7	312.27	403
8-16	8294	498	363	—	—	—	—	—	—	—	—			—	—	—	198.2	—	9.8	5.377	111.6	0.0244	220.4	9/8.2	11.5	1810.1	17558.5	312.51	404
8-15	8295	306	—	999	100/500	—	—	—	—	—	—			—	—	—	210	154299	—	—	—	—	—	—	—	—	17623.4	314.91	405
8-15	8296	296	—	999	100/500	—	—	—	—	—	—			—	—	—	210	154399	—	—	—	—	—	—	—	—	17733.3	316.31	406
8-15	8297	285	—	—	—	—	—	—	—	—	—			—	—	—	210	—	10.0	—	—	—	—	—	—	1820.1	17733.3	316.47	407
8-15	8298	108	—	999	100/500	—	—	—	—	—	—			—	—	—	210	154497	—	—	—	—	—	—	—	—	17833.2	317.37	408

ENGINE TEST SUMMARY

DATE	TEST NO.	TANK PRESS (PSIA)	INJ PRESS (PSIA)	PULSE MODE CHARACTERISTICS																	STEADY STATE CHARACTERISTICS								SUMMATION OF ON TIME (SEC)	SUMMATION OF PROPELLANT WEIGHT (LBM)	SUMMATION OF AMBIENT STARTS
				NO. PULSES	CYCLE ON OFF	CHAMBER PRESSURE INTEGRAL PULSE 1-5	CHAMBER PRESSURE INTEGRAL PULSE 90-100	CHAMBER PRESSURE INTEGRAL CAL TO PULSES	VACUUM IMPULSE PULSE 1-5	VACUUM IMPULSE PULSE 90-100	VACUUM IMPULSE CAL TO PULSES	IMPULSE (LBF-SEC)	P_C (PSIA)	SPECIFIC IMPULSE (SEC)	AVG. CENTROID (DEG) C (INBD)	AVG. CENTROID (DEG) (OUTBD)	START NO. OF PULSES	SUMMATION OF PULSES	DURATION (SEC)	THRUST (LBF)	P_C (PSIA)	FLOW RATE (LBM/SEC)	SPECIFIC IMPULSE (SEC)	ΔP_C TPT SHIFT	P_C ROUGH (PSIA)	TIME (SEC)				
8-15	8997	108	—	—	—												210	—	10.0		—					1890.1	19432	318.54	409
8-15	8998	365	—	999	100/500												210	257286	—		—					1793.1	17933	320.43	410
8-15	8999	365	—	—	—												210	—	10.0		—					1840.1	17933.1	320.60	411
8-15	9000	365	—	999	100/500												210	258286	—		—					—	18052.0	322.50	412
8-15	9001	365	—	—	—												210	—	10.0		—					1850.1	18063.9	322.67	413
8-15	9002	240	—	—	—												210	259240	—		—					—	18162.9	324.56	414
8-15	9003	365	—	999	99/500												210	—	10.0		—					1846.1	18172.9	324.73	415
8-15	9004	365	—	—	—												210	260285	—		—					—	18272.9	326.49	416
8-15	9005	365	—	997	100/500												210	—	10.0		—					1837.1	18382.9	326.67	417
8-15	9006	365	—	—	—												210	261285	—		—					—	18482.9	328.49	418
8-15	9007	240	—	662	100/500												210	—	10.0		—					1836.1	18492.9	328.67	419
8-15	9008	240	—	999	100/500												210	262285	—		—					—	18592.9	330.49	420
8-15	9009	240	—	—	—												210	—	10.0		—					1880.1	18602.9	330.67	421
8-15	9010	105	—	999	100/500												210	263285	—		—					1836.1	18692.9	332.31	422
8-15	9011	105	—	—	—												210	—	10.0		—					—	18702.9	332.49	423
8-16	9012	365	—	999	100/500												210	264285	—		—					1900.1	18802.9	334.31	424
8-16	9013	372	—	—	—												210	—	10.0		—					—	18812.9	334.49	425
8-16	9014	260	—	999	100/500												210	265285	—		—					1910.1	18912.9	336.31	426
8-16	9015	259	—	—	—												210	—	10.0		—					—	18922.9	336.49	427
8-16	9016	109	—	999	99/500												210	266285	—		—					1920.1	19022.9	338.31	428
8-16	9017	107	—	—	—												210	—	10.0		—					—	19032.9	338.49	429
8-16	9018	367	—	999	100/500												210	267285	—		—					1930.1	19132.9	340.31	430
8-16	9019	368	—	—	—												210	—	10.0		—					—	19142.9	340.49	431
8-16	9020	236	—	999	100/500												210	268285	—		—					1940.1	19242.9	342.31	432
8-16	9021	235	—	—	—												210	—	10.0		—					—	19252.9	342.49	433
8-16	9022	105	—	999	100/500												210	269285	—		—					1950.1	19352.9	344.31	434
8-16	9023	105	—	—	—												210	—	10.0		—					—	19362.9	344.49	435
8-16	9024	365	—	999	100/500												210	270285	—		—					1960.1	19382.9	346.63	436
8-16	9025	365	—	—	—												210	—	10.0		—					—	19438.1	348.53	437
8-16	9026	240	—	999	100/500												210	271285	—		—					1970.1	19448.1	348.69	438
8-16	9027	240	—	—	—												210	—	10.0		—					—	19548.0	350.50	439
8-16	9028	105	—	999	100/500												210	272285	—		—					1980.1	19558.0	350.76	440
8-16	9029	105	—	—	—												210	—	10.0		—					—			

* RAN OUT OF FUEL

ENGINE TEST SUMMARY

DATE	TEST NO.	TANK PRESS. (PSIA)	INJ. PRESS. (PSIA)	PULSE MODE CHARACTERISTICS: NO. PULSES	CYCLE ON/OFF	CHAMBER PRESSURE INTEGRAL: PULSE 1-5	PULSE 90-100	LAST 10 PULSES	VACUUM IMPULSE: PULSE 1-5	PULSE 90-100	LAST 10 PULSES	IMPULSE SHIFT (%)	P_c SHIFT (%)	SPECIFIC IMPULSE (SEC)	AVE. CENTROID TIME (MSEC): P_c (MSEC)	THRUST (MSEC)	START TEMP (°F)	SUMMATION OF PULSES	STEADY STATE CHARACTERISTICS: DURATION (SEC)	THRUST (LBF)	P_c (PSIA)	FLOW RATE (LBM/SEC)	SPECIFIC IMPULSE (SEC)	ΣPC SHIFT	P_c ROUGHNESS (±%)	SUMMATION BURN TIME (SEC)	SUMMATION OF ON TIME (SEC)	SUMMATION OF PROPELLANT USAGE (LBM)	SUMMATION OF AMBIENT STARTS
8-16	3461	365	—	999	on/400	—	—	—	—	—	—			—	—	—	210	172983	—	—	—	—	—	—	—	—	196579	352.65	441
8-16	3462	365	—	—	—	—	—	—	—	—	—			—	—	—	210	—	10.0	—	—	—	—	—	—	1990.1	196679	352.82	442
8-16	3463	240	—	999	on/400	—	—	—	—	—	—			—	—	—	210	173982	—	—	—	—	—	—	—	—	197678	354.72	443
8-16	3464	240															210		10.0							2000.1	197778	354.88	444
8-16	3465	105	—	999	on/400	—	—	—	—	—	—			—	—	—	210	174951	—	—	—	—	—	—	—	—	198777	356.79	445
8-16	3466	105	—	—	—	—	—	—	—	—	—			—	—	—	210	—	10.0	—	—	—	—	—	—	2010.1	198877	356.95	446
8-17	3467	326	320	968	on/400	11.546	10.646	18.160	.6038	.6749	.5521			196.4	105.1	101.5	236	175979	—	—	—	—	—	—	—	—	198875	359.15	447
8-17	3468	458	368	—	—	—	—	—	—	—	—			—	—	—	230	—	9.8	5.084	655	14886	218.1	15/16	12.8	2009.9	199923	359.98	448
8-17	3469	297	297	991	on/400	5.956	9.182	9.022	.5603	.3688	.4064			191.5	109.3	106.2	224	176927	—	—	—	—	—	—	—	—	200937.1	362.10	449
8-17	3470	237	189	—	—	—	—	—	—	—	—			—	—	—	244	—	9.8	2349	653	0.0140	210.6	13/16	10.2	2029.7	201067.9	362.24	450
8-17	3471	110	106	991	on/400	1.478	9.069	5.555	.1524	.2295	.2990			165.6	159.2	148.0	209	177918	—	—	—	—	—	—	—	—	202067.9	363.67	451
8-17	3472	109	109	—	—	—	—	—	—	—	—			—	—	—	208.1	—	9.8	1656	57.2	14886	199.5	25/29	22.5	2039.5	202158.8	363.75	452
8-17	3473	366	—	999	on/400	—	—	—	—	—	—			—	—	—	210	178917	—	—	—	—	—	—	—	—	203157	365.69	453
8-17	3474	365	—	—	—	—	—	—	—	—	—			—	—	—	210	—	10.0	—	—	—	—	—	—	2049.5	203257	365.81	454
8-17	3475	296	—	999	on/400	—	—	—	—	—	—			—	—	—	210	179916	—	—	—	—	—	—	—	—	204256	367.71	455
8-17	3476	235	—	—	—	—	—	—	—	—	—			—	—	—	210	—	10.0	—	—	—	—	—	—	2059.5	204356	367.88	456
8-17	3477	105	—	999	on/400	—	—	—	—	—	—			—	—	—	210	180915	—	—	—	—	—	—	—	—	205355	369.77	457
8-17	3478	105	—	—	—	—	—	—	—	—	—			—	—	—	210	—	10.0	—	—	—	—	—	—	2069.5	205455	369.90	458
8-17	3479	365	—	999	on/400	—	—	—	—	—	—			—	—	—	210	181914	—	—	—	—	—	—	—	—	206454	371.78	459
8-17	3480	365	—	—	—	—	—	—	—	—	—			—	—	—	210	—	10.0	—	—	—	—	—	—	2079.5	206554	372.00	460
8-17	3481	365	—	999	on/400	—	—	—	—	—	—			—	—	—	210	182913	—	—	—	—	—	—	—	—	207553	373.90	461
8-17	3482	240	—	—	—	—	—	—	—	—	—			—	—	—	210	—	10.0	—	—	—	—	—	—	2089.5	207653	374.07	462
8-17	3483	105	—	999	on/400	—	—	—	—	—	—			—	—	—	210	183912	—	—	—	—	—	—	—	—	208652	375.97	463
8-17	3484	105	—	—	—	—	—	—	—	—	—			—	—	—	210	—	10.0	—	—	—	—	—	—	2099.5	208752	376.13	464
8-17	3485	365	—	999	on/400	—	—	—	—	—	—			—	—	—	210	184911	—	—	—	—	—	—	—	—	209751	378.03	465
8-17	3486	365	—	—	—	—	—	—	—	—	—			—	—	—	210	—	10.0	—	—	—	—	—	—	2109.5	209851	378.20	466
8-17	3487	240	—	999	on/400	—	—	—	—	—	—			—	—	—	210	185910	—	—	—	—	—	—	—	—	210950	380.09	467
8-17	3488	240	—	—	—	—	—	—	—	—	—			—	—	—	210	—	10.0	—	—	—	—	—	—	2119.5	210950	380.26	468
8-17	3489	105	—	999	on/400	—	—	—	—	—	—			—	—	—	210	186909	—	—	—	—	—	—	—	—	211949	382.16	469
8-20	3490	105	—	—	—	—	—	—	—	—	—			—	—	—	210	—	10.0	—	—	—	—	—	—	2129.5	212049	382.32	470
8-20	3491	365	—	999	on/400	—	—	—	—	—	—			—	—	—	210	187908	—	—	—	—	—	—	—	—	213048	384.22	471
8-20	3492	365	—	—	—	—	—	—	—	—	—			—	—	—	210	—	10.0	—	—	—	—	—	—	2139.5	213148	384.39	472

ENGINE TEST SUMMARY

DATE	TEST NO.	TANK PRESS PSIA	INJ PRESS PSIA	PULSE MODE CHARACTERISTICS														STEADY STATE CHARACTERISTICS								SUMMATION OF ON TIME SEC	SUMMATION OF PROPELLANT USAGE LBM	SUMMATION OF AMBIENT STARTS
				NO. PULSES	CYCLE ON OFF	CHAMBER PRESSURE INTEGRAL PULSE 1-5	CHAMBER PRESSURE INTEGRAL PULSE 90-100	CHAMBER PRESSURE INTEGRAL LAST 10 PULSES	VACUUM IMPULSE PULSE 1-5	VACUUM IMPULSE PULSE 90-100	VACUUM IMPULSE LAST 10 PULSES	IMPULSE UNIT	P_c SHOT	SPECIFIC IMPULSE SEC	EOT CENTROID TIME MSEC C MSEC	EOT CENTROID TIME MSEC THRUST MSEC	START TEMP °F	TERMINATION OF PULSE	DURATION SEC	THRUST LBF	P_c PSIA	FLOW RATE LBM SEC	SPECIFIC IMPULSE SEC	IPC IPO SHIFT	P_c REVISION PSIA	TERMINATION TIME LBM LBM			
8-20	3461	260	—	999	100/500										—		210	PRTV	—	—	—				—	2149.7	396.72	473
8-20	3462	260	—	—	—										—		210	—	10.0	—	—				—	2149.5	2152.4	396.29	474
8-20	3463	265	—	999	100/500										—		210	99506	—	—	—				—	—	2153.4	396.19	475
8-20	3464	265	—	—	—										—		210	—	10.0	—	—				—	2159.5	2159.4	396.25	476
8-20	3465	265	—	999	100/500										—		210	99505	—	—	—				—	—	2163.5	396.21	477
8-20	3466	265	—	999	100/500										—		210	—	10.0	—	—				—	2169.5	2169.4	396.41	478
8-20	3467	265	—	—	—										—		210	99504	—	—	—				—	—	2173.4	396.31	479
8-20	3468	260	—	999	100/500										—		210	—	10.0	—	—				—	2179.5	2179.4	396.47	480
8-20	3469	260	—	—	—										—		210	99503	—	—	—				—	—	2183.3	396.37	481
8-20	3470	260	—	999	100/500										—		210	—	10.0	—	—				—	2189.3	2189.3	396.59	482
8-20	3471	265	—	—	—										—		210	99502	—	—	—				—	—	2193.2	396.49	483
8-20	3472	265	—	999	100/500										—		210	—	10.0	—	—				—	2199.2	2199.2	396.67	484
8-20	3473	265	—	—	—										—		210	99501	—	—	—				—	—	2203.1	396.50	485
8-20	3474	260	—	999	100/500										—		210	—	10.0	—	—				—	2209.1	2209.1	396.67	486
8-20	3475	260	—	—	—										—		210	99500	—	—	—				—	—	2213.0	396.57	487
8-20	3476	260	—	999	100/500										—		210	—	10.0	—	—				—	2219.1	2219.0	396.73	488
8-20	3477	260	—	—	—										—		210	99499	—	—	—				—	—	2222.9	396.63	489
8-20	3478	260	—	999	100/500										—		210	—	10.0	—	—				—	2229.0	2229.0	396.80	490
8-20	3479	260	—	—	—										—		210	99498	—	—	—				—	—	2232.9	396.70	491
8-20	3480	260	—	999	100/500										—		210	—	10.0	—	—				—	2239.0	2238.8	396.86	492
8-20	3481	236	—	—	—										—		210	99497	—	—	—				—	—	2242.7	396.76	493
8-20	3482	236	—	999	100/500										—		210	—	10.0	—	—				—	2248.9	2248.7	396.93	494
8-20	3483	103	—	—	—										—		210	99496	—	—	—				—	—	2252.6	396.83	495
8-20	3484	103	—	999	100/500										—		210	—	10.0	—	—				—	2258.6	2258.4	396.99	496
8-21	3485	236	—	—	—										—		210	99495	—	—	—				—	—	2262.3	396.89	497
8-21	3486	239	—	999	100/500										—		210	—	10.0	—	—				—	2268.3	2268.1	397.06	498
8-21	3487	239	—	—	—										—		210	99494	—	—	—				—	—	2271.9	396.95	499
8-21	3488	104	—	999	100/500										—		210	—	10.0	—	—				—	2278.0	2277.8	397.12	500
8-21	3489	104	—	—	—										—		210	99493	—	—	—				—	—	2281.8	397.02	501
8-21	3490	239	—	999	100/500										—		210	—	10.0	—	—				—	2287.8	2287.7	397.18	502
8-21	3491	235	—	—	—										—		210	99492	10.0	—	—				—	2293.8	2293.8	397.32	503
8-21	3492	240	—	201	SLEEP										—		210	99491	10.0	—	—				—	2297.5	2297.4	397.22	504

ENGINE TEST SUMMARY

PULSE MODE CHARACTERISTICS

DATE	TEST NO.	TANK PRESS. (PSIA)	INJ. PRESS. (PSIA)	NO. PULSES	CYCLE ON/OFF	CHAMBER PRESSURE INTEGRAL PULSE 1-5	CHAMBER PRESSURE INTEGRAL PULSE 90-100	CHAMBER PRESSURE INTEGRAL LAST 10 PULSES	VACUUM IMPULSE PULSE 1-5	VACUUM IMPULSE PULSE 90-100	VACUUM IMPULSE LAST 10 PULSES	IMPULSE SHIFT (%)	P_C SHIFT (%)	SPECIFIC IMPULSE (SEC)	AVE. CENTROID TIME (MSEC) P_C (MSEC)	AVE. CENTROID TIME (MSEC) THRUST (MSEC)	START TEMP. (°F)	SUMMATION OF PULSES
8-21	3495	115	—	325	SWEEP	—	—		—	—				—	—	—	210	208800
8-21	3496	240	—	999	100/900	—	—		—	—				—	—	—	210	204796
8-21	3497	240	—	—	—	—	—		—	—				—	—	—	210	—
8-21	3498	105	—	999	100/900	—	—		—	—				—	—	—	210	205748
8-21	3499	105	—	—	—	—	—		—	—				—	—	—	210	—
8-21	3500	365	365	100	20/980	1.270	2.167		.05760	.09371				156.0	50.0	52.9	205	205898
8-21	3501	363	360	100	20/480	1.097	2.250		.05175	.09504				157.9	54.3	53.8	216	205598
8-21	3502	363	360	100	50/950	3.400	4.475		.1962	.1892				160.2	47.4	46.9	211	206098
8-21	3503	363	355	100	50/450	3.966	5.507		.1217	.2290				180.0	56.7	55.8	225	206458
8-21	3504	363	358	100	100/900	7.821	10.19		.3464	.4580				188.2	82.4	81.1	218	206298
8-21	3505	366	350	100	150/850	12.75	15.02		.5772	.7095				201.6	108.5	109.0	209	206358
8-21	3506	491	472	—	—	—	—		—	—				—	—	—	225	—
8-21	3507	249	249	100	20/980	.9757	1.654		.03273	.07319				149.2	46.6	45.5	224	206458
8-21	3508	243	243	100	20/480	.8770	1.703		.03605	.07008				147.6	47.3	43.4	220	206558
8-21	3509	242	234	100	50/950	2.629	3.939		.1021	.1749				171.0	58.8	57.6	220	206658
8-21	3510	241	234	100	50/450	2.535	4.007		.1004	.1833				185.0	56.9	55.9	220	206758
8-21	3511	242	230	100	100/900	5.580	7.674		.2426	.3476				187.0	69.7	87.8	223	206858
8-21	3512	242	231	100	150/850	8.859	11.41		.3919	.5162				181.1	112.9	114.9	229	206958
8-22	3513	314	249	—	—	—	—		—	—				—	—	—	206	—
8-22	3514	104	104	100	20/980	.6298	.9991		.02248	.04126				122.3	91.0	72.6	207	207058
8-22	3515	105	103	100	20/480	.5960	.8538		.02297	.03949				90.8	93.8	66.6	205	207158
8-22	3516	105	102	100	50/950	1.632	2.521		.06507	.1063				151.9	90.1	80.8	219	207258
8-22	3517	104	102	100	50/450	1.535	2.318		.06642	.1017				132.4	126.9	120.9	216	207358
8-22	3518	104	100	100	100/900	3.046	5.090		.1225	.2130				163.5	147.5	138.6	209	207458
8-22	3519	103	100	100	150/850	4.591	7.071		.2163	.3147				176.9			213	207558
8-22	3520	104	—	—	—	—	—		—	—				—	—	—	210	—
#21 8-22	3521	367	367	100	20/980	.1258	2.130		.05207	.09765				160.0	39.3	36.0	222	207658
8-22	3522	120	105	—	—	—	—		—	—				—	—	—	210	—
8-22	3523	368	364	100	20/980	1.126	2.377		.05732	.1073				174.6	34.3	33.2	207	207858
* 8-22	3524	367	364	100	50/950	5.166	*3.825		.2196	*.2022				*167.5	*47.9	*46.7	210	207958
8-22	3525	367	360	100	50/450	3.436	5.241		.1191	.2175				169.5	52.6	52.0	214	208058
8-22	3526	367	361	100	100/900	8.17	10.32		.3562	.4615				188.9	85.68	85.20	208	208158

STEADY STATE CHARACTERISTICS

DATE	TEST NO.	DURATION (SEC)	THRUST (LBF)	P_C (PSIA)	FLOW RATE (LBM/SEC)	SPECIFIC IMPULSE (SEC)	$\Sigma PC / \Sigma FV$ SHIFT	P_C ROUGHNESS (±%)	SUMMATION BURN TIME (SEC)	SUMMATION OF ON TIME (SEC)	SUMMATION OF PROPELLANT USAGE (LBM)	SUMMATION OF AMBIENT STARTS
8-21	3495	** 20.0	—	—	—	—		—	23295.5	23042.2	417.57	505
8-21	3496	—	—	—	—	—		—	—	23162.1	419.47	506
8-21	3497	10.0	—	—	—	—		—	23305.5	23172.1	419.63	507
8-21	3498	—	—	—	—	—		—	—	23272.0	421.53	508
8-21	3499	10.0	—	—	—	—		—	23315.5	23282.0	421.70	509
8-21	3500	—	—	—	—	—		—	—	23284.0	421.76	510
8-21	3501	—	—	—	—	—		—	—	23286.0	421.82	511
8-21	3502	—	—	—	—	—		—	—	23291.0	421.93	512
8-21	3503	—	—	—	—	—		—	—	23296.0	422.06	513
8-21	3504	—	—	—	—	—		—	—	23306.0	422.30	514
8-21	3505	—	—	—	—	—		—	—	23411.0	422.66	515
8-21	3506	9.8	4839	102.1	.02264	213.3	18/19	12.1	23359.3	23420.8	422.88	516
8-21	3507	—	—	—	—	—		—	—	23412.8	422.89	517
8-21	3508	—	—	—	—	—		—	—	23424.8	422.94	518
8-21	3509	—	—	—	—	—		—	—	23425.8	423.04	519
8-21	3510	—	—	—	—	—		—	—	23434.8	423.14	520
8-21	3511	—	—	—	—	—		—	—	23444.8	423.33	521
8-21	3512	—	—	—	—	—		—	—	23455.8	423.61	522
8-22	3513	9.8	3554	76.1	.01676	212.6	21/22	8.4	23363.1	23465.6	423.78	523
8-22	3514	—	—	—	—	—		—	—	23471.6	423.81	524
8-22	3515	—	—	—	—	—		—	—	23473.6	423.85	525
8-22	3516	—	—	—	—	—		—	—	23476.6	423.92	526
8-22	3517	—	—	—	—	—		—	—	23483.6	424.00	527
8-22	3518	—	—	—	—	—		—	—	23495.6	424.13	528
8-22	3519	—	—	—	—	—		—	—	23506.6	424.31	529
8-22	3520	10.0	—	—	—	—		—	23373.1	23518.6	424.48	530
#21 8-22	3521	—	—	—	—	—		—	—	23520.6	424.54	531
8-22	3522	10.0	1614	54.2	.008080	201.8	31/32	16.0	23383.1	23530.6	424.62	532
8-22	3523	—	—	—	—	—		—	—	23532.6	424.68	533
* 8-22	3524	—	—	—	—	—		—	—	23537.6	424.80	534
8-22	3525	—	—	—	—	—		—	—	23541.6	424.93	535
8-22	3526	—	—	—	—	—		—	—	23552.6	425.17	536

* BAD TAPE
** TWO STARTS TOTAL 20 SEC 5.5

ENGINE TEST SUMMARY

DATE	TEST NO.	TANK PRESS. (PSIA)	INJ. PRESS. (PSIA)	PULSE MODE CHARACTERISTICS: NO. PULSES	CYCLE ON/OFF	CHAMBER PRESSURE INTEGRAL: PULSE 1-5	PULSE 90-100	LAST 10 PULSES	VACUUM IMPULSE: PULSE 1-5	PULSE 90-100	LAST 10 PULSES	IMPULSE SHIFT	% SHIFT	SPECIFIC IMPULSE (SEC)	AVE. CENTROID TIME (MSEC): % IMPULSE	THRUST	START TEMP. (°F)	SUMMATION OF PULSE	STEADY STATE CHARACTERISTICS: DURATION (SEC)	THRUST (LBF)	P_c (PSIA)	FLOW RATE (LBM/SEC)	SPECIFIC IMPULSE (SEC)	P_c SHIFT	P_c ROUGHNESS (PSI)	THRUST ROUGHNESS (LBF)	SUMMATION OF ON TIME (SEC)	SUMMATION OF PROPELLANT USAGE (LBM)	SUMMATION OF AMBIENT STARTS
8-22	3527	36.7	360	100	150/150	13.20	15.08		5912	6793				209.1	107.9	104.5	218												
8-22	3528	491	369	—	—	—	—		—	—				—	—	—	218		6.9	4.921	100.8	1270	214.0	16/17	7.6	2.498	2351.9	42572	598
8-22	3529	244	244	100	300/300	9799	1.669		03582	06951				104.3	46.3	42.6	215												
8-22	3530	244	244	100	200/300	9097	1.760		03208	07192				97.6	36.2	33.8	218												
8-22	3531	243	235	100	50/450	2.637	4.178		1069	1813				171.6	60.0	58.4	215												
8-22	3532	243	235	100	50/450	2.589	3.695		1098	1603				175.9	50.9	49.3	213												
8-22	3533	244	235	100	100/400	5.665	7.887		2108	3600				184.7	86.8	80.9	210												
8-22	3534	246	236	100	150/450	2.938	4.53		3958	5299				147.8	117.1	110.9	215												
#21 8-22	3535	219	229	—	—	—	—		—	—				—	—	—	221		6.9	3.592	77.2	0170	211.5	16/21	11.9	2.408	2362.3	42664	547
8-22	3536	106	105	100	200/300	5320	3782		02212	03596				116.3	91.7	78.5	208												
8-23	3537	106	105	100	200/300	5127	9276		02181	04514				130.2	66.8	61.7	217												
8-23	3538	106	104	100	50/450	1.031	2.518		05872	1076				156.9	52.0	48.0	220												
8-23	3539	107	104	100	50/450	1.957	2.805		01309	1009				131.8	126.2	119.1	212												
8-23	3540	107	104	100	100/400	3.130	5.226		1239	2122				116.3	151.0	128.3	218												
8-23	3541	106	103	100	150/450	4.742	7.115		2014	3092				169.1	155	155	215												
8-23	3542	119	163	—	—	—	—		—	—				—	—	—	222		6.9	—	—	—	—	—	—	—	2368.5	427.19	553
8-23	3543	119	103	—	—	—	—		—	—				—	—	—	219		6.9	4.626	32.6	11.91	203.2	28/30	3.0	2.478	2368.8	427.27	554
8-23	3544	440	356	—	—	—	—		—	—				—	—	—	220		7.1	5.064	35.9	0291	219.2	5/18	2.1	2.498	2368.1	427.49	554
#22 8-23	3545	316	291	—	—	—	—		—	—				—	—	—	216		7.3	5.407	76.2	0161	213.4	17/19	4.7	.441	2368.4	427.66	555
8-23	3546	107	92	—	—	—	—		—	—				—	—	—	219		7.2	4.891	26.6	0021	221.5	25/28	12.2	2.451	2368.7	427.93	556
8-23	3547	476	350	—	—	—	—		—	—				—	—	—	212		14.4	5.096	105.8	2372	219.7	11/11	7.3	1.611	2371.6	429.11	557
8-23	3548	302	232	—	—	—	—		—	—				—	—	—	213		13.4	3.68	67	0161	217.0	14/14	3.7	2.216	2373.0	430.11	558
8-23	3549	106	93	—	—	—	—		—	—				—	—	—	219		13.4	4.541	99.4	1075	209.3	25/26	13.9	2.653	2374.24	430.76	559
8-23	3550	294	233	100	150/450	5.314	7.969		2617	3728				195.6	92.4	91.5	209											2374.24	430.76	559
8-23	3551	241	233	100	150/450	4.213	11.59		4157	5363				195.3	115.3	113.3	216		6.9	3.501	75.5	1163	219.8	17/17	7.4	2.647	2378.74	431.69	561
8-24	3552	296	231	—	—	—	—		—	—				—	—	—	214											2380.12	431.78	562
#17 8-24	3553	111	110	100	200/300	.7310	1.112		02460	04490				240.9	92.3	64.4	225											2380.92	431.20	563
8-24	3554	111	111	100	200/300	.5794	1.142		02244	04932				238.3	54.0	46.2	222											2381.42	431.22	564
8-24	3555	112	111	100	100/350	1.726	2.693		06369	1126				213.5	90.8	72.9	222											2381.92	431.28	565
8-24	3556	111	111	100	50/450	1.678	2.764		04960	1111				201.8	97.1	88.0	220											2381.92	431.39	566

* FUEL VALVE CLOSED

REFERENCES

1. Transit RTG Updated Safety Analysis Report, Volume III.

   Nuclear Safety Analysis Document, September 15, 1970
   TRW (A)-11464-291

2. Safety Analysis Summary Report for the Pioneer Radioisotope Heater Unit, PFG-273-324, TRW Systems, February 19, 1971.